NASA Contractor Report 145281

Expansion of Flight Simulator Capability for Study and Solution of Aircraft Directional Control Problems on Runways — Appendixes

J. A. McGowan

McDonnell Douglas Corporation
Douglas Aircraft Company

CONTRACT NAS1-13981
JANUARY 1978

NASA

National Aeronautics and
Space Administration

Langley Research Center
Hampton, Virginia 23665

NASA CR-145281

EXPANSION OF FLIGHT SIMULATOR CAPABILITY FOR STUDY AND SOLUTION OF AIRCRAFT DIRECTIONAL CONTROL PROBLEMS ON RUNWAYS

APPENDIXES

20 JANUARY 1978

PREPARED UNDER CONTRACT NO. NAS1-13981

FOR

NASA

LANGLEY RESEARCH CENTER
NATIONAL AERONAUTICS AND SPACE ADMINISTRATION
LANGLEY STATION, HAMPTON, VIRGINIA

MCDONNELL DOUGLAS CORPORATION
DOUGLAS AIRCRAFT COMPANY
LONG BEACH, CALIFORNIA

ii

Blank

TABLE OF CONTENTS

CONVERSION FACTORS

The following table gives conversion factors from the English system to SI units for those quantities used in this report.

The sign and first two digits of each numerical entry represent a power of 10.

TO CONVERT FROM	TO	MULTIPLY BY
Fahrenheit (temperature)	Celsius	$t_c = (5/9)\ (t_f - 32)$
Foot	Meter	-01 3.048
Inch	Meter	-02 2.54
Knot (international)	Meter/Second	-01 5.144 444
Mile (U.S. Statue)	Meter	+03 1.609 344
Mile (U.S. Nautical)	Meter	+03 1.852
Pound Force (lbf avoirdupois)	Newton	+00 4.448 222
Slug	Kilograms	+01 1.459 390
Foot/Second^2	Meter/Second^2	-01 3.048
Free Fall, Standard (g's)	Meter/Second^2	+00 9.806 65
Foot^2	Meter^2	-02 9.290 304
lbf/Foot^2	Newton/Meter^2	+01 4.788 026
psi(lbf/Inch^2)	Newton/Meter^2	+03 6.894 757
Foot/second	Meter/Second	-01 3.048

The foregoing values were taken from Reference 11. Some of the values were rounded to six digits after the decimal point.

INTRODUCTION

The intention of this report is to present the models used implementing the DC-9-10 aircraft simulation for the Runway Direction Control study. The study was done on the Douglas Aircraft six-degree-of-freedom motion simulator at Long Beach.

The approach taken in documenting the models has been to describe them in algebraic form, to the extent possible. Furthermore, the effort has been directed toward presenting what was actually done rather than general forms.

The following Douglas personnel contributed to this report: P. L. Jernigan and R. E. Adams of the Systems Simulation group; G. W. Kibbee, R. A. Storley and R. P. Schiltz of Hydro-Mechanical group; and E. F. Admiral of Avionics group.

APPENDIX A

AIRCRAFT SIMULATION

The DC-9-10 aircraft was simulated using math models derived from information supplied by Aero Stability and Control, Power Plant and Hydro-Mechanical Controls groups. The supplied data was combined with classical kinematic and transformation equations to form the airframe model. The calculation flow of the airframe model is shown in Figure 1.

In developing the model it was assumed that the flight envelope would be in the low speed (mach 0-.3) and low altitude (0-500 feet) region. Also, since the runs were to be short (i.e., approach, landing and roll out), the aircraft weight was assumed to be constant and the C.G. position fixed at 25% MAC.

Three basic axes systems are used to represent the relative motions and orientations of the aircraft. The inertial system (called earth axes) has its origin at the "touchdown" point of the runway (see Figure 2). For the ground handling simulation the touchdown point was choosen to be 1000 feet in from the threshold. Another axes system called the Aircraft Body Axes System has its origin at the C.G. of the aircraft. (See Figure 3.) The sign conventions for these axes systems are as follows:

- X body axis velocity positive forward
- X earth axis velocity positive toward runway and position positive beyond touchdown point
- Y body axis velocity positive to right
- Y earth axis velocity positive to the right and position positive to the right
- Z body axis velocity positive down (negative up)
- Z earth axis velocity negative up and position negative above ground.

A third axes system used is called the Stability Axes. This system is closely related to the body axes system but is aligned with the longitudinal wind vector rather than the body of the aircraft. The stability axes are used in defining most of the aerodynamic data.

Validation of the aircraft simulation was accomplished in three phases. First, the individual sections (aero, engine, etc.) were checked to see that they were statically correct. Secondly, to the extent possible, the various models were checked dynamically using inputs which produce transient responses. These responses, recorded as time histories, were then compared with expected responses. Where direct time histories were not available comparative parameters such as frequency and time to damp were used.

The third phase of validation was to have test pilots familiar with the DC-9-10 aircraft "fly" the simulator through various maneuvers. Their comments were used to adjust some parameters to improve the "feel" of the simulation.

The data collected during some of the validation runs and the associated comparative data is part of the file of rolled charts and is labeled Validation Data.

For convenience the description of the aircraft simulation has been divided into six sections. Sections 1 and 2 cover aerodynamics and equations of motion; Section 3 describes the engine model used; Section 4 explains the environmental model (winds, and runway conditions); Section 5 covers the landing gear but does not include the antiskid system which is described in Appendices B and C; and Section 6 picks up other programs such as instrument drives, motion drives, visual system drives, etc.

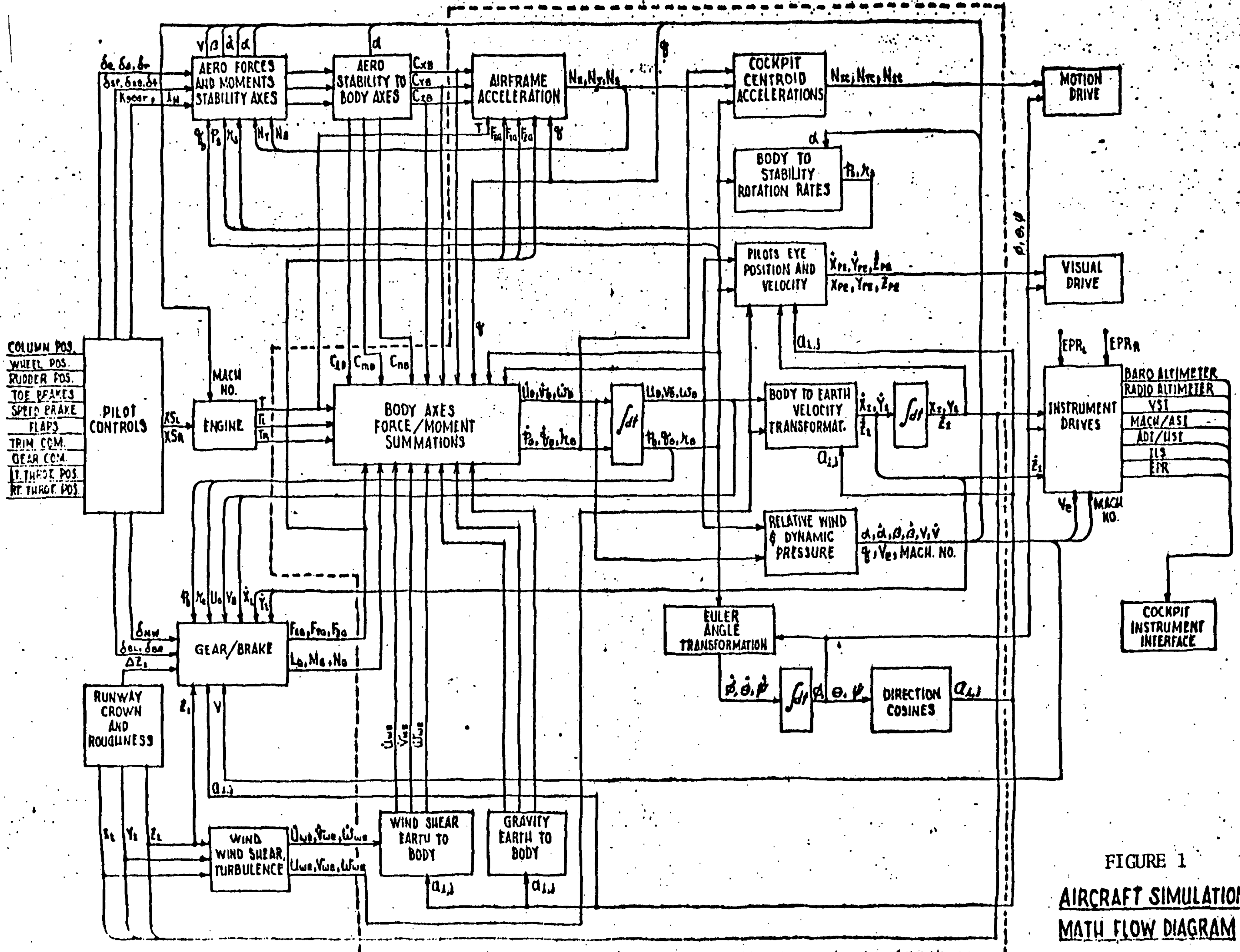

FIGURE 1

AIRCRAFT SIMULATION MATH FLOW DIAGRAM

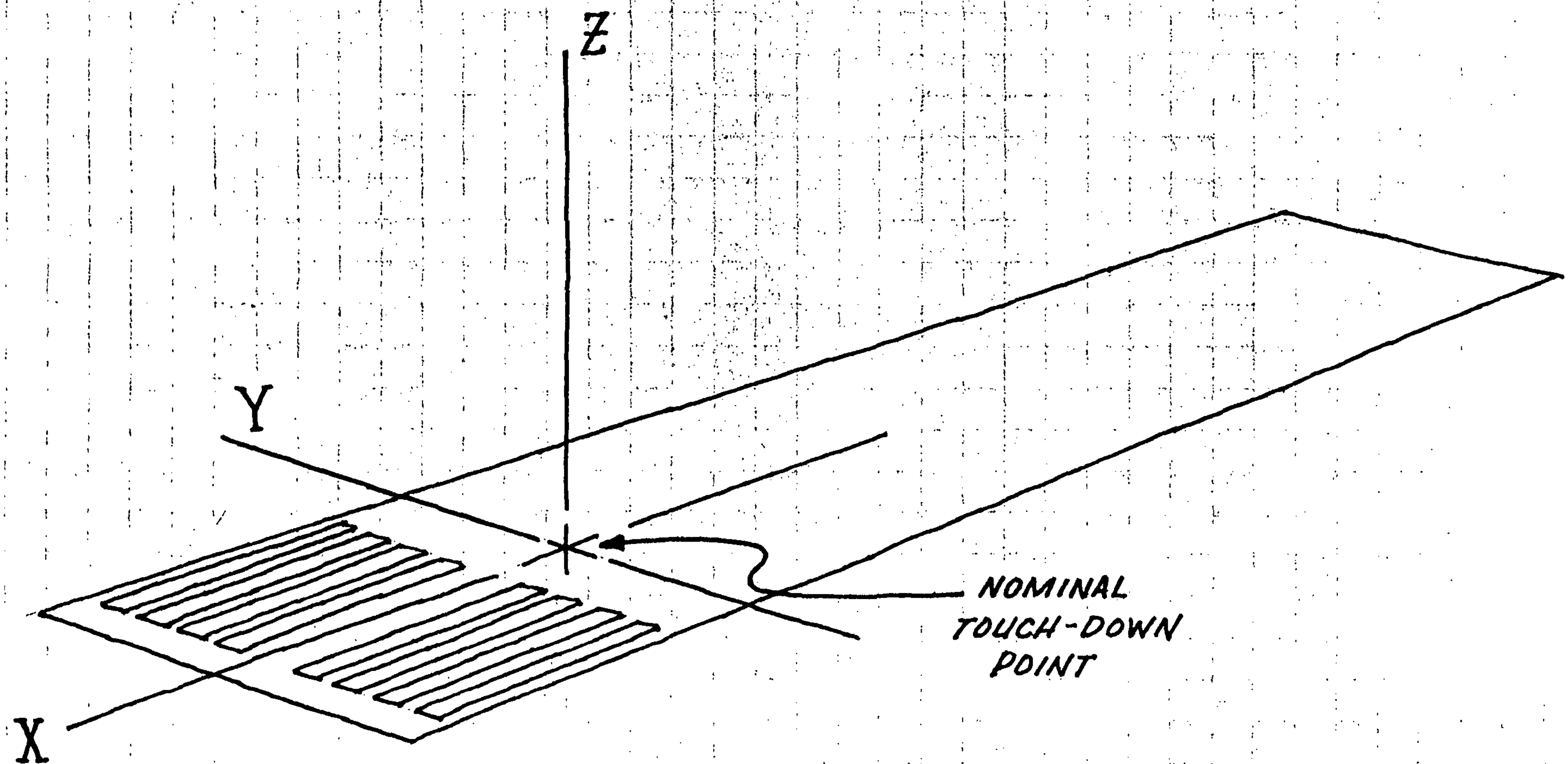

EARTH AXES

FIG. 2

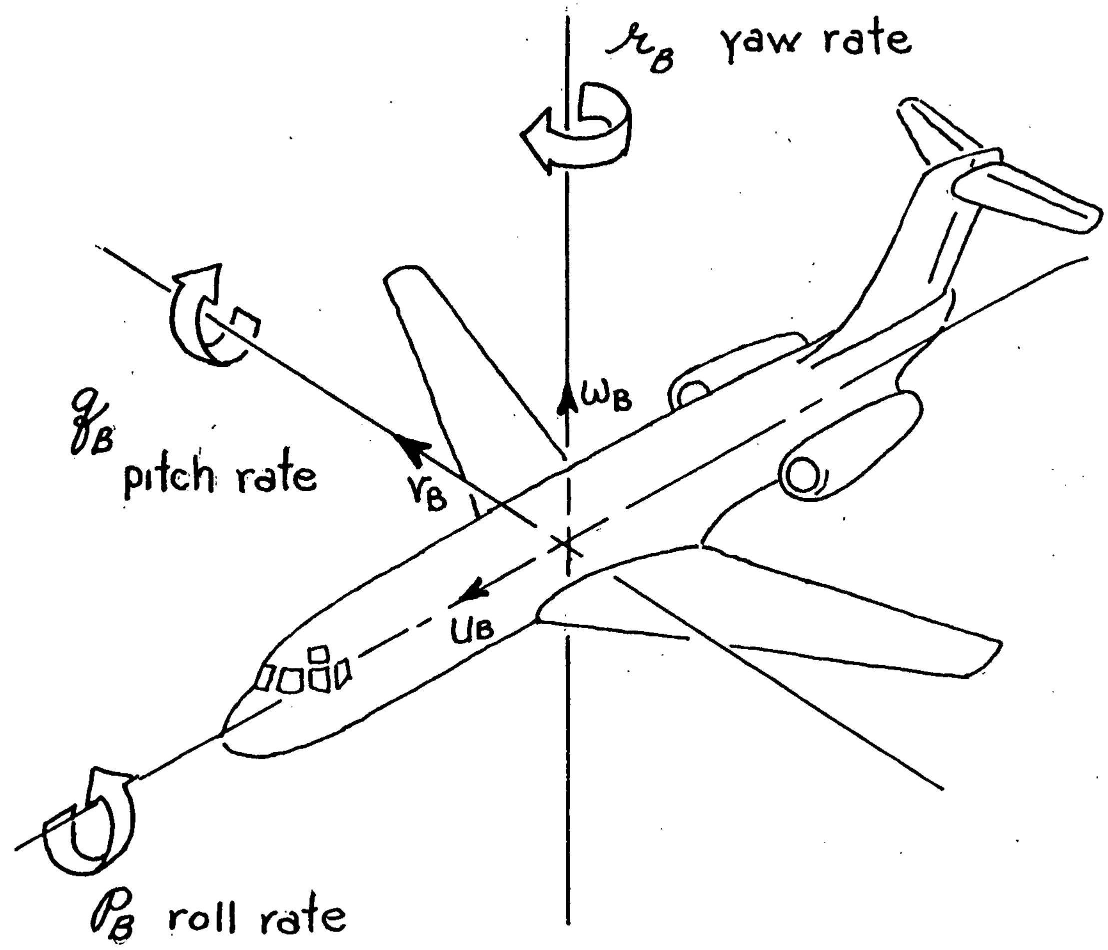

AIRCRAFT BODY AXES

FIG. 3

Section 1

Basic Airframe Equations of Motion

The calculations covered in the Equations of Motion (EOM) are those which form the six independent variables of the airframe system and preform the appropriate axes transformations between the three axes systems used. Basically these equations are those needed to describe the motions of any rigid body. The derivations of these equations are covered in almost any text on aerodynamics or rigid body dynamics. Looking at Figure 1, this section covers all the boxes enclosed by the dashed line.

The associated equations for the EOM boxes are shown in Figures 1.1 - 1.9. Table 1.1 has descriptions of all the symbols used.

The EOM used for the Ground Handling Simulation are essentially the same for any aircraft using the same axes systems. The documentation of the equations should be fairly self sufficient, however, there are a few things that might be mentioned.

The 57.3 and 1/57.3 factors show up because it was desired to have the angular state variables in units of degrees rather than radians. The method employed is to assume the angles to be in degrees and convert them back to radians for summation into the force and moment equations. The results of the summations are then converted back to degrees!

In Figure 1.4 the 1/1.69 factor in the V_e equation is the ratio of knots to feet per sec. It is more convenient to have V_e in units of knots.

The fact that weight and C.G. position were constant in this simulation meant that mass, moments of inertia, and the lever arms only had to be calculated once at initialization and remained constant during real time runs.

These EOM are designed to handle winds and wind shears, i.e., time-rate-of-change of wind speed and/or direction. This is accomplished by first defining the wind profile in the inertial (earth) axes system. The steady state part of the wind components are then summed directly onto the inertial velocities. The time-rate-of-change parts are transformed to the body axes and summed directly into the force equations. (See Figures 1.1 and 1.7). This method allows a very versatile representation of the wind conditions without sacrificing the true inertial effects of a changing wind vector on the aircraft dynamics.

It should be noted that although a transformation matrix (direction cosines) is defined, and its elements are mentioned, the EOM program uses no matrix type operations. Using the individual matrix elements streamlines the calculations by eliminating any operation where the result would be zero anyway, e.g., the gravity vector transformation into the body axes.

Validation of the EOM program consisted mainly of checking to see that the proper parameters were entered for the DC-9-10. Further tests and check runs were not made on the EOM themselves for two reasons. First, this program has been used, in almost the same form, for numerous other transport type airframe simulations. Since the changes to the EOM for the DC-9-10 were minor it was felt that any more extensive checking would not be productive. Second, and foremost, the EOM are an integral part of the whole dynamic airframe simulation. For this reason it was felt that it would be more cost effective to validate the system as a whole and only do a detailed check if it was indicated. (Which, as it turned out, it was not.)

SYMBOL TABLE EQUATIONS OF MOTION

TABLE 1.1

ALGEBRAIC SYMBOL		DESCRIPTION	UNITS
C_{nB}	CNB	COEFFICIENT OF YAWING MOMENT BODY AXIS	UNITLESS
T, T_L, T_R	THT, THL, THR	TOTAL THRUST, LEFT AND RIGHT ENGINE THRUST	lbs
i_T	—	ANGLE BETWEEN THRUST VECTOR AND FRP POSITIVE UP	deg
F_{XG}, F_{YG}, F_{ZG}	FXG, FYG, FZG	FORCE DUE TO GEAR ALONG X, Y AND Z BODY AXES	lbs
L_G, M_G, N_G	ROLLG PMG YAWG	MOMENTS DUE TO GEAR ABOUT X, Y AND Z BODY AXES	ft-lb
I_x, I_y, I_z, I_{xz}	XIX, XIY XIZ XIXZ	AIRCRAFT MOMENTS OF INERTIA BODY AXES	slug-ft²
Z_{TCG}	ZCG	DISTANCE FROM CENTER OF THRUST TO C.G.	ft
C_w	CW	WING MEAN AERODYNAMIC CHORD (MAC)	ft
$\dot{U}_{WB}, \dot{V}_{WB}, \dot{W}_{WB}$	UDW, VDW WDW	WIND SHEAR TERMS FOR X, Y AND Z BODY AXES	ft/sec²
b_w	BW	WING SPAN	ft
Y_T	—	LATERAL DISTANCE FROM AIRCRAFT CENTER LINE TO CENTER OF THRUST	ft

SYMBOL TABLE EQUATIONS OF MOTION

TABLE 1.1 (CONT.)

ALGEBRAIC SYMBOL		DESCRIPTION	UNITS
U_B, V_B, W_B	UB, VB, WB	VELOCITY COMPONENTS ALONG THE X, Y, AND Z BODY AXES	ft/sec
P_B, Q_B, R_B	PB, QB, RB	ANGULAR VELOCITIES ABOUT THE X, Y AND Z BODY AXES	deg/sec
57.3	RTD	NUMBER OF DEGREES PER RADIAN	
g	—	LOCAL ACCELERATION OF GRAVITY (NOMINALLY 32.2)	ft/sec^2
$a_{i,j}$	AT(i, j)	ELEMENT OF THE TRANSFORMATION MATRIX (DIRECTION COSINE)	UNITLESS
M	XMASS	AIRCRAFT MASS	SLUGS
$\bar{q}$	Q	DYNAMIC PRESSURE	lb/ft^2
S_w	SW	WING AREA	ft^2
C_{X_B}	CXB	COEFFICIENT OF DRAG BODY AXIS	UNITLESS
C_{Y_B}	CYB	COEFFICIENT OF SIDE FORCE BODY AXIS	"
C_{Z_B}	CZB	COEFFICIENT OF LIFT BODY AXIS	"
C_{l_B}	CLB	COEFFICIENT OF ROLLING MOMENT BODY AXIS	"
C_{M_B}	CMS	COEFFICIENT OF PITCHING MOMENT BODY AXIS	"

SYMBOL TABLE EQUATIONS OF MOTION

TABLE 1.1 (CONT.)

ALGEBRAIC SYMBOL		DESCRIPTION	UNITS
α	ALF	ANGLE OF ATTACK, ANGLE BETWEEN AIRCRAFT FLIGHT PATH VELOCITY AND X BODY AXIS IN THE PLANE OF SYMMETRY	deg
β	BET	SIDESLIP ANGLE, ANGLE BETWEEN AIRCRAFT FLIGHT PATH VELOCITY AND AIRPLANE OF SYMMETRY	deg
V	VT	FLIGHT PATH VELOCITY, TRUE	ft/sec
V_e	VEKT	EQUIVALENT AIRSPEED	KNOTS
ρ	RHO	AIR DENSITY	slug/ft^3
MACH	XMACH	AIRCRAFT MACH NUMBER	UNITLESS
SOUND	SOUND	SPEED OF SOUND	ft/sec
h_{CG}	HCG	ALTITUDE OF C.G. ABOVE GROUND	ft
h_{WHEEL}	HWHEEL	ALTITUDE OF MAIN LANDING GEAR ABOVE GROUND	ft
$X_{w,CG}$	XBWHL	LONGITUDINAL DISTANCE FROM MAIN GEAR TO C.G.	ft
$Z_{w,CG}$	ZBWHL	VERTICAL DISTANCE FROM MAIN GEAR TO C.G.	

SYMBOL TABLE EQUATIONS OF MOTION

TABLE 1.1 (CONT.)

ALGEBRAIC SYMBOL		DESCRIPTION	UNITS
$\dot{X}_I, \dot{Y}_I, \dot{Z}_I$	VIX, VIY, VIZ	AIRCRAFT VELOCITY IN INERTIAL (EARTH) AXES	ft/sec
$U_{W_E}, V_{W_E}, W_{W_E}$	VWX, VWY, VWZ	WIND VELOCITY IN EARTH AXES	ft/sec
$\dot{U}_{W_E}, \dot{V}_{W_E}, \dot{W}_{W_E}$	XDWE YDWE ZDWE	WIND ACCELERATIONS (SHEAR) IN EARTH AXES	ft/sec²
ϕ, θ, ψ	PHI, THE PSI	EULER ANGLES OF ROTATION RELATING AIRCRAFT BODY AXES TO EARTH AXES (ROLL, PITCH AND YAW)	deg
P_S, q_S, r_S	PS, QB RS	ANGULAR VELOCITIES (STABILITY AXES)	deg/sec
X_{PE}, Y_{PE}, Z_{PE}	XPE, YPE ZPE	POSITION OF PILOTS EYE IN EARTH AXES SYSTEM	ft
$\dot{X}_{PE}, \dot{Y}_{PE}, \dot{Z}_{PE}$	XDPE, YDPE ZDPE	VELOCITY OF PILOTS EYE IN EARTH AXES SYSTEM	ft/sec
U_{PE}, V_{PE}, W_{PE}	UPE, VPE WPE	VELOCITY OF PILOTS EYE IN BODY AXES SYSTEM	ft/sec
$X_{PE,CG}, Y_{PE,CG}, Z_{PE,CG}$	XBPE, YBPE ZBPE	X, Y AND Z DISTANCES FROM C.G. TO PILOTS EYE	ft
$X_{C,CG}, Y_{C,CG}, Z_{C,CG}$	XBC, YBC ZBC	X, Y AND Z DISTANCES FROM C.G. TO COCKPIT CENTROID	ft
N_X, N_Y, N_Z	ANX, ANY ANZ	AIRCRAFT ACCELERATIONS ALONG X, Y AND Z AXES (BODY AXES LOAD FACTORS)	g's
$N_{X_C}, N_{Y_C}, N_{Z_C}$	ANXC, ANYC ANZC	ACCELERATIONS OF COCKPIT CENTROID	g's

EQUATIONS OF MOTION   FIG. 1.1

FORCE AND MOMENT SUMMATIONS (LONGITUDINAL)

$$\dot{u}_B = \frac{1}{57.3}\left(v_B r_B - w_B q_B\right) + g\,a_{1,3} + \frac{1}{M}\left[\bar{q} S_w C_{X_B} + T\cos i_T + F_{XG}\right] - \dot{u}_{WB}$$

$$\dot{w}_B = \frac{1}{57.3}\left(u_B q_B - v_B p_B\right) + g\,a_{3,3} + \frac{1}{M}\left[\bar{q} S_w C_{Z_B} + T\sin i_T + F_{ZG}\right] - \dot{w}_{WB}$$

$$\dot{q}_B = \frac{1}{I_y}\left[\frac{1}{57.3}\left(I_z - I_x\right) r_B p_B + \frac{1}{57.3}\left(I_{xz}\right)\left(r_B^2 - p_B^2\right) + 57.3\, S_w c_w \bar{q}\, C_{m_B} + 57.3\, Z_{TCG}\, T + 57.3\, M_G\right]$$

EQUATIONS OF MOTION FIG. 1.2

FORCE AND MOMENT SUMMATIONS (LATERAL - DIRECTIONAL)

$$\dot{V}_B = \frac{1}{57.3}\left(w_B\, p_B - u_B\, r_B\right) + g\, a_{2,3} + \frac{1}{M}\left[\bar{q}\, S_w\, C_{Y_B} + F_{y_G}\right] - \dot{V}_{w_B}$$

$$\dot{p}_B = \frac{1}{I_x}\Big[I_{xz}\, \dot{r}_B + \frac{1}{57.3}(I_y - I_z)\, q_B\, r_B + \frac{1}{57.3}(I_{xz})\, p_B\, q_B + 57.3\, S_w\, b_w\, \bar{q}\, C_{l_B} + 57.3\, L_G \Big]$$

$$\dot{r}_B = \frac{1}{I_z}\Big[I_{xz}\, \dot{p}_B + \frac{1}{57.3}(I_x - I_y)\, p_B\, q_B - \frac{1}{57.3}(I_{xz})\, q_B\, r_B + 57.3\, S_w\, b_w\, \bar{q}\, C_{n_B} + 57.3\, \frac{1}{T}(T_L - T_R) + 57.3\, N_G \Big]$$

EQUATIONS OF MOTION FIG. 1.3

ANGLE OF ATTACK AND ANGLE OF SIDESLIP

$$\dot{\alpha} = 57.3\,(\dot{w}_B u_B - \dot{u}_B w_B) \Big/ (u_B^2 + w_B^2)$$

$$\dot{\beta} = 57.3\,(\dot{v}_B - \dot{V} v_B / V) \Big/ \sqrt{u_B^2 + w_B^2}$$

$$\sin\alpha = w_B \Big/ \sqrt{u_B^2 + w_B^2} \quad ; \quad \sin\beta = v_B \big/ V$$

$$\cos\alpha = u_B \Big/ \sqrt{u_B^2 + w_B^2} \quad ; \quad \cos\beta = \sqrt{u_B^2 + w_B^2} \Big/ V$$

$$\alpha = \tan^{-1} w_B / u_B$$

$$\beta = \tan^{-1} v_B \Big/ \sqrt{u_B^2 + w_B^2}$$

EQUATIONS OF MOTION FIG. 1.4

FLIGHT PATH VELOCITY AND ACCELERATION

$$V = \sqrt{u_B^2 + v_B^2 + w_B^2} \quad ; \quad \dot{V} = \left(\dot{u}_B u_B + \dot{v}_B v_B + \dot{w}_B w_B \right) / V$$

EQUIVALENT AIRSPEED, DYNAMIC PRESSURE AND MACH NO.

$$V_e = V \sqrt{\rho / \rho_0} \left(1/1.69 \right)$$

$$q = 1/2 \, \rho V^2$$

$$MACH = V / SOUND \quad ; \quad SOUND = 1116.89 - .003908 \, h_{CG}$$

CENTER OF GRAVITY ALTITUDE AND WHEEL HEIGHT

$$h_{CG} = - z_I$$

$$h_{WHEEL} = - \left(z_I + a_{1,3} X_{w,CG} + a_{3,3} Z_{w,CG} \right)$$

EQUATIONS OF MOTION FIG. 1.5

EULER ANGLE TRANSFORMATION

$$\dot{\psi} = (r_B \cos\phi + q_B \sin\phi) / \cos\theta$$

$$\dot{\phi} = p_B + \dot{\psi} \sin\theta$$

$$\dot{\theta} = q_B \cos\phi - r_B \sin\phi$$

TRANSFORMATION OF BODY AXES RATES TO STABILITY AXES

$$p_S = p_B \cos\alpha + r_B \sin\alpha$$

$$r_S = r_B \cos\alpha - p_B \sin\alpha$$

EQUATIONS OF MOTION FIG. 1.6

TRANSFORMATION ELEMENTS (DIRECTION COSINES)

$$a_{1,1} = \cos\psi \cos\theta$$

$$a_{2,1} = \sin\phi \sin\theta \cos\psi - \cos\phi \sin\psi$$

$$a_{3,1} = \sin\phi \sin\psi + \cos\phi \sin\theta \cos\psi$$

$$a_{1,2} = \cos\theta \sin\psi$$

$$a_{2,2} = \cos\phi \cos\psi + \sin\phi \sin\theta \sin\psi$$

$$a_{3,2} = \cos\phi \sin\theta \sin\psi - \sin\phi \cos\psi$$

$$a_{1,3} = -\sin\theta$$

$$a_{2,3} = \sin\phi \cos\theta$$

$$a_{3,3} = \cos\phi \cos\theta$$

EQUATIONS OF MOTION FIG. 1.7

BODY TO EARTH AIRCRAFT VELOCITY TRANSFORMATION

$$\dot{X}_I = a_{1,1} U_B + a_{2,1} V_B + a_{3,1} W_B + U_{WE}$$

$$\dot{Y}_I = a_{1,2} U_B + a_{2,2} V_B + a_{3,2} W_B + V_{WE}$$

$$\dot{Z}_I = a_{1,3} U_B + a_{2,3} V_B + a_{3,3} W_B + W_{WE}$$

EARTH TO BODY WIND SHEAR TRANSFORMATION

$$\dot{U}_{WB} = a_{1,1} \dot{U}_{WE} + a_{1,2} \dot{V}_{WE} + a_{1,3} \dot{W}_{WE}$$

$$\dot{V}_{WB} = a_{2,1} \dot{U}_{WE} + a_{2,2} \dot{V}_{WE} + a_{2,3} \dot{W}_{WE}$$

$$\dot{W}_{WB} = a_{3,1} \dot{U}_{WE} + a_{3,2} \dot{V}_{WE} + a_{3,3} \dot{W}_{WE}$$

EQUATIONS OF MOTION

FIG. 1.8

PILOTS EYE POSITION AND VELOCITY FOR VISUAL SYSTEM

$$X_{PE} = X_I + a_{1,1}\, X_{PE,CG} + a_{3,1}\, Z_{PE,CG}$$

$$Y_{PE} = Y_I + a_{1,2}\, X_{PE,CG} + a_{3,2}\, Z_{PE,CG}$$

$$Z_{PE} = Z_I + a_{1,3}\, X_{PE,CG} + a_{3,3}\, Z_{PE,CG}$$

NOTE: PILOT IS ASSUMED TO BE ON AIRCRAFT CENTER LINE THEREFORE $Y_{PE,CG} = 0$

$$U_{PE} = U_B + \frac{1}{57.3}(q_B)\, Z_{PE,CG}$$

$$V_{PE} = V_B + \frac{1}{57.3}(X_{PE,CG}\, r_B - Z_{PE,CG}\, P_B)$$

$$W_{PE} = W_B - \frac{1}{57.3}(q_B)\, X_{PE,CG}$$

$$\dot{X}_{PE} = U_{PE}\, a_{1,1} + V_{PE}\, a_{2,1} + W_{PE}\, a_{3,1} + U_{WE}$$

$$\dot{Y}_{PE} = U_{PE}\, a_{1,2} + V_{PE}\, a_{2,2} + W_{PE}\, a_{3,2} + V_{WE}$$

$$\dot{Z}_{PE} = U_{PE}\, a_{1,3} + V_{PE}\, a_{2,3} + W_{PE}\, a_{3,3} + W_{WE}$$

EQUATIONS OF MOTION FIG. 1.9

TRANSFORMATION OF AIRCRAFT ACCELERATIONS FROM C.G.

TO COCKPIT CENTROID FOR MOTION BASE

$$N_{XC} = N_X - \left(q_B^2 + r_B^2\right) X_{C,CG} + \left(q_B p_B - \dot{r}_B\right) Y_{C,CG} + \left(r_B p_B + \dot{q}_B\right) Z_{C,CG}$$

$$N_{YC} = N_Y + \left(p_B q_B + \dot{r}_B\right) X_{C,CG} + \left(p_B^2 + r_B^2\right) Y_{C,CG} + \left(r_B q_B - \dot{p}_B\right) Z_{C,CG}$$

$$N_{ZC} = N_Z + \left(p_B r_B - \dot{q}_B\right) X_{C,CG} + \left(q_B r_B + \dot{p}_B\right) Y_{C,CG} - \left(p_B^2 + q_B^2\right) Z_{C,CG}$$

WHERE: AIRCRAFT ACCELERATIONS

$$N_X = 1/Mg \left(\bar{q} S_W C_{X_B} + T + F_{XG} \right)$$

$$N_Y = 1/Mg \left(\bar{q} S_W C_{Y_B} + F_{YG} \right)$$

$$N_Z = -1/Mg \left(\bar{q} S_W C_{Z_B} + F_{ZG} \right)$$

FIG. 1.10

AIRCRAFT WEIGHT AND INERTIA VALUES USED FOR DC-9-10 SIMULATION

OPERATING WEIGHT EMPTY	=	49,452	lbs.
PAYLOAD	=	7,548	lbs.
FUEL	=	17,000	lbs.
GROSS WEIGHT	=	74,000	lbs.

INERTIAS

I_x	=	3.3×10^5	slug-ft^2
I_y	=	8.41×10^5	"
I_z	=	1.09×10^6	"
I_{xz}	=	$.69 \times 10^5$	"

Section 2

Aerodynamic and Control System Models

This section contains descriptions of the Pilot Controls and Aero Forces and Moments algorithms. The information is presented in two parts. The first part is called Pilot Control Inputs to Aero Equations and the second is called Aerodynamic Equations.

The primary source for the data and algorithms used in this section is the Douglas Aircraft Estimated Data for Stability and Control. (Reference 6). The references cited in the equations are to this document.

The aerodynamic equations were developed using the assumptions of low mach number and no weight change as stated. Aero elasticity terms were, however, included eventhough their value for this study is questionable.

PILOT CONTROL INPUTS TO AERO EQUATIONS

Along with the inputs from the EOM the aero force equations require eight pilot control inputs. These eight inputs are generated from seven pilot operated controls in the cockpit as follows:

Elevator Input:

$$\delta_e = (3.427 + 5.31\, X_{CG})\, \delta_{cc} \Big|_{-25}^{15}$$

Where:

X_{CG} is the C.G position as a ratio of MAC.

δ_{cc} is the position of the control column in inches and has a dead band of .25 inch.

δ_e is elevator deflection in degrees and is limited to the range of 15° trailing edge down to 25° trailing edge up.

Aileron Input:

$$\delta_a = .25\, \delta_w \Big|_{-20}^{20}$$

Where:

δ_w is wheel deflection in degrees limited to ± 113 degrees with a dead band of .25 degrees.

δ_a is aileron deflection in degrees limited to the range of 20° for both trailing edge up and down.

Rudder Input:

$$\delta_r = 6.28\, \delta_{rp} + \delta_{YD} \Big|_{-30}^{30}$$

Where:

δ_{rp} is rudder pedal deflection in inches with stops at 4.78 inches left and right and a dead band of .25 inch.

δ_r is rudder deflection in degrees limited to 30 degrees trailing edge left and right.

δ_{YD} is rudder deflection due to yaw damper. This input is limited to approximately ± 1.6 degrees. (See Section 6 YAW DAMPER.)

Spoiler Input

On the DC-9-10 the spoiler surfaces are used for three areas of flight, 1) speed brakes, all spoilers go up at once as commanded by speed brake control, 2) ground spoilers, all spoilers go full up (60 degrees) automatically if armed and main gear spin up, and 3) lateral control spoilers, spoilers are deployed one side at a time to aid the ailerons in the rolling maneuver. In this simulation both the speed brake function and the ground spoiler function (symmetric spoiler deployment) are referred to as speed brakes.

Lateral Control Spoiler Input

$$\delta_{sp} = f(\delta_{\bar{\omega}})$$

Where:

δ_{sp} is spoiler deflection in degrees, positive for right wing down and negative for left wing down.

$\delta_{\bar{\omega}}$ is control wheel deflection (same as drives the ailerons).

$f(\delta_{\bar{\omega}})$ is defined by the following table:

$\delta_{\bar{\omega}}$	$f(\delta_{\bar{\omega}})$
0	0
3	0
10	.8
20	2.5
30	5.0
40	6.7
50	7.9
60	9.3
70	12.0
75	14.2
80	17.5
90	28.7
113	60.0

The table is entered using absolute value of wheel deflection. The direction of the wheel deflection is tested and the function value is returned with a positive value for right wing down and a negative value for left wing down. This accounts for the differential nature of roll control.

Speed Brakes/Ground Spoilers

δ_{SB} is speed brake deflection (symmetrical spoilers) from 0 to 60 degrees. The speed brakes move linearly with the speed brake control handle and produce 60 degrees of spoiler deflection for full control deflection.

- OR -

$\delta_{SB} = \delta_{SBC}\left(\frac{1}{.15+1}\right)$ with 150 degrees per second rate limit. If auto ground spoilers are armed and the main gear have spun up δ_{SBC} goes from 0 to 60.

It should be noted that all of the control surfaces mentioned above have some associated lags in the actual aircraft system. These lags are of the order of .1 to .3 of a second. These lags were not implemented in the ground handling simulation. It is felt that this omission does not significantly alter the overall fidelity of the simulation.

Horizontal Stabilizer Input

i_H is the angle of incidence of the horizontal stabilizer in degrees. i_H is limited to the range of 12 degrees trailing edge up and 1.5 degrees trailing edge down.

For the ground handling simulation i_H was controlled by a thumb switch on the left side of the wheel. Pushing the switch down caused i_H to move trailing edge up and pushing the switch up caused it to move in the opposite direction. The rate of i_H movement was 1/3 of a degree per second in both directions. The maximum displacement of i_H was limited to 12 degrees trailing edge up and 1.5 degrees trailing edge down represented as -12 and + 1.5 degrees.

Flap Input

δ_f is the flap angle in degrees. δ_f is limited to the range of 0 to 50 degrees trailing edge down.

Only two flap positions were used during the ground handling study and the flap positions remained fixed during the runs. These two positions, 15 degrees and 50 degrees, represented nominal takeoff and landing configurations respectively.

If the flap handle had been changed during the runs δ_f would have moved toward the new commanded position at a rate of 2.2 degrees per second.

Landing Gear Position Input

K_{gear} represents the landing gear position

K_{gear} = 0 is gear up
K_{gear} = 1 is gear down

The gear was always down for the ground handling simulation.

SYMBOLE TABLE AERODYNAMIC SECTION

TABLE 2.1

ALGEBRAIC SYMBOL	COMPUTER SYMBOL	DESCRIPTION	UNITS
$(C_{L_{TO}})^{R}_{STATIC}$	CLTOR1	STATIC COEF. OF LIFT WITH TAIL OFF AND RIGID BODY	UNITLESS
$C_L(\alpha, \delta_f)$	CL1	CONTRIBUTION OF ANGEL OF ATTACK AND FLAPS TO STATIC LIFT	"
$\Delta C_{L_{GE}}(\alpha, \delta_f)$	DCL1GE	CONTRIBUTION OF GND. EFFECTS TO STATIC LIFT	"
K_{GE}	XKGE	GND. EFFECT FACTOR, FUNCTION OF GEAR ALT. (h_{WHEEL})	"
$\Delta C_{L_{GR}}$	—	CONTRIBUTION OF LANDING GEAR TO STATIC LIFT	"
K_{gear}	XKGEAR	FACTOR WHICH REPRESENTS GEAR POSITION (UP=0, DN=1)	"
$\Delta C_{L_{TO}}^{E}$	DCLTOE	INCREMENT TO ACCOUNT FOR STRUCTURAL ELASTISITY	"
$C_{L_\alpha}^{E/R}$	CLER	RATIO OF ELASTIC TO RIGID COEF. OF LIFT	"
q	Q	DYNAMIC PRESSURE	lbs/ft^2
N_Z	ANZ	NORMAL (VERTICAL) ACCELERATION	g's

SYMBOL TABLE AERODYNAMIC SECTION TABLE 2.1 (CONT.)

ALGEBRAIC SYMBOL	PROGRAM SYMBOL	DESCRIPTION	UNITS
$C_{L_{TO}}^{E}$	CLTOE	COEF. OF LIFE WITH TAIL OFF INCLUDING ELASTICITY	UNITLESS
$C_{L_{q_{TO}}}$	CLQTO	COEF. OF LIFE DUE TO PITCH RATE	"
q_B	QB	PITCH RATE (SEE EOM SECTION)	DEG/SEC.
$C_{L_{\dot{\alpha}_{TO}}}$	CLADTO	COEF. OF LIFE DUE TO ANGLE OF ATTACK RATE	UNITLESS
$\dot{\alpha}$	ALFD	ANGLE OF ATTACK RATE (SEE EOM SECTION)	DEG/SEC
C_W	CW	WING MEAN AERODYNAMIC CHORD (MAC)	FT.
V	VT	AIRCRAFT TOTAL VELOCITY (SEE EOM SECTION)	FT/SEC.
δ_f	FLAP	FLAP ANGLE FULL EXTEND 50°, UP 0°	DEG.
C_{T_1}	—	COEF. OF LIFT DUE TO THRUST	UNITLESS
T	THT	THRUST (SEE ENGINE SECTION)	LBS.
S_W	SW	WING AREA	FT^2
C_{Z_S}	CZS	COEF. OF LIFT FORCE IN STABILITY AXIS	UNITLESS
$C_L(\delta_{SP})$	CLGSP	COEF. OF LIFT DUE TO GND. SPOILERS	"

SYMBOL TABLE AERODYNAMIC SECTION

TABLE 2.1 (CONT.)

ALGEBRAIC SYMBOL	PROGRAM SYMBOL	DESCRIPTION	UNITS
$\left(C_{M_{TO}}\right)^{R}_{STATIC}$	CMTOR1	STATIC COEF. OF PITCHING MOMENT WITH TAIL OFF AND RIGID BODY	UNITLESS
$C_{m_1}(\alpha, \delta_f)$	CM1	CONTRIBUTION OF ALPHA AND FLAP TO STATIC PITCHING MOMENT	"
$\Delta C_{M_{GE}}(\alpha, \delta_f)$	DCM1GE	CONTRIBUTION OF GND EFFECTS TO STATIC PITCHING MOMENT	"
$\Delta C_{M_{GR}}$	–	CONTRIBUTION OF GEAR TO STATIC PITCHING MOMENT	"
$\Delta C^{E}_{M_{TO}}$	DCMTOE	INCREMENT TO PITCHING MOMENT DUE STRUCTURAL ELASTICITY	"
$C^{E}_{M_{TO}}$	CMTOE	COEF. OF PITCHING MOMENT INCLUDING ELASTIC EFFECTS	"
$f(XCG)$	FXCG	NORMALIZED DISTANCE BETWEEN C.G. AND CENTER OF LIFT	FT.
$C_{m_{q_{TO}}}$	CMQTO	COEF. OF PITCHING MOMENT DUE TO PITCH RATE	UNITLESS
$C_{m_{\dot{\alpha}_{TO}}}$	CMADTO	COEF. OF PITCHING MOMENT DUE TO ANGLE OF ATTACK RATE	UNITLESS
ϵ	EP	HORIZONTAL STABILIZER DOWN WASH ANGLE	DEG.
$\epsilon_1(\alpha, \delta_f)$	EP1	CONTRIBUTION TO ϵ DUE TO ALPHA AND FLAPS	DEG.
$\Delta\epsilon_{1_{GE}}(\alpha, \delta_f)$	DEP1GE	DOWN WASH INCREMENT DUE GND. EFFECTS	DEG.

SYMBOL TABLE AERODYNAMIC SECTION

TABLE 2.1 (CONT.)

ALGEBRAIC SYMBOL	PROGRAM SYMBOL	DESCRIPTION	UNITS
α_H	AX	HORIZONTAL STABILIZER ANGLE OF ATTACK	DEG.
i_H	XIH	HORIZONTAL STABILIZER ANGLE OF INCEDENCE	DEG.
F_H	FH	FUESLAGE BENDING FACTOR (VERTICAL PLANE)	UNITLESS
$C_{L_{\alpha_H}}^{E/R}$	CLHER	FACTOR WHICH TAKES INTO ACCOUNT THE EFFECT OF STRUCTURAL ELASTICITY	UNITLESS
$C_{L_{H}}$	CLH	COEF. OF LIFT FOR HOR. STABILIZER	"
$C_{L_{\alpha_H}}$	CLAH	COEF. OF LIFT OF HOR. STAB. FOR α_H	UNITLESS
$(C_{L_q})_H$	CLQH	COEF. OF LIFT OF HOR. STAB. FOR q_B	"
$(C_{L_{\dot\alpha}})_H$	CLADH	COEF. OF LIFT OF HOR. STAB. FOR $\dot\alpha$	"
$C_{L_{\delta_e}}$	CLDE	COEF. OF LIFT OF HOR. STAB. FOR δ_e	"
δ_e	DE	ELEVATOR ANGLE	DEG.
C_{M_H}	CMH	COEF. OF PITCHING MOMENT DUE HOR. STAB.	UNITLESS
l_{HCG}	XLH	DISTANCE FROM C.G. TO HOR. STAB.	FT.

SYMBOL TABLE AERODYNAMIC SECTION

TABLE 2.1 (CONT.)

ALGEBRAIC SYMBOL	PROGRAM SYMBOL	DESCRIPTION	UNITS
C_{MS}	CMS	COEF. OF PITCHING MOMENT FOR STABILITY AXIS	UNITLESS
$\Delta C_M(\delta_{SP})$	CMGSP	INCREMENT OF PITCHING MOMENT COEF. DUE TO GND SPOILERS	"
$\Delta C_{D_{GR}}$	CDIGR	INCREMENT OF DRAG COEF. DUE TO LANDING GEAR	"
$\Delta C_{D_{gr_0}}$	CDIGRO	INTERCEPT POINT OF LINEAR FUNCTION	"
$\Delta C_{D_{gr_1}}$	CDIGR1	SLOPE OF LINEAR FUNCTION	"
$C_{D_{iGE}}$	CDIGE	COEF. OF INDUCED DRAG DUE TO GND. EFFECTS	"
C_D	CD	COEF. OF DRAG	"
$C_{D_p}(\alpha, \delta_f)$	CDO	COEF. OF PARASITIC DRAG	"
$C_{D_i}(\alpha, \delta_f)$	CDI	COEF. OF INDUCED DRAG	"
$\Delta C_D(\delta_{sp})$	CDGSP	INCREMENT OF DRAG COEF. DUE TO GND SPOILERS	"
C_{XS}	CXS	COEF. OF DRAG IN STABILITY AXIS	"

SYMBOL TABLE AERODYNAMIC SECTION

TABLE 2.1 (CONT.)

ALGEBRAIC SYMBOL	PROGRAM SYMBOL	DESCRIPTION	UNITS
C_{XB}	CXB	COEF. OF DRAG BODY AXIS	UNITLESS
C_{ZB}	CZB	COEF. OF LIFT BODY AXIS	"
C_{mB}	CMS	COEF. OF PITCHING MOMENT BODY AXIS	"
F_V	FV	FUSELAGE BENDING LATERAL PLANE	UNITLESS
$C_{l_{\beta_{TO}}}$	CLBTO	COEF. OF ROLLING MOMENT (TAIL OFF) DUE TO SIDE SLIP ANGLE (BETA)	UNITLESS
$C_{l_{\beta_1}}$	CLB1	INTERCEPT POINT FUNCTION OF ANGLE OF ATTACK AND FLAP ANGLE	UNITLESS
$C_{l_{\beta_2}}$	CLB2		UNITLESS
$C_{l_p}^{E/R}$	CLPER	RATIO OF RIGID TO ELASTIC FORCE FOR THE EFFECT OF ROLL RATE ON THE COEF. OF ROLLING MOMENT	UNITLESS
$C_{l_{\delta_{SP}}}^{E/R}$	CLSPER	RIGID TO ELASTIC FACTOR FOR THE EFFECT OF SPOILERS	UNITLESS
$C_{l_{\delta_a}}^{E/R}$	DAER	RIGID TO ELASTIC FACTOR FOR THE EFFECT OF AILERON'S	UNITLESS
$C_{l_{r_{TO}}}$	CLRTO	COEF. OF ROLLING MOMENT DUE TO YAW RATE	"
$C_{l_{TOS}}$	CLTOS	COEF. OF ROLLING MOMENT IN STABILITY AXIS WITH TAIL OFF	"

SYMBOL TABLE AERODYNAMIC SECTION

TABLE 2.1 (CONT.)

ALGEBRAIC SYMBOL	PROGRAM SYMBOL	DESCRIPTION	UNITS
$C_{\ell_{\beta_{TO}}}$	CLBTO	COEF. OF ROLLING MOMENT DUE TO SIDE SLIP ANGLE	UNITLESS
$C_{\ell_{\dot{p}}}$	CLPD	COEF. OF ROLLING MOMENT DUE TO ROLLING ACCELERATION	UNITLESS
$C_{\ell_{p_{TO}}}$	CLPTO	COEF. OF ROLLING MOMENT DUE TO ROLL RATE	"
b_w	BW	WING SPAN	FT.
$C_{\ell_{\delta_a}}$	CLDA	COEF. OF ROLLING MOMENT DUE TO AILERON DEFLECTION	UNITLESS
$C_\ell\ (\alpha, \delta_{sp}, \delta_f)$	CLSP	COEF. OF ROLLING MOMENT DUE TO SPOILER DEFLECTION, ANGLE OF ATTACK, AND FLAP	"
$C_{y_{\beta_{TO}}}$	CYBTO	COEF. OF SIDE FORCE DUE TO ANGLE OF SIDE SLIP, TAIL OFF	"
$C_{y_{p_{TO}}}$	CYPTO	COEF. OF SIDE FORCE DUE TO ROLL RATE	"
$C_{y_{\delta_a}}$	CYDA	COEF. OF SIDE FORCE DUE TO AILERON DEFLECTION	"
$C_{y_{\delta_{sp}}}$	CYDSP	COEF. OR SIDE FORCE DUE TO SPOILER DEFLECTION	"
$C_{y_{TO}}$	CYTO	COEF. OF SIDE FORCE WITH TAIL OFF	"
β	BET	SIDE SLIP ANGLE (BETA)	DEG.
p_s	PS	ROLL RATE STABILITY AXIS	DEG/SEC

SYMBOL TABLE AERODYNAMIC SECTION

TABLE 2.1 (CONT.)

ALGEBRAIC SYMBOL	PROGRAM SYMBOL	DESCRIPTION	UNITS
$C_{L_{\alpha_V}}^{E/R}$	CLAVER	ELASTIC TO RIGID RATIO FOR "	
$C_{y_{\dot{\beta}}}$	CYBD	COEF. OF SIDE FORCE DUE TO SIDE SLIP ANGLE RATE	UNITLESS
$C_{y_{\dot{p}_V}}$	CYPDV	COEF. OF SIDE FORCE AT THE VERTICAL TAIL DUE TO ROLL ACCELERATION	"
$C_{y_{\beta_V}}$	CYBV	COEF. OF SIDE FORCE AT THE VERTICAL TAIL DUE TO SIDE SLIP ANGLE	"
$C_{y_{p_V}}$	CYPV	COEF. OF SIDE FORCE AT THE VERTICAL TAIL DUE TO ROLL RATE	"
$C_{y_{r_V}}$	CYRV	COEF. OF SIDE FORCE AT THE VERTICAL TAIL DUE TO YAW RATE	"
$C_{y_{\dot{r}}}$	CYRD	COEF. OF SIDE FORCE DUE TO YAW ACCELERATION	UNITLESS
$C_{y_{N_Y}}$	CYNY	COEF. OF SIDE FORCE DUE TO LATERAL ACCELERATION	"
C_{y_V}	CYV	COEF. OF SIDE FORCE ON VERTICAL TAIL	UNITLESS
$C_{y_{\delta_r}}^{E/R}$	DRER	ELASTIC TO RIGID RATIO FOR EFFECT OF RUDDER ON SIDE LOAD	"
$C_{y_{\delta_r}}$	CYDR	COEF. OF SIDE LOAD DUE TO RUDDER	"
$C_y(\delta_r)$	CYRU	TOTAL COEF. OF SIDE LOAD DUE TO RUDDER	"

SYMBOL TABLE AERODYNAMIC SECTION

TABLE 2.1 (CONT.)

ALGEBRAIC SYMBOL	PROGRAM SYMBOL	DESCRIPTION	UNITS
$C_{n_{p_{TO}}}$	CNPTO	COEF. OF YAWING MOMENT DUE TO ROLL RATE	UNITLESS
$C_{n_{r_{TO}}}$	CNRTO	COEF. OF YAWING MOMENT DUE TO YAW RATE	"
$C_{n_{\delta_a}}$	CNDA	COEF. OF YAWING MOMENT DUE AILERON DEFLECTION	"
$C_{n_{TOS}}$	CNTOS	TOTAL COEF. OF YAWING MOMENT FOR TAIL OFF STABILITY AXIS	"
$C_{n_{\beta_{TO}}}(\alpha, \delta_f)$	CNBTO	COEF. OF YAWING MOMENT DUE SIDE SLIP ANGLE FUNCTION OF ANGLE OF ATTACK AND FLAP ANGLE	"
$C_n(\alpha, \delta_{SP}, \delta_f)$	CNSP	COEF. OF YAWING MOMENT DUE TO SPOILER DEFLECTION ALSO FUNCTION OF ANGLE OF ATTACK AND FLAP ANGLE	"
p_s	PS	ROLL RATE STABILITY AXIS	DEG/SEC.
r_s	RS	YAW RATE STABILITY AXIS	"
C_{l_B}	CLB	TOTAL COEF. OF ROLLING MOMENT FOR BODY AXIS	UNITLESS
d_{vcg}	ZVCG	VERTICAL DISTANCE FROM C.G. TO AERO CENTER OF VERTICAL STABILIZER	FT.
d_{vcg_r}	ZVCGU	VERTICAL DISTANCE FROM C.G. TO AERO CENTER OF RUDDER SURFACE	FT.

SYMBOL TABLE AERODYNAMIC SECTION

TABLE 2.1 (CONT.)

ALGEBRIC SYMBOL	PROGRAM SYMBOL	DESCRIPTION	UNITS
C_{y_B}	CYB	TOTAL COEF. OF SIDE FORCE IN BODY AXIS	UNITLESS
C_{n_B}	CNB	TOTAL COEF. OF YAWING MOMENT IN BODY AXIS	"
ℓ_{vcg}	XVCG	LONGITUDINAL DISTANCE FROM C.G. TO VERTICAL STABILIZER	FT.
ℓ_{vcgr}	XVCGU	LONGITUDINAL DISTANCE FROM C.G. TO RUDDER SURFACE	"
ℓ_{xcg}	FXCG2	LONGITUDINAL DISTANCE FROM C.G. AT 25% MAC TO ACTUAL C.G. (TERM IS ZERO FOR C.G. AT 25% MAC)	"
δ_{SP}	DSP	SPOILER DEFLECTION DUE TO WHEEL MOTION	DEG
δ_{SB}	DSB	SPOILER DEFLECTION DUE TO SPEED BRAKE HANDLE	DEG

EQUATIONS AERODYNAMIC SECTION

FIG. 2.1

LONGITUDINAL AERO FORCE COEFFICIENTS

COEFFICIENT OF LIFT (TAIL OFF WITH ELASTIC CORRECTIONS)

$$C_{L_{TO}}^{E} = \left(C_{L_{TO}}\right)^{R}_{STATIC} + \Delta C_{L_{TO}}^{E} + \left[\left(C_{L_q}\right)_{TO} q_B + \left(C_{L_{\dot{\alpha}}}\right)_{TO} \dot{\alpha}\right] c_w/2V + \frac{\partial C_L}{\partial C_T}(\delta_f)\, C_T$$

WHERE:

$$\left(C_{L_{TO}}\right)^{R}_{STATIC} = C_L(\alpha, \delta_f) + \Delta C_{L_{GE}}(\alpha, \delta_f)\, K_{GE} + \Delta C_{L_{GR}}\, K_{gear}$$

$$\Delta C_{L_{TO}}^{E} = -\left(C_{L_{TO}}\right)^{R}_{STATIC}\left(1 - C_{L_\alpha}^{E/R}\right) + \left(C_{L_n}\right)^{E}_{TO} N_z$$

$$C_T = T/qS_w \qquad \frac{\partial C_L}{\partial C_T}(\delta_f) = .36 - .001\,\delta_f$$

$$C_{L_\alpha}^{E/R} = 1 - .00034\, q$$

$K_{GE} = f(h_{WHEEL})$ (SEE TABLE 2.4)

EQUATIONS AERODYNAMIC SECTION

FIG. 2.2

LONGITUDINAL AERO FORCE COEFFICIENTS

COEFFICIENT OF PITCHING MOMENT (TAIL OFF WITH ELASTIC CORRECTIONS)

$$C_{m_{TO}}^{E} = \left(C_{m_{TO}}\right)_{STATIC}^{R} + \Delta C_{m_{TO}}^{E} + C_{L_{TO}}^{E} f(X_{cG}) + \left[C_{m_{q_{TO}}} q_B + C_{m_{\dot{\alpha}_{TO}}} \dot{\alpha}\right] c_w/2V$$

WHERE:

$$\left(C_{m_{TO}}\right)_{STATIC}^{R} = C_m(\alpha, \delta_f) + \Delta C_{m_{GE}}(\alpha, \delta_f) K_{GE} + \Delta C_{m_{GR}} K_{gear}$$

$$\Delta C_{m_{TO}}^{E} = \left(\Delta C_{m_0}\right)_{TO}^{E} q + \left(\frac{\partial C_m}{\partial C_L}\right)_{TO}^{E} q\, C_{L_{TO}}^{E} - \left(C_{m_n}\right)_{TO}^{E} N_z$$

$$f(X_{cG}) = .25 - X_{cG}$$ ($X_{cG} = .25$ FOR THE GND HANDLING STUDY)

$$K_{GE} = f(h_{WHEEL})$$ (SEE TABLE 2.4)

EQUATIONS AERODYNAMIC SECTION

FIG. 2.3

LONGITUDINAL AERO CONSTANTS

LIFT:

$(C_{L_q})_{TO} = .104$ REF: (DC9-A14.59, P.55)

$(C_{L_{\dot{\alpha}}})_{TO} = .012$ ″

$\Delta C_{L_{GR}} = .026$

$(C_{L_n})^{E}_{TO} = .01$ (DC9-A5-185, P.200)

PITCHING MOMENT:

$C_{m_{q_{TO}}} = -.087$ (DC9-A14.60A, P.56) $(C_{m_n})^{E}_{TO} = .003$ (DC9-A5-185, P.200)

$C_{m_{\dot{\alpha}_{TO}}} = -.017$ ″ $\Delta C_{m_{GR}} = 0$

$(\Delta C_{m_0})^{E}_{TO} = .00001$ (DC9-A5-184, P.199)

$\left(\frac{\partial C_m}{\partial C_L}\right)^{E}_{TO} = .000077$ ″

FIG. 2.4

LONGITUDINAL AERO COEFFICIENTS

HORIZONTAL STABILIZER (LIFT)

$$C_{L_H} = F_H \Big[\alpha_H \, C_{L_{\alpha_H}} C_{L_{\alpha_H}}^{E/R} + (C_{L_n})_H^E \, N_Z + C_{L_{\delta_e}} C_{L_{\delta_e}}^{E/R} \, \delta_e$$

$$+ C_{L_{\alpha_H}}^{E/R} \Big((C_{L_q})_H \, q_B + (C_{L_{\dot\alpha}})_H \, \dot\alpha \Big) \, c_w / 2V \Big]$$

WHERE:

$F_H = 1 - .00067\, \bar{q}$ REF: (DC9-C4.776, P. 203)

$\alpha_H = \alpha - \epsilon + i_H$

$\epsilon = \epsilon_1(\alpha, \delta_f) + \Delta\epsilon_{GE}(\alpha, \delta_f)\, K_{GE} + \Delta\epsilon(\delta_{SB})$

$C_{L_{\alpha_H}}^{E/R} = 1 - .00035\, \bar{q}$ (DC9-C4.880, P. 204)

$C_{L_{\delta_e}}^{E/R} = 1 - .0007\, \bar{q}$ (DC9-C4.775, P. 205)

EQUATIONS AERODYNAMIC SECTION

FIG. 2.5

LONGITUDINAL AERO COEFFICIENTS

HORIZONTAL STABILIZER (PITCHING MOMENT)

$$C_{m_H} = - C_{L_H} \, l_{HCG}$$

WHERE:

$$l_{HCG} = l_{H\bar{c}/4} + (.25 - x_{cg})$$

TOTAL PITCHING MOMENT COEFFICIENT

$$C_{m_S} = C_{m_{TO}}^{E} + C_{m_H} + \Delta C_m (\delta_{SB})$$

TOTAL LIFT COEFFICIENT

$$C_{Z_S} = -\left(C_{L_{TO}}^{E} + C_{L_H}\right) - \Delta C_L (\delta_{SB})$$

FIG. 2.6

LONGITUDINAL AERO CONSTANTS

HORIZONTAL STABILIZER:

$C_{L_{\alpha_H}} = .0169$ REF: (DC9-C4.964, P.41)

$(C_{L_\eta})_H^E = .0035$ (DC9-C4-449, P.202)

$C_{L_{\delta_e}} = .00932$ (DC9-C4.964, P.41)

$(C_{L_q})_H = .138$ (DC9-A14-59, P.55)

$(C_{L_{\dot\alpha}})_H = .046$ "

$l_{H c/4} = X_{H,CG}/c_w = 3.969$

GENERAL CONSTANTS:

$b_w = 89.35$ ft.

$c_w = 11.79$ ft.

$S_w = 934.3$ ft.^{2}

FIG. 2.7

LONGITUDINAL AERO COEFFICIENTS

COEFFICIENT OF DRAG

$$C_D = C_{D_p}(\delta_f) + C_{D_{iGE}}(C_{Z_S})^2\, C_{D_i}(\delta_f) + \Delta C_{D_{GR}}\, K_{gear} + \Delta C_D(\delta_{SB})$$

WHERE:

$$C_{D_{iGE}} = 1 - e^{\left[-2.48(2\,h_{cg}/b_w)^{.768}\right]}$$

$$\Delta C_{D_{GR}} = .0249 - .0002732\,\delta_f$$

TOTAL DRAG COEFFICIENT

$$C_{X_S} = -C_D$$

FUNCTION TABLE AERODYNAMIC SECTION

TABLE 2.2

FUNCTION : $C_{D_i}(\delta_f)$

δ_f	$C_{D_i}(\delta_f)$	δ_f	$C_{D_i}(\delta_f)$
0	.04914	30	.04430
5	.04650	35	.04401
10	.04564	40	.04371
15	.04535	45	.04349
20	.04504	50	.04322
25	.04470		

REF : (A-4 7149-4-63)

FUNCTION TABLE AERODYNAMIC SECTION

TABLE 2.3

FUNCTION: $C_{D_P}(\delta_f)$

δ_f	$C_{D_P}(\delta_f)$	δ_f	$C_{D_P}(\delta_f)$
0	.0217	30	.0677
5	.0252	35	.0810
10	.0300	40	.0970
15	.0360	45	.1160
20	.0447	50	.1391
25	.0550		

REF: (A-4 7149-4-63)

FUNCTION TABLE AERODYNAMIC SECTION

FUNCTION: K_{GE} (h_{WHEEL})   TABLE 2.4

h_{WHEEL}	K_{GE}	h_{WHEEL}	K_{GE}	h_{WHEEL}	K_{GE}
0	1.0	25	.13	50	.01
5	.61	30	.09	55	.008
10	.39	35	.06	60	.007
15	.26	40	.04	65	.004
20	.185	45	.015	70	0

REF: DC9 - A28

THESE FUNCTIONS HAVE BEEN LINEARIZED

$$\Delta \epsilon (\delta_{SB}) = 0.0$$

$$\Delta C_m (\delta_{SB}) = -.00203 \, \delta_{SB}$$

$$\Delta C_L (\delta_{SB}) = -.01063 \, \delta_{SB}$$

$$\Delta C_D (\delta_{SB}) = .00198 \, \delta_{SB}$$

FLAP = .00

ALF	CL	CL GE	CM	CM GE	EP	EP GE
-4.00000	-.19000	-.15000	-.08085	-.02203	.38000	1.00000
-3.00000	-.10250	-.04625	-.07954	-.02208	.68500	1.15000
-2.00000	-.01500	.05750	-.07823	-.02213	.99000	1.30000
-1.00000	.07250	.16125	-.07691	-.02218	1.29500	1.45000
.00000	.16000	.26500	-.07560	-.02274	1.60000	1.60000
1.00000	.25040	.37000	-.07424	-.02361	1.93000	1.74286
2.00000	.34080	.47500	-.07289	-.02448	2.26000	1.88571
3.00000	.43120	.57500	-.07114	-.02531	2.59000	2.02857
4.00000	.52160	.67500	-.06866	-.02614	2.92000	2.17143
5.00000	.61200	.77000	-.06617	-.02692	3.25000	2.31429
6.00000	.70240	.86500	-.06368	-.02771	3.58000	2.45710
7.00000	.79280	.95750	-.06120	-.02786	3.91000	2.60000
8.00000	.88320	1.05000	-.05767	-.02763	4.24000	2.74290
9.00000	.97360	1.13000	-.05406	-.02795	4.57000	2.88570
10.00000	1.06400	1.21000	-.04916	-.02940	4.90000	3.02860
11.00000	1.15500	1.27750	-.04370	-.03210	5.25000	3.17140
12.00000	1.24600	1.34500	-.03755	-.03615	5.60000	3.31430
13.00000	1.32000	1.18333	-.03200	-.02875	6.00000	3.45710
14.00000	1.37500	1.02167	-.02787	-.02770	6.40000	3.60000
15.00000	1.41800	.86000	-.02600	-.02767	6.85000	3.60000
16.00000	1.43000	.86000	-.02600	-.02767	7.30000	3.60000
17.00000	1.33750	.86000	-.03069	-.02767	7.30000	3.60000
18.00000	1.24500	.86000	-.03762	-.02767	7.30000	3.60000
19.00000	1.15250	.86000	-.04385	-.02767	7.30000	3.60000
20.00000	1.06000	.86000	-.04940	-.02767	7.30000	3.60000

DELT CL GEAR = .00000 DELT CM GEAR = .00000

THIS TABLE CONTAINS THE FOLLOWING FUNCTIONS:

$C_L(\alpha, \delta_f)$, $\Delta C_{LGE}(\alpha, \delta_f)$, $C_M(\alpha, \delta_f)$, $\Delta C_{MGE}(\alpha, \delta_f)$

$\epsilon_1(\alpha, \delta_f)$, $\Delta \epsilon_{GE}(\alpha, \delta_f)$

TABLE 2.5

FLAP = 5.00

ALF	CL	CL GE	CM	CM GE	EP	EP GE
-4.00000	-.07500	.00000	-.10150	-.07307	.56000	1.25000
-3.00000	.01375	.10187	-.10145	-.07304	.90125	1.38750
-2.00000	.10250	.20375	-.10112	-.07104	1.24250	1.52500
-1.00000	.19125	.30563	-.10078	-.06942	1.58370	1.66245
.00000	.28000	.40750	-.10045	-.06781	1.92500	1.80000
1.00000	.37020	.51000	-.10011	-.06618	2.28500	1.93482
2.00000	.46040	.61250	-.09902	-.06456	2.64500	2.06964
3.00000	.55060	.70625	-.09755	-.06311	3.00500	2.20446
4.00000	.64080	.80000	-.09588	-.06225	3.36500	2.33930
5.00000	.73100	.89000	-.09397	-.06143	3.72500	2.47410
6.00000	.82120	.98000	-.09176	-.06017	4.08500	2.60890
7.00000	.91140	1.06625	-.08860	-.05913	4.44500	2.74380
8.00000	1.00160	1.15250	-.08542	-.05862	4.80500	2.87860
9.00000	1.09180	1.22875	-.08114	-.05857	5.16340	3.01340
10.00000	1.18200	1.30500	-.07686	-.05884	5.52190	3.14820
11.00000	1.27250	1.37375	-.07165	-.06004	5.89530	3.28300
12.00000	1.35800	1.44250	-.06652	-.06050	6.26880	3.41790
13.00000	1.43500	1.27167	-.06400	-.05868	6.67970	3.55270
14.00000	1.49750	1.10083	-.06400	-.05875	7.09060	3.68750
15.00000	1.55400	.93000	-.06400	-.06090	7.53910	3.68750
16.00000	1.51800	.93000	-.06400	-.06090	7.98750	3.68750
17.00000	1.42970	.92995	-.06400	-.06090	7.98750	3.68750
18.00000	1.34150	.93000	-.06751	-.06090	7.98750	3.68750
19.00000	1.25330	.93005	-.07280	-.06090	7.98750	3.68750
20.00000	1.16500	.93000	-.07766	-.06089	7.98750	3.68750

DELT CL GEAR = .00000 DELT CM GEAR = .00000

TABLE 2.5 (CONT.)

FLAP = 10.00

ALF	CL	CL GE	CM	CM GE	EP	EP GE
-4.00000	.04000	.15000	-.12530	-.12200	.74000	1.50000
-3.00000	.13000	.25000	-.12597	-.11799	1.11750	1.62500
-2.00000	.22000	.35000	-.12665	-.11400	1.49500	1.75000
-1.00000	.31000	.45000	-.12732	-.10999	1.87250	1.87500
.00000	.40000	.55000	-.12800	-.10600	2.25000	2.00000
1.00000	.49000	.65000	-.12755	-.10200	2.64000	2.12679
2.00000	.58000	.75000	-.12710	-.09867	3.03000	2.25357
3.00000	.67000	.83750	-.12595	-.09633	3.42000	2.38040
4.00000	.76000	.92500	-.12460	-.09400	3.81000	2.50710
5.00000	.85000	1.01000	-.12250	-.09180	4.20000	2.63390
6.00000	.94000	1.09500	-.11980	-.09010	4.59000	2.76070
7.00000	1.03000	1.17500	-.11695	-.08850	4.98000	2.88750
8.00000	1.12000	1.25500	-.11380	-.08607	5.37000	3.01430
9.00000	1.21000	1.32750	-.11055	-.08354	5.75690	3.14110
10.00000	1.30000	1.40000	-.10650	-.08100	6.14370	3.26780
11.00000	1.39000	1.47000	-.10245	-.08217	6.54060	3.39460
12.00000	1.47000	1.54000	-.09780	-.08300	6.93750	3.52140
13.00000	1.55000	1.36000	-.09300	-.08240	7.35940	3.64820
14.00000	1.62000	1.18000	-.08840	-.08840	7.78120	3.77500
15.00000	1.69000	1.00000	-.08280	-.09200	8.22810	3.77500
16.00000	1.60600	1.00000	-.08952	-.09200	8.67500	3.77500
17.00000	1.52200	1.00000	-.09468	-.09200	8.67500	3.77500
18.00000	1.43800	1.00000	-.09972	-.09200	8.67500	3.77500
19.00000	1.35400	1.00000	-.10407	-.09200	8.67500	3.77500
20.00000	1.27000	1.00000	-.10785	-.09200	8.67500	3.77500

DELT CL GEAR = .00000 DELT CM GEAR = .00000

TABLE 2.5 (CONT.)

FLAP = 15.00

ALF	CL	CL GE	CM	CM GE	EP	EP GE
-4.00000	.18500	.30500	-.16225	-.16450	.92000	1.75000
-3.00000	.27525	.40313	-.16441	-.16435	1.33370	1.86245
-2.00000	.36550	.50125	-.16701	-.15977	1.74750	1.97500
-1.00000	.45575	.59938	-.16870	-.15518	2.16120	2.08745
.00000	.54600	.69750	-.16936	-.15059	2.57500	2.20000
1.00000	.63625	.79250	-.16932	-.14677	2.99500	2.31875
2.00000	.72650	.88750	-.16887	-.14296	3.41500	2.43750
3.00000	.81675	.97150	-.16816	-.13959	3.83500	2.55630
4.00000	.90700	1.05550	-.16636	-.13641	4.25500	2.67500
5.00000	.99725	1.13525	-.16455	-.13348	4.67500	2.79380
6.00000	1.08750	1.21500	-.16187	-.13043	5.09500	2.91250
7.00000	1.17750	1.29125	-.15917	-.12706	5.51500	3.03130
8.00000	1.26750	1.36750	-.15574	-.12368	5.93500	3.15000
9.00000	1.35750	1.43500	-.15207	-.12105	6.35030	3.26870
10.00000	1.44750	1.50250	-.14804	-.11876	6.76560	3.38750
11.00000	1.53630	1.57005	-.14351	-.11820	7.18590	3.50620
12.00000	1.62000	1.53125	-.13870	-.11820	7.60620	3.62490
13.00000	1.69500	1.36750	-.13383	-.12369	8.03910	3.74380
14.00000	1.76000	1.20375	-.13350	-.13093	8.47190	3.86250
15.00000	1.75330	1.03997	-.13350	-.13698	8.91720	3.86250
16.00000	1.66970	1.04003	-.13547	-.13698	9.36250	3.86250
17.00000	1.58600	1.04000	-.14077	-.13698	9.36250	3.86250
18.00000	1.50230	1.03997	-.14537	-.13698	9.36250	3.86250
19.00000	1.41870	1.04003	-.14943	-.13698	9.36250	3.86250
20.00000	1.33500	1.04000	-.15299	-.13698	9.36250	3.86250

DELT CL GEAR = .00000 DELT CM GEAR = .00000

TABLE 2.5 (CONT.)

FLAP = 20.00

ALF	CL	CL GE	CM	CM GE	EP	EP GE
-4.00000	.33000	.46000	-.20450	-.21379	1.10000	2.00000
-3.00000	.42050	.55625	-.20862	-.20865	1.55000	2.10000
-2.00000	.51100	.65250	-.21111	-.20349	2.00000	2.20000
-1.00000	.60150	.74875	-.21201	-.19834	2.45000	2.30000
.00000	.69200	.84500	-.21246	-.19319	2.90000	2.40000
1.00000	.78250	.93500	-.21291	-.18837	3.35000	2.51071
2.00000	.87300	1.02500	-.21227	-.18356	3.80000	2.62140
3.00000	.96350	1.10550	-.21136	-.17925	4.25000	2.73210
4.00000	1.05400	1.18600	-.20965	-.17495	4.70000	2.84290
5.00000	1.14450	1.26050	-.20739	-.17097	5.15000	2.95360
6.00000	1.23500	1.33500	-.20472	-.16698	5.60000	3.06430
7.00000	1.32500	1.40750	-.20142	-.16287	6.05000	3.17500
8.00000	1.41500	1.48000	-.19812	-.15670	6.50000	3.28570
9.00000	1.50500	1.54250	-.19475	-.15160	6.94370	3.39640
10.00000	1.59500	1.60500	-.19025	-.14685	7.38750	3.50710
11.00000	1.68250	1.67000	-.18587	-.14489	7.83120	3.61780
12.00000	1.77000	1.52250	-.17940	-.15320	8.27500	3.72860
13.00000	1.84000	1.37500	-.17380	-.16484	8.71880	3.83930
14.00000	1.90000	1.22750	-.16900	-.17273	9.16250	3.95000
15.00000	1.81670	1.08003	-.17567	-.18062	9.60620	3.95000
16.00000	1.73330	1.07997	-.18233	-.18062	10.05000	3.95000
17.00000	1.65000	1.08000	-.18750	-.18062	10.05000	3.95000
18.00000	1.56670	1.08003	-.19167	-.18062	10.05000	3.95000
19.00000	1.48330	1.07997	-.19561	-.18062	10.05000	3.95000
20.00000	1.40000	1.08000	-.19867	-.18062	10.05000	3.95000

DELT CL GEAR = .00000 DELT CM GEAR = .00000

TABLE 2.5 (CONT.)

FLAP = 25.00

ALF	CL	CL GE	CM	CM GE	EP	EP GE
-4.00000	.48000	.61000	-.24950	-.21329	1.31670	2.16670
-3.00000	.57050	.70063	-.24950	-.21329	1.77500	2.26667
-2.00000	.66100	.79125	-.25057	-.21329	2.23330	2.36663
-1.00000	.75150	.88187	-.25215	-.21329	2.69170	2.46670
.00000	.84200	.97250	-.25310	-.21329	3.15000	2.56667
1.00000	.93250	1.05750	-.25333	-.21329	3.61250	2.67321
2.00000	1.02300	1.14250	-.25315	-.21106	4.07500	2.77980
3.00000	1.11350	1.22025	-.25180	-.20700	4.53750	2.88630
4.00000	1.20400	1.29800	-.25039	-.20293	5.00000	2.99290
5.00000	1.29450	1.36900	-.24782	-.19920	5.46250	3.09940
6.00000	1.38500	1.44000	-.24526	-.19415	5.92500	3.20600
7.00000	1.47370	1.50745	-.24145	-.18838	6.38750	3.31250
8.00000	1.56250	1.57500	-.23697	-.18288	6.85000	3.41900
9.00000	1.65250	1.63500	-.23146	-.17923	7.30450	3.52560
10.00000	1.73500	1.69500	-.22536	-.17648	7.75900	3.63210
11.00000	1.81250	1.75000	-.21884	-.17625	8.21350	3.73860
12.00000	1.89000	1.58750	-.21167	-.18185	8.66810	3.84530
13.00000	1.95500	1.42500	-.21075	-.19544	9.12260	3.95180
14.00000	1.94290	1.26254	-.21075	-.20478	9.57710	4.05840
15.00000	1.85900	1.09995	-.21454	-.21329	9.57710	4.05840
16.00000	1.77520	1.09996	-.22204	-.21329	9.57710	4.05840
17.00000	1.69140	1.09997	-.22883	-.21329	9.57710	4.05840
18.00000	1.60760	1.09998	-.23449	-.21330	9.57710	4.05840
19.00000	1.52380	1.09999	-.23900	-.21329	9.57710	4.05840
20.00000	1.44000	1.10000	-.24300	-.21329	9.57710	4.05840

DELT CL GEAR = .00000 DELT CM GEAR = .00000

TABLE 2.5 (CONT.)

FLAP = 30.00

ALF	CL	CL GE	CM	CM GE	EP	EP GE
-4.00000	.63000	.76000	-.28790	-.24703	1.53330	2.33330
-3.00000	.72050	.84500	-.29061	-.24703	2.00000	2.43333
-2.00000	.81100	.93000	-.29316	-.24703	2.46670	2.53337
-1.00000	.90150	1.01500	-.29452	-.24703	2.93330	2.63330
.00000	.99200	1.10000	-.29588	-.24703	3.40000	2.73333
1.00000	1.08250	1.18000	-.29559	-.24294	3.87500	2.83570
2.00000	1.17300	1.26000	-.29513	-.23883	4.35000	2.93810
3.00000	1.26350	1.33500	-.29373	-.23500	4.82500	3.04050
4.00000	1.35400	1.41000	-.29192	-.23080	5.30000	3.14290
5.00000	1.44450	1.47750	-.28855	-.22495	5.77500	3.24520
6.00000	1.53500	1.54500	-.28357	-.21925	6.25000	3.34760
7.00000	1.62250	1.60750	-.27809	-.21421	6.72500	3.45000
8.00000	1.71000	1.67000	-.27065	-.21035	7.20000	3.55240
9.00000	1.80000	1.72750	-.26300	-.20850	7.66530	3.65480
10.00000	1.87500	1.78500	-.25512	-.20849	8.13060	3.75720
11.00000	1.94250	1.83000	-.24804	-.20850	8.59580	3.85950
12.00000	2.01000	1.65250	-.24071	-.21143	9.06110	3.96190
13.00000	2.07000	1.47500	-.23300	-.22517	9.52640	4.06430
14.00000	1.98570	1.29749	-.24350	-.23692	9.99170	4.16670
15.00000	1.90140	1.11997	-.25235	-.24601	9.99170	4.16670
16.00000	1.81710	1.11996	-.26120	-.24601	9.99170	4.16670
17.00000	1.73290	1.12004	-.26871	-.24601	9.99170	4.16670
18.00000	1.64860	1.12003	-.27587	-.24601	9.99170	4.16670
19.00000	1.56430	1.12001	-.28196	-.24600	9.99170	4.16670
20.00000	1.48000	1.12000	-.28660	-.24601	9.99170	4.16670

DELT CL GEAR = .00000 DELT CM GEAR = .00000

TABLE 2.5 (CONT.)

FLAP = 35.00

ALF	CL	CL GE	CM	CM GE	EP	EP GE
-4.00000	.73000	.86000	-.32400	-.28077	1.75000	2.50000
-3.00000	.82037	.94062	-.32400	-.28077	2.22500	2.60000
-2.00000	.91075	1.02125	-.32400	-.28077	2.70000	2.70000
-1.00000	1.00110	1.10185	-.32402	-.28068	3.17500	2.80000
.00000	1.09150	1.18250	-.32594	-.27664	3.65000	2.90000
1.00000	1.18190	1.25878	-.32705	-.27283	4.13750	2.99820
2.00000	1.27220	1.33495	-.32653	-.26901	4.62500	3.09640
3.00000	1.36260	1.40623	-.32531	-.26520	5.11250	3.19460
4.00000	1.45300	1.47750	-.32236	-.25896	5.60000	3.29290
5.00000	1.54340	1.54190	-.31830	-.25344	6.08750	3.39110
6.00000	1.63370	1.60620	-.31330	-.24801	6.57500	3.48930
7.00000	1.71900	1.66563	-.30712	-.24341	7.06250	3.58750
8.00000	1.80420	1.72495	-.30086	-.24075	7.55000	3.68570
9.00000	1.88890	1.78065	-.29314	-.24075	8.02600	3.78390
10.00000	1.96220	1.83370	-.28644	-.24075	8.50210	3.88220
11.00000	2.02940	1.82202	-.27973	-.24075	8.97810	3.98030
12.00000	2.06030	1.64340	-.27628	-.24513	9.45420	4.07860
13.00000	2.08560	1.46479	-.27520	-.26008	9.93020	4.17680
14.00000	2.00260	1.28611	-.28271	-.27145	10.40600	4.27480
15.00000	1.91970	1.10752	-.29033	-.28040	10.40600	4.27480
16.00000	1.83670	1.10745	-.29790	-.28040	10.40600	4.27480
17.00000	1.75380	1.10749	-.30460	-.28040	10.40600	4.27480
18.00000	1.67090	1.10753	-.31061	-.28040	10.40600	4.27480
19.00000	1.58790	1.10746	-.31629	-.28040	10.40600	4.27480
20.00000	1.50500	1.10750	-.32002	-.28039	10.40600	4.27480

DELT CL GEAR = .00000 DELT CM GEAR = .00000

TABLE 2.5 (CONT.)

FLAP = 40.00

ALF	CL	CL GE	CM	CM GE	EP	EP GE
-4.00000	.83000	.96000	-.35200	-.31452	1.96670	2.66670
-3.00000	.92025	1.03625	-.35200	-.31452	2.45000	2.76667
-2.00000	1.01050	1.11250	-.35250	-.31391	2.93330	2.86663
-1.00000	1.10070	1.18870	-.35677	-.31017	3.41670	2.96670
.00000	1.19100	1.26500	-.35925	-.30644	3.90000	3.06667
1.00000	1.28120	1.33745	-.35950	-.30289	4.40000	3.16070
2.00000	1.37150	1.41000	-.35878	-.29895	4.90000	3.25480
3.00000	1.46170	1.47745	-.35634	-.29299	5.40000	3.34880
4.00000	1.55200	1.54500	-.35318	-.28710	5.90000	3.44290
5.00000	1.64220	1.60620	-.34896	-.28174	6.40000	3.53690
6.00000	1.73250	1.66750	-.34355	-.27603	6.90000	3.63100
7.00000	1.81550	1.72375	-.33830	-.27300	7.40000	3.72500
8.00000	1.89850	1.78000	-.33187	-.27300	7.90000	3.81900
9.00000	1.97770	1.83370	-.32572	-.27300	8.38680	3.91310
10.00000	2.04950	1.88250	-.31933	-.27300	8.87360	4.00710
11.00000	2.11630	1.81405	-.31740	-.27300	9.36040	4.10120
12.00000	2.11060	1.63429	-.31740	-.27914	9.84720	4.19520
13.00000	2.10110	1.45449	-.31740	-.29502	10.33400	4.28930
14.00000	2.01950	1.27473	-.32216	-.30597	10.82100	4.38350
15.00000	1.93790	1.09496	-.32881	-.31452	10.82100	4.38350
16.00000	1.85630	1.09495	-.33513	-.31451	10.82100	4.38350
17.00000	1.77480	1.09504	-.34101	-.31451	10.82100	4.38350
18.00000	1.69320	1.09502	-.34591	-.31452	10.82100	4.38350
19.00000	1.61160	1.09501	-.35080	-.31451	10.82100	4.38350
20.0	1.53000	1.09500	-.35395	-.31452	10.82100	4.38350

DELT CL GEAR = .00000 DELT CM GEAR = .00000

TABLE 2.5 (CONT.)

FLAP = 45.00

ALF	CL	CL GE	CM	CM GE	EP	EP GE
-4.00000	.93000	1.06000	-.38000	-.34826	2.18330	2.83330
-3.00000	1.02010	1.13185	-.38148	-.34673	2.67500	2.93333
-2.00000	1.11020	1.20370	-.38782	-.34329	3.16670	3.03337
-1.00000	1.20040	1.27565	-.39175	-.33986	3.65830	3.13330
.00000	1.29050	1.34750	-.39265	-.33642	4.15000	3.23333
1.00000	1.38060	1.41622	-.39235	-.33247	4.66250	3.32320
2.00000	1.47070	1.48495	-.39048	-.32634	5.17500	3.41310
3.00000	1.56090	1.54878	-.38823	-.32070	5.68750	3.50300
4.00000	1.65100	1.61250	-.38483	-.31480	6.20000	3.59290
5.00000	1.74110	1.67060	-.38055	-.30846	6.71250	3.68270
6.00000	1.83130	1.72880	-.37576	-.30525	7.22500	3.77260
7.00000	1.91200	1.78187	-.37061	-.30525	7.73750	3.86250
8.00000	1.99270	1.83495	-.36546	-.30525	8.25000	3.95240
9.00000	2.06660	1.88685	-.35986	-.30525	8.74760	4.04230
10.00000	2.13670	1.93120	-.35960	-.30525	9.24510	4.13210
11.00000	2.20310	1.80597	-.35960	-.30525	9.74270	4.22200
12.00000	2.16080	1.62509	-.35960	-.31342	10.24000	4.31160
13.00000	2.11670	1.44428	-.35960	-.32997	10.73800	4.40190
14.00000	2.03640	1.26334	-.36219	-.34045	11.23500	4.49130
15.00000	1.95620	1.08251	-.36779	-.34825	11.23500	4.49130
16.00000	1.87600	1.08255	-.37291	-.34826	11.23500	4.49130
17.00000	1.79570	1.08249	-.37795	-.34825	11.23500	4.49130
18.00000	1.71550	1.08252	-.38176	-.34825	11.23500	4.49130
19.00000	1.63520	1.08246	-.38558	-.34826	11.23500	4.49130
20.00000	1.55500	1.08250	-.38837	-.34825	11.23500	4.49130

DELT CL GEAR = .00000 DELT CM GEAR = .00000

TABLE 2.5 (CONT.)

FLAP = 50.00

ALF	CL	CL GE	CM	CM GE	EP	EP GE
-4.00000	1.03000	1.16000	-.41100	-.37920	2.40000	3.00000
-3.00000	1.12000	1.22750	-.41920	-.37605	2.90000	3.10000
-2.00000	1.21000	1.29500	-.42420	-.37290	3.40000	3.20000
-1.00000	1.30000	1.36250	-.42600	-.36975	3.90000	3.30000
.00000	1.39000	1.43000	-.42600	-.36530	4.40000	3.40000
1.00000	1.48000	1.49500	-.42480	-.35945	4.92500	3.48570
2.00000	1.57000	1.56000	-.42345	-.35360	5.45000	3.57140
3.00000	1.66000	1.62000	-.42090	-.34750	5.97500	3.65710
4.00000	1.75000	1.68000	-.41775	-.34000	6.50000	3.74290
5.00000	1.84000	1.73500	-.41400	-.33312	7.02500	3.82860
6.00000	1.93000	1.79000	-.40950	-.32625	7.55000	3.91430
7.00000	2.00850	1.84000	-.40549	-.31900	8.07500	4.00000
8.00000	2.08700	1.89000	-.40078	-.31150	8.60000	4.08570
9.00000	2.15550	1.94000	-.39500	-.30159	9.10830	4.17140
10.00000	2.22400	1.98000	-.38812	-.29320	9.61670	4.25720
11.00000	2.29000	1.79800	-.38020	-.32525	10.12500	4.34290
12.00000	2.21110	1.61599	-.38967	-.34800	10.63300	4.42820
13.00000	2.13220	1.43398	-.39710	-.36494	11.14200	4.51460
14.00000	2.05330	1.25197	-.40280	-.37491	11.65000	4.60000
15.00000	1.97440	1.06996	-.40728	-.38200	11.65000	4.60000
16.00000	1.89560	1.07004	-.41122	-.38200	11.65000	4.60000
17.00000	1.81670	1.07003	-.41517	-.38200	11.65000	4.60000
18.00000	1.73780	1.07002	-.41818	-.38200	11.65000	4.60000
19.00000	1.65890	1.07001	-.42094	-.38200	11.65000	4.60000
20.00000	1.58000	1.07000	-.42330	-.38200	11.65000	4.60000

DELT CL GEAR = .00000 DELT CM GEAR = .00000

STOP 0

TABLE 2.5 (CONT.)

EQUATIONS AERODYNAMIC SECTION

FIG. 2.8

LONGITUDINAL AERO EQUATIONS

STABILITY TO BODY AXIS TRANSFORMATION

$$C_{X_B} = C_{X_S} \cos\alpha - C_{Z_S} \sin\alpha$$

$$C_{Z_B} = C_{X_S} \sin\alpha + C_{Z_S} \cos\alpha$$

$$C_{M_O} = C_{m_S}$$

EQUATIONS AERODYNAMIC SECTION

FIG. 2.9

LATERAL - DIRECTIONAL AERO COEFFICIENTS

COEFFICIENT OF ROLLING MOMENT:

$$C_{l_{TO_S}} = C_{l_{\beta_{TO}}} \beta + C_{l_{\dot{p}}} \dot{p}_B + \left(C_{l_{p_{TO}}} C_{l_p}^{E/R} p_S + C_{l_{r_{TO}}} r_S \right) b_W / 2V$$
$$+ C_{l_{\delta_a}} C_{l_{\delta_a}}^{E/R} \delta_a + C_{l_{\delta_{SP}}}^{E/R} C_l (\alpha, \delta_{SP}, \delta_f)$$

WHERE:

$$C_{l_{\beta_{TO}}} = C_{l_{\beta_1}}(\delta_f) + \left(\Delta C_{l_{\beta_{C_{L_{TO}}=0}}} \right)_{TO}^{E} + \left(C_{l_{\beta_2}}(\delta_f) - \left(\Delta \frac{\partial C_{l_\beta}}{\partial C_L} \right)_{TO}^{E} \right) C_{L_{TO}}^{E}$$
$$+ \left(\frac{\partial C_{l_\beta}}{\partial n} \right)_{TO}^{E} N_Z$$

$C_{l_{\dot{p}}} = .00002$ REF: (DC9-A10.432.1, P. 210)

$C_{l_{p_{TO}}} = -.0075$ (DC9-C20-623.1, P. 68)

$C_{l_{r_{TO}}} = -.0000254\,\delta_f + .00488\,C_{L_{TO}}^{E}$ (DC9-A11.74A, P. 70)

FIG. 2.10

LATERAL – DIRECTIONAL AERO COEFFICIENTS

ROLLING MOMENT CON'T

$C_{l_{\delta_a}} = .00093$	REF: (DC9-C2D-392, P. 73 & 79)
$C_{l_{\delta_a}}^{E/R} = 1 - .00107\,\bar{q}$	(DC9-C2D-667, P. 212)
$C_{l_{\delta_{SP}}}^{E/R} = 1 - .00055\,\bar{q}$	(DC9-C2D-664, P. 213)
$\left(\Delta C_{l_{\beta_{C_{L_{TO}}=0}}}\right)_{TO}^{E} = .00025$	(DC9-A9.67, P. 209)
$\left(\Delta \dfrac{\partial C_{l_\beta}}{\partial C_L}\right)_{TO}^{E} = .00005\,\bar{q}$	"
$\left(\dfrac{\partial C_{l_\beta}}{\partial n}\right)_{TO}^{E} = .0001$	"
$C_{l_p}^{E/R} = 1 - .00058\,\bar{q}$	(DC9-C2D-665, P. 211)

FUNCTION TABLE AERODYNAMIC SECTION

TABLE 2.6

FUNCTION: $C_l(\alpha, \delta_{sp}, \delta_f)$ FOR $\delta_f = 0$

δ_{sp} \ α	−4	0	4	8	12
0	0	0	0	0	0
20	.0104	.011	.0114	.0120	.0120
35	.0177	.0187	.0195	.0204	.0204
50	.0244	.0256	.0269	.0282	.0282
60	.0280	.0295	.0310	.0326	.0326

REF: DC-9-C2D.803
LB-32322 P.82

FUNCTION TABLE AERODYNAMIC SECTION

TABLE 2.6 (CONT.)

FUNCTION: $C_\ell(\alpha, \delta_{sp}, \delta_f)$ FOR $\delta_f = 20$

δ_{sp} \ α	-4	0	4	8	12
0	0	0	0	0	0
5	.003	.0031	.0033	.0035	.0037
10	.0071	.0075	.0080	.0085	.0090
15	.0124	.0131	.0142	.0149	.0157
20	.0172	.0182	.0197	.0207	.0216
25	.0212	.0225	.0242	.0255	.0266
30	.0245	.0260	.0279	.0293	.0305
40	.0298	.0319	.0340	.0358	.0374
50	.0342	.0367	.0390	.0412	.0431
60	.0380	.0410	.0435	.0460	.0484

REF: ibid.

FUNCTION TABLE AERODYNAMIC SECTION

TABLE 2.6 (CONT.)

FUNCTION: $C_\ell(\alpha, \delta_{sp}, \delta_f)$ FOR $\delta_f = 50$

δ_{sp} \ α	-4	0	4	8	12
0	0	0	0	0	
4	.0040	.0042	.0045	.0048	
8	.0150	.0158	.0173	.0180	
16	.0396	.0410	.0425	.0444	
20	.0470	.0498	.0522	.0554	
25	.0522	.0575	.0612	.0665	
30	.0558	.0623	.0674	.0739	
35	.0589	.0654	.0715	.0780	
40	.0616	.0681	.0745	.0807	
50	.0667	.0734	.0798	.0855	
60	.0715	.0781	.0846	.0900	

REF: ibid.

FUNCTION TABLE AERODYNAMIC SECTION

TABLE 2.7

FUNCTION: $C_{l_{\beta_2}}(\delta_f)$

δ_f	$C_{l_{\beta_2}}(\delta_f)$	δ_f	$C_{l_{\beta_2}}(\delta_f)$
0	−.00225	30	−.00242
5	−.00230	35	−.00244
10	−.00232	40	−.00245
15	−.00235	45	−.00247
20	−.00238	50	−.00250
25	−.00240		

TABLE 2.8

FUNCTION: $C_{l_{\beta_1}}(\delta_f)$

δ_f	$C_{l_{\beta_1}}(\delta_f)$	δ_f	$C_{l_{\beta_1}}(\delta_f)$
0	-.00004	30	.00159
5	.00020	35	.00187
10	.00045	40	.00219
15	.00073	45	.00248
20	.00100	50	.00280
25	.00128		

FIG. 2.11

LATERAL-DIRECTIONAL AERO COEFFICIENTS

COEFFICIENT OF YAWING MOMENT:

$$C_{n_{TOS}} = C_{n\beta_{TO}}\,\beta + C_{n\delta_a}\,\delta_a + C_n(\alpha, \delta_{sp}, \delta_f) + (C_{np_{TO}}\,p_s + C_{nr_{TO}}\,r_s)\,b_w/2V$$

WHERE:

$$C_{n\beta_{TO}} = -.002 + .000011\,\delta_f$$ REF: (DC9-A11.40, P.59)

$$C_{n\delta_a} = .000025\left[\delta_f - 20\right]_0^{30} - .0000075\,\alpha + .00001$$ (DC9-C20.496, P.80)

$$C_{np_{TO}} = .0000084\,\delta_f - .00148\,C_{L_{TO}}^{E}$$ (DC9-A9.29, 30, P.64 & 65)

$$C_{nr_{TO}} = -.00005 - .000011\,\delta_f - .00019\left(C_{L_{TO}}^{E}\right)^2$$ (DC9-A11.69A, P.69)

FUNCTION TABLE AERODYNAMIC SECTION

TABLE 2.9

FUNCTION: $C_n(\alpha, \delta_{SP}, \delta_f)$ FOR $\delta_f = 0$

δ_{SP} \ α	-4	0	4	8	12
0	0	0	0	0	0
8	.0006	.0009	.0006	.0009	.0006
12	.0010	.0014	.0012	.0014	.0010
20	.0018	.0024	.0022	.0026	.0018
60	.0068	.0080	.0074	.0086	.0086

REF: DCG-C20.437
LB-31624 P. 113

FUNCTION TABLE AERODYNAMIC SECTION

TABLE 2.9 (CONT.)

FUNCTION: $C_n(\alpha, \delta_{sp}, \delta_f)$ FOR $\delta_f = 20$

δ_{sp} \ α	-4	0	4	8	12
0	0	0	0	0	0
5	.0011	.0010	.0007	.0004	.0004
10	.0030	.0025	.0016	.0010	.0010
20	.0058	.0050	.0037	.0026	.0026
40	.0098	.0090	.0075	.0061	.0061
60	.0136	.0128	.0111	.0094	.0094

REF: ibid.

FUNCTION: $C_n(\alpha, \delta_{SP}, \delta_f)$ FOR $\delta_f = 50$

δ_{SP} \ α	-4	0	4	8	12
0	0	0	0	0	
5	.0022	.0017	.0012	.0009	
10	.0051	.0041	.0030	.0022	
15	.0084	.0070	.0054	.0041	
20	.0112	.0098	.0080	.0063	
25	.0132	.0117	.0101	.0080	
30	.0146	.0131	.0114	.0092	
40	.0167	.0150	.0133	.0110	
50	.0184	.0166	.0149	.0126	
60	.0199	.0180	.0163	.0138	

REF: ibid.

FIG. 2.12

LATERAL - DIRECTIONAL AERO COEFFICIENTS

COEFFICIENT OF SIDE FORCE FOR FUSELAGE WITH TAIL OFF

$$C_{y_{TO}} = C_{y\beta_{TO}}\,\beta + C_{y_{p_{TO}}}\left(p_s\right) b_w/2V$$

WHERE:

$$C_{y\beta_{TO}} = -.0051 - .000018\,\delta_f \qquad \text{REF: (DC9-A11.41, P.60)}$$

$$C_{y_{p_{TO}}} = .00115 - .0000068\,\delta_f + .00284\,C_{L_{TO}}^{E} \qquad \text{(DC9-A9.22 \& 23, P.66 \& 67)}$$

EQUATIONS AERODYNAMIC SECTION

FIG. 2.13

LATERAL- DIRECTIONAL AERO COEFFICIENTS

COEFFICIENT OF SIDE FORCE DUE TO VERTICAL TAIL WITHOUT RUDDER

$$C_{y_V} = F_V \left[C_{L_{\alpha_V}}^{E/R} C_{y_{\beta_V}} \beta + C_{y_{\dot{r}}} \dot{r}_B + C_{y_{n_y}} N_Y + C_{L_{\alpha_V}}^{E/R} \left(C_{y_{\dot{\beta}}} \dot{\beta} + C_{y_{p_V}} p_B + C_{y_{r_V}} r_B + \frac{C_{y_{\dot{p}_V}}}{V} \dot{p}_B \right) b_w / 2V \right]$$

WHERE:

$F_V = 1 - .00016\, \bar{q}$ (DC9-C6.206, P.206)

$C_{L_{\alpha_V}}^{E/R} = 1 - .00021\, \bar{q}$ "

$C_{y_{\dot{r}}} = -.000045$ (DC9-C6.218, P.208)

$C_{y_{n_y}} = .0014$ "

$C_{y_{\dot{\beta}}} = .0003 + .000036\, \delta_f$ (DC9-A15-194-1, P.71)

$C_{y_{\beta_V}} = -.0106 - .000043\, \delta_f$ (DC9-A11.41, P.60)

$C_{y_{p_V}} = -.00115$ (DC9-A9.22 ; 23, P.66 ; 67)

$C_{y_{r_V}} = .0088 + .000032\, \delta_f$ (DC9-A11.69A, P.69)

$C_{y_{\dot{p}_V}} = .0319 - .000058\, \delta_f$ (DC9-A9.13, P.72)

$b_w = 89.35$ ft.

FIG. 2.14

LATERAL - DIRECTIONAL AERO COEFFICIENTS

COEFFICIENT OF SIDE FORCE DUE TO RUDDER

$$C_y(\delta_r) = F_V \, C_{y_{\delta_r}}^{E/R} \, C_{y_{\delta_r}} \, \delta_r$$

WHERE:

$$C_{y_{\delta_r}}^{E/R} = 1 - .00035\bar{q}$$ REF: (DC9-C6.219, P. 207)

$$C_{y_{\delta_r}} = .0049 2 - .000024\,\alpha + .0000116\,\delta_f$$ (DC9-C6.166, P.120)

COEFFICIENT OF TOTAL SIDE FORCE, BODY AXIS

$$C_{y_B} = C_{y_{TO}} + C_{y_V} + C_y(\delta_r)$$

FIG. 2.15

LATERAL - DIRECTIONAL AERO COEFFICIENTS

COEFFICIENTS OF ROLLING AND YAWING MOMENT, BODY AXIS

$$C_{l_B} = C_{l_{TOS}} \cos\alpha - C_{n_{TOS}} \sin\alpha + d_{VCG}\, C_{y_V} + d_{VCG_r}\, C_y(\delta_r)$$

$$C_{n_B} = C_{n_{TOS}} \cos\alpha + C_{l_{TOS}} \sin\alpha - l_{VCG}\, C_{y_V} - l_{VCG_r}\, C_y(\delta_r) - l_{X_{CG}}\, C_{y_{TO}}$$

WHERE:

$$d_{VCG} = Z_{V,CG}/b_W = .1394$$

$$d_{VCG_r} = Z_{V,CG_r}/b_W = .134$$

$$l_{VCG} = l_{VCG\,c/4} + (.25 - X_{CG})\, c_W/b_W \quad ; \quad l_{V,CG\,c/4} = X_{V,CG}/b_W = .407$$

$$l_{VCG_r} = l_{VCG_r\,c/4} + (.25 - X_{CG})\, c_W/b_W \quad ; \quad l_{V,CG_r\,c/4} = X_{V,CG_r}/b_W = .407$$

$$l_{X_{CG}} = (.25 - X_{CG})\, c_W/b_W$$

Section 3

Engine Model

The simulation model for the JT8D DC-9 engine was developed from static and dynamic data provided by Pratt & Whitney and Douglas Flight Test. The static data for forward and reverse thrust were formed into a table with mach number and E.P.R. as arguments. (See Table 3.1) Likewise, a table of E.P.R. versus cross shaft angle was formed. (See Table 3.2) Table 3.2was taken directly from the published engine performance data for the sea level static case. The values of E.P.R. were taken from the 59 degree F curve with the exception that the reverse E.P.R.'s were made negative to facilitate entry into the thrust vs. E.P.R./mach no. table, Table 3.1.The dynamic data (consisting of typical engine acceleration and deceleration time histories) was used to estimate a representative time constant.

The engine model was configured as shown in Figure 3.1. The sensor on the cockpit throttle pedestal provides a positive signal for the position of the main throttle handles and a negative signal for the position of the reverse thrust levers. When this plus/minus signal reaches the computer it is biased and scaled to represent cross shaft angle (XS) which has a range of 2.5 to 90 degrees. A cross shaft angle between 2.5 and 20 degrees indicates reverse thrust and an XS angle between 45 and 90 degrees indicates forward thrust. The idle position is 38.4 degrees of XS.

The past value of XS is subtracted from the current XS value to form a differential. After limiting the differential is integrated to form a new current value of XS angle. This process results in a first order lag which approximates the engine dynamics. The lagged XS position is then used as an argument in Table 3.2to find E.P.R. and E.P.R. along with mach number is used to find thrust from Table 3.1. The absolute value of E.P.R. is limited and sent to the E.P.R. instrument in the cockpit and thrust is made available to the equations of motion for force calculations.

With the main throttle handles in the idle position, "reverse thrust" is commanded by pulling the reverse thrust levers up to a detent. At the detent the amber "UNLOCK" light is lit and a logic signal is sent to the engine program which starts a 2 second timer. After 2 seconds the computer returns a logic signal which causes the green "REVERSE THRUST" light to be lit and at the same time causes the detent to be retracted allowing the levers to move on up, thus increasing reverse thrust.

Returning the reverse thrust levers to the stowed position turns out the amber light and causes the computer to turn out the green light and reset the detent.

The engine model was validated by first comparing E.P.R. and thrust values for various cross shaft angles with supplied data. Secondly, the dynamic response of the engine model was adjusted using pilot comments and comparisons to supplied data.

NOTE: The actual engine acceleration and deceleration responses are not simple lags as used in the model. The deceleration of the engine is fairly close to a first order lag while the acceleration is more akin to a second order type response. Nevertheless, it has been found in past simulations, that a first order lag gives a very acceptable representation of engine dynamics. The data indicated a time constant of about 3 seconds, however, pilots seemed to prefer something a little less than 2 seconds. A time constant of 2 seconds was used in the simulation.

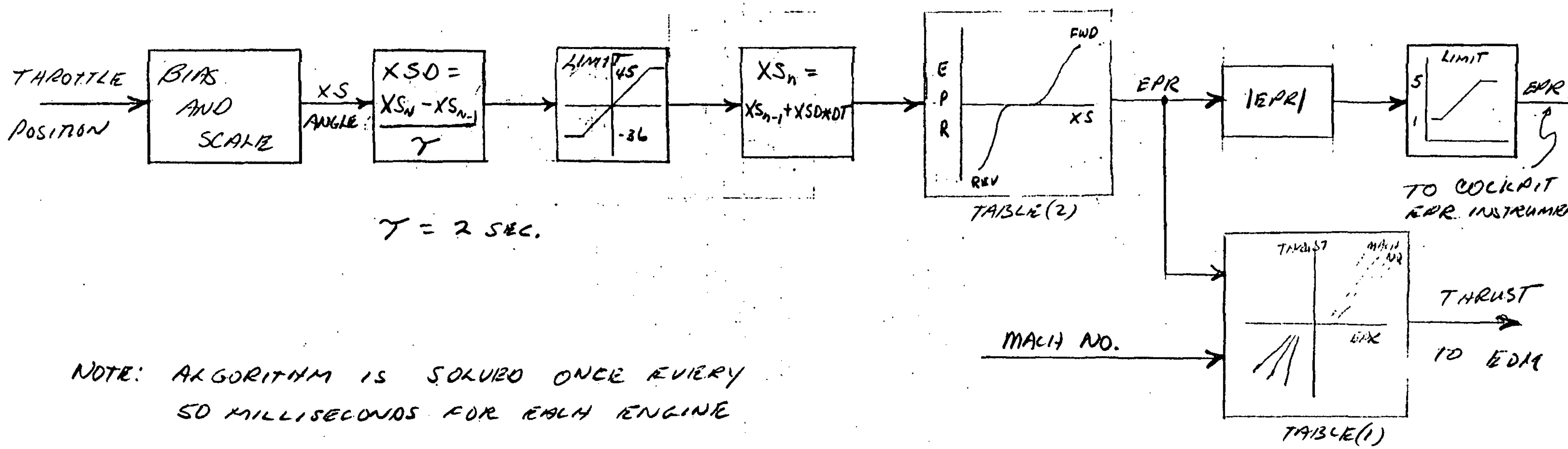

τ = 2 SEC.

NOTE: ALGORITHM IS SOLVED ONCE EVERY 50 MILLISECONDS FOR EACH ENGINE

ENGINE MODEL BLOCK DIAGRAM

FIGURE 3.1

ENGINE MODEL FUNCTION TABLES

TABLE 3.1
THRUST VS. EPR AND MACH NO.

-2.2	-1.8	-1.4	-1	-.6	EPR
1.	1.3	1.6	1.9	2.2	EPR
-7150.	-4360.	-1920.	-100.	0.	M = 0.
0.	5250.	9520.	13200.	16400.	M = 0 .
-9200.	-6230.	-3400.	-820.	0.	M = .1
0.	4750.	8750.	12320.	15400.	M = .1
-11920.	-8510.	-5130.	-1880.	0.	M = .2
90.	4400.	8240.	11780.	14890.	M = .2
-15200.	-11400.	-7600.	-3740.	0.	M = .3
200.	4300.	8000.	11470.	14700.	M = .3

TABLE 3.2
EPR VS. CROSS SHAFT ANGLE

2.5	10.	15.	20.	35.	36.	XS
45.	55.	73.5	90.			XS
-2.13	-1.60	-1.27	-1.03	-1.03	1.03	EPR
1.03	1.03	1.70	2.16			EPR

Section 4
Environmental Models

This section covers the runway condition models (crown, roughness and friction), the wind model and the turbulence model.

The crown, roughness and friction models are fully described in MCAIR report - titled "DC-9 Landing Gear Math Model for Directional Control On Runway Flight Simulation", by Harry Passmore, Reference 4. The crown model is the same as that in the report and the roughness and friction models are essentially the same except for the following changes:

1) The runway roughness table used was the same as the table 7-1 of the Passmore report except that all the bump heights were multiplied by 2. Also, the starting point of the table was set 500 feet "in" from the threshold to allow a "smooth" area for trimming the airframe simulation on the ground.

2) The DC-9 Nose Tire Cornering Coefficient (see figure 7-4 of the Passmore report) was multiplied by a factor of 5/7. This was done to reduce nose wheel steering sensitivity but did not take the resulting cornering force outside of an acceptable range. The main gear curves were the same as in the report.

3) The patchy runway condition profiles used in the study were essentially the same as cases 3 and 4 of figure 7-3 of the Passmore report. The exception is that in case 4, the patchy asymmetric profile, the "ICE"

segments were replaced with "WET" or "FLOODED" segments (see figure 4.1 below).

Turbulence Model:

The air turbulence model used for the ground handling study was developed from the Dryden* spectra (as opposed to the von Karman spectra). The independent longitudinal, lateral and vertical gust components are generated by filtering Gaussian random signals with the following three filters:

Longitudinal
$$F_u(S) = \sigma_u \sqrt{\frac{L_u}{\pi V}} \; \frac{1}{1 + \frac{L_u}{V} S}$$

Lateral
$$F_v(S) = \sigma_v \sqrt{\frac{L_v}{2\pi V}} \; \frac{1 + \sqrt{3}\frac{L_v}{V} S}{\left(1 + \frac{L_v}{V} S\right)^2}$$

Vertical
$$F_w(S) = \sigma_w \sqrt{\frac{L_w}{2\pi V}} \; \frac{1 + \sqrt{3}\frac{L_w}{V} S}{\left(1 + \frac{L_w}{V} S\right)^2}$$

where:

σ_u, σ_v, σ_w = RMS gust intensities.

These sigma values are a function of altitude.

ALT	σ_u AND σ_v	σ_w
20	.65	0
75	1.63	.15
150	3.61	.25
300	4.75	.31
450	.5	.09
600	.25	.06

*See, for example, Reference 7.

PATCHY RUNWAY CONDITION PROFILES

RUNWAY DISTANCE, FT	PATCHY SYMMETRIC				PATCHY UNSYMMETRIC		
	LMG	NG	RMG		LMG	NG	RMG
0-500	WET	WET	WET	A 1	WET	WET	WET
500-1000	WET	WET	WET	B 2	WET	WET	WET
1000-1500	WET	WET	WET	C 3	WET	WET	WET
1500-2000	WET	WET	WET	D 4	WET	WET	WET
2000-2500	WET	WET	WET	E 5	WET	WET	WET
2500-3000	WET	WET	WET	F 6	WET	WET	WET
3000-3500	WET	WET	WET	G 7	WET	WET	WET
3500-4000	WET	WET	WET	H 8	WET	WET	WET
4000-4500	FLOODED	FLOODED	FLOODED	I 9	FLOODED	WET	WET
4500-5000	WET	WET	WET	J 10	WET	WET	DRY
5000-5050	FLOODED	FLOODED	FLOODED	K 11	DRY	DRY	WET
5050-5100	WET	WET	WET	L 12	WET	WET	FLOODED
5100-5150	FLOODED	FLOODED	FLOODED	M 13	DRY	DRY	WET
5150-5200	WET	WET	WET	N 14	WET	WET	FLOODED
5200-5250	DRY	DRY	DRY	O 15	FLOODED	WET	WET
5250-5300	FLOODED	FLOODED	FLOODED	P 16	WET	WET	DRY
5300-5350	WET	WET	WET	Q 17	DRY	DRY	WET
5350-5400	FLOODED	FLOODED	FLOODED	A 18	WET	WET	FLOODED
5400-5450	WET	WET	WET	B 19	DRY	DRY	WET
5450-5500	DRY	DRY	DRY	C 20	WET	WET	FLOODED
5500-5600	WET	WET	WET	D 21	FLOODED	WET	WET
5600-5700	FLOODED	FLOODED	FLOODED	E 22	WET	WET	FLOODED
5700-5800	WET	WET	WET	F 23	FLOODED	WET	WET
5800-5900	DRY	DRY	DRY	G 24	WET	WET	FLOODED
5900-6000	WET	WET	WET	H 25	FLOODED	WET	WET
6000-6500	FLOODED	FLOODED	FLOODED	I 26	WET	WET	FLOODED
6500-7000	WET	WET	WET	J 27	FLOODED	WET	WET
7000-7500	DRY	DRY	DRY	K 28	WET	WET	FLOODED
7500-8000	WET	WET	WET	L 29	FLOODED	WET	WET
8000-8500	FLOODED	FLOODED	FLOODED	M 30	WET	WET	FLOODED
8500-9000	WET	WET	WET	N 31	FLOODED	WET	WET
9000-9500	WET	WET	WET	O 32	WET	WET	FLOODED
9500-10000	WET	WET	WET	P 33	FLOODED	WET	WET

NOTE: Patchy symmetrical same as Case #3 used in McAir simulator runs

FIGURE 4.1

L_u, L_v, L_w = scale lengths. These are normally functions of altitude, however, for the ground handling study they were held constant.

$$L_u = L_v = 400 \quad , \quad L_w = 200$$

V = the true airspeed of the aircraft. For this study the used for the filters was held constant at 100 f.p.s.

S = the Laplace transform variable.

The turbulence model was activated by using a numerical Gaussian random number generator to supply the inputs to the filters. The outputs of the filters are then considered to be the X, Y and Z gust components.

$$GUST_X = RAN(1) * F_u(S)$$
$$GUST_Y = RAN(2) * F_v(S)$$
$$GUST_Z = RAN(3) * F_w(S)$$

where:

$GUST_X$, $GUST_Y$, $GUST_Y$ = gust velocity components in feet per second.

$RAN(1)$, $RAN(2)$, $RAN(3)$ = three Gaussian random numbers which range from zero to ± 1 and are generated in series from a common seed.

$F_u(S)$, $F_v(S)$, $F_w(S)$ = the three filters shown above.

The actual digital algorithm was patterned after that in a NASA-Ames Program Specification, titled "Wind," by R. E. McFarland. (Reference 8). The algorithm used in the ground handling simulation did not include the rotational terms and had $1/\sqrt{2}$ less gain than the "Wind" algorithm.

Wind Model:

The wind model allowed for the specification of the wind components in the earth axes system. The X, Y and Z wind components could be specified as constants or functions of either range or altitude. Several of these tables of winds could be stored and the particular table desired could be called up before a run. Actually the tables for the gust paraemters were also handled by the wind routine making it the complete definer of the wind conditions.

After calculating the various elements these elements were summed to form the total wind component for each axes.

$$U_{WE} = SHEAR_x + STEADY_x + GUST_x$$
$$V_{WE} = SHEAR_y + STEADY_y + GUST_y$$
$$W_{WE} = SHEAR_z + STEADY_y + GUST_z$$

These wind components are then differentiated to form the wind acceleration components.

$$\dot{U}_{WE}, \quad \dot{V}_{WE} \quad \text{AND} \quad \dot{W}_{WE}$$

The six wind velocities and accelerations are picked up in the EOM where the velocity components are added to the inertial velocity components and the acceleration components are transformed to the body axis where they are added to the body axis force equations. See Figures 1.1, 1.2 and 1.7 of the EOM section.

The ground handling study only required a constant side wind and turbulence so that all terms except $STEADY_Y$ and the three GUST terms were zero. Note that σ_ω was zero below 20 feet so that $GUST_Z$ was zero on the ground. See description of turbulence model above.

Section 5
Struts Subroutine Implementation Notes

The STRUTS subroutine, written in FORTRAN, is an implementation of the mathematical model defined in Ref. 4, "DC-9 Landing Gear Math Model for Directional Control on Runway Flight Simulation." Most of the FORTRAN names defined in that report are used in STRUTS. The basic structure of STRUTS is similar to the subroutine LNDGR mentioned in the above report. Figure E1 is a general flow chart of STRUTS with line number references to the listing of STRUTS. The differences between STRUTS and LNDGR occur in the implementation of coordinate transformations, strut dynamic model and antiskid model. Most of the changes were made to decrease compute time.

An examination of the numerous coordinate transformations required in the gear model indicates that many of the transformation matrices are sparce. (They have several elements which are zero.) Therefore, compute time can be saved by coding the transform equations directly rather than using a general matrix multiply subroutine. Compute time is saved by eliminating the overhead required for a subroutine linkage.

Simulation of the strut dynamics (strut plus wheel mass dynamics) as defined in the above report consumes a lot of compute time. The natural frequency of that mass suspended between the tire spring and the strut spring is 15-20 Hz. Therefore, these equations must be solved approximately 200 times each second.

In the RDC simulation, STRUTS was called 20 times each second and these high frequency equations were solved 7 times for each pass through STRUTS. Satisfactory results were obtained with this solution rate of 140 times a second.

Compute time can be substantially reduced by minimizing the number of operations performed in the iterative loop used to solve for the strut dynamics. This was accomplished in STRUTS by expanding the dynamic equations and collecting all terms which are constant. All constant terms were moved outside the iterative loop and computed once for each pass through STRUTS to initialize the iterative loop.

Included in this initialization are calculations designed to minimize the step inputs to the strut dynamics. If the aircraft lands with a vertical velocity of 10 FPS and the simulation is solved 20 times a second, the step input to the landing gear can be 6 inches. This is a large step when compared to the total tire and strut movement. Therefore, the step change in height input to STRUTS is divided by the number of passes through the strut dynamics. This makes each step into the strut dynamics less than 1 inch. No investigation was made of the efficacy of this technique.

It is recommended that elimination of the strut dynamics be investigated in future RDC programs. Adequate results can probably be obtained by allowing the aircraft mass to land on a non linear spring with a combined characteristic of the strut and tire. The savings in coding complexity and, therefore, compute time in the strut routine would be substantial.

See Appendix B for a detailed description of the software antiskid system.

A great deal of time was spent developing the low speed taxiing characteristics of the simulation. During checkout, the pilots had the sensation of skidding too much at low speeds. Also, after coming to a complete halt, an oscillation would occur which was very unreal. Adjustments of tire and strut damping did not affect the oscillation. Since the very low speed regime was not considered important in this program, speed logic and simple geometric relations were added to remedy these irregularities.

The following equations were added to the equations of motion (see subroutine EOM, lines 135-39 & 196-201).

VE = SQRT (VIX*VIX+VIY*VIY) = $\sqrt{VIX^2+VIY^2}$

ROLLG = YAWG = 0.0

FYG = XMASS*(UB*RB*DTR - QSM*CYB - 32.2*AT(2,3))

RB = VE*DNS* .0229

PB = -PHI

ANY = VE*RB*.000542

VE is the ground velocity of the aircraft in feet per second. When VE is less than 20 these simplified equations are used. The roll and yaw moments due to the gear are zeroed. The lateral force due to the gear, FYG, is set to a value that balances the aircraft side force equation. Body yaw rate, RB, is computed as simple circular motion based on the nose wheel steering angle, DNS, and VE. See Figure E2 for a derivation of the simplified RB equation. Body roll rate, PB, is set equal to negative roll angle to washout any roll angle that exists when the low speed logic is entered. Lateral acceleration, ANY, is also computed based on simple circular motion.

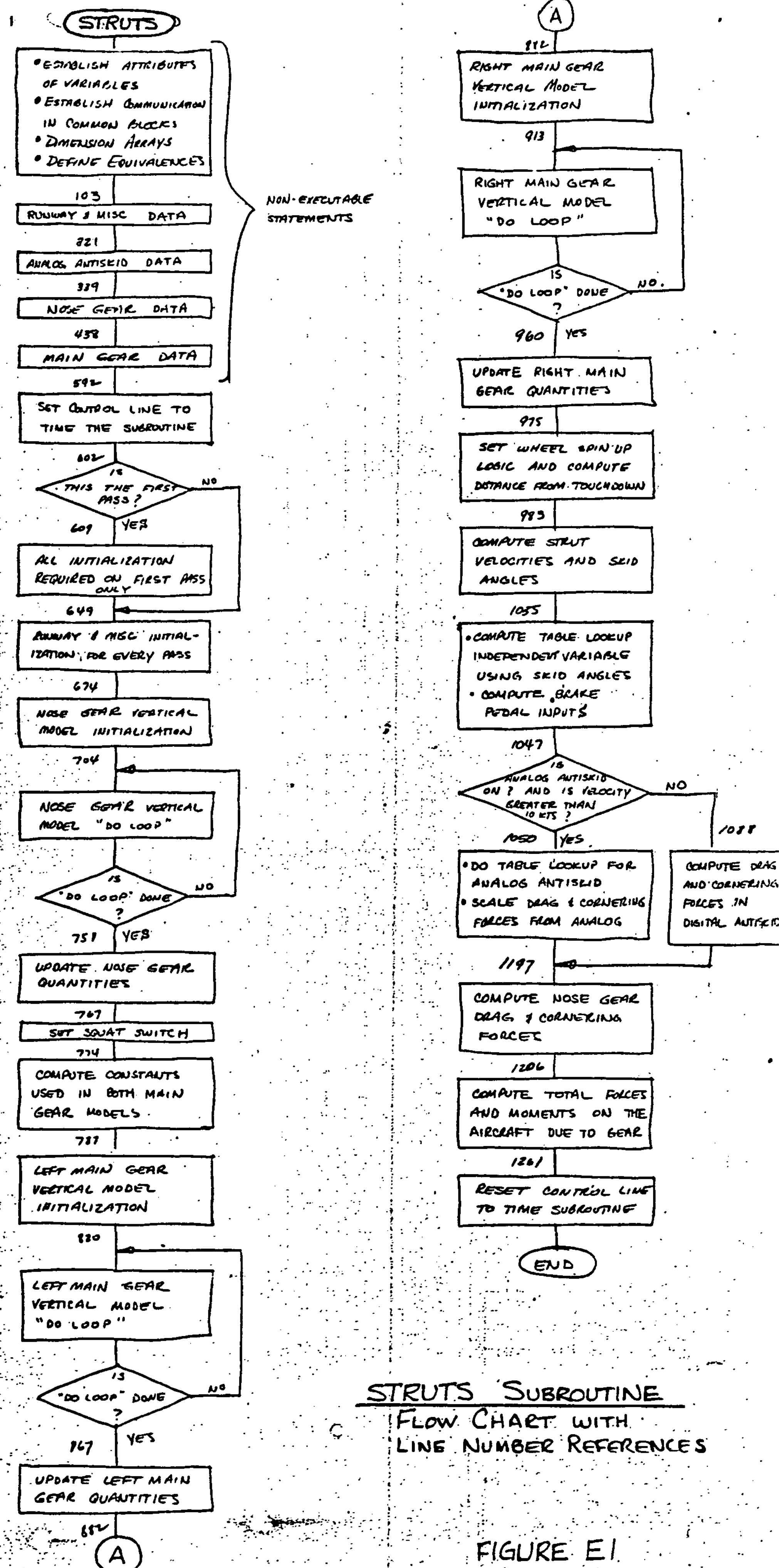

STRUTS SUBROUTINE

FLOW CHART WITH LINE NUMBER REFERENCES

FIGURE E1

DERIVATION OF YAW RATE DUE TO NOSE WHEEL STEERING FOR LOW SPEED STEERING EQUATION

FIGURE E2

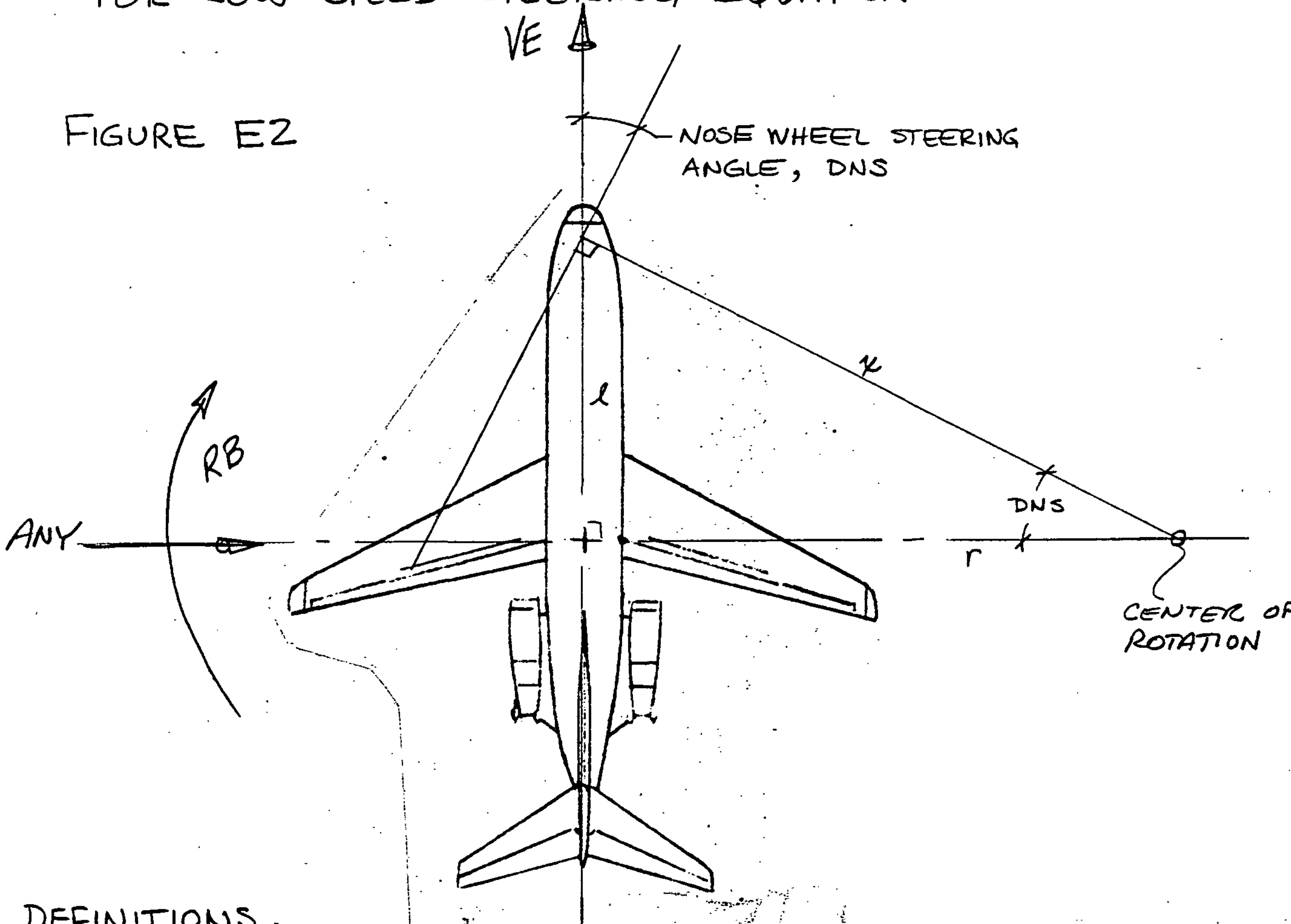

DEFINITIONS,

DNS = NOSE WHEEL STEERING ANGLE, DEG

x = NORMAL FROM NOSE WHEEL PLANE TO CENTER OF ROTATION

ℓ = DISTANCE FROM CG TO NOSE WHEEL, FT $\simeq$ 44.6

r = RADIUS OF ROTATION, FT

VE = AIRCRAFT SPEED, FPS

RB = AIRCRAFT BODY YAW RATE, DEG/SEC

ANY = AIRCRAFT LATERAL ACCELERATION, g's

FROM TRIGONOMETRIC RELATIONS

$$r = x \cos DNS$$

$$\ell = x \sin DNS$$

$$\therefore \; r = \ell / \tan DNS$$

$$= (44.6/DNS)\,57.3 \quad FT \quad \text{FOR SMALL ANGLES}$$

FROM SIMPLE CIRCULAR MOTION,

$$RB = 57.3\,VE/r \;; \quad ANY = VE * RB * \frac{1}{57.3 * 32.2}$$

$$\boxed{\begin{array}{ll} \therefore \; RB = VE * DNS * .0224 & \text{DEG/SEC.} \\ ANY = VE * RB * .000542 & g\text{'s} \end{array}}$$

DEFINITIONS FOR NAMES USED IN FORTRAN SUBROUTINE STRUTS

NAME	DEFINITION	UNITS
$COFRBL	LEFT TIRE BRAKING COEFFICIENT, ARRAY OF SIZE 4, EACH ELEMENT IS A DIFFERENT RUNWAY CONDITION, (1)= DRY, (2)= WET, (3)= FLOODED, (4)= ICY	
$COFRBR	RIGHT TIRE BRAKING COEFFICIENT, ARRAY SIMILAR TO $COFRBL	
$COFRSL	LEFT TIRE SIDEFORCE COEFFICIENT, ARRAY SIMILAR TO $COFRBL	
$COFRSN	NOSE TIRE SIDEFORCE COEFFICIENT, ARRAY SIMILAR TO $COFRBL	
$COFRSR	RIGHT TIRE SIDEFORCE COEFFICIENT, ARRAY SIMILAR TO $COFRBL	
$DATA	DUMMY ARRAY TO PAD COMMON BLOCK $DATA	
$UMAXL	LEFT TIRE MAXIMUM COEFFICIENT OF FRICTION	
$UMAXR	RIGHT TIRE MAXIMUM COEFFICIENT OF FRICTION	
$VARB	ARRAY THROUGH WHICH MAJORITY OF DATA IS TRANSMITTED TO AND FROM STRUTS	
ABRK	EFFECTIVE BRAKE AREA	IN^2
ABS	FORTRAN FUNCTION FOR FINDING ABSOLUTE VALUE	
ACMT	MAIN GEAR TIRE VISCOUS DAMPING COEFFICIENT	LB/IN/SEC

DEFINITIONS (con't)

NAME	DEFINITION	UNITS
ACNT	NOSE GEAR TIRE VISCOUS DAMPING COEFFICIENT	LB/IN/SEC
AEA	AUXILLARY EULER ANGLE FOR TRANSFORMATION BETWEEN GEAR AXES AND AIRCRAFT BODY AXES.	RAD.
AKMT	MAIN GEAR TIRE LINEAR SPRING CONSTANT	LB/IN
AKNT	NOSE GEAR TIRE LINEAR SPRING CONSTANT	LB/IN
AMAX	FORTRAN FUNCTION FOR FINDING THE MAXIMUM OF TWO REAL VALUES	
AMIN	FORTRAN FUNCTION FOR FINDING THE MINIMUM OF TWO REAL VALUES	
AMOD	FORTRAN FUNCTION FOR FINDING THE REMAINDER IN THE QUOTIENT OF TWO GIVEN REAL VALUES	
ARPTALT	AIRPORT ALTITUDE	FT.
AT	TRANSFORMATION MATRIX, INERTIAL AXES TO AIRCRAFT BODY AXES	
BPEDL	LEFT BRAKE PEDAL POSITION, NORMALIZED	
BPEDR	RIGHT BRAKE PEDAL POSITION, NORMALIZED	
CAEA	COSINE OF ANGLE AEA	

DEFINITIONS (con't)

NAME	DEFINITION	UNITS
CBAR	LENGTH OF MEAN AERODYNAMIC CHORD (MAC)	IN
CFSTK	CONVERSION FACTOR, FPS TO KNOTS	KNOTS/FPS
CG	AIRCRAFT CENTER OF GRAVITY AS A FRACTION OF MAC	
CKTFS	CONVERSION FACTOR, KNOTS TO FPS	FPS/KNOT
CMD	MAIN GEAR STRUT VISCOUS DAMPING COEFFICIENT	LB/IN/SEC
CMVL	LEFT MAIN GEAR STRUT V^2 DAMPING COEFFICIENT	$LB/(IN/SEC)^2$
CMVN	NOSE GEAR STRUT V^2 DAMPING COEFFICIENT	$LB/(IN/SEC)^2$
CMVR	RIGHT MAIN GEAR STRUT V^2 DAMPING COEFFICIENT	$LB/(IN/SEC)^2$
CND	NOSE GEAR STRUT VISCOUS DAMPING COEFFICIENT	LB/IN/SEC
COFEBT	TABLE OF MAIN TIRE EFFECTIVE BRAKING COEFFICIENT	
COFRBL	LEFT TIRE BRAKING COEFFICIENT	
COFRBR	RIGHT TIRE BRAKING COEFFICIENT	
COFRSL	LEFT TIRE SIDEFORCE COEFFICIENT	
COFRSN	NOSE TIRE SIDEFORCE COEFFICIENT	

DEFINITIONS (con't)

NAME	DEFINITION	UNITS
COFRSNT	TABLE OF NOSE TIRE SIDEFORCE COEFFICIENT	
COFRSR	RIGHT TIRE SIDEFORCE COEFFICIENT	
COFSBT	TABLE OF MAIN TIRE SIDEFORCE COEFFICIENT	
COFSNT	TABLE OF NOSE TIRE SIDEFORCE COEFFICIENT	
COSKAL	COSINE OF LEFT TIRE SKID ANGLE	
COSKAN	COSINE OF NOSE TIRE SKID ANGLE	
COSKAR	COSINE OF RIGHT TIRE SKID ANGLE	
CPGCAE	PRODUCT OF COSINES OF PGM AND AEA	
CPGM	COSINE OF PGM	
CPGN	COSINE OF PGN	
CPHI	COSINE OF AIRCRAFT ROLL ANGLE	
CPHSTH	PRODUCT OF COSINE OF AIRCRAFT ROLL ANGLE AND SINE OF AIRCRAFT PITCH ANGLE	
CPL	LEFT GEAR ANTISKID CYCLE PERIOD	SEC.
CPR	RIGHT GEAR ANTISKID CYCLE PERIOD	SEC.
CPSI	COSINE OF AIRCRAFT HEADING	

DEFINITIONS (con't)

NAME	DEFINITION	UNITS
CRGM	COSINE OF RGM	
CTBLI	DIFFERENCE EQUATION COEFFICIENT FOR BRAKE HYDRAULIC PRESSURE LAG	
CTHE	COSINE OF AIRCRAFT PITCH ANGLE	
CTL	LEFT GEAR ANTISKID CYCLE DUTY (FRACTION OF TIME BRAKE IS ON)	
CTNWSI	DIFFERENCE EQUATION COEFFICIENT FOR NOSE WHEEL STEERING LAG	
CTR	RIGHT GEAR ANTISKID CYCLE DUTY (FRACTION OF TIME BRAKE IS ON)	
CXB	AIRCRAFT EQUATIONS OF MOTION LONGITUDINAL COEFFICIENT	
CYB	AIRCRAFT EQUATIONS OF MOTION LATERAL COEFFICIENT	
DEADZ	FUNCTION TO SIMULATE DEADZONE	
DELT	SIMULATION STEP SIZE (NOT ZERO DURING RESET)	SEC
DH	ALTITUDE OF AIRCRAFT CG ABOVE THE AIRPORT	FT.
DHUBHL	CHANGE IN LEFT GEAR HUB HEIGHT FOR EACH PASS THROUGH THE VERTICAL MODEL ITERATIVE LOOP	IN.

DEFINITIONS (con't)

NAME	DEFINITION	UNITS
DHUBHN	SIMILAR TO DHUBHL FOR NOSE GEAR	IN.
DHUBHR	SIMILAR TO DHUBHR FOR RIGHT GEAR	IN.
DIN	TABLE OF CONTROL INPUTS FROM COCKPIT	10 VOLTS/UNITY
DME	LENGTH OF MAIN STRUT EXTENDED	FT.
DML	LEFT STRUT LENGTH	FT.
DMR	RIGHT STRUT LENGTH	FT
DN	NOSE STRUT LENGTH	FT.
DNE	LENGTH OF NOSE STRUT EXTENDED	FT.
DRCCG	DISTANCE FROM RUNWAY CENTERLINE TO AIRCRAFT CG	FT.
DRCLM	DISTANCE FROM RUNWAY CENTERLINE TO LEFT MAIN WHEEL	FT.
DRCNW	DISTANCE FROM RUNWAY CENTERLINE TO NOSE WHEEL	FT.
DRCRM	DISTANCE FROM RUNWAY CENTERLINE TO RIGHT MAIN WHEEL	FT.
DRTCG	X DISTANCE FROM GLIDESLOPE SHACK TO AIRCRAFT CG	FT
DRTLM	X DISTANCE FROM GLIDESLOPE SHACK TO LEFT MAIN WHEEL +500	FT

DEFINITIONS (con't)

NAME	DEFINITION	UNITS
DRTNW	X DISTANCE FROM GLIDESLOPE SHACK TO NOSE WHEEL + 500	FT.
DRTRM	X DISTANCE FROM GLIDESLOPE SHACK TO RIGHT MAIN WHEEL + 500	FT.
DT	INTEGRATION STEP SIZE	SEC.
DTONP	INTEGRATION STEP SIZE USED IN VERTICAL STRUT MODEL ITERATIVE LOOP	SEC
DTR	CONVERSION FACTOR, DEGREES TO RADIANS	RAD/DEG
DXMALE	DISTANCE FROM THE LEADING EDGE OF THE MAC TO MAIN STRUT ATTACH POINT	FT
DXNALE	DISTANCE FROM THE LEADING EDGE OF THE MAC TO NOSE STRUT ATTACH POINT	FT
EXP	FORTRAN FUNCTION FOR FINDING e^x	
EXTRA	GENERAL PURPOSE ARRAY FOR PASSING DATA TO AND FROM SUBROUTINE, PART OF $VARB.	
FBLCOM	LEFT MAIN WHEEL COMMANDED BRAKING FORCE	LB.
FBLMAX	LEFT MAIN WHEEL MAXIMUM AVAILABLE BRAKING FORCE	LB.
FBRCOM	RIGHT MAIN WHEEL COMMANDED BRAKING FORCE	LB.

DEFINITIONS (con't)

NAME	DEFINITION	UNITS
FBRMAX	RIGHT MAIN WHEEL MAXIMUM AVAILABLE BRAKING FORCE	LB.
FCON	SLOPE OF UNBRAKED CORNERING FORCE FUNCTION IN ANALOG ANTISKID	LB/DEG
FCOL	LEFT MAIN WHEEL UNBRAKED CORNERING FORCE IN ANALOG ANTISKID	LB
FCOR	RIGHT MAIN WHEEL UNBRAKED CORNERING FORCE IN ANALOG ANTISKID	LB
FDAMPL	LEFT MAIN STRUT TOTAL DAMPING FORCE	LB
FDAMPN	NOSE STRUT TOTAL DAMPING FORCE	LB
FDAMPR	RIGHT MAIN STRUT TOTAL DAMPING FORCE	LB.
FGML	LEFT MAIN TIRE FORCES ALONG STRUT Z-AXIS	LB.
FGMR	RIGHT MAIN TIRE FORCES ALONG STRUT Z-AXIS	LB.
FGN	NOSE TIRE FORCES ALONG STRUT Z-AXIS	LB.
FLE	LEFT MAIN TIRE FORCE ⊥ GROUND	LB.
FLEMUM	PRODUCT OF FLE & $UMAXL DIVIDED BY 2, USED IN ANALOG ANTISKID	LB.
FLV	LEFT MAIN TIRE FORCES IN GEAR VELOCITY AXES, AN ARRAY OF 3, (1)= X-FORCE, (2)= Y-FORCE & (3)= Z-FORCE	LB

DEFINITIONS (con't)

NAME	DEFINITION	UNITS
FML	LEFT MAIN TIRE FORCES IN AIRCRAFT BODY AXES, AN ARRAY OF 3; (1)= X-FORCE, (2)= Y-FORCE, (3)= Z-FORCE	LB
FMR	RIGHT MAIN TIRE FORCES IN AIRCRAFT BODY AXES, SIMILAR TO ARRAY FML	LB
FN	NOSE TIRE FORCES IN AIRCRAFT BODY AXES, SIMILAR TO ARRAY FML	LB
FNE	NOSE TIRE FORCE ⊥ GROUND	LB
FNV	NOSE TIRE FORCES IN GEAR VELOCITY AXES, SIMILAR TO ARRAY FLV	LB
FRE	RIGHT MAIN TIRE FORCE ⊥ GROUND	LB
FREMUM	PRODUCT OF FRE & $UMAXR DIVIDED BY 2, USED IN ANALOG ANTISKID	LB
FRV	RIGHT MAIN TIRE FORCES IN GEAR VELOCITY AXES, SIMILAR TO ARRAY FLV	LB
FS	ARRAY OF SCALE FACTORS TO CONVERT ARRAY DIN INTO ENGINEERING UNITS	VARIOUS
FSL	LEFT MAIN STRUT NONLINEAR SPRING FORCE	LB
FSMCMVM	TABLE OF MAIN STRUT NONLINEAR SPRING FORCES AND V^2 DAMPING COEFFICIENT	LB & LB/IN/SEC

DEFINITIONS (con't)

NAME	DEFINITION	UNITS
FSN	NOSE STRUT NONLINEAR SPRING FORCE	LB
FSNCMVN	TABLE OF NOSE STRUT NONLINEAR SPRING FORCES AND V^2 DAMPING COEFFICIENT	LB & LB/IN/SEC
FSR	RIGHT MAIN STRUT NONLINEAR SPRING FORCE	LB
FUN1D	FORTRAN SUBROUTINE FOR FINDING A FUNCTION OF ONE VARIABLE	
FXG	GEAR FORCES ALONG AIRCRAFT BODY X-AXIS	LB.
FYG	GEAR FORCES ALONG AIRCRAFT BODY Y-AXIS	LB
FZG	GEAR FORCES ALONG AIRCRAFT BODY Z-AXIS	LB
F3CL	EMPIRICAL FUNCTION USED TO REDUCE LEFT BRAKED DRAG FORCE AS A FUNCTION OF SKID ANGLE IN ANALOG ANTISKID	LB
F3CR	SAME AS F3CL FOR RIGHT WHEEL	LB
F3CT	TABLE OF VALUES FOR F3CL & F3CR	LB
GEOCON	ARRAY OF GEOMETRIC CONSTANTS	VARIOUS
HBUMP	RUNWAY BUMPS, AN ARRAY OF SIZE 3, (1)= NOSE GEAR, (2)= LEFT GEAR & (3)= RIGHT GEAR	IN.

DEFINITIONS (con't)

NAME	DEFINITION	UNITS
HCROWN	RUNWAY CROWN, AN ARRAY SIMILAR TO HBUMP	IN.
HUBHL	LEFT MAIN WHEEL HUB ALTITUDE	IN
HUBHLD	LEFT MAIN STRUT ATTACH POINT ALTITUDE CHANGE FOR EACH PASS THROUGH THE VERTICAL MODEL ITERATIVE LOOP	IN
HUBHLP	LEFT MAIN STRUT ATTACH POINT ALTITUDE PAST VALUE	IN
HUBHLO	LEFT MAIN STRUT ATTACH POINT INITIAL ALTITUDE FOR ITERATIVE LOOP	IN
HUBHN	NOSE STRUT EQUIVALENT OF HUBHL	IN
HUBHND	NOSE STRUT EQUIVALENT OF HUBHLD	IN
HUBHNP	NOSE STRUT EQUIVALENT OF HUBHLP	IN
HUBHNO	NOSE STRUT EQUIVALENT OF HUBHLO	IN
HUBHR	RIGHT MAIN STRUT EQUIVALENT OF HUBHL	IN
HUBHRD	RIGHT MAIN STRUT EQUIVALENT OF HUBHLD	IN
HUBHRP	RIGHT MAIN STRUT EQUIVALENT OF HUBHLP	IN
HUBHRO	RIGHT MAIN STRUT EQUIVALENT OF HUBHLO	IN
I	GENERAL PURPOSE INTEGER	

DEFINITIONS (con't)

NAME	DEFINITION	UNITS
I1140	DUMMY ARRAY TO PAD COMMON BLOCK I1140	
J	GENERAL PURPOSE INTEGER	
JCASE	RUNWAY CONDITION CASE NUMBER, 1 = SYMMETRICAL PATCHY, 2 = ASYMMETRICAL PATCHY, 3 = DRY, 4 = WET, 5 = FLOODED	
JDFRT	INTEGER DISTANCE FROM RUNWAY THRESHOLD TO AIRCRAFT CG	FT.
JPRWY	RUNWAY CONDITION CODE	
JPRWYD	TABLE OF RUNWAY CONDITION CODES	
JRWYCLM	RUNWAY CONDITION AT LEFT MAIN WHEEL, 1 IS DRY, 2 IS WET, 3 IS FLOODED	
JRWYCNG	RUNWAY CONDITION AT NOSE WHEEL	
JRWYCRM	RUNWAY CONDITION AT RIGHT MAIN WHEEL	
JRWYD	SUBSCRIPT FOR TABLE JPRWYD DERIVED FROM JDFRT	
K	GENERAL PURPOSE INTEGER	
KOUNT	DUMMY VARIABLE IN COMMON BLOCK $TIME	
K1 to K8	TEMPORARY CONSTANTS USED IN BOTH MAIN STRUTS, PART OF TRANSFORMATIONS	
LOG	LOGIC SWITCHES, AN ARRAY OF SIZE 30	

DEFINITIONS (con't)

NAME	DEFINITION	UNITS
MAX	FORTRAN FUNCTION FOR FINDING THE MAXIMUM OF TWO OR MORE INTEGERS	
MFSL	MEMORY FOR LEFT STRUT NONLINEAR SPRING TABLE LOOKUP, FSL	
MFSN	MEMORY FOR FSN TABLE LOOKUP	
MFSR	MEMORY FOR FSR TABLE LOOKUP	
MF3CL	MEMORY FOR F3CL TABLE LOOKUP	
MF3CR	MEMORY FOR F3CR TABLE LOOKUP	
MIN	FORTRAN FUNCTION FOR FINDING THE MINIMUM OF TWO OR MORE INTEGERS	
MMUL	MEMORY FOR MUMAXL TABLE LOOKUP	
MMUR	MEMORY FOR MUMAXR TABLE LOOKUP	
MOD	INTEGER VERSION OF AMOD (see above)	
MSKBL	MEMORY FOR $COFRBL TABLE LOOKUP	
MSKBR	MEMORY FOR $COFRBR TABLE LOOKUP	
MSKN	MEMORY FOR $COFRSN TABLE LOOKUP	
MSKSBL	MEMORY FOR $COFRSL TABLE LOOKUP	
MSKSBR	MEMORY FOR $COFRSR TABLE LOOKUP	

DEFINITIONS (con't)

NAME	DEFINITION	UNITS
MSKSNL	MEMORY FOR $COFRSL TABLE LOOKUP	
MSKSNR	MEMORY FOR $COFRSR TABLE LOOKUP	
MUMAXL	LEFT MAIN WHEEL MAXIMUM COEFFICIENT OF FRICTION, AN ARRAY OF SIZE 4, (1) = DRY, (2) = WET, (3) = FLOODED, (4) = ICY	
MUMAXR	RIGHT MAIN WHEEL MAXIMUM COEFFICIENT OF FRICTION, AN ARRAY SIMILAR TO MUMAXL	
MUMAXT	TABLE OF VALUES FOR MUMAXL & MUMAXR	
MVFG1	FORTRAN SUBROUTINE TO FIND A FUNCTION OF ONE VARIABLE	
MVFG2	FORTRAN SUBROUTINE TO FIND A FUNCTION OF TWO VARIABLES	
MVTBL	MEMORY FOR $COFRBL TABLE LOOKUP	
MVTBR	MEMORY FOR $COFRBR TABLE LOOKUP	
MVTN	MEMORY FOR $COFRSN TABLE LOOKUP	
MVTSBL	MEMORY FOR $COFRSL TABLE LOOKUP	
MVTSBR	MEMORY FOR $COFRSR TABLE LOOKUP	
MVTSNL	MEMORY FOR $COFRSL TABLE LOOKUP	
MVTSNR	MEMORY FOR $COFRSR TABLE LOOKUP	

DEFINITIONS (con't)

NAME	DEFINITION	UNITS
NFSM	NUMBER OF STRUT POINTS IN FSMCMVM	
NFSN	NUMBER OF STRUT POINTS IN FSNCMVN	
NF3C	NUMBER OF SKID ANGLE POINTS IN F3CT	
NMU	NUMBER OF VELOCITY POINTS IN MUMAXT	
NPASS	NUMBER OF PASSES THROUGH VERTICAL STRUT MODEL ITERATIVE LOOPS	
NSKB	NUMBER OF SKID ANGLE POINTS IN COFEBT	
NSKN	NUMBER OF SKID ANGLE POINTS IN COFRSNT	
NSKSB	NUMBER OF SKID ANGLE POINTS IN COFSBT	
NSKSN	NUMBER OF SKID ANGLE POINTS IN COFSNT	
NVTB	NUMBER OF VELOCITY POINTS IN COFEBT	
NVTN	NUMBER OF VELOCITY POINTS IN COFRSNT	
NVTSB	NUMBER OF VELOCITY POINTS IN COFSBT	
NVTSN	NUMBER OF VELOCITY POINTS IN COFSNT	
OUTIN	DUMMY ARRAY TO PAD COMMON BLOCK $OUTIN	
PB	AIRCRAFT BODY ROLL RATE	DEG/SEC
PGM	ANGLE BETWEEN THE AIRCRAFT STATION LINE AND MAIN STRUT CENTER LINE	DEG

DEFINITIONS (con't)

NAME	DEFINITION	UNITS
PGN	NOSE STRUT EQUIVALENT TO PGM	DEG.
PMG	AIRCRAFT BODY AXIS PITCHING MOMENT DUE TO GEARS	FT-LB.
PRWY	POSITION ON A 2400 FOOT SEGMENT OF RUNWAY, USED TO FIND HBUMP	FT.
QSM	AIRCRAFT EQUATIONS OF MOTION COEFFICIENT	LB/SLUG
RB	AIRCRAFT BODY AXIS YAW RATE	DEG/SEC
RFLATM	MINIMUM RADIUS OF MAIN TIRE	IN
RFLATN	MINIMUM RADIUS OF NOSE TIRE	IN
RGM	ANGLE BETWEEN AIRCRAFT BUTT LINE AND MAIN STRUT CENTER LINE	DEG
RMLA	LEFT MAIN STRUT ATTACH POINT LOCATION IN BODY AXES, AN ARRAY OF 3, (1) = X-POSITION, (2) = Y-POSITION, (3) = Z-POSITION	FT
RMLW	LEFT MAIN WHEEL HUB LOCATION IN BODY AXES, AN ARRAY OF 3 SIMILAR TO RMLA	FT
RMRA	RIGHT MAIN STRUT EQUIVALENT TO RMLA	FT
RMRW	RIGHT MAIN WHEEL EQUIVALENT TO RMLW	FT

DEFINITIONS (con't)

NAME	DEFINITION	UNITS
RNA	NOSE STRUT EQUIVALENT TO RMLA	FT.
RNW	NOSE WHEEL EQUIVALENT TO RMLW	FT.
ROLLG	AIRCRAFT BODY AXIS ROLL MOMENT DUE TO GEARS	FT-LB.
RTD	CONVERSION FACTOR, RADIANS TO DEGREES	DEG/RAD.
RTIM	RADIUS OF UNDEFLECTED MAIN TIRE	IN.
RTIN	RADIUS OF UNDEFLECTED NOSE TIRE	IN.
RWYBUMP	TABLE OF VALUES FOR HBUMP	IN.
SAEA	SINE OF AEA	
SFBUMP	SCALE FACTOR ON HBUMP	
SFCROWN	SCALE FACTOR ON HCROWN	
SIGN	FORTRAN FUNCTION FOR ATTACHING THE SIGN OF ONE VARIABLE TO ANOTHER	
SINCOS	FORTRAN SUBROUTINE FOR FINDING THE SINE AND COSINE OF AN ANGLE	
SISKAL	SINE OF SKANGL	
SISKAN	SINE OF SKANGN	
SISKAR	SINE OF SKANGR	

DEFINITIONS (con't)

NAME	DEFINITION	UNITS
SKANGL	LEFT MAIN TIRE SKID ANGLE	DEG
SKANGN	NOSE TIRE SKID ANGLE (NO STEERING)	DEG
SKANGR	RIGHT MAIN TIRE SKID ANGLE	DEG
SKANGT	TOTAL NOSE TIRE SKID ANGLE	DEG
SL	LEFT MAIN STRUT DEFLECTION	IN.
SLD	LEFT MAIN STRUT DEFLECTION RATE	IN/SEC
SLDD	LEFT MAIN STRUT DEFLECTION ACCEL.	IN/SEC^2
SMMAX	MAIN STRUT MAXIMUM DEFLECTION	IN
SN	NOSE STRUT DEFLECTION	IN
SND	NOSE STRUT DEFLECTION RATE	IN/SEC
SNDD	NOSE STRUT DEFLECTION ACCEL.	IN/SEC^2
SNMAX	NOSE STRUT MAXIMUM DEFLECTION	IN
SPGCAE	PRODUCT OF SPGM AND CAEA	
SPGM	SINE OF PGM	
SPGN	SINE OF PGN	
SPHI	SINE OF AIRCRAFT ROLL ANGLE	
SPHSTH	PRODUCT OF SPHI AND STHE	

DEFINITIONS (con't)

NAME	DEFINITION	UNITS
SPSI	SINE OF AIRCRAFT HEADING	
SQRT	FORTRAN FUNCTION FOR FINDING SQUARE ROOT	
SR	RIGHT MAIN STRUT DEFLECTION	IN
SRD	RIGHT MAIN STRUT DEFLECTION RATE	IN/SEC
SRDD	RIGHT MAIN STRUT DEFLECTION ACCEL	IN/SEC^2
SRGM	SINE OF RGM	
STHE	SINE OF AIRCRAFT PITCH ANGLE	
STRANG	NOSE WHEEL STEERING ANGLE	DEG
THT	ENGINE THRUST ALONG AIRCRAFT X-AXIS	LB
TIML	LEFT WHEEL ANTISKID TIMER	SEC.
TIMR	RIGHT WHEEL ANTISKID TIMER	SEC.
TRIG	FORTRAN SUBROUTINE FOR FINDING THE ARCTANGENT GIVEN TWO VALUES	
TO to T9	TEMPORARY STORAGE LOCATIONS FOR INTERMEDIATE VALUES.	
UB	AIRCRAFT VELOCITY, BODY X-AXIS	FT/SEC
USMM	UNSPRUNG MASS OF MAIN STRUT + WHEEL	$LB\text{-}SEC^2/IN$

DEFINITIONS (con't)

NAME	DEFINITION	UNITS
USMN	UNSPRUNG MASS OF NOSE STRUT + WHEEL	LB-SEC^2/IN
VB	AIRCRAFT VELOCITY, BODY Y-AXIS	FT/SEC
VDW	WIND ACCELERATION, AIRCRAFT BODY Y-AXIS	FT/SEC^2
VE	AIRCRAFT EQUIVALET AIRSPEED	FT/SEC
VIX	AIRCRAFT VELOCITY, INERTIAL X-AXIS	FT/SEC
VIY	AIRCRAFT VELOCITY, INERTIAL Y-AXIS	FT/SEC
VTLW	LEFT WHEEL TOTAL VELOCITY IN GROUND PLANE	FT/SEC
VTNW	NOSE WHEEL TOTAL VELOCITY IN GROUND PLANE	FT/SEC
VTRW	RIGHT WHEEL TOTAL VELOCITY IN GROUND PLANE	FT/SEC
VWL	LEFT WHEEL VELOCITY, INERTIAL AXES, AN ARRAY OF 3, (1) = X-AXIS, (2) = Y-AXIS, (3) = NOT USED	FT/SEC
VWN	NOSE WHEEL VELOCITY SIMILAR TO VWL	FT/SEC
VWR	RIGHT WHEEL VELOCITY SIMILAR TO VWL	FT/SEC
XCG	SAME AS CG	
XMASS	AIRCRAFT MASS	SLUGS

DEFINITIONS (con't)

NAME	DEFINITION	UNITS
XRO	ROLLOUT DISTANCE	FT
XTD	TOUCHDOWN POINT FROM GLIDESLOPE SHACK	FT
YAWG	AIRCRAFT YAW MOMENT DUE TO GEARS	FT-LB
ZI	AIRCRAFT POSITION, INERTIAL Z-AXIS	FT

Section 6

Auxiliary Equations

This section contains descriptions of the models for the ILS and marker beacons; the instrument drive algorithms; and the yaw damper model. Also included are short descriptions of the interfaces to the motion base and the visual system.

ILS (Instrument Landing System):

The ILS consists of a glide slope beam (G/S) and a localizer beam (LOC). The G/S provides a descending path to the runway touch-down point which is about 1000' in from the threshold. Typically this path is about 3 degrees. The LOC provides lateral guidance by defining a path down the center of the runway. The origins of the LOC beam is at the far end of the runway.

The ILS model essentially does two things: 1) establish the position of the ILS receivers, on the aircraft, with respect to the transmitters on the ground, and 2) calculates the angular errors from the fixed beams.

The positions of the ILS sensors are transformed to the earth axes by the following equations:

G/S

$$X_{GI} = X_I + X_{BGS}A_{1,1} + Z_{BGS}A_{3,1}$$

$$Z_{GI} = Z_I + X_{BGS}A_{1,3} + Z_{BGS}A_{3,3} + AP_{ALT}$$

LOC

$$X_{LI} = X_I + X_{BL}A_{1,1} + Z_{BL}A_{3,1}$$

$$Y_{LI} = Y_I + X_{BL}A_{1,2} + Z_{BL}A_{3,2}$$

Where:

- X_{BGS}, Z_{BGS} = the body axes coordinates of the G/S antenna.*
- X_{BL}, Y_{BL} = The body axes coordinates of the LOC antenna.*
- $A_{i,j}$ = Elements of the body to earth transformation matrix (direction cosines).
- X_I, Y_I, Z_I = Earth axes coordinates of the aircraft.
- AP_{ALT} = Airport altitude
- X_{GI}, Z_{GI} = Earth axes coordinates of the G/S antenna.
- X_{LI}, Y_{LI} = Earth axes coordinates of the LOC antenna.

* NOTE: Body axes coordinates are based on a longitudinal C.G. position at the quarter chord and on the aircraft center line.

The earth axes positions of the ILS sensors on the aircraft are used to calculate the voltage errors as follows:

$$E_{G/S} = [G/S\ X - (\text{Arctan}\ {}^{Z_{GI}}/_{X_{GI}})\ 57.3]\ .214$$

$$E_{LOC} = [(\text{Arctan}\ {}^{Y_{LI}}/_{X_{LI}} - RWY_L)\ 57.3]\ .075$$

Where:

G/S X = The fixed glide path angle defined by the glide slope transmitter.

RWY_L = The length of the runway from the touch-down point to the far end (position of the localizer transmitter).

57.3 = Numbers of degrees in radian. Used here to convert from radians to degrees.

.214 = Volts per degree of G/S error.

.075 = Volts per degree of LOC error.

$E_{G/S}$ = Glide slope error in volts.

E_{LOC} = Localizer error in volts.

The glide slope and localizer error signals are sent to the indicators in the ADI and HSI instruments. The ILS displays are scaled in "DOTS" where .075 volts equals one dot for both G/S and LOC.

Marker Beacons:

Two marker beacons were simulated for the RDC study. Typically airports will have 2 or 3 of these beacons spaced out along the runway approach. These beacons activate a beeper and lights in the cockpit. There is a light for each beacon.

The simulation model consisted of using comparisons on longitudinal and lateral aircraft displacement to define two rectangles within which the beeper and appropriate light are activated.

For the RDC study the following dimensions were used:

Outer Marker:

$-35856 < X_I < -33456$ range out from touch down point in feet

$-2100 < Y_I < +2100$ lateral displacement in feet

Middle Marker:

$-4640 < X_I < -3440$ range out from touch-down point in feet

$-1000 < Y_I < +1000$ lateral displacement in feet

The rectangle sizes are the approximate size of the beacon radiation pattern if the aircraft were following a 3 degree glide slope.

Instrument Drives:

The six primary flight instruments were active at both the Captain's and First Officer's positions. The Captain's instruments were DC-9 types and the First Officer's were DC-10 types. In addition the center panel contained two DC-9 type Engine Pressure Ratio (EPR) instruments. Both the DC-9 and DC-10 instruments were driven with the same parameters, for the most part.

ADI (Attitude and Director Indicator)

Artificial horizon - driven by pitch and roll (θ and ϕ).
ILS indicators - driven by the ILS parameters $E_{G/S}$ and E_{LOC}.
The flight director bars, speed command bug and skid ball were not driven.

HSI (Horizontal Situation Indicator)

Compas - driven by heading (ψ)
ILS - same as ADI
DME (Distance Measuring Equipment) indicator was not used.

BARO altimeter - driven by C.G. attitude (h_{CG})

Radio altimeter - The altitude of the radio altimeter antenna is found as follows:

$$h_{RA} = -h_{RABIAS} - (Z_I + X_{BRA}A_{1,3} + Z_{BRA}A_{3,3} + AP_{ALT})$$

Where:

h_{RA} = radio altimeter altitude

h_{RABIAS} = Bias such that the radio altimeter will read zero when the main gear just touch the ground and the aircraft pitch angle is 6 degrees.

Z_I = earth axes Z component ($-h_{CG}$).

X_{BRA} = X body axes component of radio altimeter antenna position.*

Z_{BRA} = Z body axes component of radio altimeter antenna position.*

$A_{i,j}$ = elements of body to earth transformation matrix.

AP_{ALT} = airport altitude

*NOTE: Body axes coordinates are based on a longitudinal C.G. position at the quarter chord and on the aircraft center line.

In order to drive the radio altitude indicator h_{RA} must be changed to a voltage. The h_{RA} voltage relationship is non-linear as follows:

h_{RA}	VOLTS
0	.4
200	4.4
400	8.4
600	12.151
800	14.947
1000	17.130
1200	18.920
1400	20.438
1600	21.756
1800	22.920
2000	23.962
2200	24.907
2400	25.769
2600	26.6
2800	32. *

* This point is used to drive the DC-10 tape instrument display out of sight.

VSI (Vertical Speed Indicator)

The VSI instrument was driven with a first order lag as shown.

VSI drive = $\dot{Z}_I/\gamma S+1$

Where:

$\dot{Z}_I$ = aircraft vertical rate component in earth axes

γ = .5 second

IAS (Indicated Air Speed)

IAS was driven with equivalent airspeed (V_e) as calculated by EOM.

EPR (Engine Pressure Ratio)

EPR indicators were driven with EPR as calculated in the engine algorithm (see Section 3).

Yaw Damper

The DC-9 model used for the RDC study included a yaw damper. The yaw damper model used was optimized for the approach configuration. A block diagram of the yaw damper algorithm is shown in Figure 6.1.

The body axes yaw rate (r_B) is the primary damping loop while the body axes roll rate (P_B) provides some turn coordination. The limiter is used to limit the authority of the yaw damper. K_7 is needed to change the commanded rudder deflection in hinge coordinates to stream coordinates. Stream coordinates are used in the computation of aero forces.

Motion Base Drive

The algorithms for the motion base drive have been taken from NASA report TN D-7350 (Reference 3). The only changes made by Douglas to the algorithms, other than those which relate to the geometry of the platform, were as follows:

1) The braking acceleration circuit was not used.

2) The lead compensation was applied directly to the jack signals and not to the centroid position as shown in the report.

3) The washout parameters used are very similar to those shown in Table 2 of a NASA paper presented at an AIAA conference (Reference 9). Table 6.1 below shows the actual values used for the Douglas motion base.

DC-9 YAW DAMPER and TURN COORDINATION

MANUAL APPROCH MODE

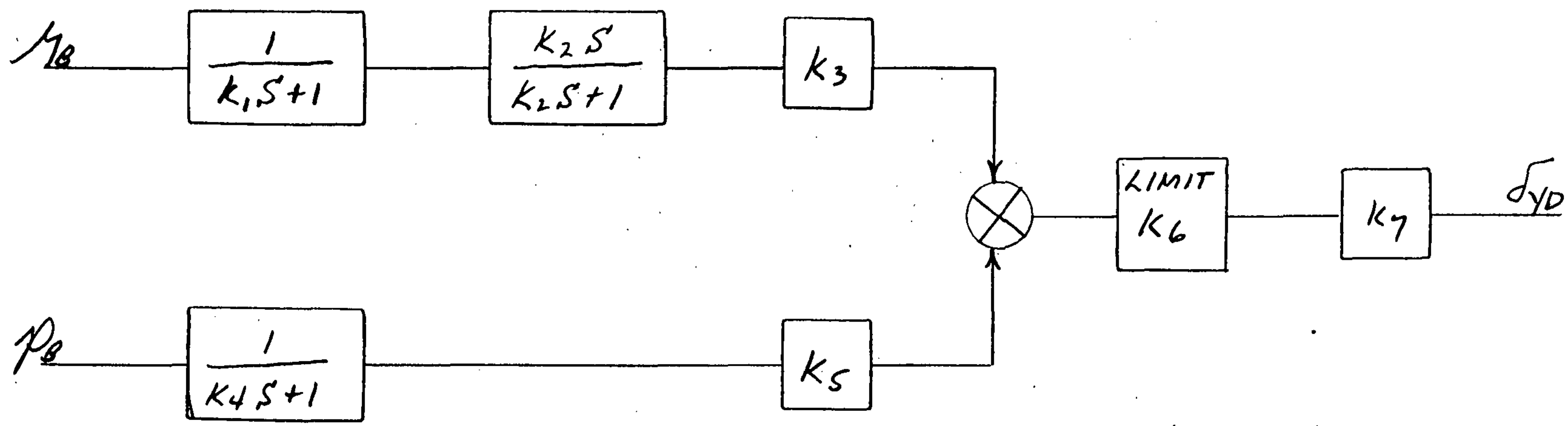

$K_1 = .05$

$K_2 = 1.45$

$K_3 = 2.5$

$K_4 = .01$

$K_5 = -.34$

$K_6 = \pm 2.12$ degrees

$K_7 = .7692$ degrees stream/degrees hinge

FIG. 6.1

MOTION BASE WASHOUT PARAMETERS

TABLE 6.1

VARIABLE MATH	COMPUTER	UNITS	VALUE
		HIGH PASS FILTER	
$K_{Z,1}$	C1(3)	-	0.8
$\xi_{Z,1}$	ZET1(3)	-	0.7
$\omega_{n,Z,1}$	OM1(3)	rad/sec	2.0
$K_{Z,2}$	C2(3)	-	1.0
		LOW PASS FILTER	
$K_{\theta,1}$	C1(1)	-	0.5
ξ_{θ}	ZET1(1)	-	0.7
$\omega_{n,\theta}$	OM1(1)	rad/sec	5.0
$K_{\theta,2}$	C2(1)	-	0
$K_{\phi,1}$	C1(2)	-	0.05
ξ_{ϕ}	ZET1(2)	-	0.7
$\omega_{n,\phi}$	OM1(2)	rad/sec	5.0
$K_{\phi,2}$	C2(2)	-	0
		SIGNAL-SHAPING NETWORK	
$K_{q,T,1}$	C3(1)	per ft.	0.001
$K_{q,T,2}$	C3(1)	sec	30.0
$K_{q,T,3}$	C5(1)	per sec.	0.05
$K_{p,T,1}$	C3(2)	per ft.	-0.001 *
$K_{p,T,2}$	C4(2)	sec	30.0
$K_{p,T,3}$	C5(2)	per sec	0.05
$K_{r,1}$	C3(3)	per ft.	0.004
$K_{r,2}$	C4(3)	sec	3.8
$K_{r,3}$	C5(3)	per sec.	0.05

* The minus value takes the place of the minus signs in the $\dot{\phi}_T$ equation. (See page 21 of NASA report.)

MOTION BASE WASHOUT PARAMETERS
TABLE 6.1 (Cont'd)

VARIABLE		UNITS	VALUE
MATH	COMPUTER		
	SCALE AIRPLANE ANGULAR RATES		
K_p	C6(1)	-	0.7
K_q	C6(2)	-	0.5
K_r	C6(3)	-	0.2
	TRANSLATIONAL WASHOUT		
a_1	C7(1)	rad/sec	1.414
a_2	C7(2)	rad/sec	2.1
a_3	C7(3)	rad/sec	2.1
b_1	C8(1)	rad/sec	1.0
b_2	C8(2)	rad/sec	2.25
b_3	C8(3)	rad/sec	2.25

Visual System Drive

The visual system used during the RDC study was a T.V. viewed model type called a Visual Flight Attachment (VFA), made by Redifon of England.

The VFA T.V. camera is mounted on a moving platform which can be moved over the model. The moving platform is driven by servos with the controlling signals originating in a "mini" digital computer. The drive algorithms, which were supplied by Redifon*, are calculated in the mini computer. The basic aircraft position, rate and orientation signals are calculated and transformed to the pilot's eye position in the main simulation computer. These signals are then transmitted to the mini over an analog link.

The main simulation computer calculates the input signals for the VFA at a frame rate of 20 per second. The mini does its calculations at a frame rate of 50 per second.

It should be mentioned that the analog link is just that, the signals from the main computer are put through digital to analog converters (DAC's) and transmitted over analog trunk lines to the VFA area where they are re-digitized by an analog-to-digital converter (ADC) and sent to the mini. It also should be mentioned that it is generally felt that an analog link is probably not the best way to interface two digital computers!

---

* See Reference 10.

APPENDIX B

SOFTWARE ANTISKID

The software antiskid model defined in Ref. 4 , "DC-9 Landing Gear Math Model For Directional Control on Runway Flight Simulation", pages 36-38, was changed slightly to simplify the logic, decrease compute time and obtain the desired performance. This appendix will document those changes. The same notation is used here except the subscript, j, has been deleted in this appendix with the understanding that the equations and diagrams apply to both right and left main gears.

Figure B1 is a flow chart of the antiskid system as implemented in STRUTS, the Douglas subroutine implementation of the above report. Figure B2 is a typical time history of braking force with period Cp and duty C_t. In the original model, when $F_{BCOM} > F_{BON}$ (see Figure B1) antiskid cycling is started. In STRUTS, this decision point was made independent of C_t because at high speeds on wet runways C_t is small which makes F_{BON} large and the antiskid did not cycle as desired. In STRUTS, F_{BCOM} is compared to the product of the effective coefficient of friction, μ_D, normal tire load, F_E, and a constant, 1.35, to determine the onset of antiskid cycling. F_{BCOM} was also increased by changing the effective braking area from 5 to 8 square inches. In retrospect, this value of F_{BCOM} was probably too high. However, since maximum performance stops were used on most test runs, the high command level was not obvious. The precise onset of antiskid cycling was not investigated.

During checkout of the simulation, the antiskid system was evaluated by Douglas pilots and compared with the analog (hardware) antiskid system. The result of this check was a modification to the period and duty of the antiskid cycling. This change is illustrated in Figure B3. The period, C_p, was increased 0.8 seconds over the entire speed range and the duty, C_t, was increased for wet and flooded runway conditions.

SOFTWARE ANTISKID

FIGURE B1

FLOW CHART

TYPICAL (RIGHT & LEFT)

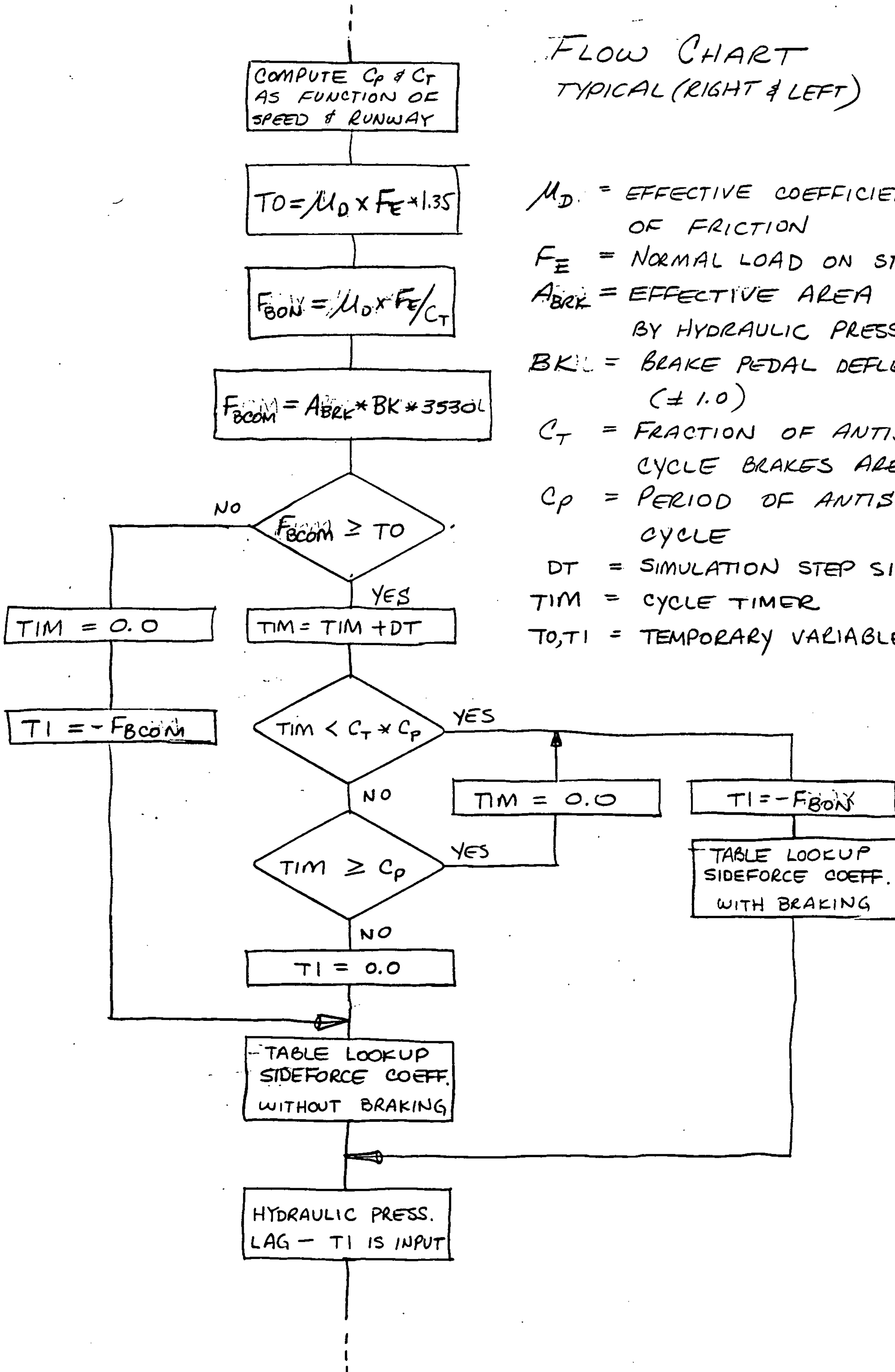

μ_D = EFFECTIVE COEFFICIENT OF FRICTION

F_E = NORMAL LOAD ON STRUT

A_{BRK} = EFFECTIVE AREA WORKED BY HYDRAULIC PRESSURE

BK = BRAKE PEDAL DEFLECTION ($\neq 1.0$)

C_T = FRACTION OF ANTISKID CYCLE BRAKES ARE ON

C_P = PERIOD OF ANTISKID CYCLE

DT = SIMULATION STEP SIZE

TIM = CYCLE TIMER

TO, TI = TEMPORARY VARIABLES.

RDC PROGRAM - DIGITAL ANTISKID

C_P - PERIOD OF ANTISKID CYCLES
C_T - FRACTION OF PERIOD BRAKES ARE ON (DUTY)

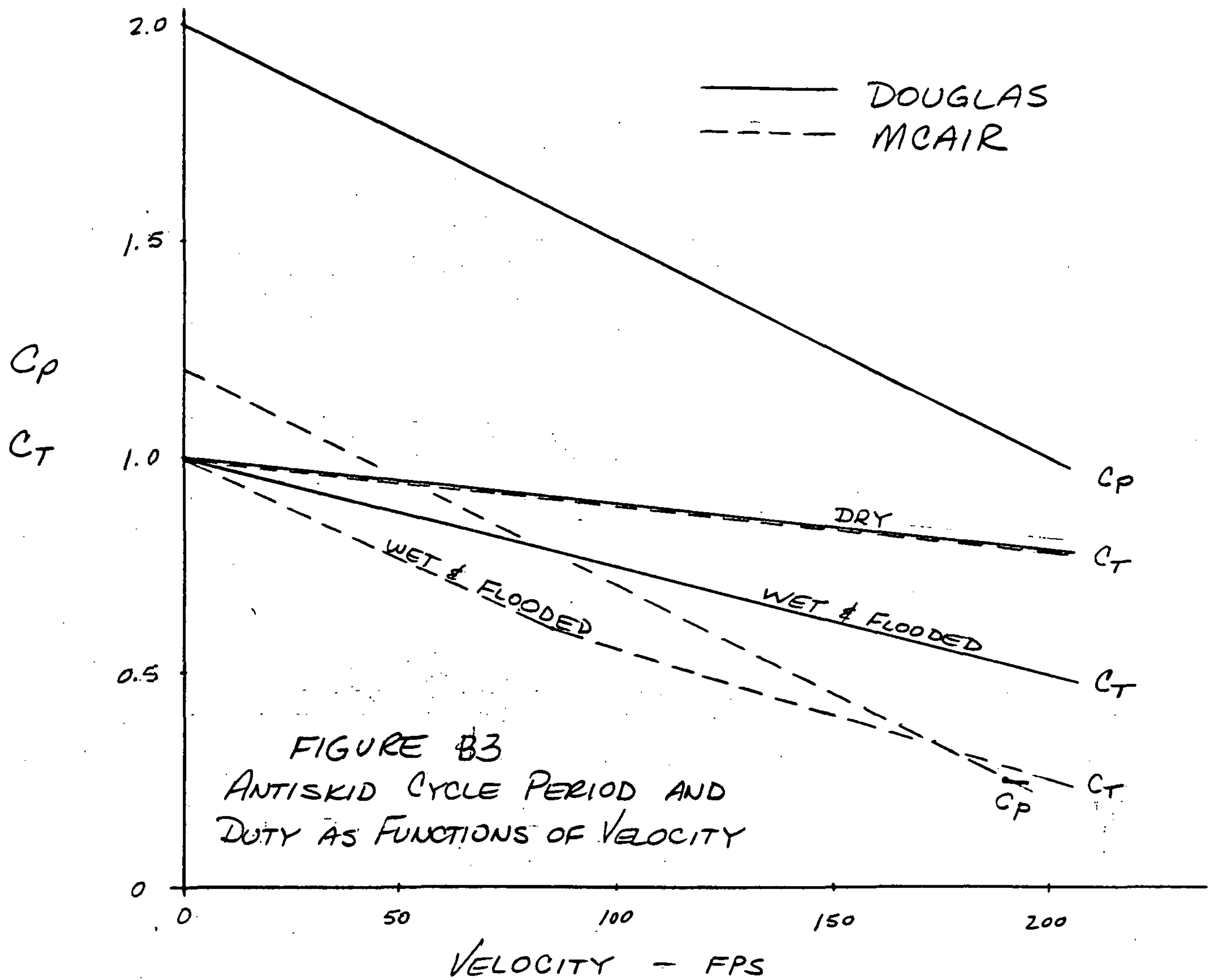

FIGURE B3
ANTISKID CYCLE PERIOD AND
DUTY AS FUNCTIONS OF VELOCITY

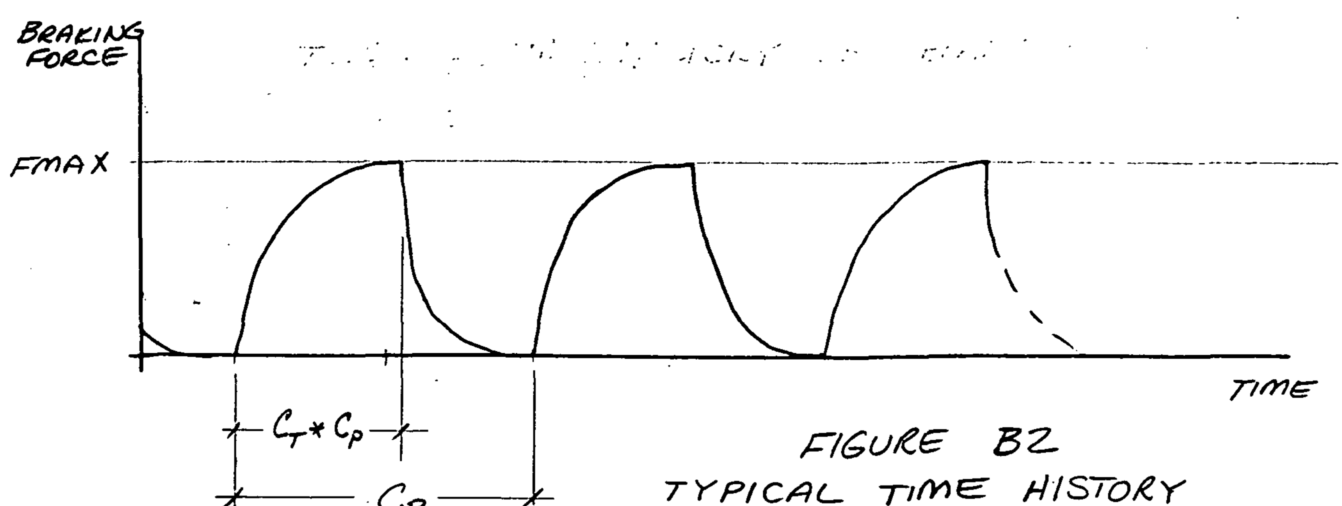

FIGURE B2
TYPICAL TIME HISTORY
OF BRAKING FORCE

APPENDIX C
ANALOG/HARDWARE ANTISKID

Section 1. INTRODUCTION

The analog/hardware antiskid simulator is a system that produces real time drag and cornering tire forces for the aircraft simulation. The system consists of an analog computer and actual aircraft hardware implemented as shown in Figure C-1.

The analog computer receives inputs from the digital aircraft simulation and brake pressure from the hydraulics and calculates in real time the tire drag and cornering forces and wheel speed. The wheel speed is output to the antiskid control box and the forces are output to the aircraft simulation. The antiskid control box produces an antiskid control valve signal that controls brake pressure.

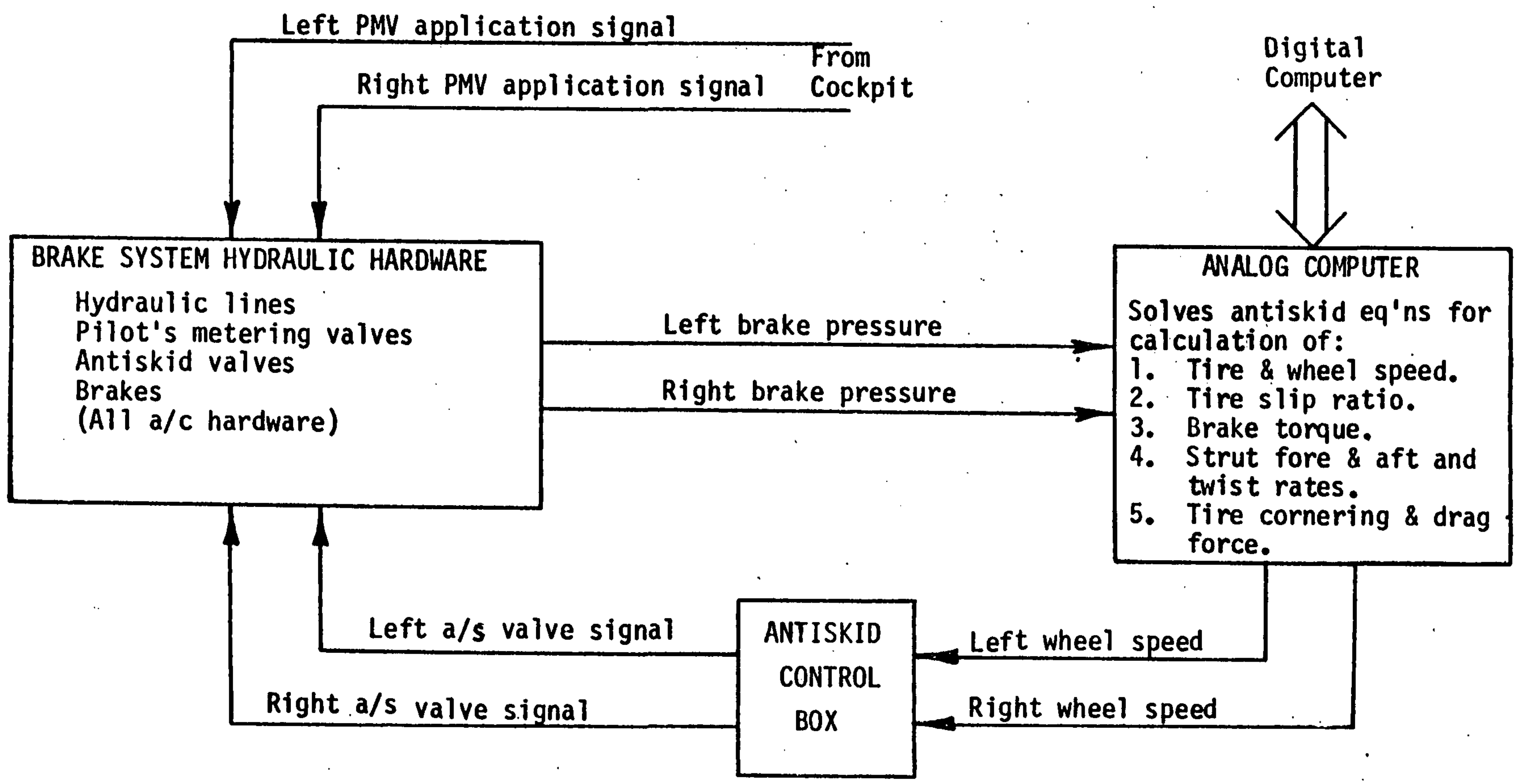

FIGURE C-1 ANALOG ANTISKID BLOCK DIAGRAM

Section 2. MODEL DERIVATION

The math flow diagram of the model for one strut is shown in Figure C-2. Both strut mechanizations are identical. These equations are implemented on an analog computer because of the high frequencies involved.

PRIMARY TIRE CORNERING AND DRAG FORCE

Originally it was planned to generate tire cornering and drag forces similarly to the method developed in Exhibit A of Reference 2. However, the method gave excessive side loads in the unbraked condition. Figure C-3 illustrates this problem. A new empirical method was developed based on data from Reference 5. This new method is developed in Primary Tire Cornering and Drag Force Analysis.

SECOND TIRE CORNERING AND DRAG FORCES, STRUT FORE-AFT AND TWIST RATES, BRAKE TORQUE, TIRE AND WHEEL SPEED, AND TIRE SLIP RATIO

The remainder of the items shown in Figure C-3 are developed in the above named analysis.

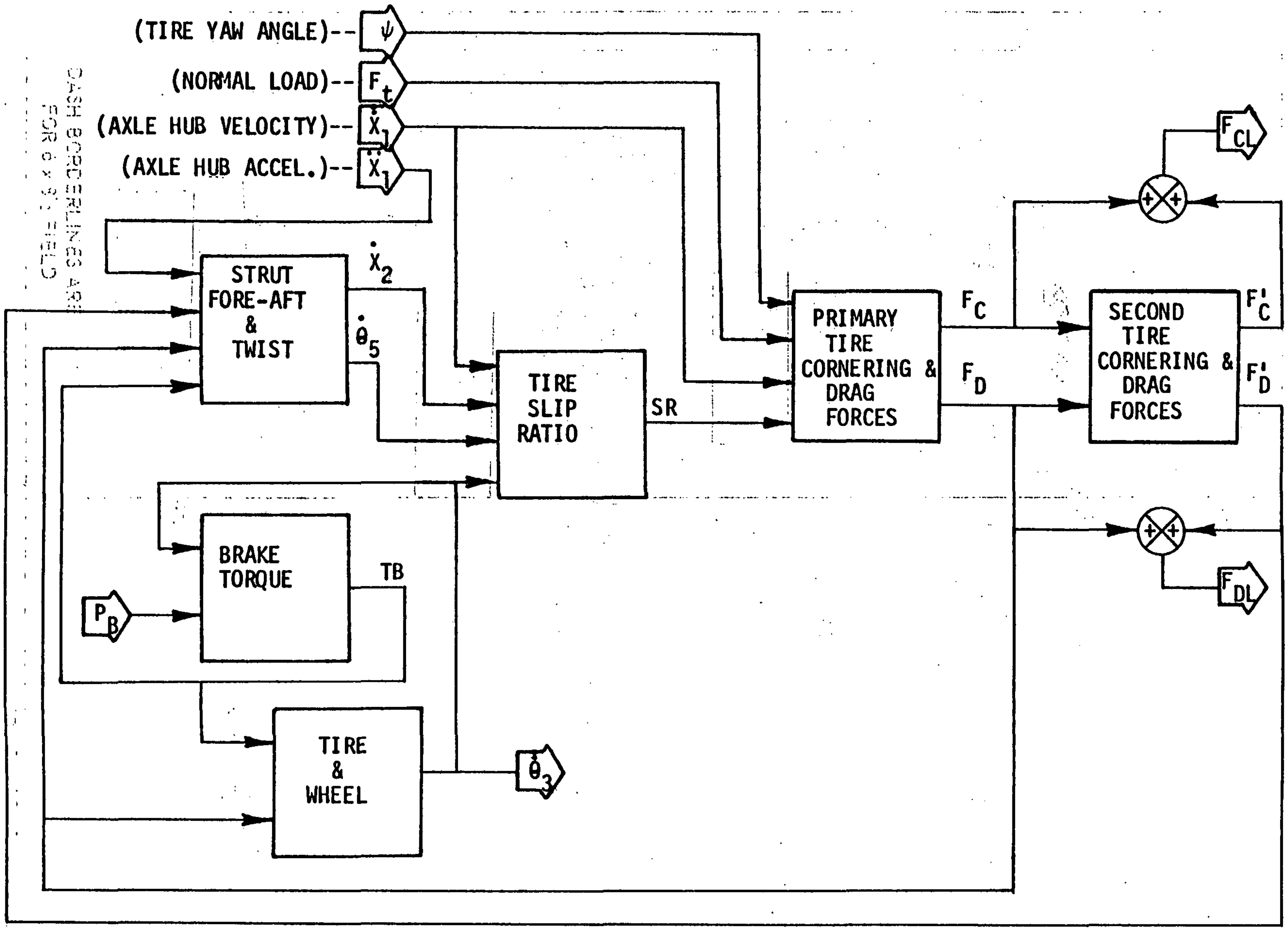

FIGURE C-2 MATH FLOW BLOCK DIAGRAM - STRUT EQUATIONS

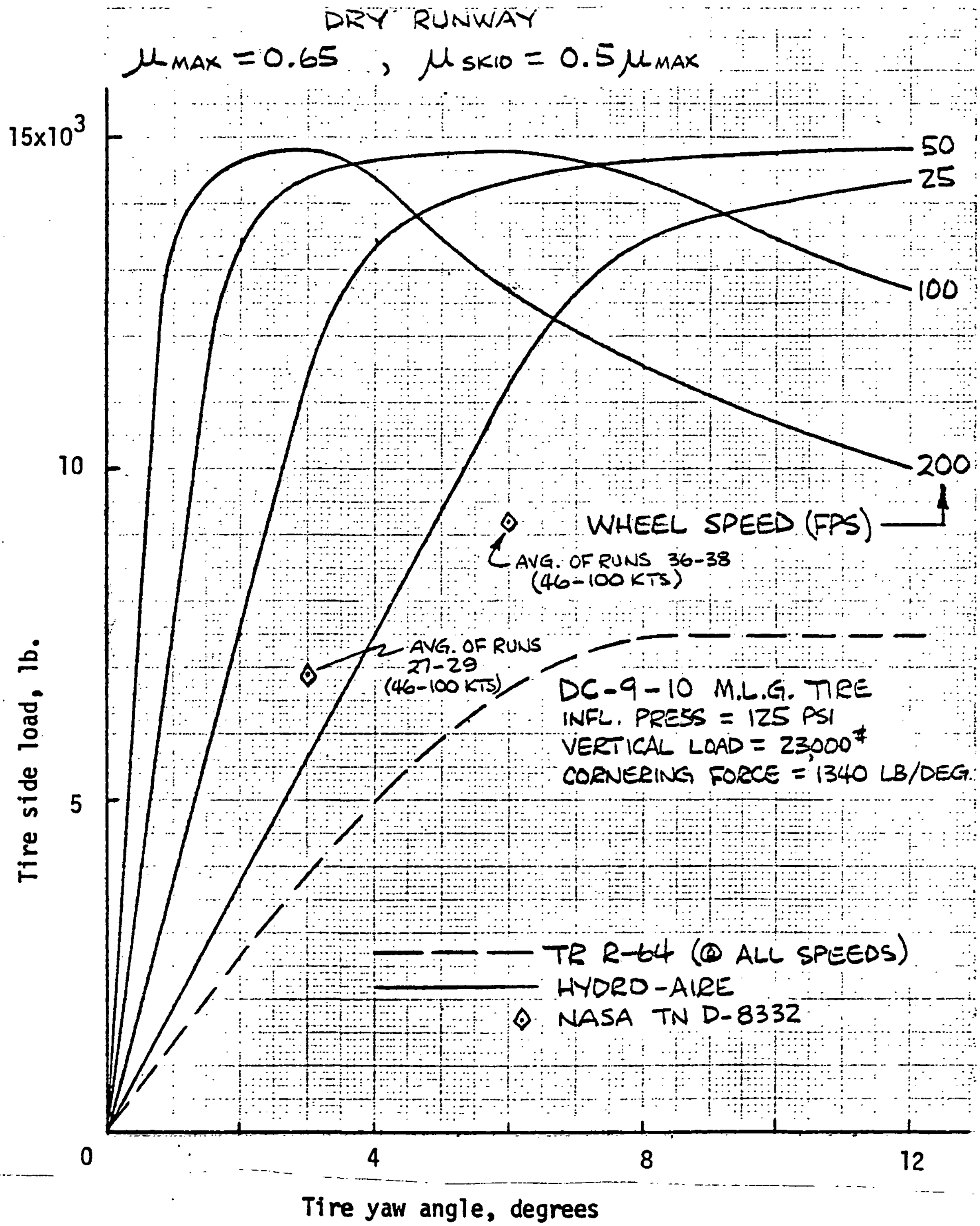

FIGURE C-3 COMPARISON OF HYDRO AIRE'S TIRE CORNERING THEORY WITH THAT OF NASA TR R-64 --- WITHOUT BRAKING

INTRODUCTION

THIS SECTION DEVELOPS, DESCRIBES, AND CORRELATES THE FRICTION FORCE MODELS USED FOR CORNERING AND DRAG IN THE ANALOG ANTISKID SIMULATION.

THE MODEL WAS DEVELOPED TO EXHIBIT THE TRENDS SHOWN IN TESTING CONDUCTED AT NASA LANGLEY AIRCRAFT LANDING LOADS AND DOCUMENTED IN REFERENCE 1. THE MODEL ALSO EXHIBITS EXPECTED LARGE ANGLE PERFORMANCE.

THE MODEL BASICALLY REDUCES THE UNBRAKED CORNERING FORCE AS A FUNCTION OF SLIP RATIO AND REDUCES THE DRAG FRICTION FORCE WITH INCREASING TIRE YAW ANGLE.

MODEL DEFINITION

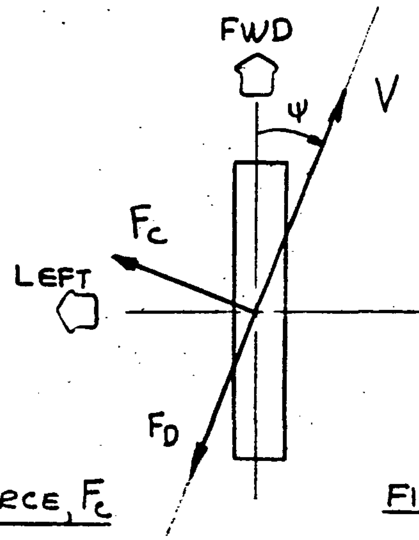

CORNERING FRICTION FORCE, F_C

FIGURE 1
TIRE FORCES

THE CORNERING FRICTION FORCE IS DETERMINED BY REDUCING THE UNBRAKED CORNERING FORCE AS A FUNCTION OF INCREASING SLIP RATIO.

UNBRAKED CORNERING FORCE, F_{CO}

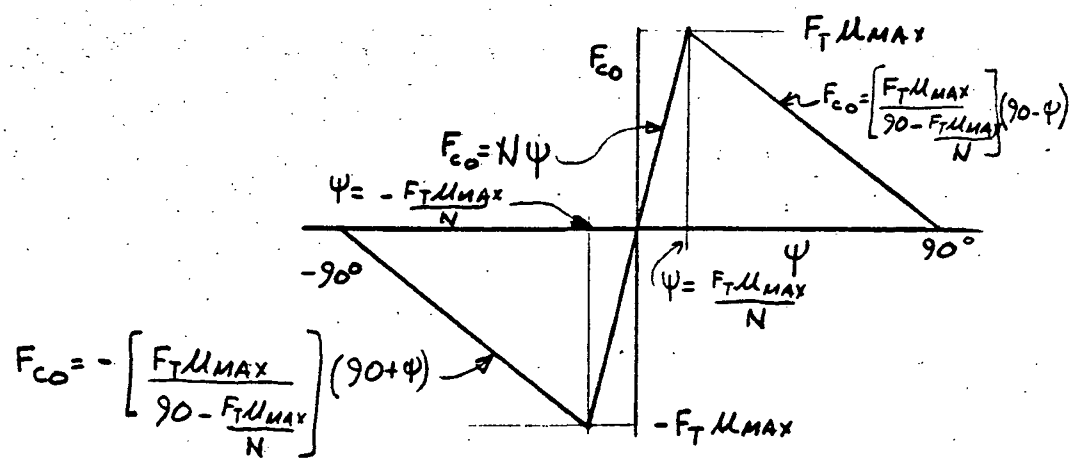

FIGURE 2 UNBRAKED CORNERING FORCE

FOR SMALL YAW ANGLES

EQN 1 $\quad F_{CO}=N\psi \qquad \left(-\frac{F_T\mu_{MAX}}{N}<\psi<\frac{F_T\mu_{MAX}}{N}\right)$

WHERE N = TIRE CORNERING POWER
ψ = TIRE YAW ANGLE
μ_M = MAXIMUM TIRE FRICTION COEFFICIENT
F_T = TIRE NORMAL LOAD

FOR LARGE POSITIVE YAW ANGLES

EQN 2
$$F_{CO} = \left(\frac{F_T \mu_{MAX}}{90 - \frac{F_T \mu_{MAX}}{N}} \right) (90 - \psi) \qquad \left(\frac{F_T \mu_{MAX}}{N} \leq \psi < 90^\circ \right)$$

FOR LARGE NEGATIVE YAW ANGLES

EQN 3
$$F_{CO} = -\left(\frac{F_T \mu_{MAX}}{90 - \frac{F_T \mu_{MAX}}{N}} \right) (90 + \psi) \qquad \left(-90 < \psi \leq -\frac{F_T \mu_{MAX}}{N} \right)$$

NOTE: THIS REPRESENTATION IS A SIMPLIFICATION OF A PROCEDURE THAT CAN BE DEVELOPED USING RELATIONSHIPS GIVEN IN REFERENCE 2. THIS PROCEDURE WOULD BE AS FOLLOWS: (EQN NUMBERS ARE FOR REF 2)

1. DETERMINE TIRE DEFLECTION δ FROM NORMAL LOAD F_Z USING EQNS 23 & 24.
2. DETERMINE CORNERING POWER N FROM TIRE DEFLECTION WITH EQN 82.
3. DETERMINE TIRE NORMAL FORCE $F_{\psi, r, e}$ FROM TIRE YAW ANGLE ψ AND CORNERING POWER WITH EQNS 79 & 80.
4. DETERMINE CORNERING FORCE F_c FROM NORMAL FORCE WITH EQN 81.

THE CORNERING FORCE F_C IS DETERMINED BY REDUCING F_{C_0} WITH INCREASING SLIP RATIO.

EQN 4 $$F_C = F_{C_0} \cdot f_S(SR)$$

WHERE SR = SLIP RATIO

$f_S(SR)$ = MONOTONICALLY DECREASING FUNCTION WITH A VALUE OF 1. AT SR=0, 0 AT SR=1., AND ADJUSTED TO DUPLICATE EXPERIMENTAL RESULTS BETWEEN. (FIGURE 3)

DRAG FRICTION FORCE

THE DRAG FRICTION COEFFICIENT RATIO $\frac{\mu}{\mu_{MAX}}$ IS

EQN 5 $$\frac{\mu}{\mu_{MAX}} = f_3(SR, \psi)$$

WHERE $f_3(SR, \psi)$ IS AN EXPERIMENTALLY DETERMINED FUNCTION AS SHOWN IN FIGURE 4.

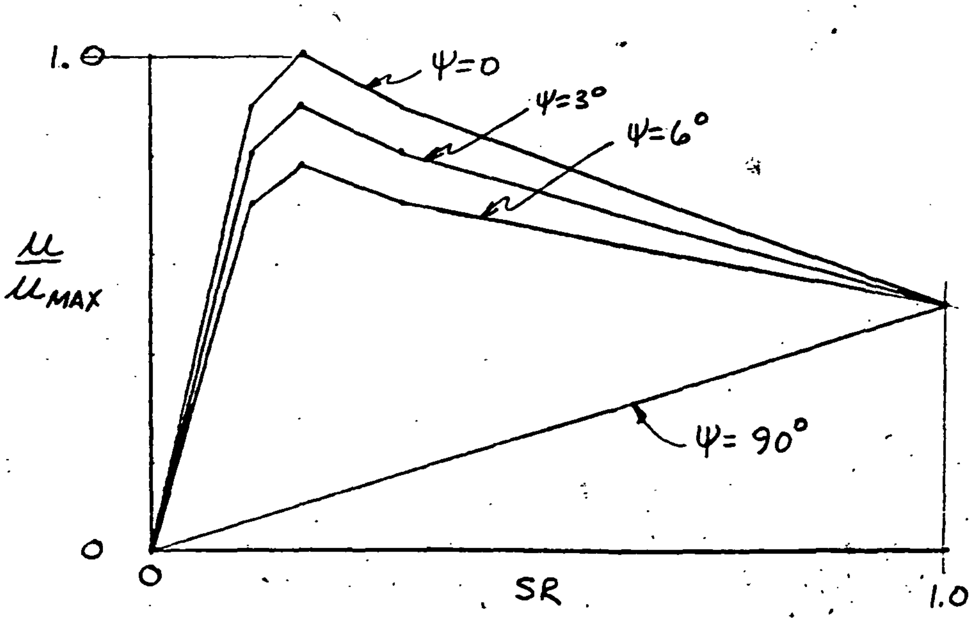

$$f_3(SR,\psi) = f_{3B}(SR) + f_{3A}(SR) \times f_{3C}(\psi)$$

WHERE, $f_{3A}(SR)$ IS AS SHOWN IN FIGURE 5,

$f_{3B}(SR)$ " " " " " 6, &

$f_{3C}(\psi)$ " " " " " 7.

THE DRAG FRICTION FORCE IS

EQN 6 $$F_D = \frac{\mu}{\mu_{MAX}} \times F_T \mu_{MAX}$$

MAXIMUM FRICTION COEFFICIENT

THE MAXIMUM FRICTION COEFFICIENT IS EXPRESSED AS A FUNCTION OF VELOCITY

EQN 7 $$\mu_{MAX} = f_4(\dot{X}_1')$$

WHERE $\dot{X}_1'$ = TOTAL VELOCITY

$f_4(\dot{X}_1)$ = FIGURE 19 OF REFERENCE 1 (SHOWN HERE IN FIGURE 8)

BLOCK DIAGRAM

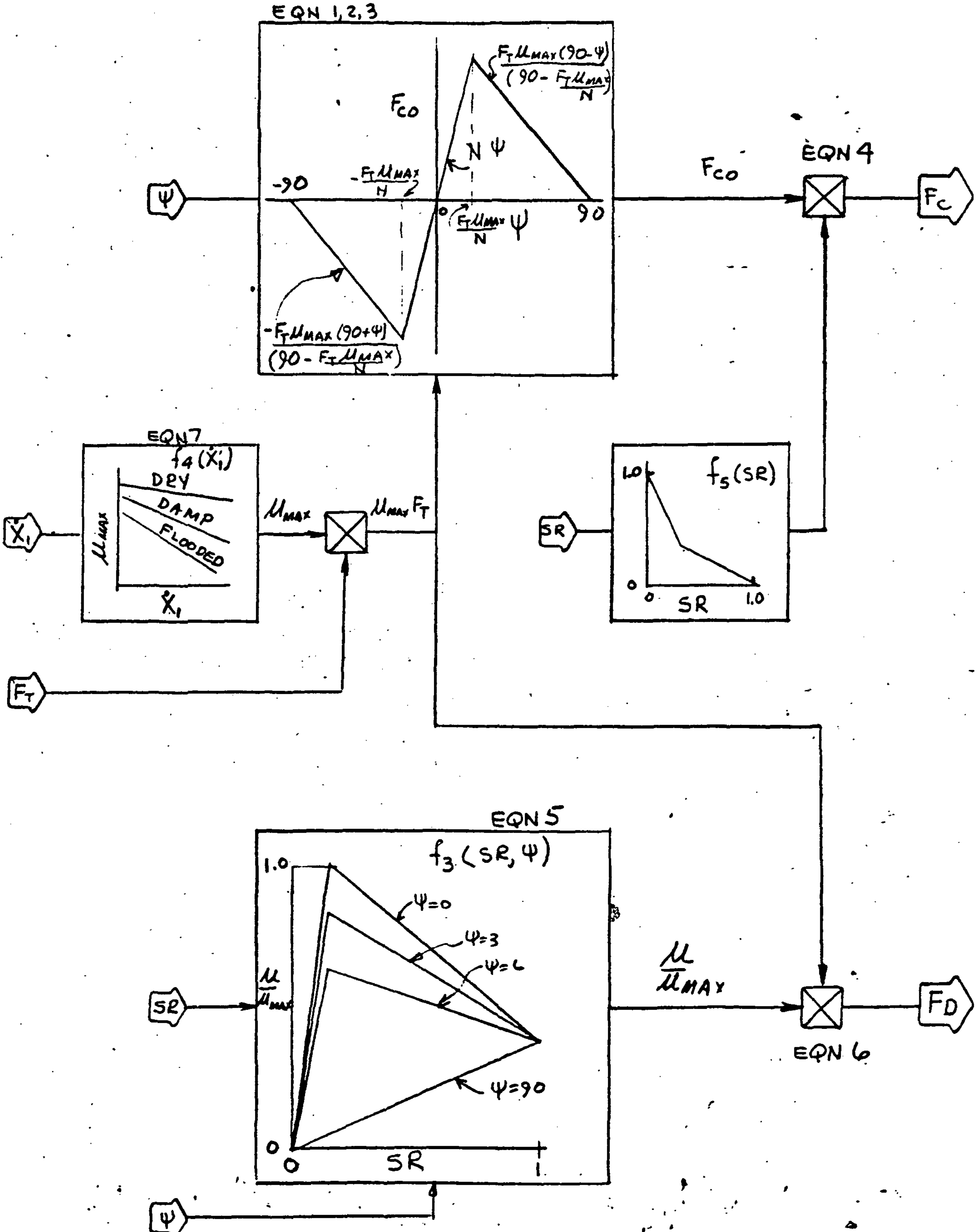

SYMBOLS

SYMBOL	CONSTANT	VARIABLE	NUMERICAL VALUE	UNITS	DESCRIPTION
F_C		X	—	LBS	TIRE CORNERING FORCE PERPENDICULAR TO VELOCITY
F_{CO}		X	—	LBS	ZERO SLIP CORNERING FORCE
F_D		X	—	LBS	TIRE DRAG FORCE PARALLEL TO VELOCITY
F_T		X	—	LBS	VERTICAL TIRE LOAD
$f_3(SR,\psi)$	X		SEE PG 138	—	NORMALIZED μ-SLIP CURVE
$f_4(\dot{X}_1)$	X		SEE PG 141	—	μ_{MAX} - VELOCITY CURVES
$f_5(SR)$	X		SEE PG 137	—	CORNER FORCE REDUCTION VS SLIP RATIO
N	X		1491	LBS/DEG	CORNERING POWER
SR		X	—	—	SLIP RATIO
$\dot{X}_1$		X	—	FT/SEC	TOTAL VELOCITY
ψ		X	—	DEG	TIRE YAW ANGLE
μ_{MAX}		X	—	—	MAXIMUM FRICTION COEFFICIENT
$\frac{\mu}{\mu_{MAX}}$		X	—	—	DRAG FRICTION COEFFICIENT RATIO

$f_s(SR)$ - CORNER FORCE REDUCTION

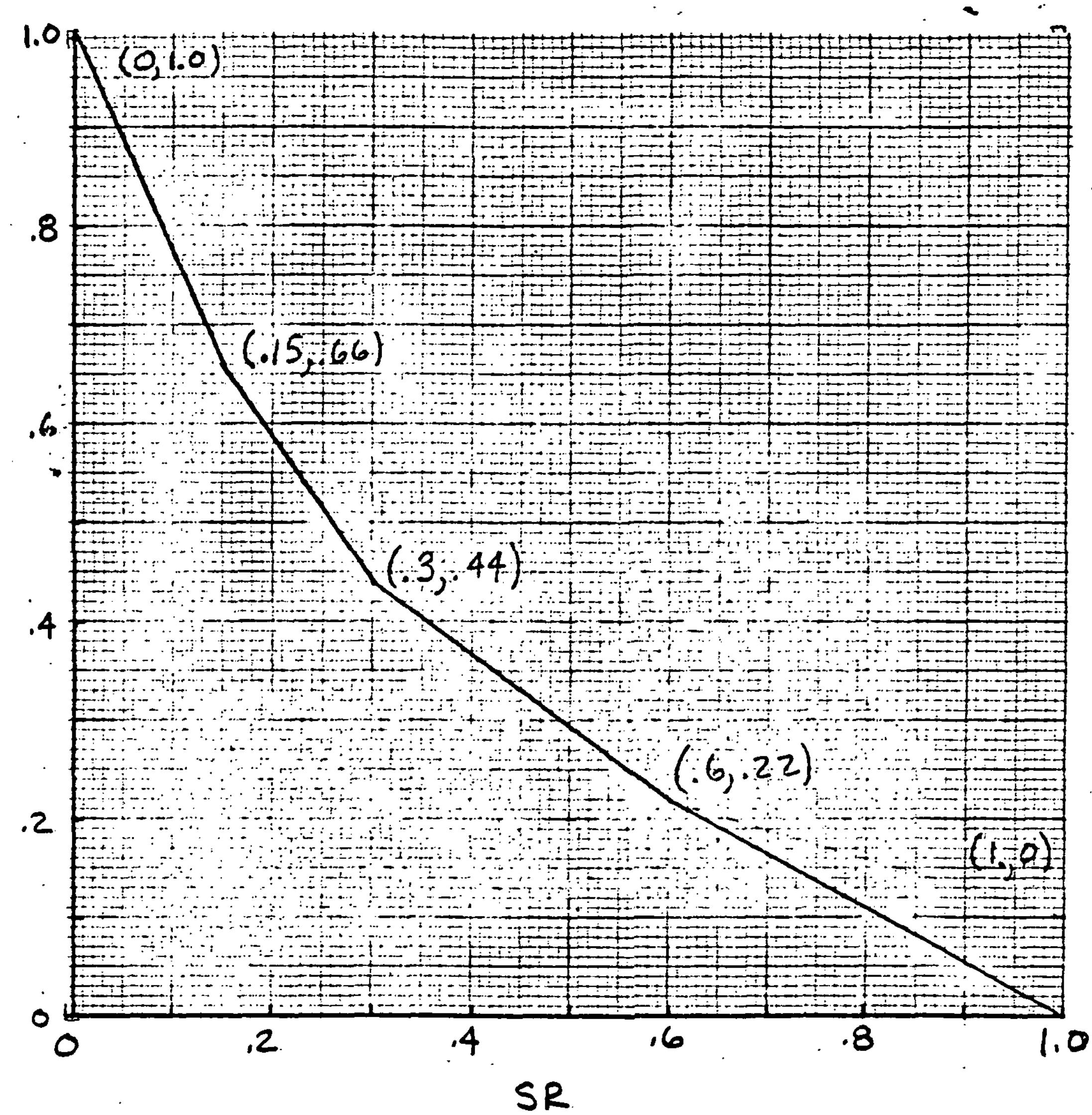

FIGURE 3

$f_3(SR, \psi)$ NORMALIZED μ-SLIP CURVE

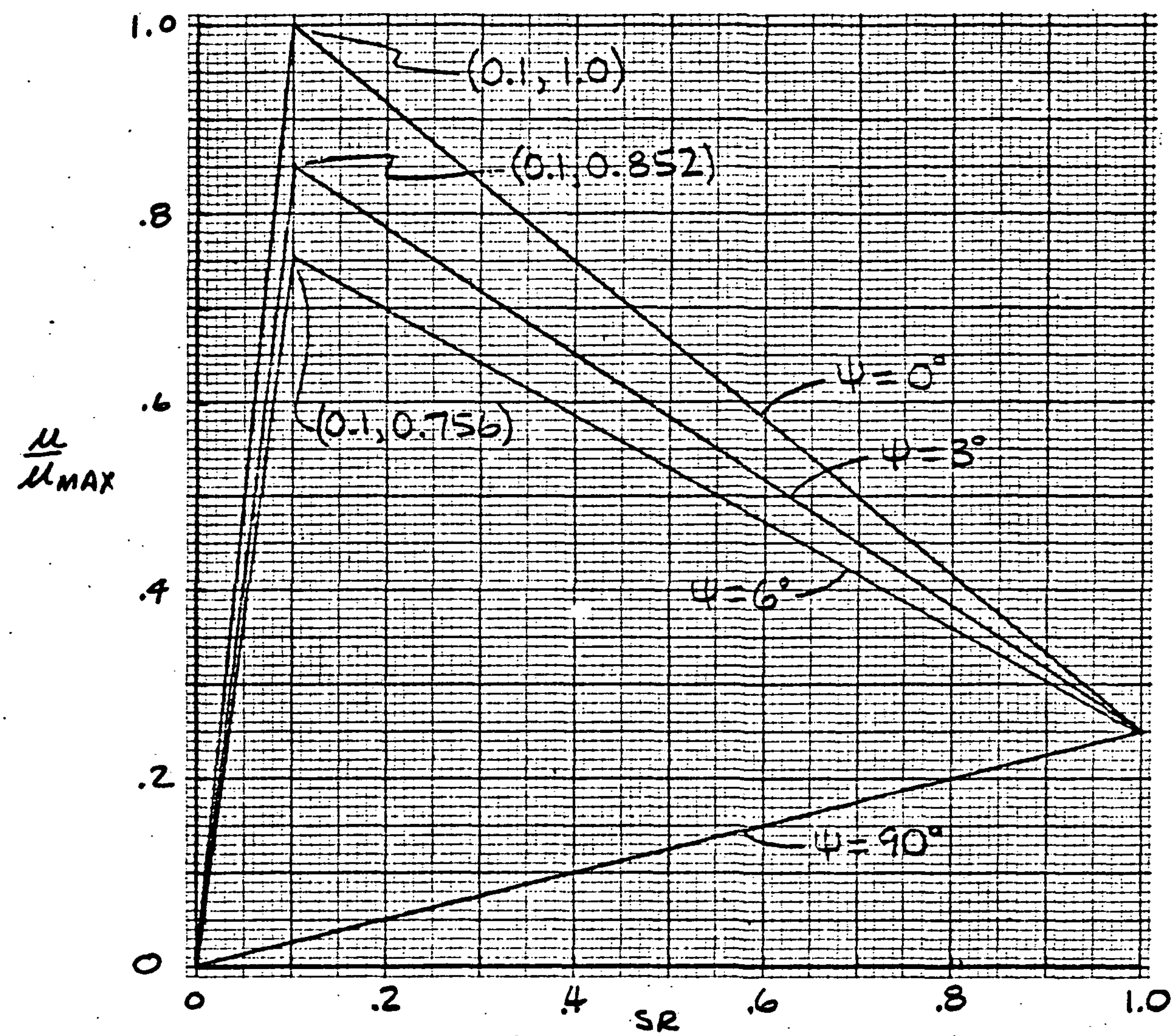

FIGURE 4

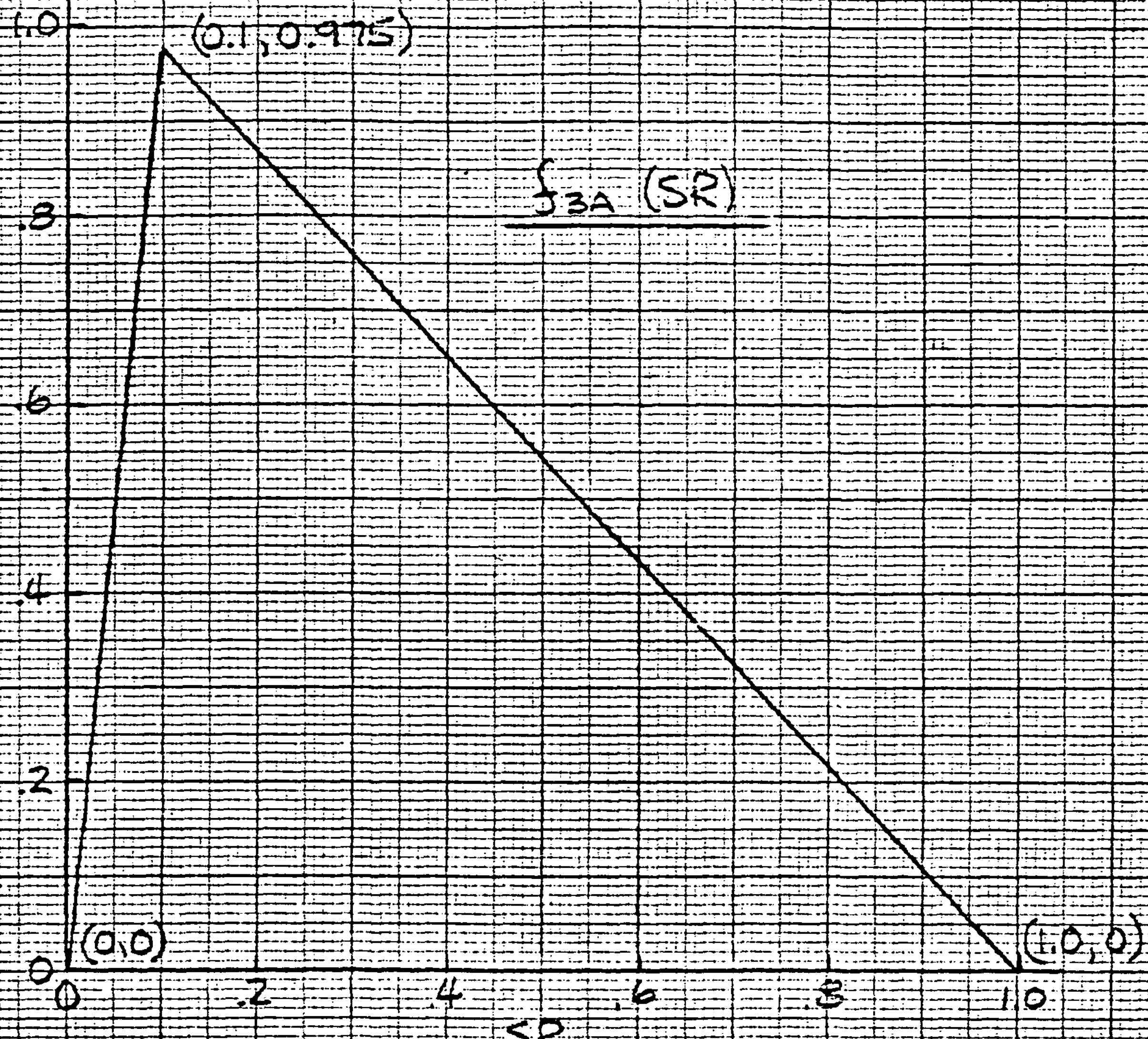

FIGURE 5

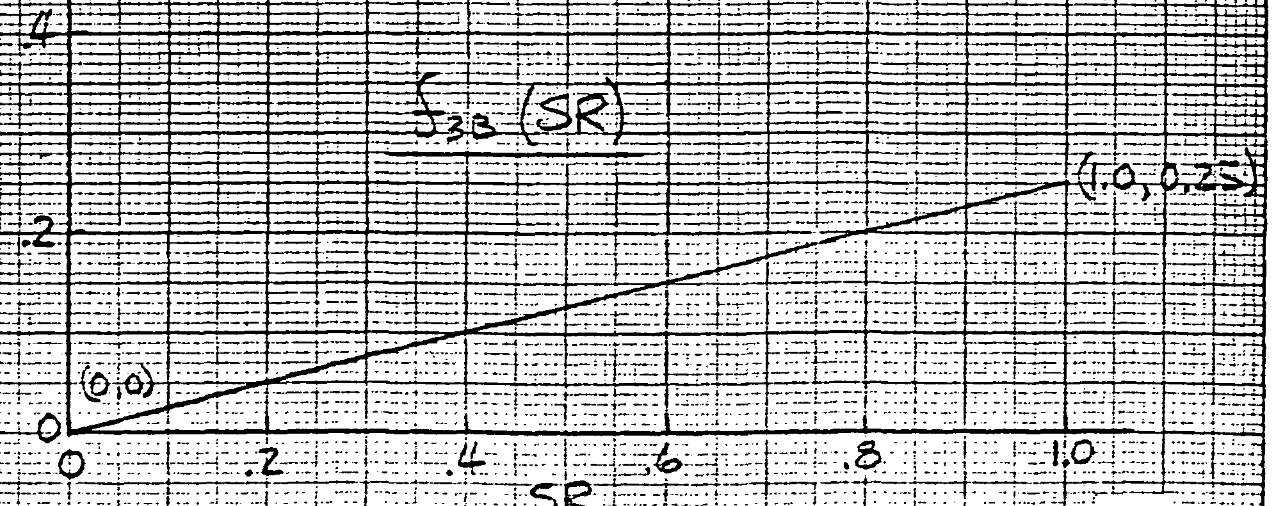

FIGURE 6

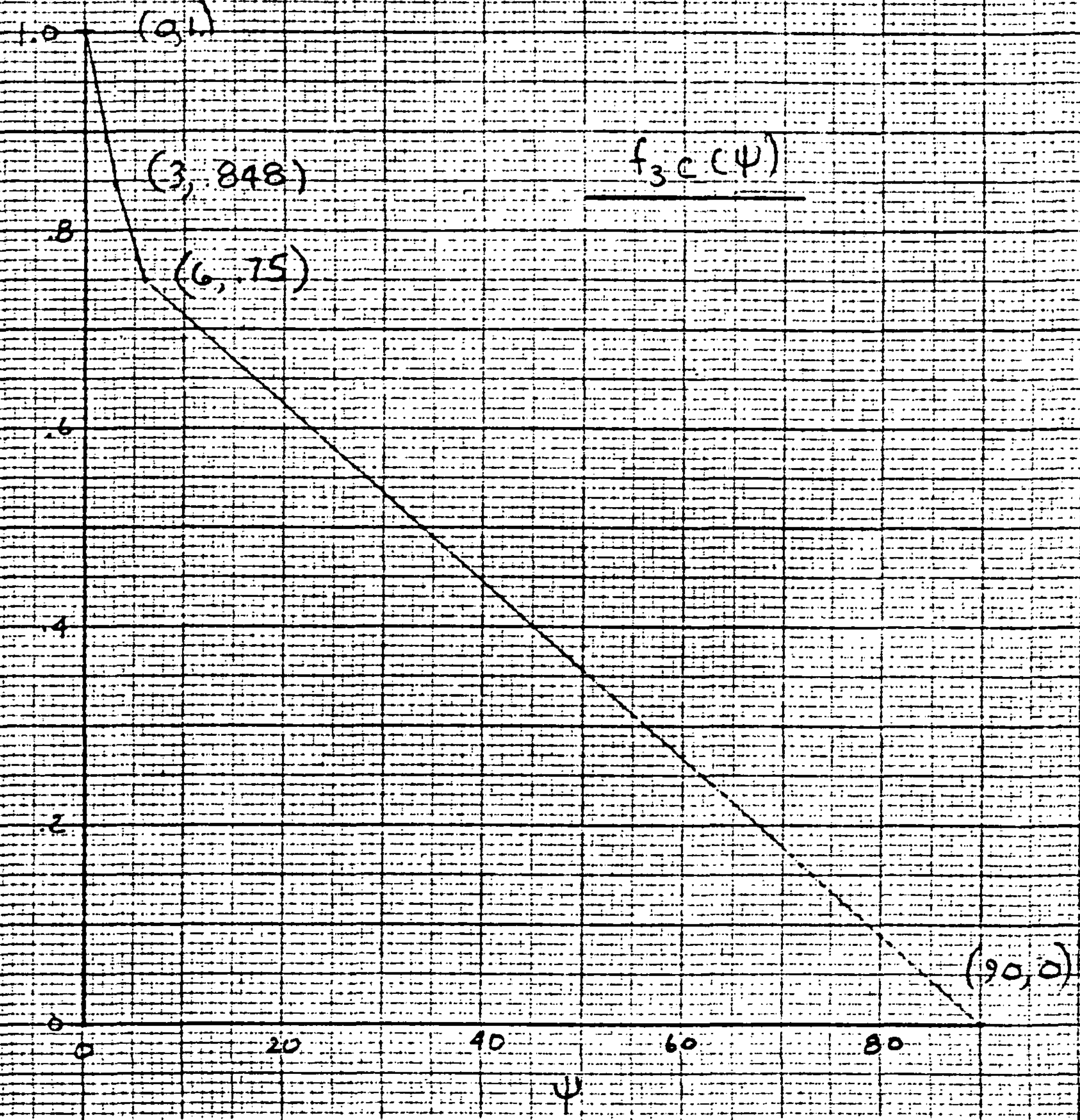

FIGURE 7

μ_{MAX} VERSUS VELOCITY (REF 1 FIG 19)

$f_4(\dot{X}_1)$

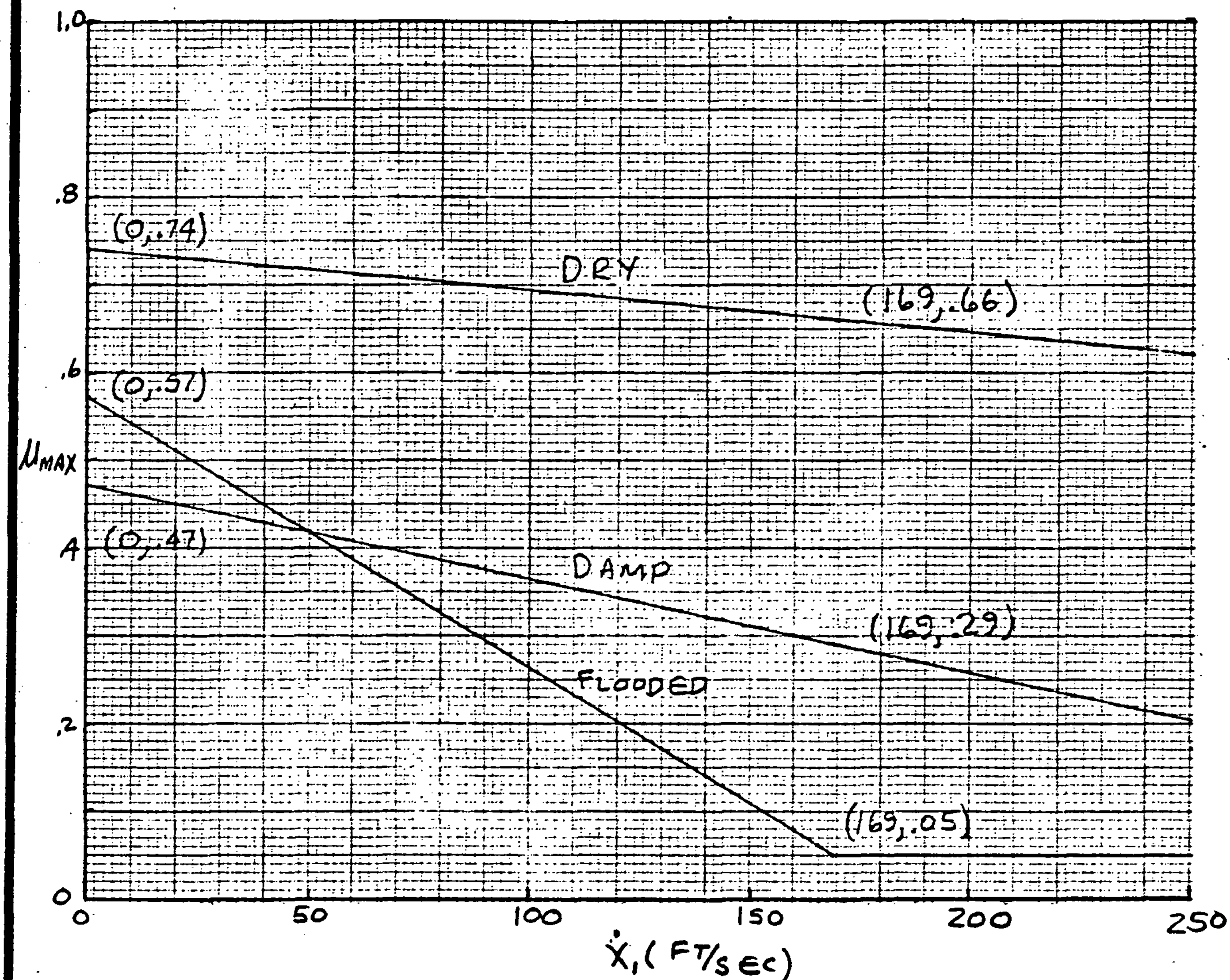

FIGURE 8

MODEL CORRELATION

TO ASSESS THE MODEL ACCURACY, PLOTS OF CORNERING AND DRAG FORCE VERSUS SLIP RATIO WERE MADE USING THE MODEL FOR 6 TEST CONDITIONS TESTED IN REFERENCE 1. TEST DATA IS THEN PLOTTED IN THE PROPER PLOT.

TEST DATA FROM REF 1

CONDITIONS						EXPERIMENTAL VALUES			
RUN.	ψ °	$\dot{X}_1$ FT/SEC	F_T LBS	TIME SEC	S_R —	μ_s —	F_c LBS	μ_d —	F_D LBS
1	0	78	12300	1.4	.02	–	–	.57	7011
				2.0	.04	–	–	.61	7503
				2.5	.08	–	–	.65	7995
				3.0	.09	–	–	.70	8610
				3.5	.10	–	–	.75	9225
				3.9	.12	–	–	.76	9348
				4.05	.9	–	–	.2	2460
27	3	78	13900	.5	0	.32	4448	.05	695
				1.2	.04	.3	4170	.4	5560
				1.5	.09	.29	4031	.59	8201
				2.0	.10	.28	3892	.55	7645
				2.5	.10	.24	3336	.6	8340
				3.0	.12	.22	3058	.64	8896
				3.2	.9	.05	695	.2	2780
36	6	78	18800	2.0	0	.45	8460	.08	1504
				3.5	.04	.4	7520	.5	9400
				4.0	.08	.37	6956	.5	9400
				4.8	.72	.05	940	.25	4700
				6.0	.09	.38	7144	.48	9024
				7.0	.10	.31	5828	.52	9776
				8.0	.13	.3	5640	.58	10904
				8.5	.18	.26	4883	.6	11280

TEST DATA FROM REF 1

CONDITIONS						EXPERIMENTAL VALUES			
RUN	ψ °	$\dot{X}_1$ FT/SEC	F_T LBS	TIME SEC	SR	μ_s	F_c LBS	μ_d	F_D LBS
4	0	166	13700	1.3	.05	-	-	.38	5206
				1.6	.09	-	-	.55	7535
				2.0	.10	-	-	.58	7946
				2.6	.18	-	-	.68	9316
				3.0	.90	-	-	.32	4384
				3.5	.03	-	-	.2	2740
				4.0	.06	-	-	.38	5206
				5.0	.08	-	-	.5	6850
				6.0	.10	-	-	.6 (.55-.7)	8220
				7.0	.11	-	-	.65 ([illegible])	8905
29	3	169	17000	1.0	.01	.3	5100	.05	850
				2.5	.02	.31	5270	.14	2380
				2.7	.05	.30	5100	.28	4760
				2.8	.08	.30	5100	.38	6460
				3.0	.09	.31	5270	.42	7140
				3.5	.09	.30	5100	.48	8160
				4.0	.10	.31	5270	.50	8500
				4.5	.11	.29	4930	.52	8840
				5.0	.12	.28	4760	.56	9520
38	6	169	18700	1.0	.04	.43	8041	.07	1309
				2.6	.09	.40	7480	.27	5049
				2.75	.12	.34	6358	.40	7480
				3.0	.13	.31	5797	.45	8415
				3.5	.18	.28	5236	.45	8415
				4.0	.20	.20	3740	.45	8415
				4.25	.22	.18	3366	.50	9350
				4.4	.50	.08	1496	.40	7480

ANALYTICAL VALUES COMPUTED BY MODEL

RUN	ψ °	$N\psi$ LBS	$F_T \mu_{MAX}$ LBS	$\dot{X}_1$ FT/SEC	$f_4(V)$ μ_{MAX}	F_T LBS	SR	$f_3(SR,\psi)$ μ/μ_{MAX}	$f_5(SR)$	F_C LBS	F_D LBS
1	0	0	8610	78	.7	12300	0	0	1.00	0	0
							.05	.50	.89	0	4305
							.10	1.00	.77	0	8610
							.15	.96	.66	0	8266
							.20	.915	.58	0	7878
							.40	.75	.37	0	6458
							.60	.58	.22	0	4994
							.80	.415	.11	0	3573
							1.00	.25	0	0	2152
27	3	4473	9730	78	.7	13900	0	0	1.00	4473	0
							.05	.426	.89	3981	4145
							.10	.852	.77	3444	8290
							.15	.82	.66	2952	7979
							.20	.78	.58	2594	7589
							.40	.65	.37	1655	6154
							.60	.515	.22	984	5011
							.80	.38	.11	492	3697
							1.00	.25	0	0	2433
36	6	8946	13160	78	.7	18800	0	0	1.00	8946	0
							.05	.378	.89	7962	4975
							.10	.756	.77	6888	9949
							.15	.725	.66	5904	9541
							.20	.70	.58	5189	9210
							.40	.585	.37	3310	7699
							.60	.47	.22	1968	6185
							.80	.36	.11	984	4738
							1.00	.25	0	0	3290

ANALYTICAL VALUES COMPUTED BY MODEL

RUN	ψ °	$N\psi$ LBS	$F_T \mathcal{U}_{MAX}$ LBS	$\dot{X}_1$ FT/SEC	$f_4(V)$ $\mathcal{U}_{MAX}$	F_T LBS	SR	$f_3(SR,\psi)$	$f_5(SR)$	F_C LBS	F_D LBS
4	0	0	9042	166	.66	13700	0	0	1.00	0	0
							.05	.50	.89	0	4521
							.10	1.00	.77	0	9042
							.15	.96	.66	0	8680
							.20	.915	.58	0	8273
							.40	.75	.37	0	6781
							.60	.58	.22	0	5244
							.80	.415	.11	0	3752
							1.00	.25	0	0	2261
29	3	4473	11220	169	.66	17000	0	0	1.00	4473	0
							.05	.426	.89	3981	4780
							.10	.852	.77	3444	9559
							.15	.82	.66	2952	9200
							.20	.78	.58	2594	8752
							.40	.65	.37	1655	7293
							.60	.515	.22	984	5778
							.80	.38	.11	492	4264
							1.00	.25	0	0	2805
38	6	8946	12408	169	.66	18800	0	0	1.00	8946	0
							.05	.378	.89	7962	4690
							.10	.756	.77	6888	9380
							.15	.725	.66	5904	8996
							.20	.70	.58	5189	8686
							.40	.585	.37	3310	7259
							.60	.47	.22	1968	5832
							.80	.36	.11	984	4467
							1.00	.25	0	0	3102

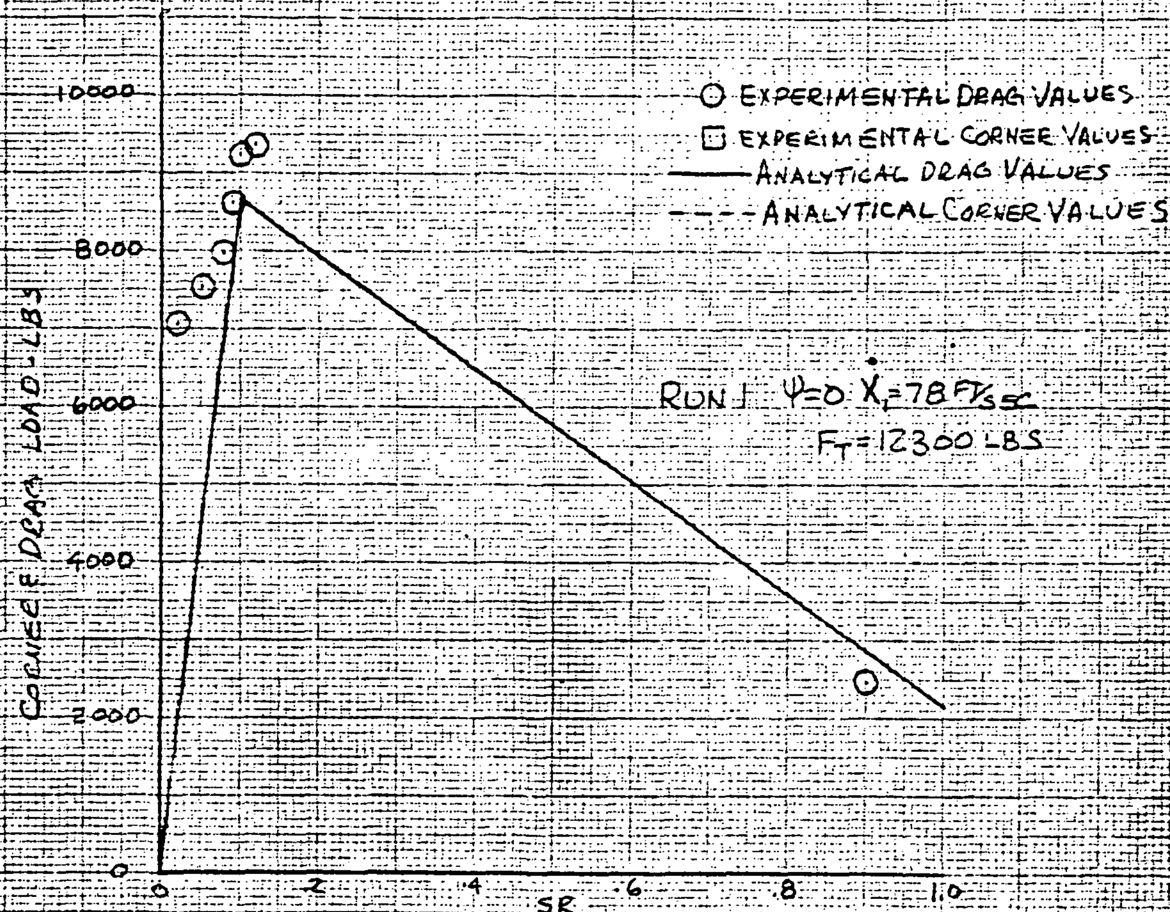

○ EXPERIMENTAL DRAG VALUES
□ EXPERIMENTAL CORNER VALUES
——— ANALYTICAL DRAG VALUES
- - - - ANALYTICAL CORNER VALUES
RUN 1 Ψ=0 Ẋ₁=78 FT/SEC
F_T = 12300 LBS
CORNER DRAG LOAD - LBS
10000
8000
6000
4000
2000
0
0
.2
.4
.6
.8
1.0
SR

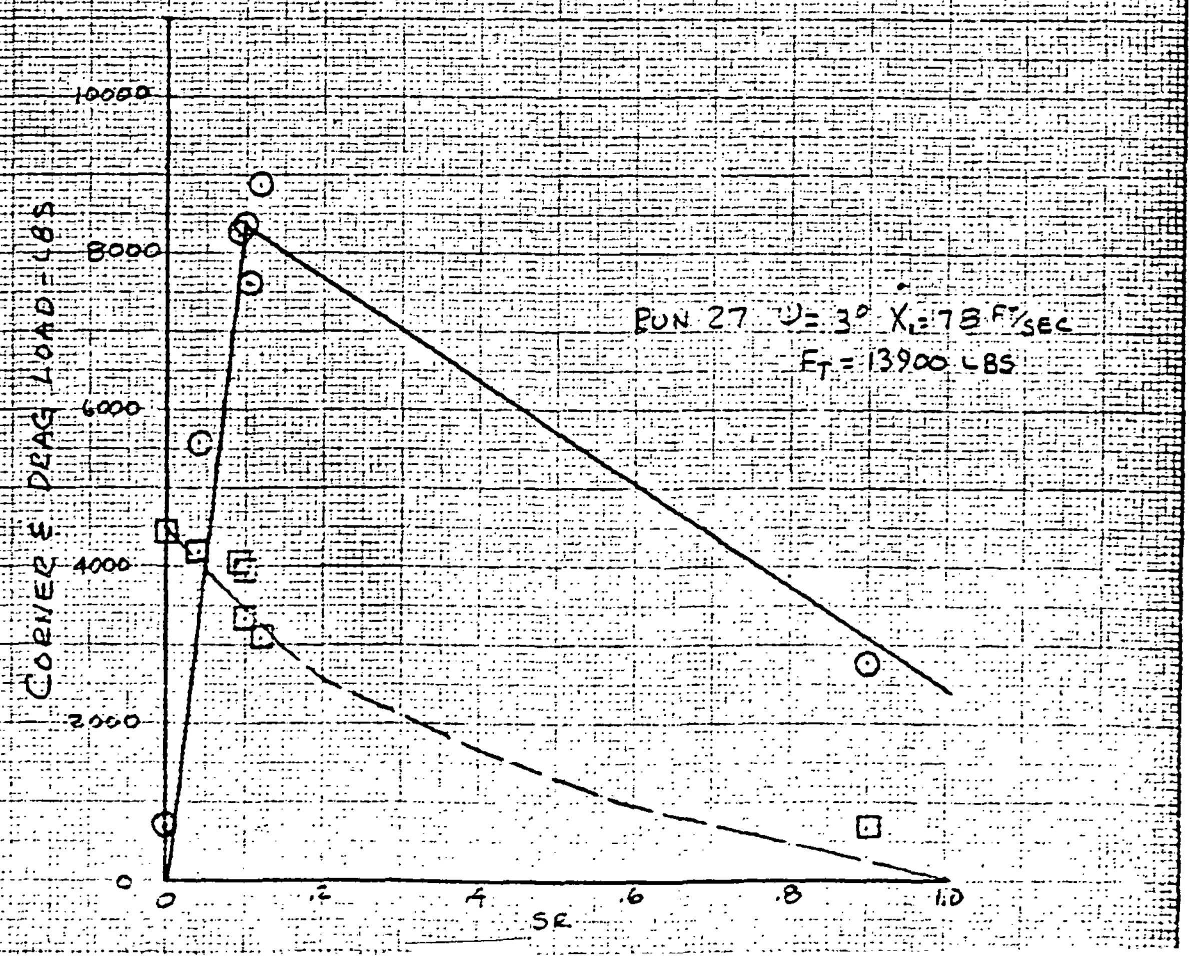

RUN 27 Ψ= 3° Ẋ₁=78 FT/SEC
F_T = 13900 LBS
CORNER & DRAG LOAD - LBS
10000
8000
6000
4000
2000
0
0
.2
.4
.6
.8
1.0
SR

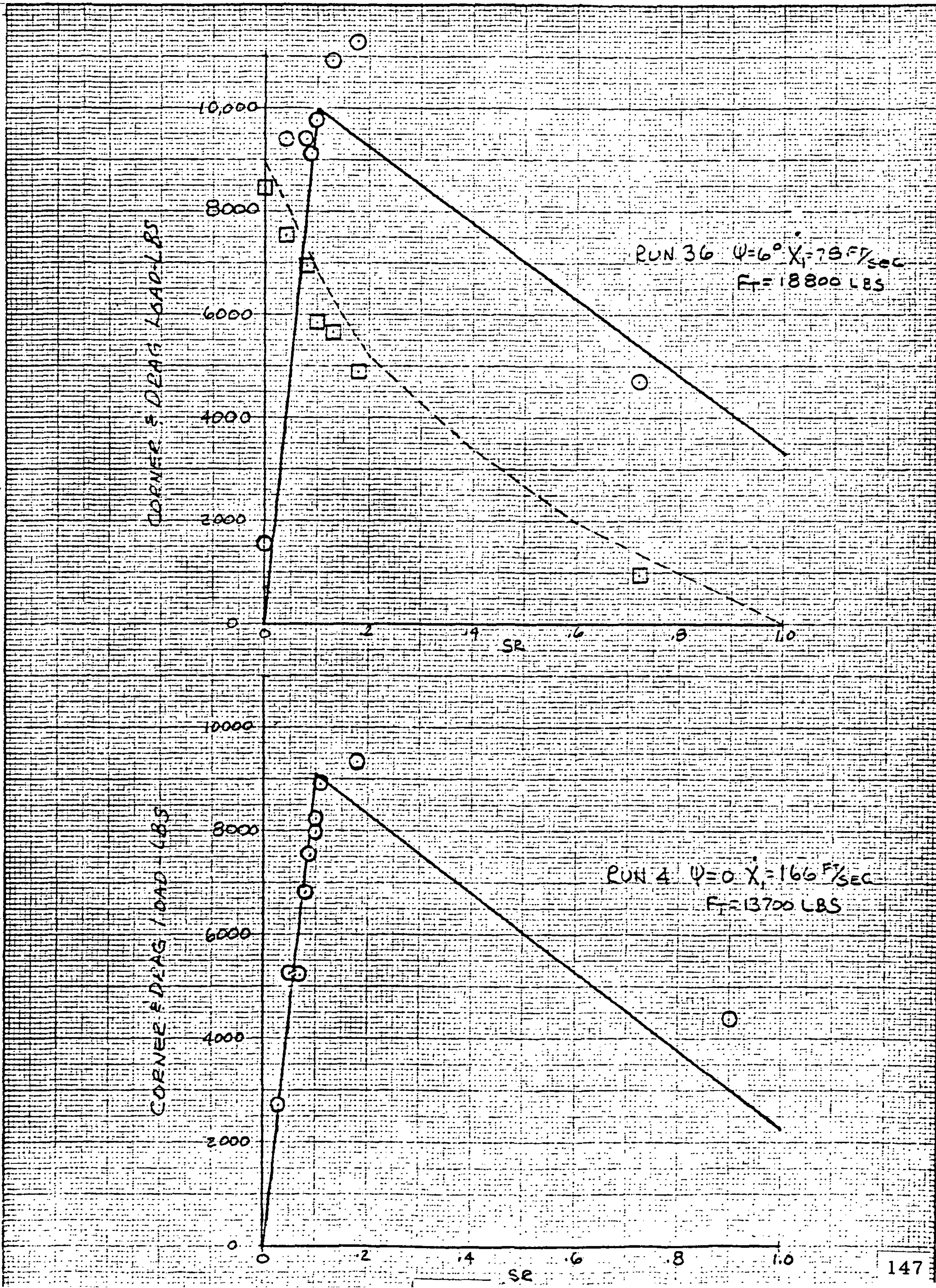

K+E ALBANENE® TRACING PAPER LA 4940

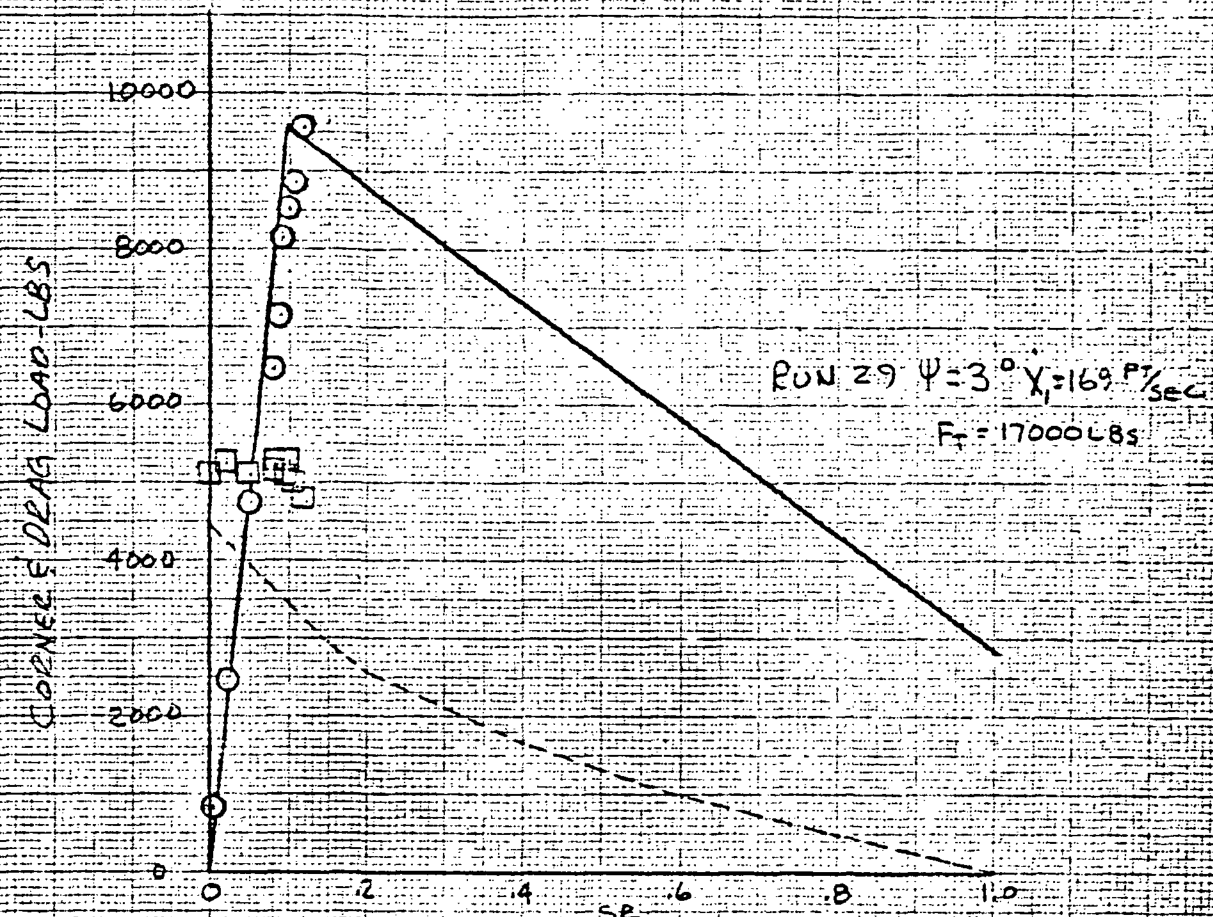

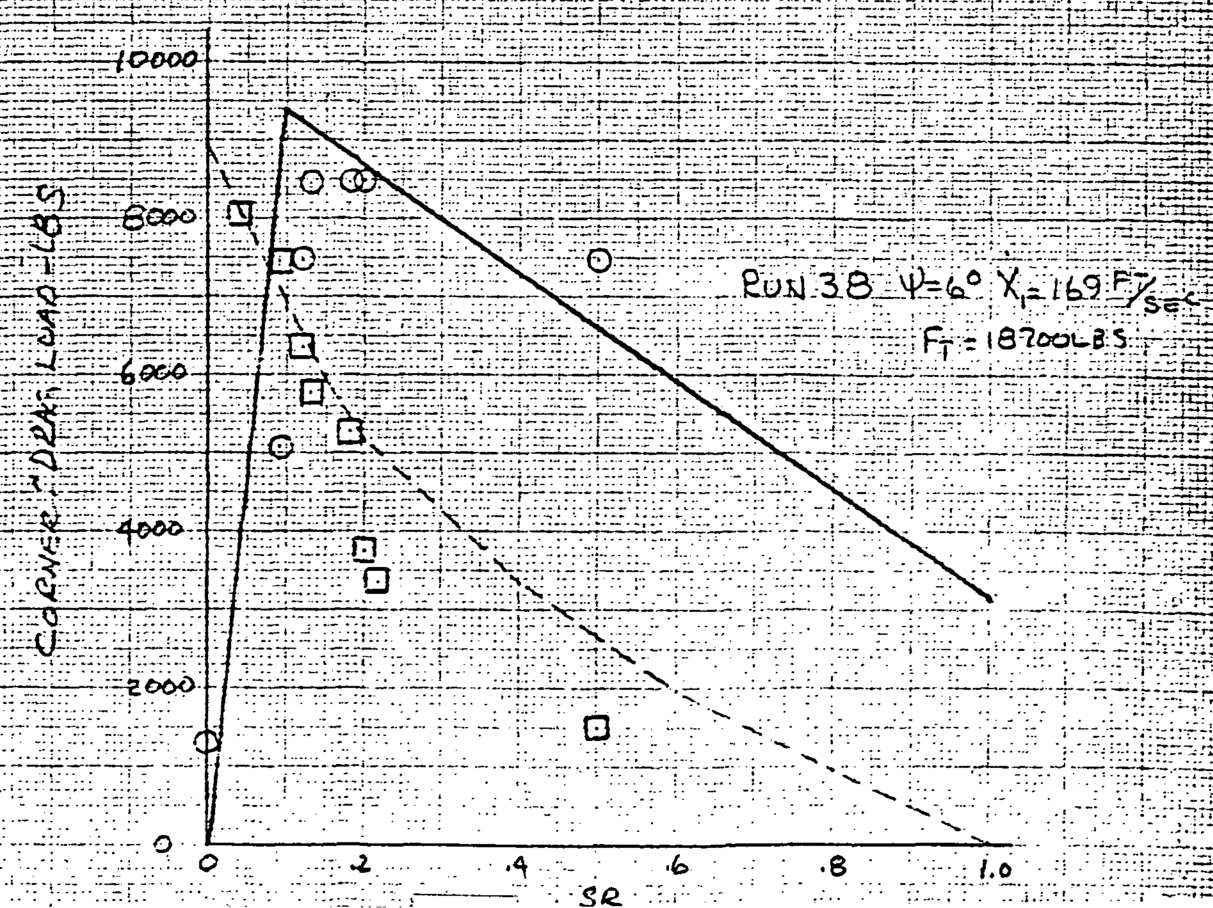

K+E ALBANENE® TRACING PAPER LA 4940

INTRODUCTION

THIS SECTION DEVELOPS THE EQUATIONS FOR STRUT AXLE DEFORMATIONS, BRAKE TORQUE, TIRE AND WHEEL DYNAMICS, AND TIRE SLIP RATIO COMPUTATION.

MODEL DEFINITION

AXLE DEFLECTION

DURING BRAKING THE WHEEL AXLE DEFLECTS. THE DEFLECTIONS ARE LARGE ENOUGH THAT THE DEFLECTION VELOCITIES ARE IMPORTANT CONSIDERATIONS TO THE ANTISKID OPERATION. THE WHEEL AXLE DEFLECTION IS THE SUM OF THE FORE-AFT DEFLECTION OF THE STRUT AND THE AXLE TWIST ABOUT THE STRUT.

STRUT FORE-AFT DEFLECTION

INFLUENCE COEFFICIENTS ARE USED TO DERIVE THE STRUT FORE-AFT EQUATIONS OF MOTION. THE FORCES BENDING THE STRUT ARE DRAG FORCES, BRAKE TORQUE, INERTIA FORCES, AND STRUT DAMPING FORCES.

STRUT DAMPING FORCE - VISCOUS DAMPING IS ASSUMED IN THE MODEL. THE EXPRESSION FOR THE FORCE IS DERIVED AS FOLLOWS:

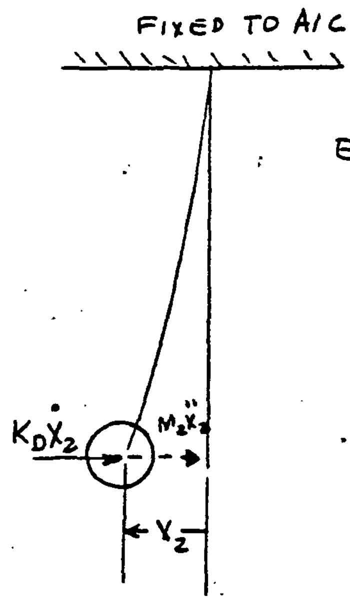

FIG. 1 DAMPING FORCE

FROM FIGURE 1

EQN 1 $\quad X_2 = -M_2\ddot{X}_2\delta_{11} - K_D\dot{X}_2\delta_{11}$

WHERE $X_2, \dot{X}_2, \ddot{X}_2$ = STRUT DISP, VEL, ACC REL TO A/C
δ_{11} = INFLUENCE COEFF - DEFLECTION AT STRUT DUE TO 1 LB LOAD
M_2 = EFFECTIVE STRUT MASS
K_D = EFFECTIVE STRUT DAMPING COEF.

REARRANGING EQN 1 GIVES

EQN 2 $\quad \ddot{X}_2 + \dfrac{K_D}{M_2}\dot{X}_2 + \dfrac{1}{M_2\delta_{11}}X_2 = 0$

BY EQUATING LIKE COEFFICIENTS TO A SINGLE DEGREE OF FREEDOM EQUATION OF MOTION GIVES

EQN 3 $\quad K_D = 2\zeta_{x_2}\sqrt{\dfrac{M_2}{\delta_{11}}}$

WHERE ζ_{x_2} = CRITICAL DAMPING RATIO

INERTIA FORCE $= M_2(\ddot{X}_1 + \ddot{X}_2)$ SEE FIG 2

WHERE $\ddot{X}_1$ = AIRCRAFT LONGITUDINAL ACCELERATION

DRAG FORCE $= F_D + F_D'$

WHERE F_D = PRIMARY TIRE DRAG FORCE
F_D' = SECOND TIRE DRAG FORCE

BRAKE TORQUE - FOR SIMPLIFICATION, THE ASSUMPTION IS MADE THAT THE TOTAL BRAKE TORQUE ACTING ON THE STRUT IS TWICE THE PRIMARY BRAKE TORQUE T_B.

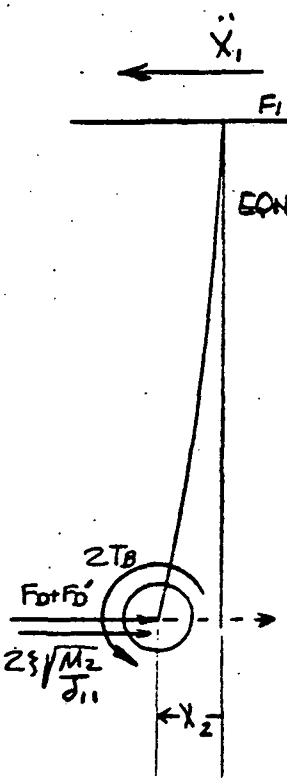

FIG-2 STRUT FORCES

THE STRUT DISPLACEMENT IS

EQN 4 $$X_2 = -(F_D+F_D')\delta_{11} - 2T_B\delta_{12} - M_2(\ddot{X}_1+\ddot{X}_2)\delta_{11} - 2\xi_{X_2}\sqrt{M_2\delta_{11}}\,\dot{X}_2$$

WHERE δ_{12} = INFLUENCE COEFF - DEFLECTION AT STRUT DUE TO A 1 FT-LB TORQUE

REARRANGING EQN 4 GIVES

EQN 5 $$\ddot{X}_2 = -\frac{X_2}{M_2\delta_{11}} - \frac{(F_D+F_D')}{M_2} - \frac{2T_B\delta_{12}}{M_2\delta_{11}} - \frac{2\xi_x\dot{X}_2}{\sqrt{M_2\delta_{11}}} - \ddot{X}_1$$

EQN 6 $$\dot{X}_2 = \dot{X}_2(0) + \int_0^t \ddot{X}_2\,dt$$

EQN 7 $$X_2 = X_2(0) + \int_0^t \dot{X}_2\,dt$$

INITIAL CONDITIONS $\dot{X}_2(0)$ AND $X_2(0)$ ARE ZERO.

AXLE TORSIONAL DEFLECTION

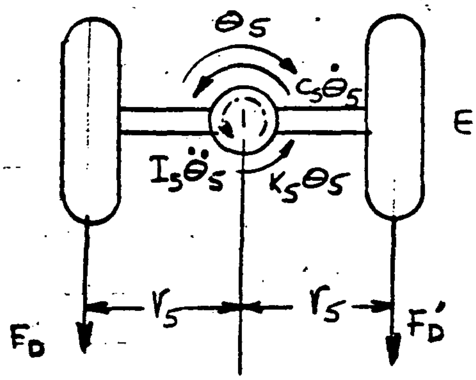

FIGURE 3 STRUT TWIST

THE STRUT TORSION MOMENT EQUATION IS

EQN 8 $$I_S\ddot{\theta}_S + C_S\dot{\theta}_S + K_S\theta_S = r_S\,(F_D - F_D')$$

WHERE $\theta_S, \dot{\theta}_S, \ddot{\theta}_S$ ARE AXLE ROTATIONAL DISPLACEMENT, VELOCITY AND ACCELERATION

I_S = MOMENT OF INERTIA
C_S = ROTATIONAL DAMPING FACTOR
K_S = ROTATIONAL SPRING FACTOR
r_S = DISTANCE FROM STRUT TO TIRE

BRAKE TORQUE MODEL

BRAKE TORQUE IS ASSUMED TO BE THE PRODUCT OF TWO FUNCTIONS

EQN 9 $$T_B = f_1(\dot{\theta}_3) \times f_2(\bar{P}_B)$$

WHERE

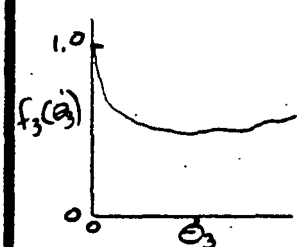

$f_1(\dot{\theta}_3)$ IS AN EMPIRICAL FUNCTION THAT INTRODUCES THE EFFECT OF BRAKE TORQUE VARIATION WITH BRAKE ROTATIONAL SPEED WHEN BRAKE PRESSURE IS HELD CONSTANT. A DIFFERENT FUNCTION IS USED FOR LANDINGS AND TAKEOFFS.

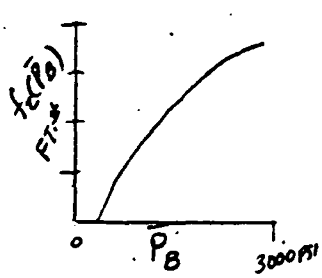

$f_2(\bar{P}_B)$ IS AN EMPIRICAL FUNCTION THAT INTRODUCES THE NON LINEAR RELATIONSHIP BETWEEN BRAKE TORQUE AND BRAKE PRESSURE WHEN ROTATIONAL SPEED IS HELD CONSTANT.

FIG 4 BRAKE FUNCTIONS

$\bar{P}_B$ FILTERED BRAKE PRESSURE

TO ACCOUNT FOR A TIME DELAY BETWEEN BRAKE TORQUE CHANGE AND BRAKE PRESSURE CHANGE, $\overline{P}_B$ IS DETERMINED FROM THE RELATIONSHIP

EQN 10 $$\dot{\overline{P}}_B = \frac{1}{\tau_B}\left(P_B - \overline{P}_B\right)$$

WHERE P_B IS THE MEASURED BRAKE PRESSURE AT THE BRAKE

τ_B = TIME CONSTANT FOR BRAKE

EQN 11 $$\overline{P}_B = \overline{P}_B(0) + \int_0^T \dot{\overline{P}}_B \, dt$$

WHERE THE INITIAL CONDITION $\overline{P}_B(0)$ IS ZERO

TIRE AND WHEEL DYNAMICS

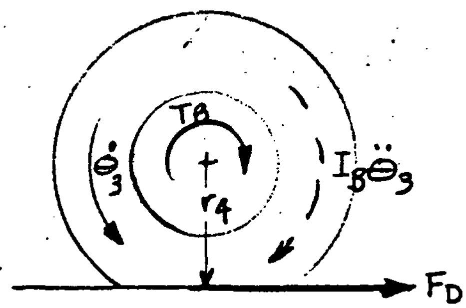

FIG 6 TIRE AND WHEEL

SUMMING MOMENTS GIVES

EQN 12 $$I_B\ddot{\theta}_3 + T_B - r_4 F_D = 0$$

WHERE

I_B = INERTIA OF TIRE, WHEEL & BRAKE

r_4 = AXLE HEIGHT

OR

EQN 13 $$\ddot{\theta}_3 = \frac{r_4 F_D - T_B}{I_B}$$

EQN 14 $$\dot{\theta}_3 = \dot{\theta}_3(0) + \int_0^T \ddot{\theta}_3 \, dt$$

WHERE $\dot{\theta}_3(0)$ IS THE INITIAL TIRE ROTATIONAL SPEED.

TIRE SLIP RATIO

THE SLIP RATIO OF THE PRIMARY TIRE IS

EQN 15
$$V_{SB} = \frac{(\dot{X}_1 + \dot{X}_2 - r_5 \dot{\Theta}_5 - r_r \dot{\Theta}_3)}{\dot{X}_1 + \dot{X}_2 - r_5 \dot{\Theta}_5}$$

WHERE r_r = EFFECTIVE ROLLING RADIUS

SECOND TIRE CORNERING & DRAG FORCES

THE SECOND TIRE FORCES ARE ASSUMED TO BE LAGGED FROM THE PRIMARY FORCES BY THE RELATION

EQN 16
$$\dot{F}_C' = \frac{1}{\tau_C}(F_C - F_C')$$

EQN 17
$$\dot{F}_D' = \frac{1}{\tau_D}(F_D - F_D')$$

WHERE F_C' AND F_D' ARE THE SECONDARY CORNERING AND DRAG FORCES RESPECTFULLY
τ_C = CORNERING TIME CONSTANT
τ_D = DRAG TIME CONSTANT

EQN 18
$$F_C' = F_C'(0) + \int_0^T \dot{F}_C' \, dt$$

EQN 19
$$F_D' = F_D'(0) + \int_0^T \dot{F}_D' \, dt$$

WHERE $F_C'(0)$ AND $F_D'(0)$ ARE INITIAL CONDITIONS

Section 3. PROGRAM

ANALOG PROGRAM

The analog computer program is shown in Figure C-4. The program was set up so that it could be used in either the stand alone or normal mode. This allowed the program to be developed independently of the total simulator.

INTERFACE AND PROGRAMMING CONSIDERATIONS

The simulation was interfaced with the digital simulation and hardware as illustrated in the Analog Antiskid Interface Description.

Analog computer to Hardware Interface - Wheel speed from the computer drove voltage controlled oscillators. The oscillator outputs were impressed on the antiskid control box to simulate the signal from each tire. The frequency corresponded to 40 pulses per wheel revolution.

The squat signal was 28 vdc when the nose gear was fully extended and zero when the gear compressed one and one half inches.

The PMV servos drove the PMV in response to brake pedal position.

Brake pressure was monitored by pressure transducers connected to amplifiers with appropriate gains for the analog circuit.

Digital Computer to Analog Computer Interface - The signal from the digital computer was processed by a Digital-to-Analog converter. To take advantage of the digital computer capabilities the product of normal load and maximum friction coefficient was formed in the digital computer. The unbraked cornering force and $f_{3c}(\psi)$ were also calculated in the digital computer because of nature of the computations and the relatively slow changes experienced by these parameters. Aircraft axle velocities and aircraft acceleration were also input to the analog computer. Cornering and drag loads were impressed on analog-to-digital converters for communication with the digital computer.

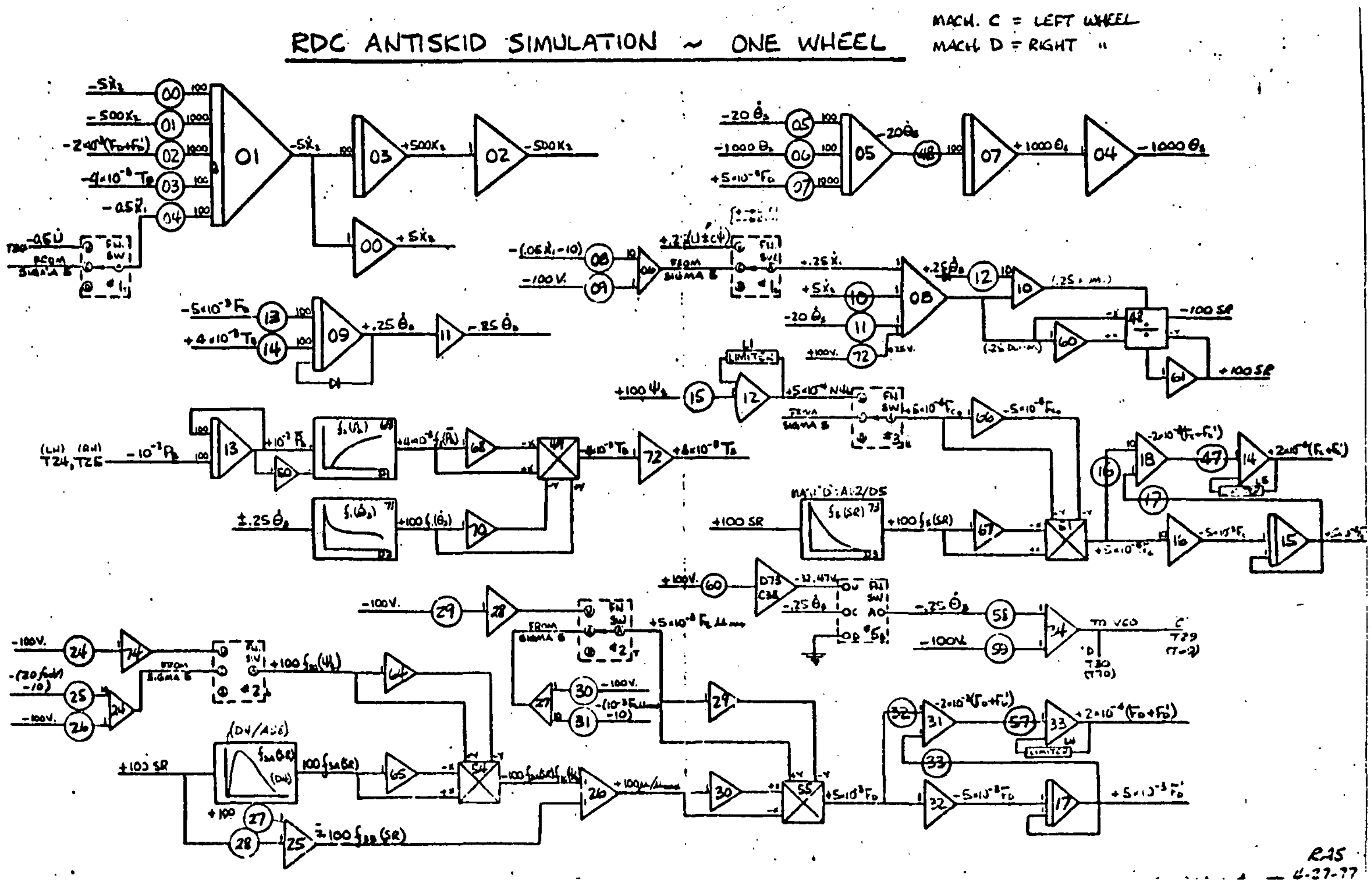

FIGURE C-4 WIRING DIAGRAM -- ANALOG ANTISKID SIMULATOR

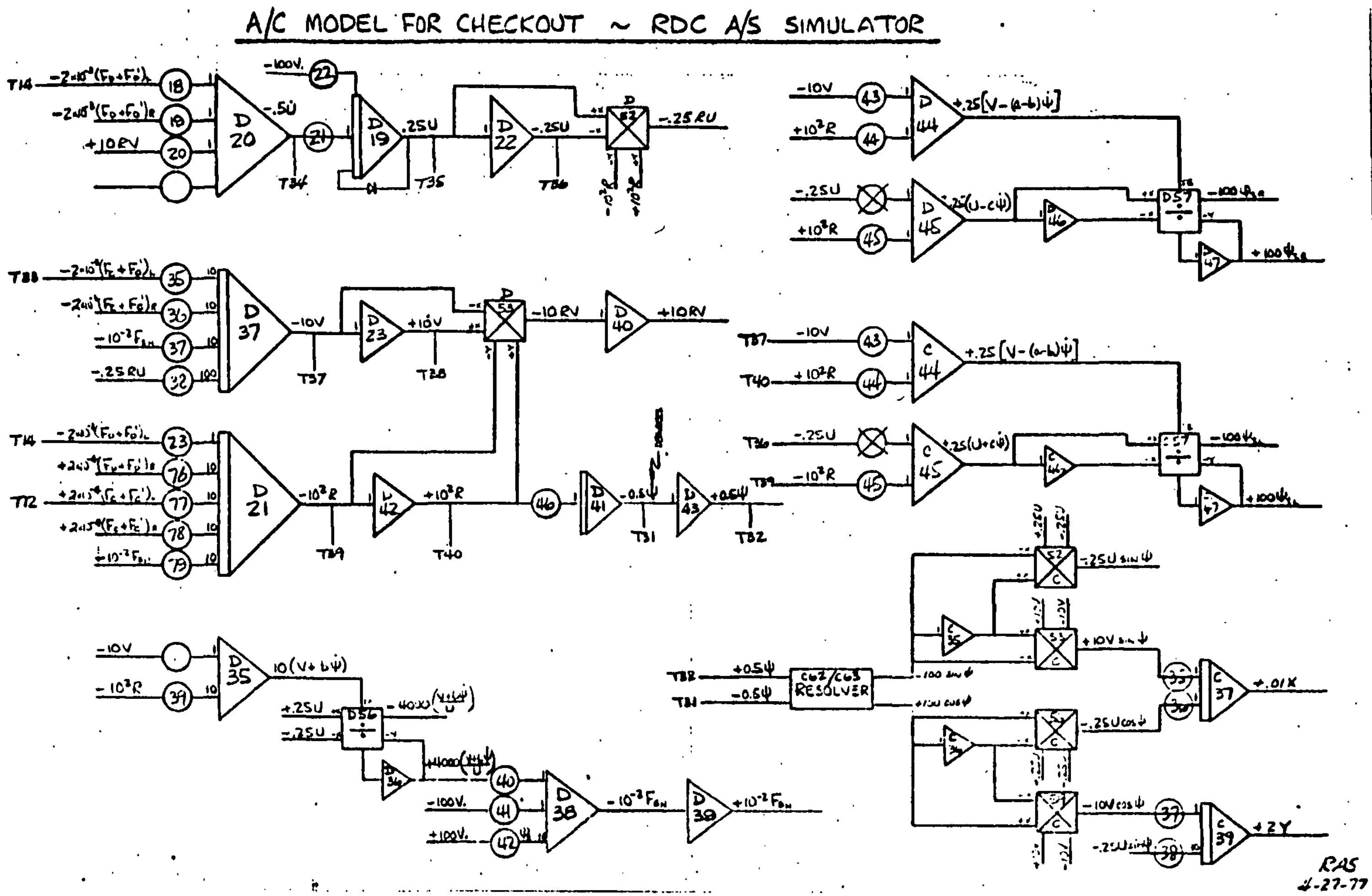

FIGURE C-4 WIRING DIAGRAM -- ANALOG ANTISKID SIMULATOR (CONCLUDED)

ANALOG ANTISKID SIMULATION INTERFACE DESCRIPTION

THE PHYSICAL BLOCK DIAGRAM FOR THE SIMULATION IS SHOWN ON THE NEXT PAGE. ITEMS WITH ARROWS TOWARD SIMULATION COME TO THE SIMULATION FROM THE AIRFRAME SIMULATION WITH THE EXCEPTION OF THE PMU CONTROLS WHICH COME FROM THE COCKPIT. ITEMS WITH ARROWS AWAY FROM SIMULATION GO TO THE AIRFRAME SIMULATION. THE FOLLOWING TABLE DEFINES THE VARIABLES.

SYMBOL	DEFINITION
LEFT/RIGHT PMU CONTROL	LEFT/RIGHT PILOTS METERING VALVE COMMAND - PROPORTIONAL TO BRAKE PEDAL POSITION
SQUAT SIGNAL	INDICATION THAT NOSE GEAR HAS COMPRESSED 3 INCHES - NECESSARY FOR ANTISKID BOX OPERATION
$(F_T \mu_{MAX})_{L/R}$	VALUE OF LEFT/RIGHT GEAR NORMAL LOAD MULTIPLIED BY MAXIMUM FRICTION COEFFICIENT
$F_{CO\,L/R}$	LEFT/RIGHT UNBRAKED CORNERING FORCE
$f_{3C}(\Psi_{L/R})$	EMPIRICAL FUNCTION USED TO REDUCE BRAKED DRAG FORCE AS A FUNCTION OF YAW ANGLE.
$\dot{X}_{1\,L/R}$, $\ddot{X}_{1\,L/R}$	LEFT/RIGHT AXLE VELOCITY, ACCELERATION
$F_{C\,L/R}$	LEFT/RIGHT CORNERING FORCE
$F_{D\,L/R}$	LEFT/ RIGHT DRAG FORCE
COMPUTER CONTROL	SIGNAL TO ANALOG COMPUTER TO RESET, HOLD, COMPUTE

ANALOG ANTISKID SIMULATION

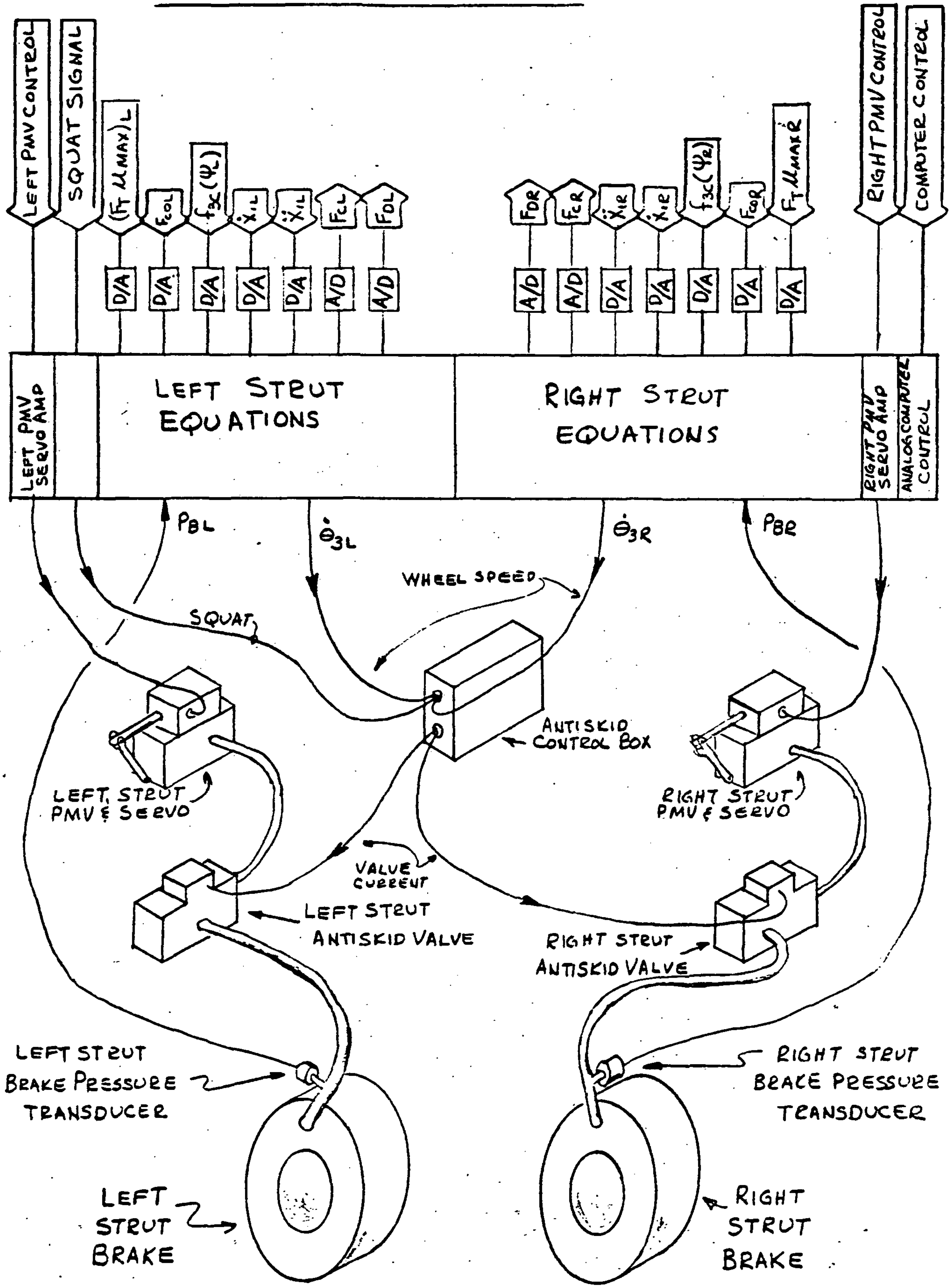

Section 4. HARDWARE

The hardware needed for this program is outlined in the Task Assignment Drawing Z7802765. Details of the hardware are given in Drawing Z7935344.

Equipment serial numbers used in the simulation were as follows:

LH A/S Valve	P/N 39-101	S/N 797C
RH A/S Valve	P/N 39-101	S/N 799C
LH PMV	P/N 7920966-5503	S/N 416309A
RH PMV	P/N 7920966-5503	S/N 416308A
Control Box	P/N 42-089-5	S/N 256
LH Brake	P/N 9560788	S/N MAY66-8E
RH Brake	P/N 9560788	S/N NOV66-31

25-1821 (10-68)

REVISIONS			
LTR	DESCRIPTION	DATE	APPROVED
A	SEE E.O.	5-6-77	K.A.S
B	SEE E.O.	10-14-77	K.A.S.

TEST 0971 MAR 30 1977

SCHEDULE INFORMATION		DATE
TEST INITIATED		
FINAL REPORT SUBMITTAL		
DESIGN APPROVAL		DATE
LAB TEST		
STRENGTH		
PR ENGR	[illegible signature]	3/25/7
GR ENGR	G.W. KIBBEE	3-25-77
PREP BY	R. A. Storley	3-17-77

DOUGLAS AIRCRAFT COMPANY

MCDONNELL DOUGLAS — LONG BEACH, CALIFORNIA

TITLE ANTISKID SIMULATION - RUNWAY DIRECTIONAL CONTROL SIMULATOR DC-9 SERIES 10

TASK ASSIGNMENT DRAWING

SIZE A | TAD | Z7802765

EWO | S.O. | SHEET 1

DAC XA60-13A4 (REV. 3-74)

TABLE OF CONTENTS AND REVISION LETTER RECORD

TABLE OF CONTENTS	SHEET NUMBER	LETTER	
TITLE PAGE	1	A	B
TABLE OF CONTENTS	2	A	B
INTRODUCTION	3		
PURPOSE	4		
REQUIRED EQUIPMENT	5		B
TEST REQUIREMENTS	6		
&LD WORK ITEMS	7		B
SCHEDULE	8		
FIGURE 1	9		
FIGURE 2	10	A	

DOUGLAS	SIZE	CODE IDENT NO.	
	A	88277	Z7802765
		REV LTR B	SHEET 2.

SYM

INTRODUCTION

This Task Assignment Drawing details the requirements for an analog/hardware antiskid simulation to be interfaced with the motion-base flight simulator. Actual brake and antiskid system hardware will be used, operating in conjunction with an analog computer.

PURPOSE

The purpose of these tests is to extend existing flight simulator capability for the study and solution of aircraft directional control problems on runways. A man-in-loop DC-9 aircraft ground handling simulator will be developed, correlated and then demonstrated to NASA personnel. A realistic simulation would be very useful in evaluating factors which influence aircraft ground handling performance up to and beyond the operational limits of the aircraft without risk to equipment and pilot.

REQUIRED EQUIPMENT

1. Hydro-Aire DC-9 Hydraulic Brake System Simulator
2. Hydraulic Power Supply (Skydrol, 3000 psi, 15 GPM min.)
3. Brake Application Servo (two required)
4. Six Strain Gage Power Supplies
5. Six Channel Bridge Balance
6. Six Preston Model 8300 DO Amplifiers
7. Two Comcor Ci-175 Analog Computers
8. DC-9 Transformer/Rectifier
9. Two VCO's (HP 3310A or equivalent)

*10. Function Generator (HP 3300A), with "Offset" plug-in (HP 3304A)

*11. Electronic Counter (HP 5512A or equivalent)

*12. X-Y Plotter

13. Beckman Six Channel Recorder

*14. Scope

15. Two Pressure Gages (0-5000 psi)
16. Six Pressure Transducers (0-5000 psi)
17. Two Break-out Boards (Z7935344-13 and -15)
18. Connector Cables (Z7935344-17,-19, -21, -23)
19. Six Amplifier Pressure Monitoring Board (No identification) - Available on DC-10 Antiskid Simulator

A general layout of the required equipment is shown in Figure 1.

*Not required full time

TEST REQUIREMENTS

The following tests will be conducted:

1. A predemonstration evaluation of the simulator will be made, utilizing a FAA and a Douglas pilot. Corrective action will be taken to resolve any problem areas.

2. The complete simulation will be evaluated by both a FAA and a Douglas pilot. This demonstration program will be designed to qualitatively evaluate:

   a. The benefits of using the antiskid simulation in conjunction with the aircraft simulator.

   b. The degree of correlation between the simulator and the pilot's experience and available DC-9 flight test data.

SYM B

F&LD WORK ITEMS

1. Obtain* and install Hydro-Aire DC-9 hydraulic brake system simulator.

2. Install hydraulic piping between hydraulic power supply and brake system simulator.

3. Develop and install brake application system.

4. Install pressure transducers and gages on brake system simulator (see Figure 2).

5. Operate hydraulic system as required.

6. Restore hydraulic brake system simulator to original condition and return to Hydro-Aire upon completion of test.

7. Obtain and install pressure instrumentation (strain gage power supplies, bridge balance, and Preston amplifiers) per drawing # Z7935344 (-501 rack assembly).

8. Fabricate two break-out boards per drawing # Z7935344 (-13 and -15 panel assemblies).

9. Fabricate and install connector cables. Fabricate per drawing # Z7935344-17, -19, -21, -23. Install per drawing # Z7935344.

10. Set up instrumentation rack per drawing # Z7935344 (-503 rack assembly).

11. Set up and maintain two Comcor Ci-175 computers and the Beckman recorder (setup in enclosed platform adjacent to motion-base).

12. Obtain VCO's, function generators, electronic counter, X-Y plotter and scope. Place near Comcor computers.

13. Return all instruments to stockroom at completion of test.

*Write consignment purchase order and provide transportation. Unit will be available from 1 May 1977 until 29 July 1977.

SYM

SCHEDULE

Set-up of the Comcor Ci-175 computers is required by 22 April 1977 so that programming can be started. Fabrication and/or installation of all other required equipment is to be complete by 6 May 1977. System integration (with the flight simulator), checkout and demonstration will continue through 29 July 1977.

FORM XA60-13A2 (1-68)

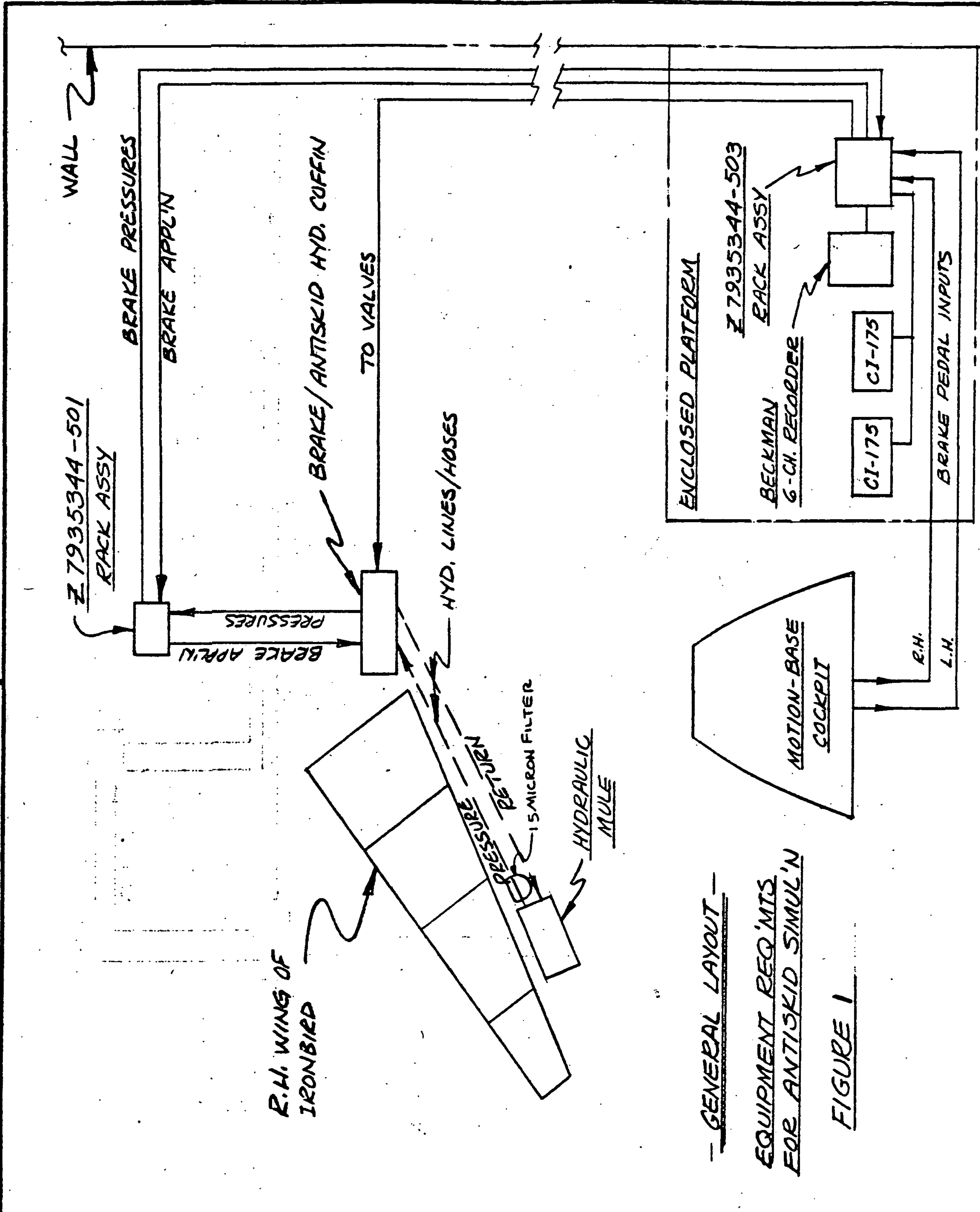

— GENERAL LAYOUT —
EQUIPMENT REQ'MTS
FOR ANTISKID SIMUL'N
FIGURE 1

DOUGLAS	SIZE	CODE IDENT NO.	
	A	88277	Z7802765
			REV LTR

SHEET 9

SYM A

RAS 6-2-76

DC-9-10 ANTISKID SIMULATOR HYDRAULIC SCHEMATIC

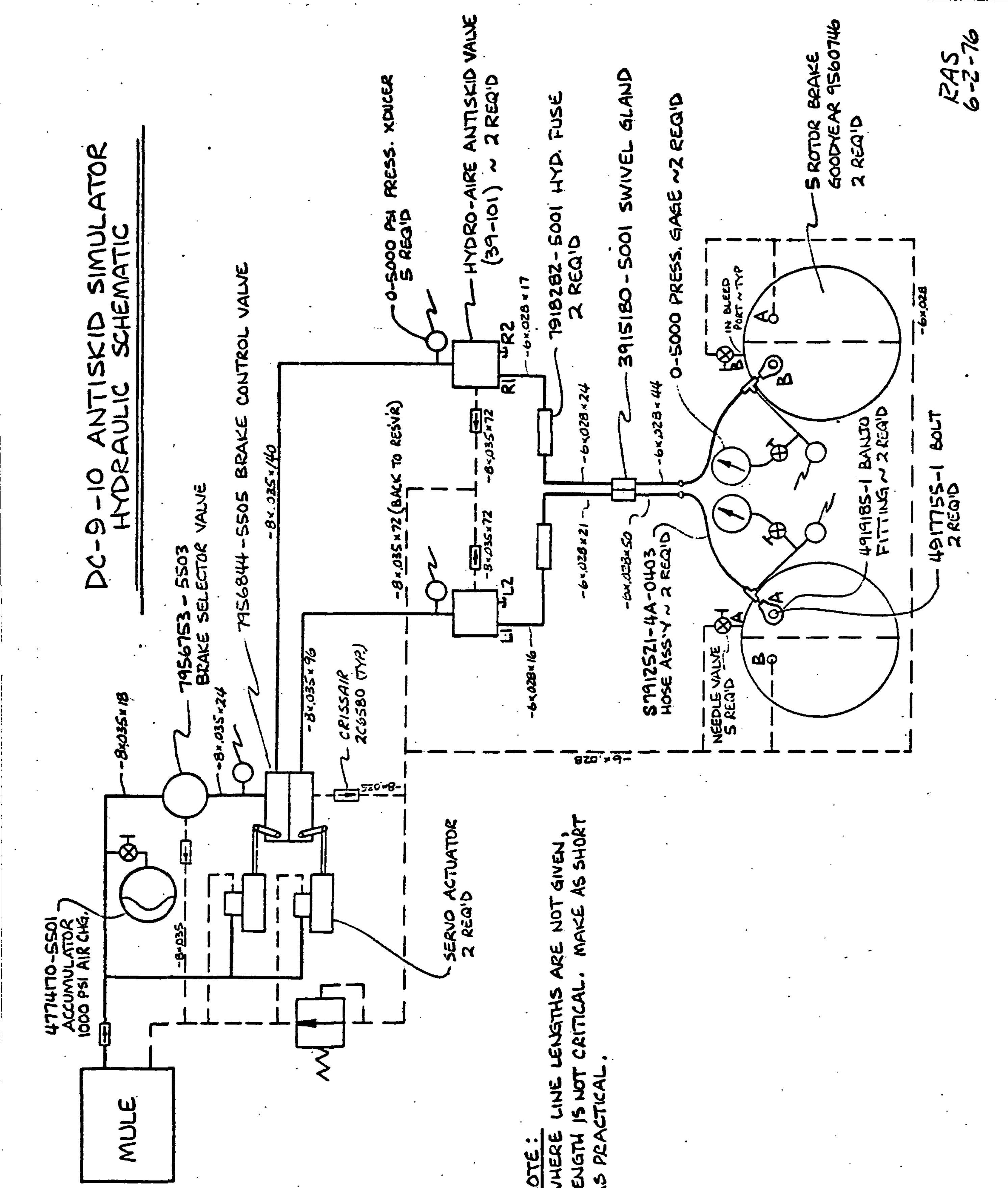

NOTE: WHERE LINE LENGTHS ARE NOT GIVEN, LENGTH IS NOT CRITICAL. MAKE AS SHORT AS PRACTICAL.

FIGURE 2

DOUGLAS AIRCRAFT COMPANY	TAD	SIZE A	Z 7802765
	EWO	S.O.	SHEET 10

ENGINEERING ORDER

DOUGLAS AIRCRAFT COMPANY, LONG BEACH, CALIFORNIA — MCDONNELL DOUGLAS CORPORATION

DAC 25-1709K (REV. 6-75)

RC	MI	MW	AW	FS	OTHER MODEL USAGE	DESIGN SECTION: LDM	TYPE RELEASE	MAJOR SUB. MDC	TOTAL NO. PI INPUT SHEETS
							DEVELOPMENT A / PRODUCTION B / NON PROD. C		ADV DATE; SHEET 1 OF 1

SIZE — DRAWING NUMBER: Z7935344

DATE	1	DRAWING CHANGED	A
DATE	2	ADVANCE DWG CHG	
DATE	3	SERIAL EO	
DATE	4	NEW REVISED RLSE	
DATE	5	REISSUE TO REVISE	R

HANDLING INSTRUCTIONS (HI)

0. INTERCHANGEABILITY OF PARTS NOT AFFECTED. USAGE OF CHANGED OR UNCHANGED PARTS OPTIONAL.
2. PARTS MUST CONFORM AT NOTED EFFECTIVITY.
3. PARTS MUST CONFORM AT NOTED EFFECTIVITY. SPECIAL REWORK FOR PARTS MADE INCLUDED.
4. SCRAP.
5. NOTED.
6. RETROFIT (DELIVERED ARTICLES).

ENGRG TIME CHG (COST CHARGE NO.): 1660 1402

TITLE: ANTI-SKID SIMULATION EQUIP. — MOTION-BASE SYSTEM

EWO | DOG | WRO | ROUTING CODE | CHG CLASS | SEO REWORK DWG REQUIRES DWG CHG YES NO | DWG REPLACES REPLACED BY | RELEASE STOP ORDER DATED

SYS | COE | PATTERN DIE MOLD AFFECTED YES NO | EXPECTED SEO CHG INCORP DATE | INCORP SEO Q4EO NO.

EO MADE BY 10-11-77 R.A. STORLEY | DESIGN APPROVAL 10-11-77 R.A. STORLEY | CHECK EO | WEIGHTS | PROJ ENGR | PRODUCT SUPPORT | RELEASE DATE | CUSTOMER AUTH | INCORP VIR NO

DWG MADE CHGD BY | SPEC COMPLIANCE | CHECK DWG | STRESS | CHANGE CONTROL | MATERIAL | CUSTOMER

	1.2 LTR	MODEL	SECTION	RELEASE CCN	HI NO.	1ST FUS AFF	EFFECTIVITY (4 SERIAL NUMBERS PER LINE MAXIMUM)	CONFIGURATION	REQ PER ARTICLE NEW	REQ PER ARTICLE FORMER	NEXT ASSEMBLY DRAWING NO	U CD	
1		CRAD											1
2													2
3													3
4													4
5													5

FOR RECORD PURPOSES ONLY.

THIS E.O. DOCUMENTS CORRECTIONS MADE TO THE DC-9 ANTISKID SYSTEM SIMULATION WHICH WAS A PART OF THE MOTION-BASE RUNWAY DIRECTIONAL CONTROL SIMULATOR.

SHEET 11 — IDENTIFIED WIRING CONNECTION POINTS ON ELEMENTS 2N2324 & 2N2647.

SHEET 13 — IDENTIFIED RATING ON RESISTORS (BETWEEN BRAKE PEDALS & COCKPIT/LOCAL SWITCH)

SHEET 20 — ADDED WIRING BETWEEN PTS. 33, 36, 37, 38 & 39 ON J1 CONNECTOR & -7 PANEL.

SHEET 30 — ADDED RESISTORS TO B/M (REF. SHEET 13)

	YES	NO
OATP AFF		
SCHEMATICS AFF		
FINISH SPEC AFF		
DAMS & DRAINS AFF		
VENTILATION AFF		
SEALING AFF		
ELEC BONDING AFF		
LUBRICATION AFF		

PRINT DISTRIBUTION	Yes	No
DEVELOPMENT		
Orig at ____ Dup at ____		VER
SUPPLIER RELEASE WITH DAC PLANNING ACTION REQUIRED		KP

SB SC NO. | EXTRA EO'S: NAME | QTY | DEPT | MAIL CODE | EXTRA DWGS: NAME | QTY | DEPT | MAIL CODE | DRAWING NUMBER Z7935344

12/3 ENGINEER ORDER

DOUGLAS AIRCRAFT COMPANY, LONG BEACH, CALIFORNIA — McDONNELL DOUGLAS CORPORATION

DAC 25-1709K (2-72)

DRO 114643

11464

OTHER MODEL USAGE	DESIGN SECTION	RELEASE		MAJOR SUB-MDC	TOTAL NO. PL INPUT SHEETS	SIZE	DRAWING NUMBER
	53	DEVELOPMENT	A		ADV DATE		Z7935344
		PRODUCTION	B				
	LDM	NON PROD.	C ✓		SHEET 1 OF 30		

RC	MI	MW	AW	FS	LDM

HANDLING INSTRUCTIONS (HI)
0. INTERCHANGEABILITY OF PARTS NOT AFFECTED. USAGE OF CHANGED OR UNCHANGED PARTS OPTIONAL.
2. PARTS MUST CONFORM AT NOTED EFFECTIVITY.
3. PARTS MUST CONFORM AT NOTED EFFECTIVITY. SPECIAL REWORK FOR PARTS MADE INCLUDED.
4. SCRAP.
5. NOTED.
6. RETROFIT (DELIVERED ARTICLES).

ENGRG TIME CHG (Sales Order): 1660 / 1402

TITLE: ANTI-SKID SIMULATION EQUIP. — MOTION-BASE SYSTEM

DATE	1	DRAWING CHANGED
DATE	2	ADVANCE DWG CHG
DATE	3	SERIAL EO
DATE	4	NEW REVISED RLSE — NEW
DATE	5	REISSUE TO REVISE — R

EWO	DOG	WRO	ROUTING CODE	CHG CLASS	SEO/REWORK DWG REQUIRES DWG CHG — YES / NO	DWG REPLACES / REPLACED BY	RELEASE STOP ORDER DATED
SYS	COE				PATTERN DIE MOLD AFFECTED — YES / NO	EXPECTED SEO CHG INCORP DATE	INCORP SERIAL EO NO.

EO MADE BY	DESIGN	CHECK EO	WEIGHTS	PROJECT	PRODUCT SUPPORT	RELEASE / DATE	CUSTOMER AUTH	INCORP VIR NO.
R.R. DEAN	3-31-77 STORLEY			3-31-77 [illegible signature]				
DWG MADE-CHGD BY	SPEC COMPLIANCE	CHECK DWG	STRESS	CHANGE CONTROL	MATERIAL	CUSTOMER		

	1.2 LTR	MODEL	SECTION	RELEASE S.O.	HI NO.	1ST FUS AFF	EFFECTIVITY (4 SERIAL NUMBERS PER LINE MAXIMUM)	DWG CONFIGURATIONS	REQ PER ARTICLE NEW	REQ PER ARTICLE FORMER	NEXT ASSEMBLY DRAWING NO.	U CD	
1													1
2		C RAD											2
3													3
4													4
5													5

THIS E.O. CONTAINS ALL INFORMATION REQ'D TO ASSEMBLE THE NECESSARY EQUIPMENT FOR DC-9 ANTI-SKID PORTION OF THE GROUND-HANDLING TESTS. CONTACT DICK STORELY X-37291 OR BOB DEAN, X-36311 FOR FURTHER INFO.

ADV. TYPE TEST RELEASE
DRAWING NOT TO BE ALTERED
DATE 4-5-77 REL SC

	YES	NO
OATP AFF		
FIA/FMEA AFF		
SCHEMATICS AFF		
FUNC'L MOCK UP AFF		
FINISH SPEC AFF		
SPARE TYPE PART AFF		
DAMS & DRAINS AFF		
VENTILATION AFF		
SEALING AFF		
ELEC BONDING AFF		
LAB TEST AFF		
LUBRICATION AFF		

SERVICE CHG	EXTRA EO'S NAME	QTY	DEPT	MAIL CODE	EXTRA DWGS NAME	QTY	DEPT	MAIL CODE

PRINT DISTRIBUTION	Yes	No
DEVELOPMENT		
Orig at ____		
Dup at ____		
MAJ SUB MDC RLSE WITH DAC PLANNING ACTION REQUIRED		

DRAWING NUMBER: Z7935344

ENGINEERING ORDER

DAC 25-17098 (6-71)

DOUGLAS AIRCRAFT COMPANY
LONG BEACH, CALIFORNIA
McDONNELL DOUGLAS
CORPORATION

SHEET	SIZE	DRAWING NUMBER
2		Z7935344

DATE	1	DRAWING CHANGED	
DATE	2	ADVANCE DWG CHG	
DATE	3	SERIAL EO	
DATE	4	NEW/REVISED RELEASE	NEW
DATE	5	REISSUE TO REVISE	R

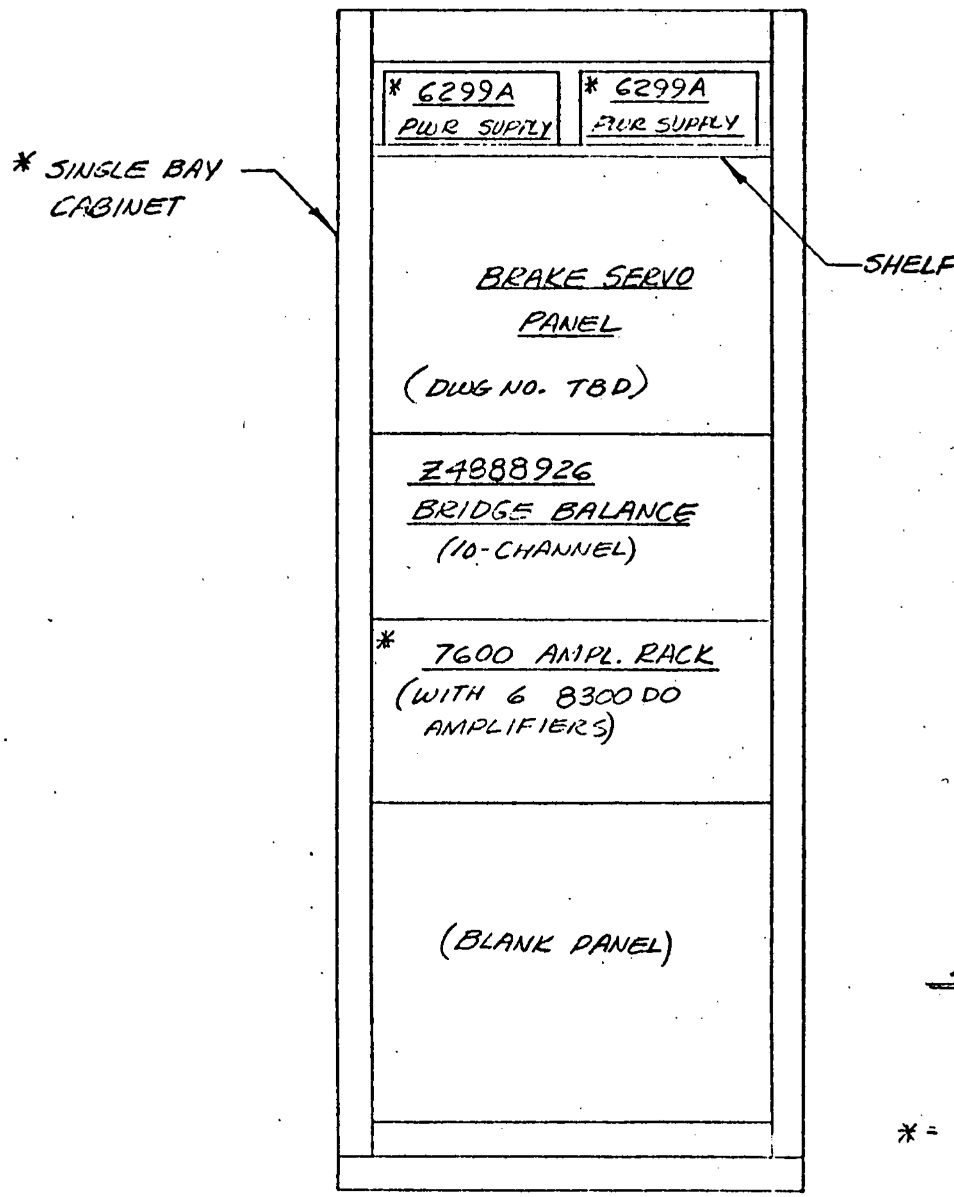

DETAIL -501 RACK ASSY

(SEE CABLE DIAGRAM, SHEET 3)

* = EXISTING EQUIP.

DWG NO. Z7935344

ENGINEERING ORDER

DAC 25-17095 (6-71)

DOUGLAS AIRCRAFT COMPANY
LONG BEACH, CALIFORNIA
MCDONNELL DOUGLAS
CORPORATION

SHEET	SIZE	DRAWING NUMBER
3		Z7935344

DATE	1	DRAWING CHANGED	
DATE	2	ADVANCE DWG CHG	
DATE	3	SERIAL EO	
DATE	4	NEW/REVISED RELEASE	NEW
DATE	5	REISSUE TO REVISE	R

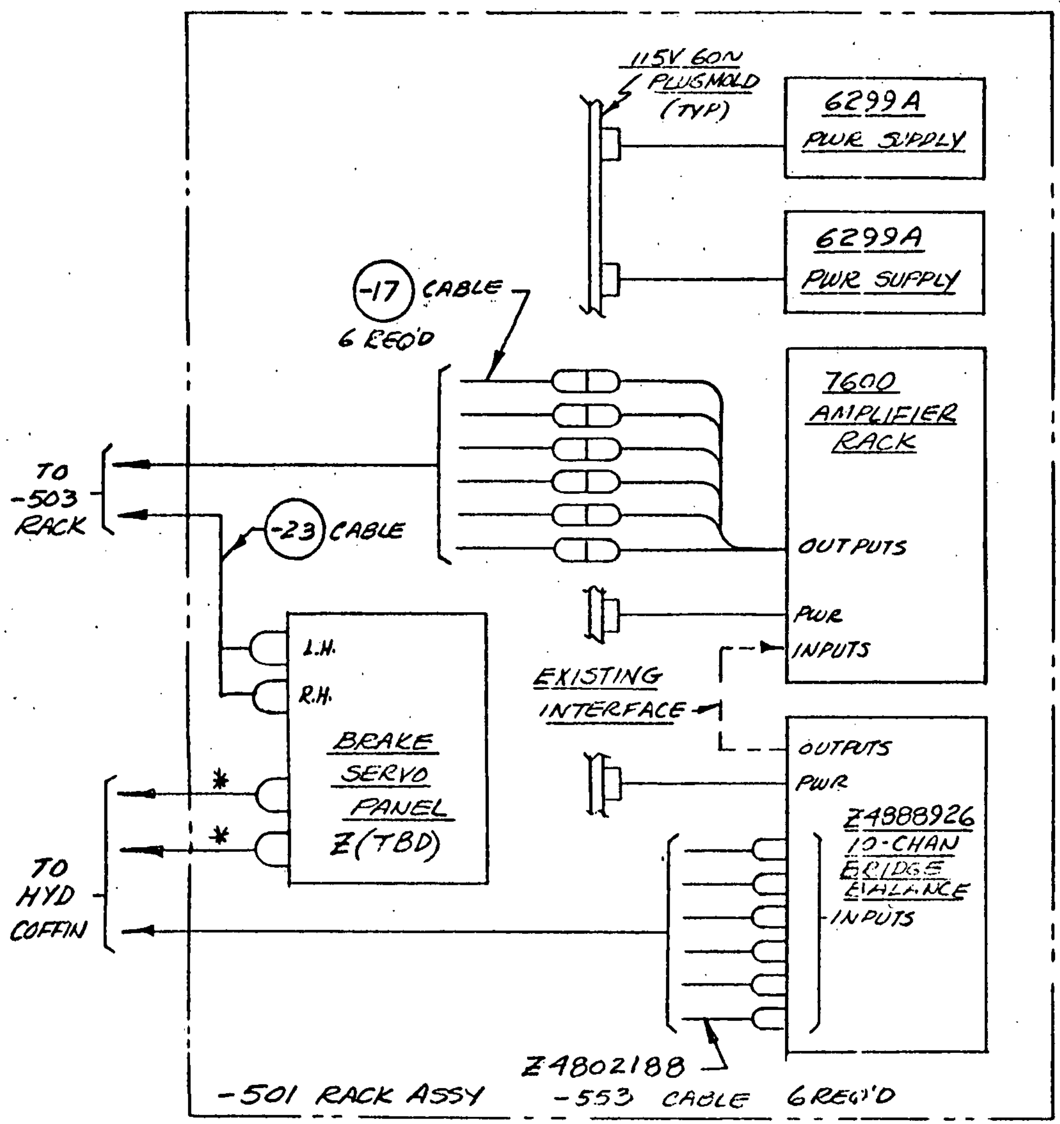

DETAIL -501 RACK ASSY

* THESE CABLES TO BE PART OF Z (TBD) DWG.
CONTACT R. ECKWEILER X 39788 FOR FURTHER INFO.

DWG NO. Z7935344

ENGINEERING ORDER

DAC 25-17098 (6-71)

DOUGLAS AIRCRAFT COMPANY
LONG BEACH, CALIFORNIA
MCDONNELL DOUGLAS
CORPORATION

SHEET	SIZE	DRAWING NUMBER
4		Z7935344

DATE	1	DRAWING CHANGED	
DATE	2	ADVANCE DWG CHG	
DATE	3	SERIAL EO	
DATE	4	NEW/REVISED RELEASE	NEW
DATE	6	REISSUE TO REVISE	R

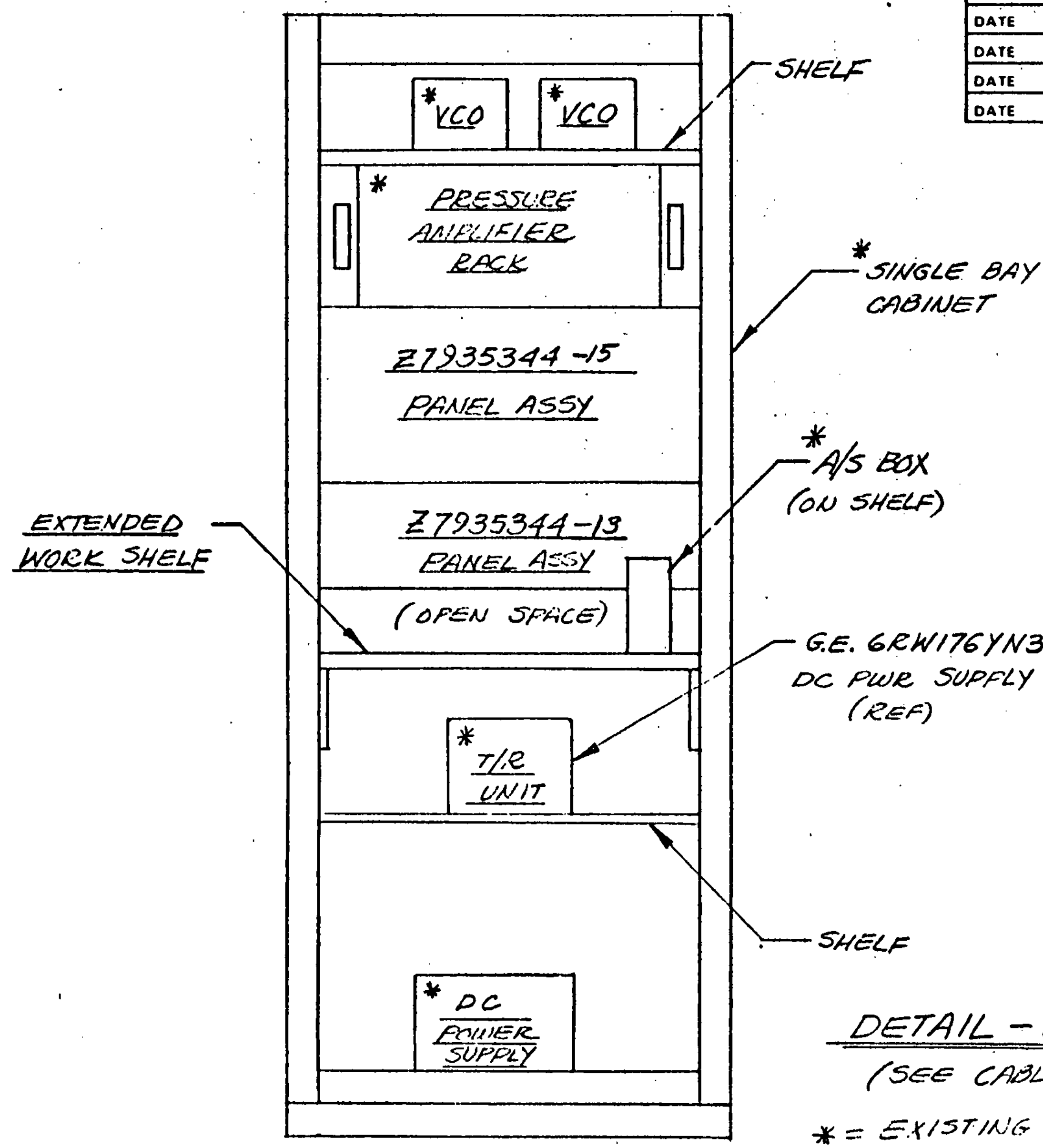

DETAIL - 503 RACK ASSY

(SEE CABLE DIAGRAM, SHEET 5)

* = EXISTING EQUIP.

DWG NO. Z7935344

ENGINEERING ORDER

DAC 25-17098 (6-71)

DOUGLAS AIRCRAFT COMPANY, LONG BEACH, CALIFORNIA
MCDONNELL DOUGLAS CORPORATION

SHEET	SIZE	DRAWING NUMBER
5		Z 7935344

DATE	1	DRAWING CHANGED	
DATE	2	ADVANCE DWG CHG	
DATE	3	SERIAL EO	
DATE	4	NEW/REVISED RELEASE	NEW
DATE	5	REISSUE TO REVISE	R

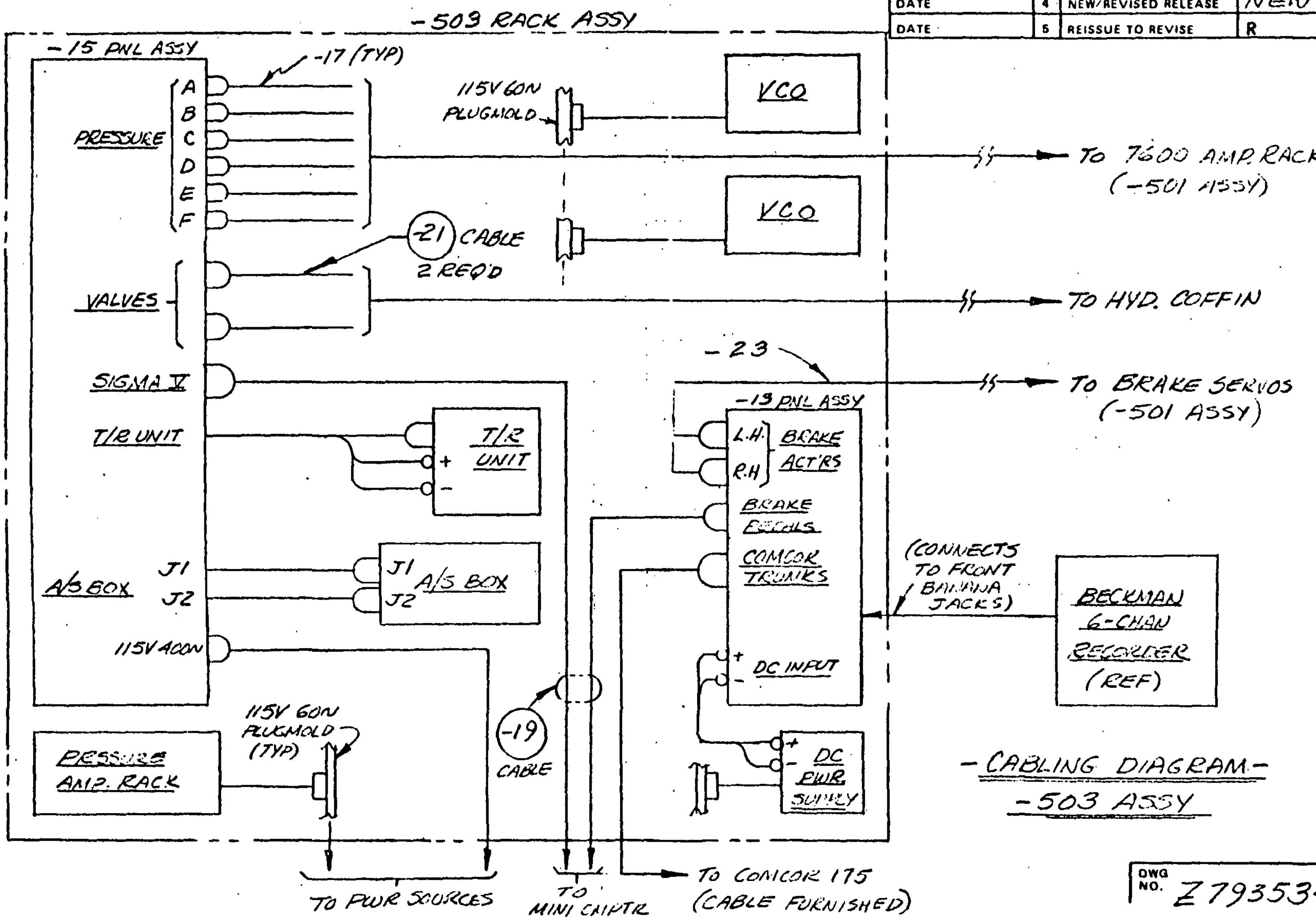

-CABLING DIAGRAM-
-503 ASSY

DWG NO. Z 7935344

ENGINEERING ORDER

DAC 25-17098 (6-71)

DOUGLAS AIRCRAFT COMPANY
LONG BEACH, CALIFORNIA
McDONNELL DOUGLAS CORPORATION

SHEET	SIZE	DRAWING NUMBER
6		Z7935344

DATE	1	DRAWING CHANGED	
DATE	2	ADVANCE DWG CHG	
DATE	3	SERIAL EO	
DATE	4	NEW/REVISED RELEASE	NEW
DATE	5	REISSUE TO REVISE	R

NOTES:
1. SEE PARTS LIST FOR TABULATION OF PART NO.'S VS LOCATION.
2. APPLY APPROPRIATE SIZE BLACK DRY-TRANSFER LETTERS & FIGURES APPROX AS SHOWN. OVERSPRAY WITH CLEAR ACRYLIC LACQUER.

(G) = GREEN (●) = BLACK (R) = RED (B) = BLUE ○ = BROWN

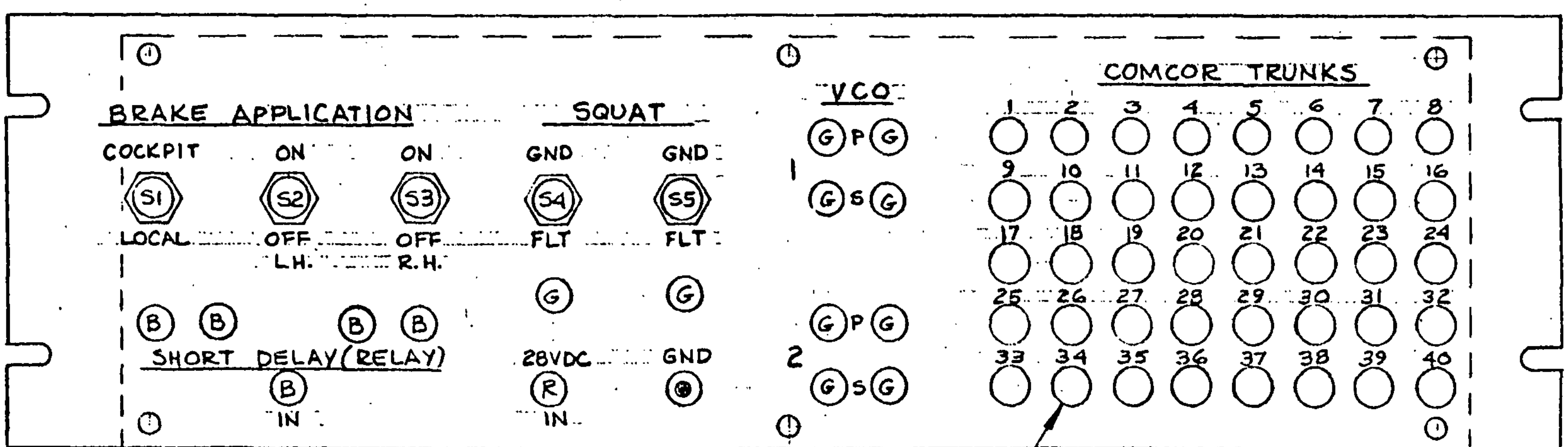

NO. 1498 BANANA JACK 57 REQ'D
(SEE COLOR CODE ABOVE)

DETAIL - LETTERING & PARTS LOCATION (FRONT)
-13 PANEL ASSY

DWG NO. Z7935344

ENGINEERING ORDER

DAC 25-17098 (6-71)

DOUGLAS AIRCRAFT COMPANY
LONG BEACH, CALIFORNIA
MCDONNELL DOUGLAS
CORPORATION

SHEET	SIZE	DRAWING NUMBER
7		Z 7935344

DATE	1	DRAWING CHANGED	
DATE	2	ADVANCE DWG CHG	
DATE	3	SERIAL EO	
DATE	4	NEW-REVISED RELEASE	NEW
DATE	5	REISSUE TO REVISE	R

NOTE: WIRE PER SHEETS 12 & 13.

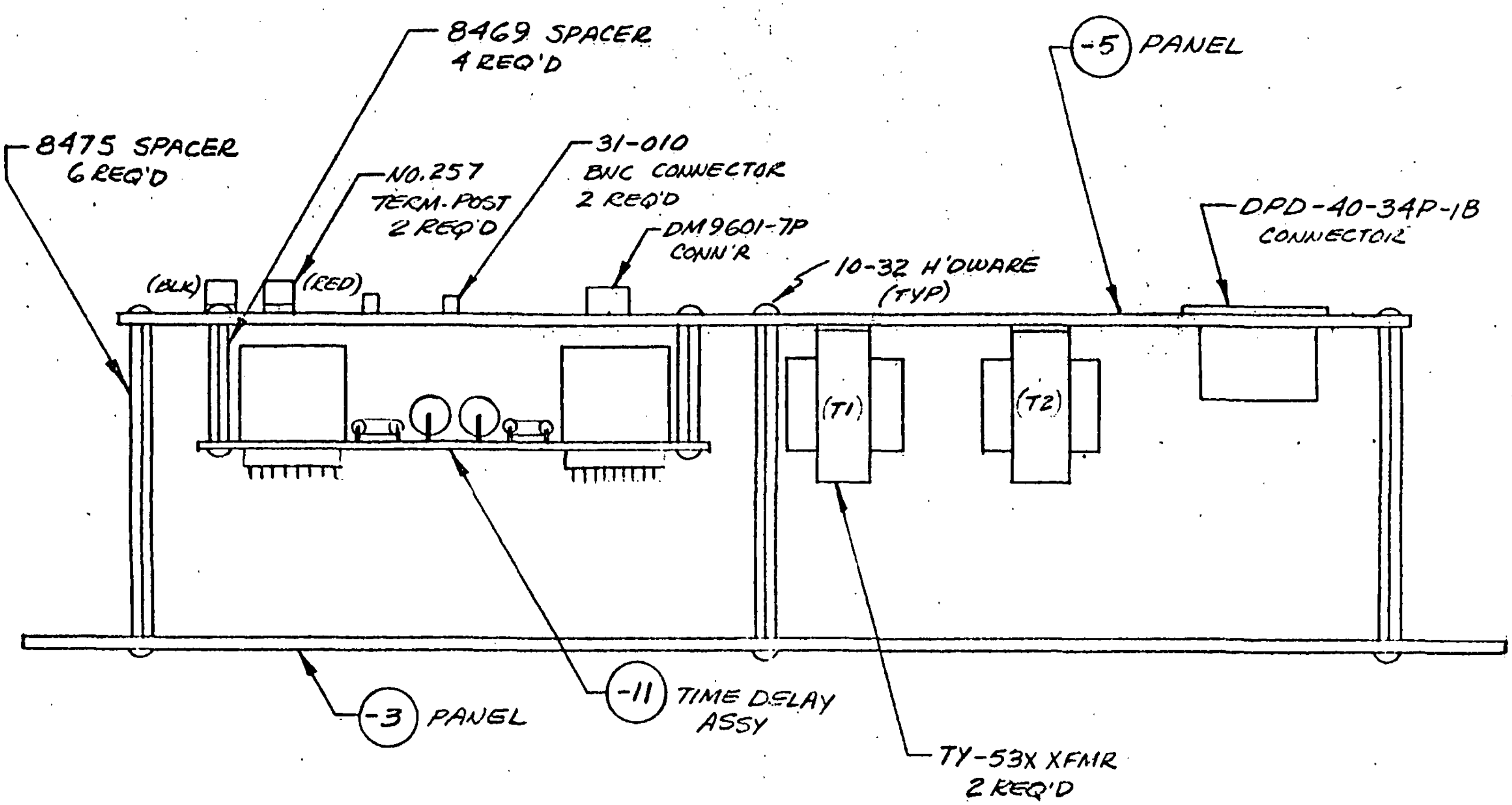

ASSY DETAIL -13 PANEL (TOP VIEW)

DWG NO. Z 7935344

ENGINEERING ORDER

DAC 25-17098 (6-71)

DOUGLAS AIRCRAFT COMPANY
LONG BEACH, CALIFORNIA
MCDONNELL DOUGLAS

SHEET	SIZE	DRAWING NUMBER
8		Z7935344

DATE	1	DRAWING CHANGED	
DATE	2	ADVANCE DWG CHG	
DATE	3	SERIAL EO	
DATE	4	NEW/REVISED RELEASE	NEW
DATE	5	REISSUE TO REVISE	R

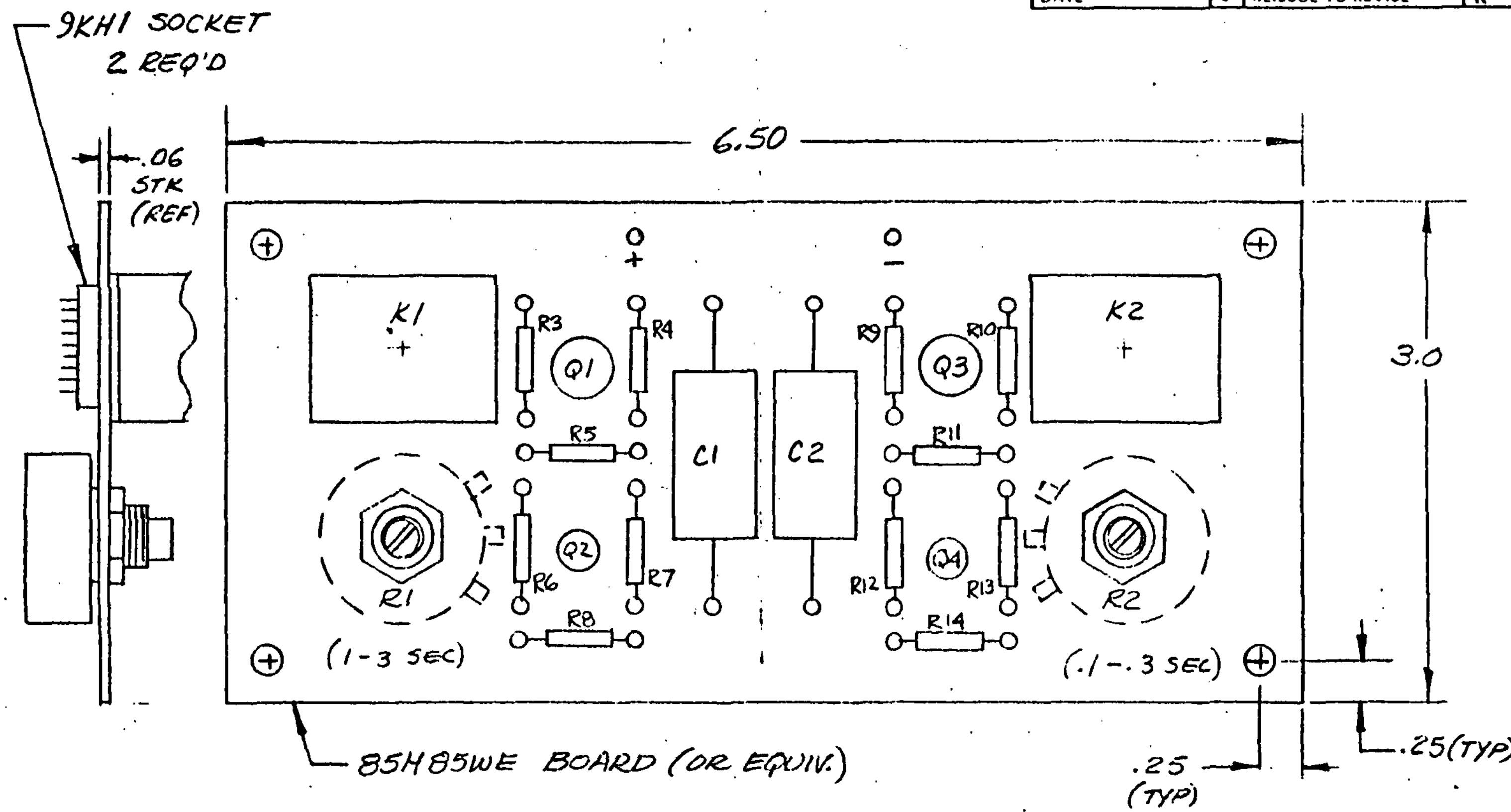

DETAIL – 11 TIME DELAY ASSY

NOTES:
1. LOCATE COMPONENTS APPROX. AS SHOWN; USE SUITABLE TERMINALS TO MOUNT CAP'S & RESISTORS.
2. IDENTIFY EACH COMPONENT FOR REFERENCE.
3. WIRE PER SHEET 11.
4. SEE PARTS LIST FOR PART NO.'S NOT SHOWN.

DWG NO. Z7935344

ENGINEERING ORDER

DAC 28-1709B (6-71)

DOUGLAS AIRCRAFT COMPANY
LONG BEACH, CALIFORNIA
MCDONNELL DOUGLAS

SHEET	SIZE	DRAWING NUMBER
9		Z 7935344

DATE	1	DRAWING CHANGED	
DATE	2	ADVANCE DWG CHG	
DATE	3	SERIAL EO	
DATE	4	NEW-REVISED RELEASE	NEW
DATE	5	REISSUE TO REVISE	R

NOTES: 1. -3 PANEL TO BE PAINTED LIGHT BEIGE ENAMEL (BINGHAM BEIGE).

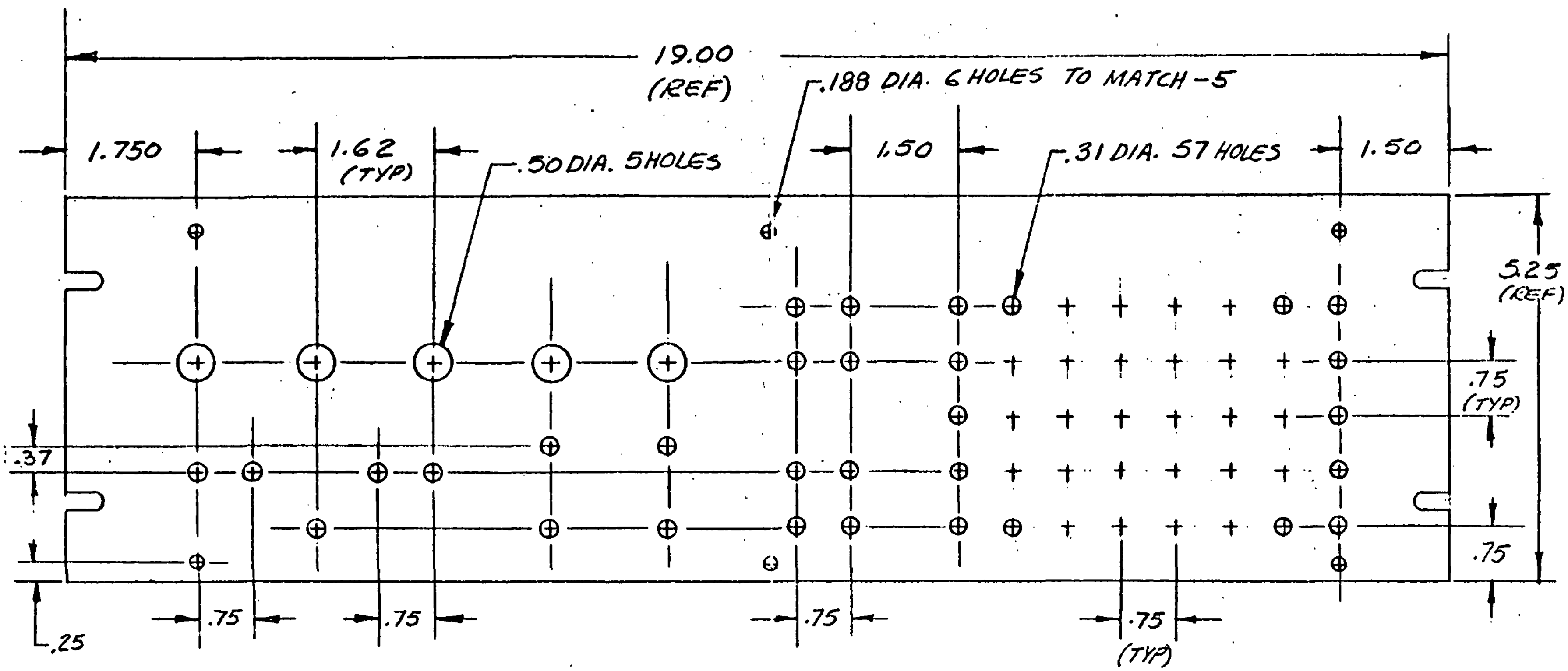

DETAIL -3 PANEL

DWG NO. Z 7935344

ENGINEERING ORDER

DAC 26-17098 (8-71)

DOUGLAS AIRCRAFT COMPANY
LONG BEACH, CALIFORNIA
McDONNELL DOUGLAS CORPORATION

SHEET	SIZE	DRAWING NUMBER
10		Z7935344

DATE	1	DRAWING CHANGED	
DATE	2	ADVANCE DWG CHG	
DATE	3	SERIAL EO	
DATE	4	NEW-REVISED RELEASE	NEW
DATE	5	REISSUE TO REVISE	R

NOTES: 1. APPLY BLACK DRY-TRANSFER LETTERING APPROX. AS SHOWN; OVERSPRAY WITH CLEAR ACRYLIC LACQUER.

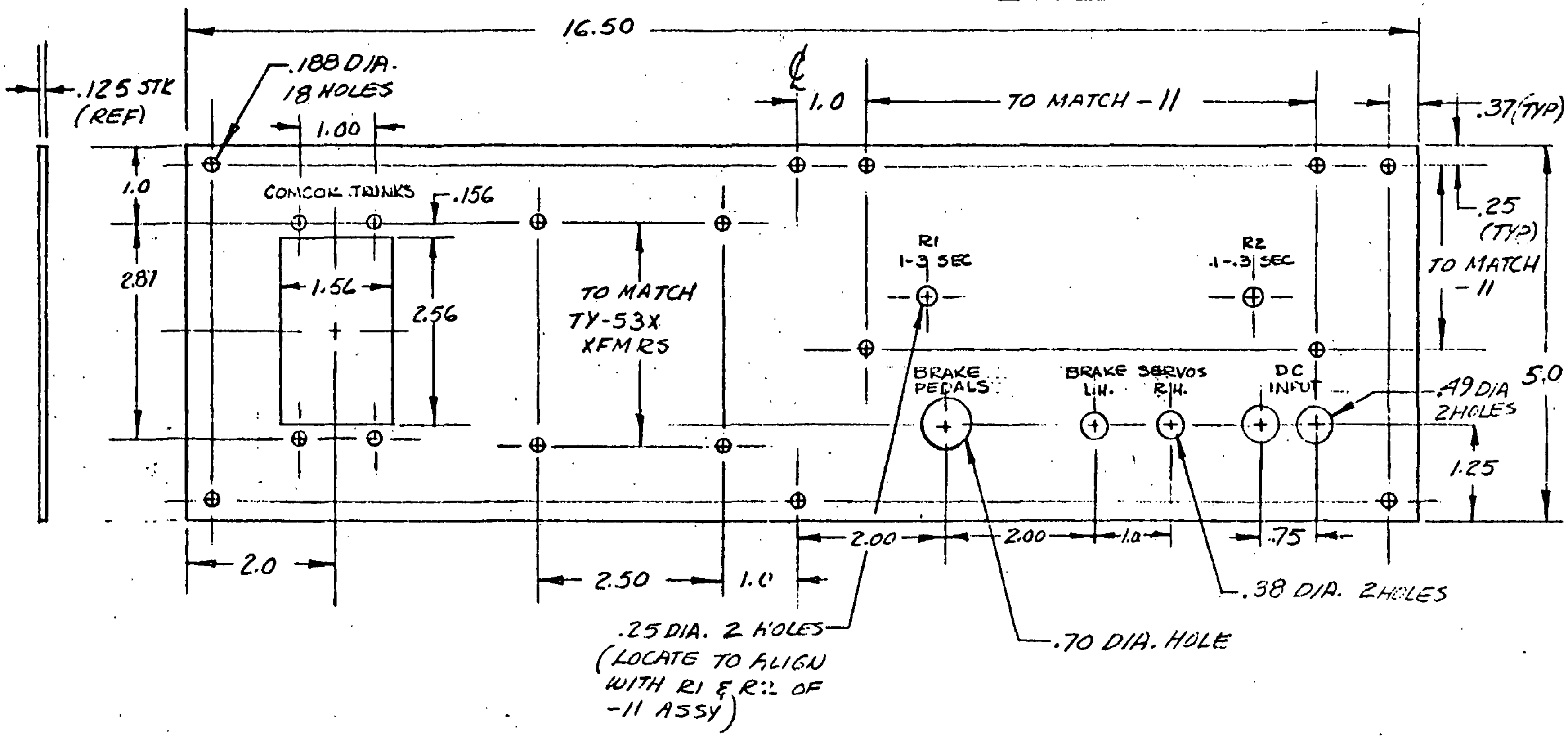

DETAIL -5 PANEL
(MAT'L: 6061-T6 ALUM.)

DWG NO. Z7935344

ENGINEERING ORDER

DAC 25-1709B (6-71)

DOUGLAS AIRCRAFT COMPANY
LONG BEACH, CALIFORNIA
MCDONNELL DOUGLAS

SHEET	SIZE	DRAWING NUMBER
11		Z 7935344

DATE	1	DRAWING CHANGED	
DATE	2	ADVANCE DWG CHG	
DATE	3	SERIAL EO	
DATE	4	NEW/REVISED RELEASE	NEW
DATE	5	REISSUE TO REVISE	R

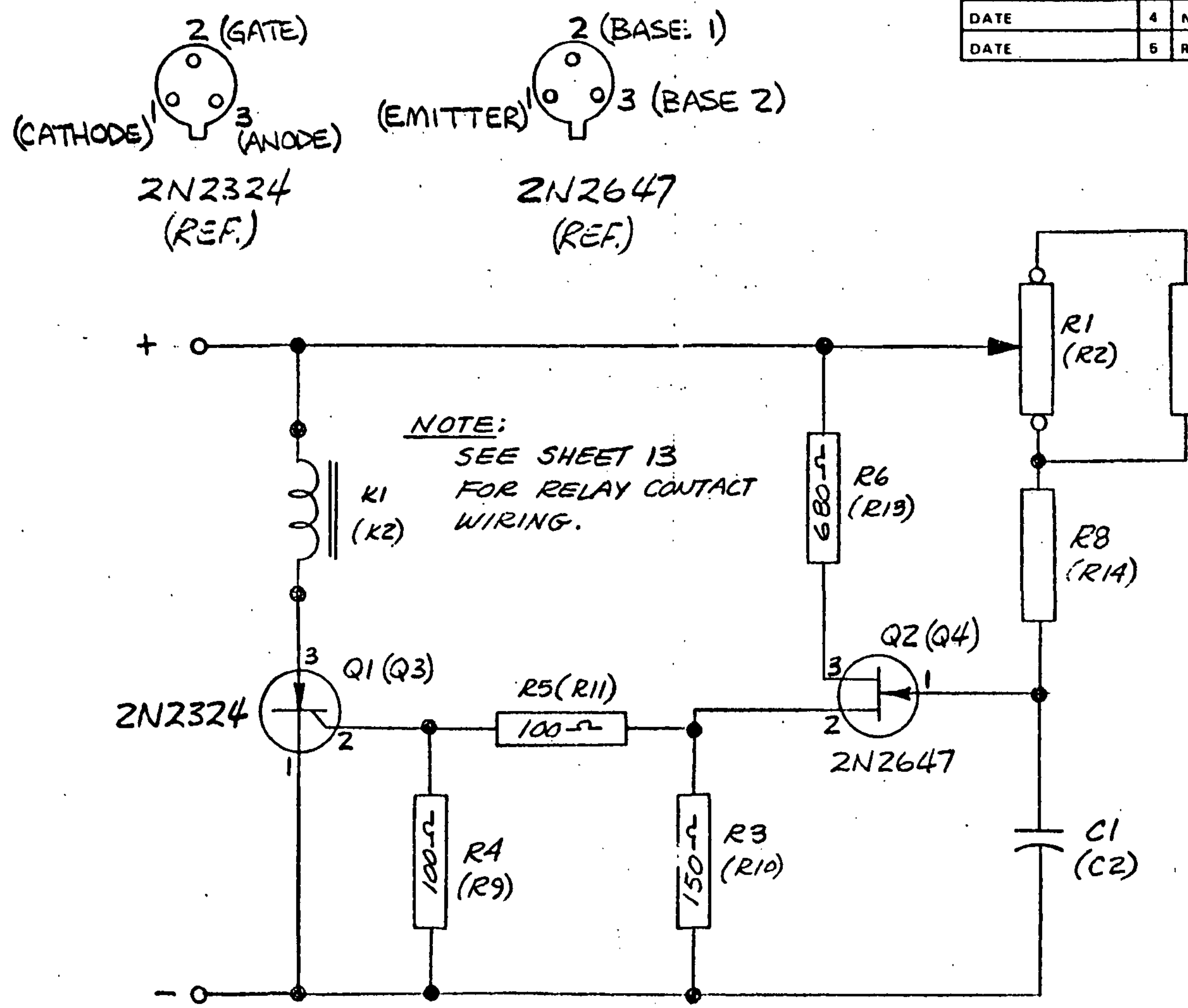

NOTE:
SEE SHEET 13 FOR RELAY CONTACT WIRING.

(1-3 SEC)
R1 - .1MEG
R7 - 330KΩ
R8 - 62KΩ
C1 - 15MFD

(.1-.3 SEC.)
R2 - .25MEG
R12 - 180KΩ
R14 - 15.7KΩ
C2 - 4MFD

WIRING DIAGRAM - 11 TIME DELAY ASSY

DWG NO. Z 7935344

ENGINEERING ORDER

DAC 26-1709B (6-71)

DOUGLAS AIRCRAFT COMPANY
LONG BEACH, CALIFORNIA
McDONNELL DOUGLAS

SHEET	SIZE	DRAWING NUMBER
12		Z7935344

DATE	1	DRAWING CHANGED	
DATE	2	ADVANCE DWG CHG	
DATE	3	SERIAL EO	
DATE	4	NEW/REVISED RELEASE	NEW
DATE	5	REISSUE TO REVISE	R

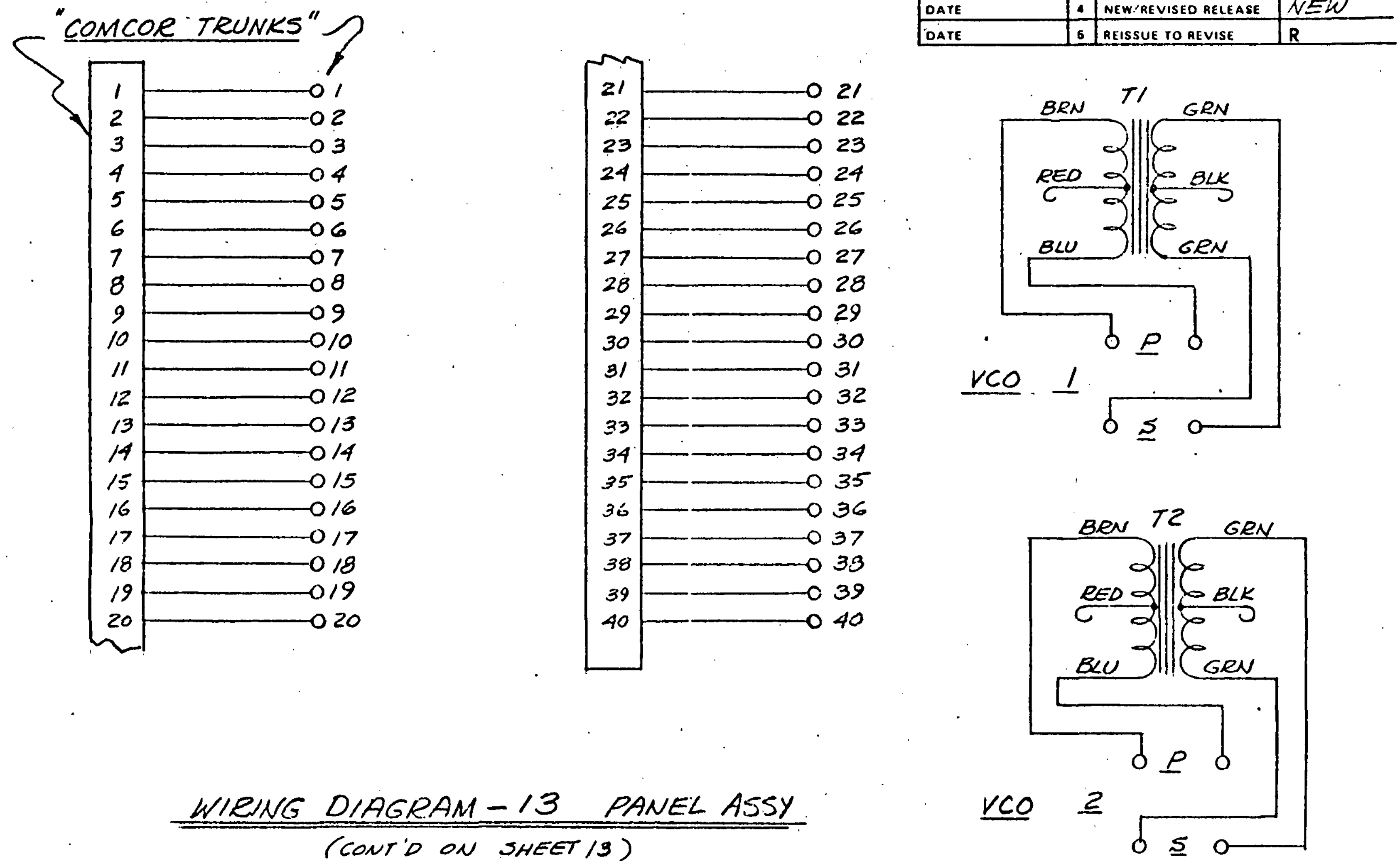

WIRING DIAGRAM - 13 PANEL ASSY

(CONT'D ON SHEET 13)

DWG NO. Z7935344

ENGINEERING ORDER

DAC 25-17098 (6-71)

DOUGLAS AIRCRAFT COMPANY
LONG BEACH, CALIFORNIA
McDONNELL DOUGLAS CORPORATION

SHEET	SIZE	DRAWING NUMBER
13		Z7935344

DATE	1	DRAWING CHANGED	
DATE	2	ADVANCE DWG CHG	
DATE	3	SERIAL EO	
DATE	4	NEW REVISED RELEASE	NEW
DATE	5	REISSUE TO REVISE	R

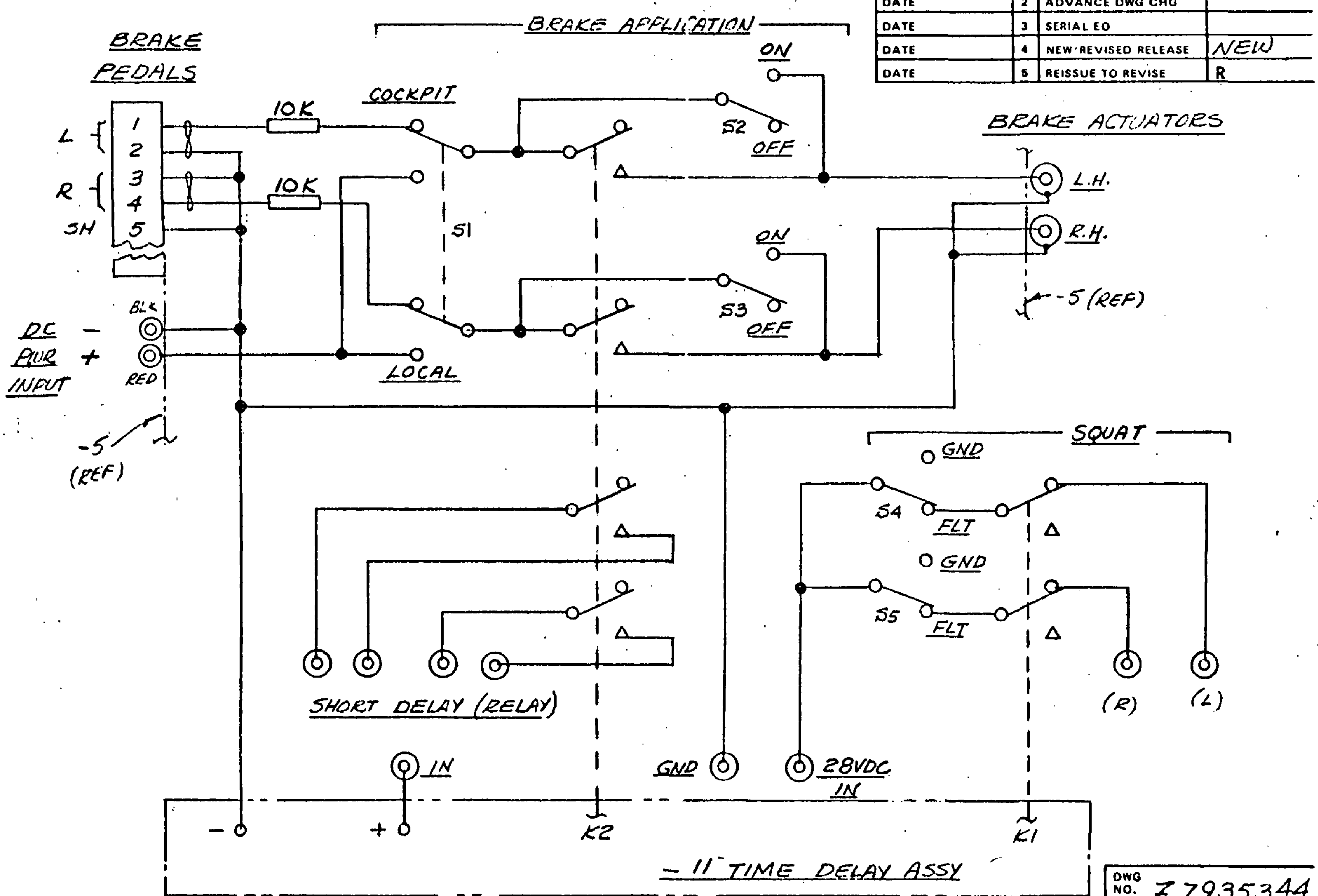

WIRING DIAGRAM - 13 PANEL ASSY (CONT'D)

DWG NO. Z7935344

ENGINEERING ORDER

DAC 25-17098 (6-71)

DOUGLAS AIRCRAFT COMPANY
LONG BEACH, CALIFORNIA
MCDONNELL DOUGLAS CORPORATION

SHEET	SIZE	DRAWING NUMBER
14		Z7935344

DATE	1	DRAWING CHANGED	
DATE	2	ADVANCE DWG CHG	
DATE	3	SERIAL EO	
DATE	4	NEW/REVISED RELEASE	NEW
DATE	5	REISSUE TO REVISE	R

NOTES:
1. SEE PARTS LIST FOR TABULATION OF PART NUMBERS VS. LOCATION.
2. APPLY APPROPRIATE SIZE BLACK DRY-TRANSFER LETTERS & FIGURES APPROX. AS SHOWN. OVERSPRAY WITH CLEAR ACRYLIC LACQUER.
3. ◯ = GREEN ⊚ = YELLOW ◉ = BLACK Ⓡ = RED Ⓑ = BLUE

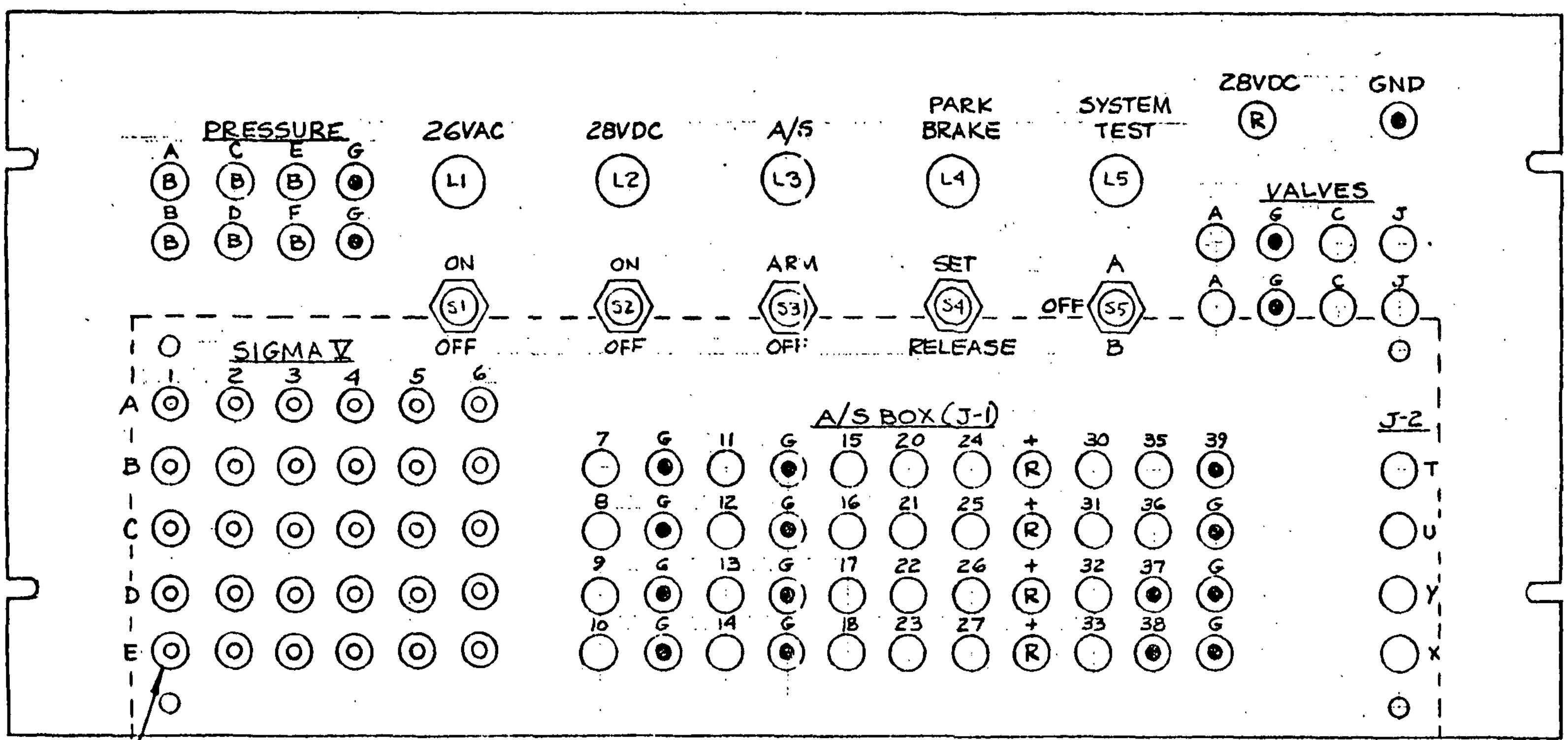

NO.1498 BANANA JACK 91 REQ'D (SEE NOTE 3 FOR COLOR)

DETAIL — LETTERING & PARTS LOCATION (FRONT)
-15 PANEL ASSY

DWG NO. Z7935344

ENGINEERING ORDER

DAC 25-17098 (6-71)

DOUGLAS AIRCRAFT COMPANY
LONG BEACH, CALIFORNIA
MCDONNELL DOUGLAS CORPORATION

SHEET	SIZE	DRAWING NUMBER
15		Z7935344

DATE	1	DRAWING CHANGED	
DATE	2	ADVANCE DWG CHG	
DATE	3	SERIAL EO	
DATE	4	NEW/REVISED RELEASE	NEW
DATE	5	REISSUE TO REVISE	R

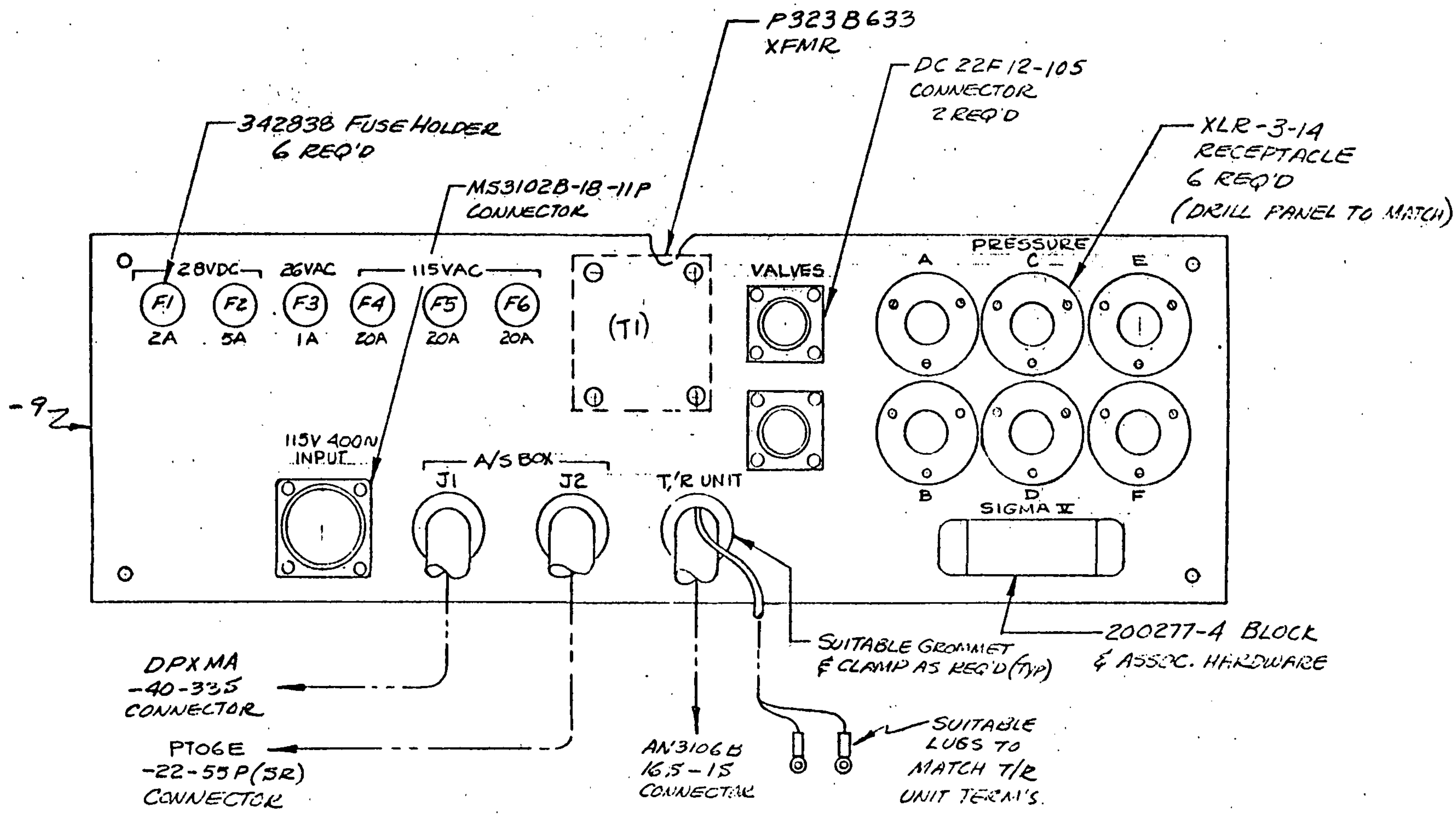

DETAIL - PARTS LAYOUT & LETTERING

-9 PANEL

DWG NO. Z7935344

ENGINEERING ORDER

DAC 25-17098 (6-71)

DOUGLAS AIRCRAFT COMPANY
LONG BEACH, CALIFORNIA
MCDONNELL DOUGLAS
CORPORATION

SHEET	SIZE	DRAWING NUMBER
16		Z7935344

DATE	1	DRAWING CHANGED	
DATE	2	ADVANCE DWG CHG	
DATE	3	SERIAL EO	
DATE	4	NEW/REVISED RELEASE	NEW
DATE	5	REISSUE TO REVISE	R

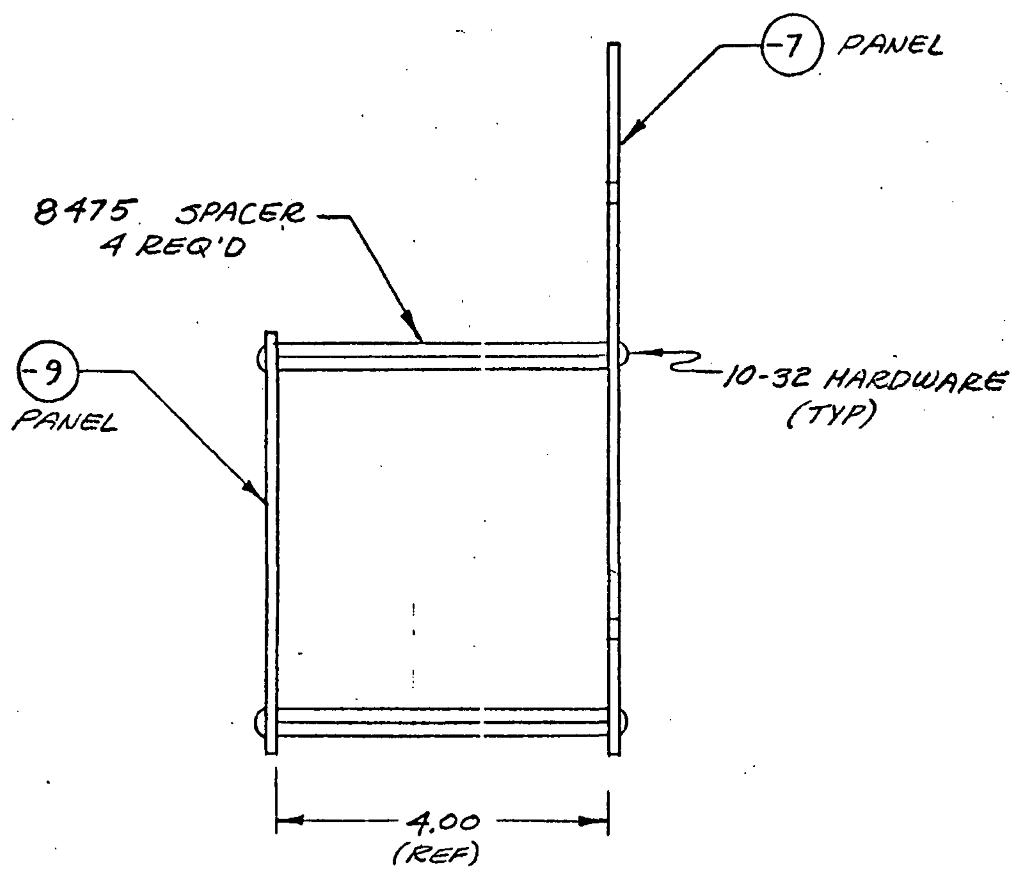

DETAIL - REAR CONNECTOR PANEL MTG (SIDE VIEW)

-15 PANEL ASSY

DWG NO. Z7935344

ENGINEERING ORDER

DAC 25-1709B (6-71)

DOUGLAS AIRCRAFT COMPANY
LONG BEACH, CALIFORNIA
McDONNELL DOUGLAS
CODE IDENT NO. 88277

SHEET	SIZE	DRAWING NUMBER
17		Z7935344

DATE	1	DRAWING CHANGED	
DATE	2	ADVANCE DWG CHG	
DATE	3	SERIAL EO	
DATE	4	NEW/REVISED RELEASE	NEW
DATE	5	REISSUE TO REVISE	R

NOTES: 1. -7 PANEL TO BE PAINTED LIGHT BEIGE ENAMEL. (BINGHAM BEIGE)

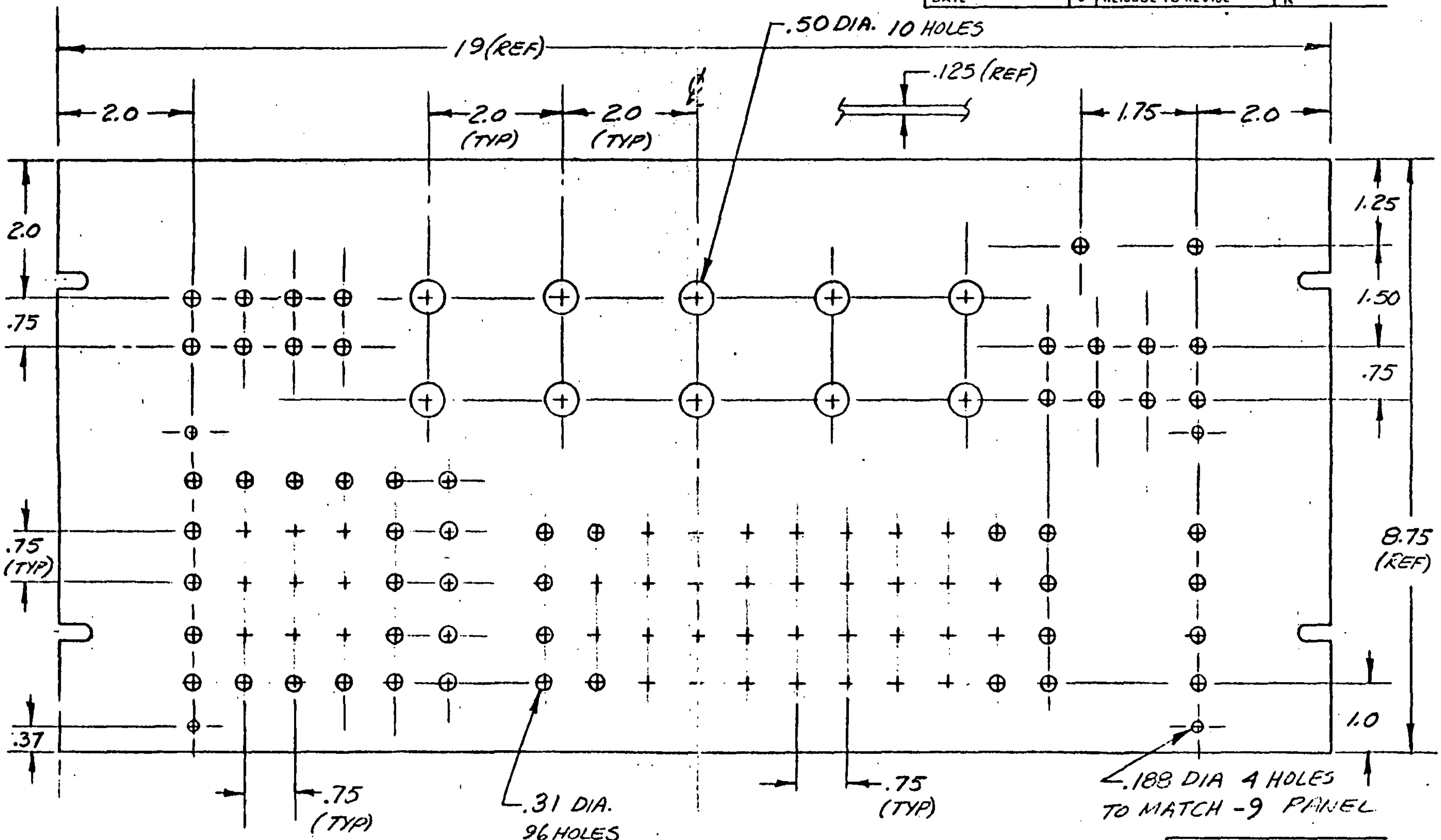

DETAIL -7 PANEL

DWG NO. Z7935344

ENGINEERING ORDER

DAC 25-17098 (6-71)

DOUGLAS AIRCRAFT COMPANY
LONG BEACH, CALIFORNIA
MCDONNELL DOUGLAS
CODE IDENT NO. 88277 CORPORATION

SHEET	SIZE	DRAWING NUMBER
18		Z7935344

DATE	1	DRAWING CHANGED	
DATE	2	ADVANCE DWG CHG	
DATE	3	SERIAL EO	
DATE	4	NEW/REVISED RELEASE	NEW
DATE	5	REISSUE TO REVISE	R

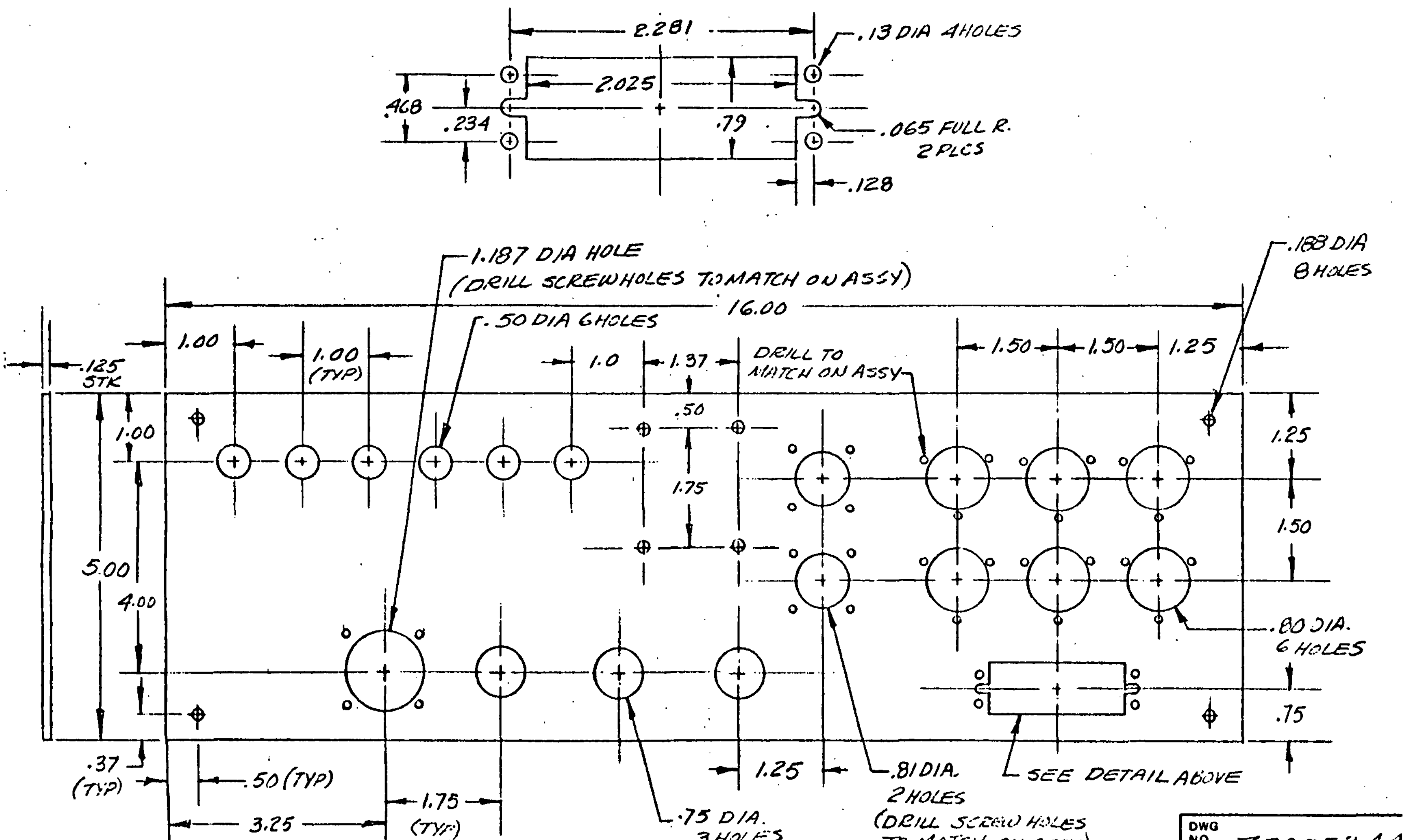

DETAIL - 9 PANEL (MT'L: 6061-T6 ALUM.)

DWG NO. Z7935344

ENGINEERING ORDER

DAC 25-1709B (6-71)

DOUGLAS AIRCRAFT COMPANY
LONG BEACH, CALIFORNIA
McDONNELL DOUGLAS

SHEET	SIZE	DRAWING NUMBER
19		Z 7935344

DATE	1	DRAWING CHANGED	
DATE	2	ADVANCE DWG CHG	
DATE	3	SERIAL EO	
DATE	4	NEW/REVISED RELEASE	NEW
DATE	5	REISSUE TO REVISE	R

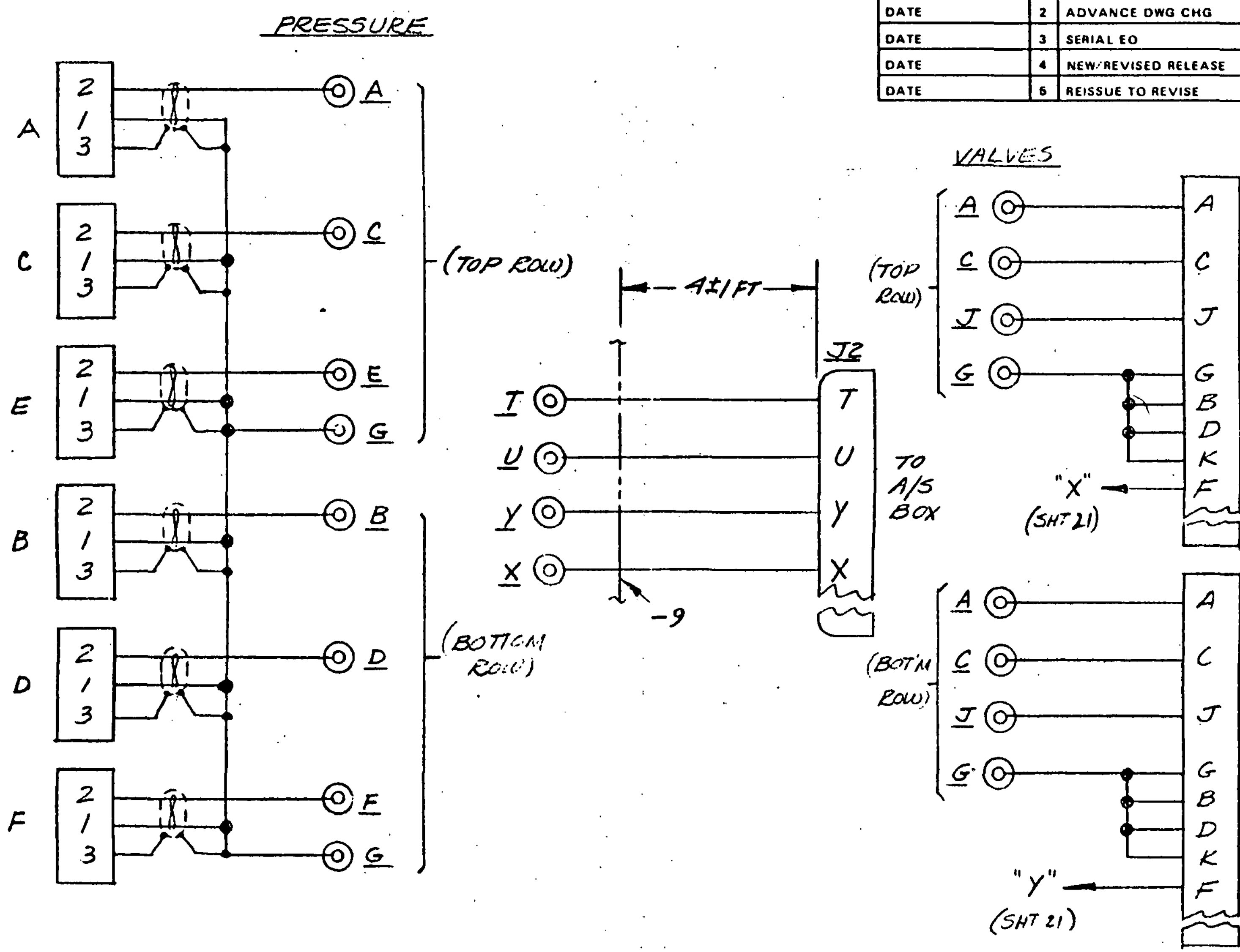

WIRING DIAGRAM – 15 PANEL ASSY

(CONT'D ON SHEETS 20 & 21)

DWG NO. Z 7935344

ENGINEERING ORDER

DAC 25-17098 (6-71)

DOUGLAS AIRCRAFT COMPANY
LONG BEACH, CALIFORNIA
McDONNELL DOUGLAS
CORPORATION

SHEET	SIZE	DRAWING NUMBER
20		Z7935344

DATE	1	DRAWING CHANGED	
DATE	2	ADVANCE DWG CHG	
DATE	3	SERIAL EO	
DATE	4	NEW/REVISED RELEASE	NEW
DATE	5	REISSUE TO REVISE	R

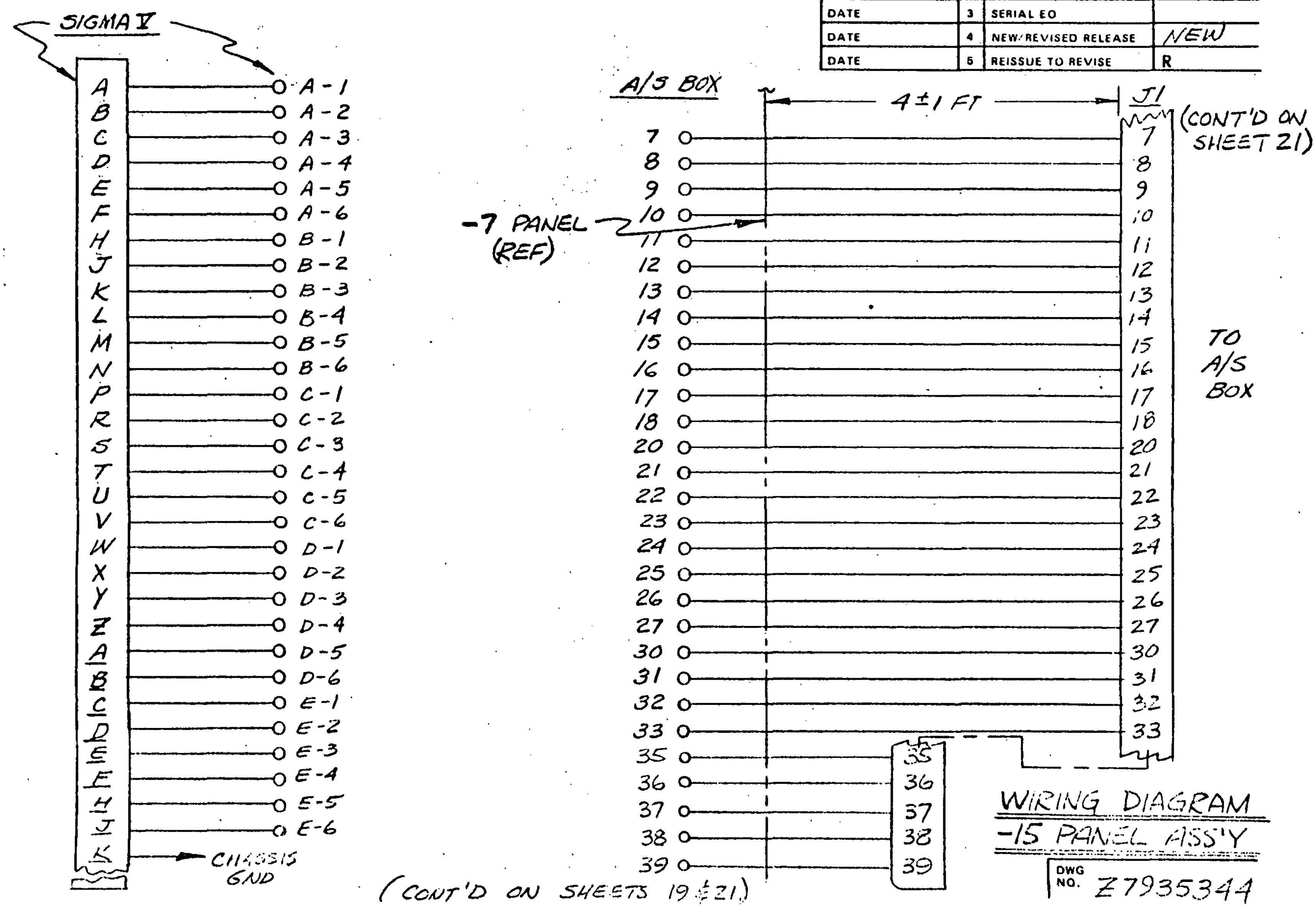

WIRING DIAGRAM
-15 PANEL ASS'Y

DWG NO. Z7935344

ENGINEERING ORDER

DAC 25-17098 (6-71)

DOUGLAS AIRCRAFT COMPANY
LONG BEACH, CALIFORNIA
McDONNELL DOUGLAS
CORPORATION

SHEET	SIZE	DRAWING NUMBER
21		Z 7935344

DATE	1	DRAWING CHANGED	
DATE	2	ADVANCE DWG CHG	
DATE	3	SERIAL EO	
DATE	4	NEW/REVISED RELEASE	NEW
DATE	5	REISSUE TO REVISE	R

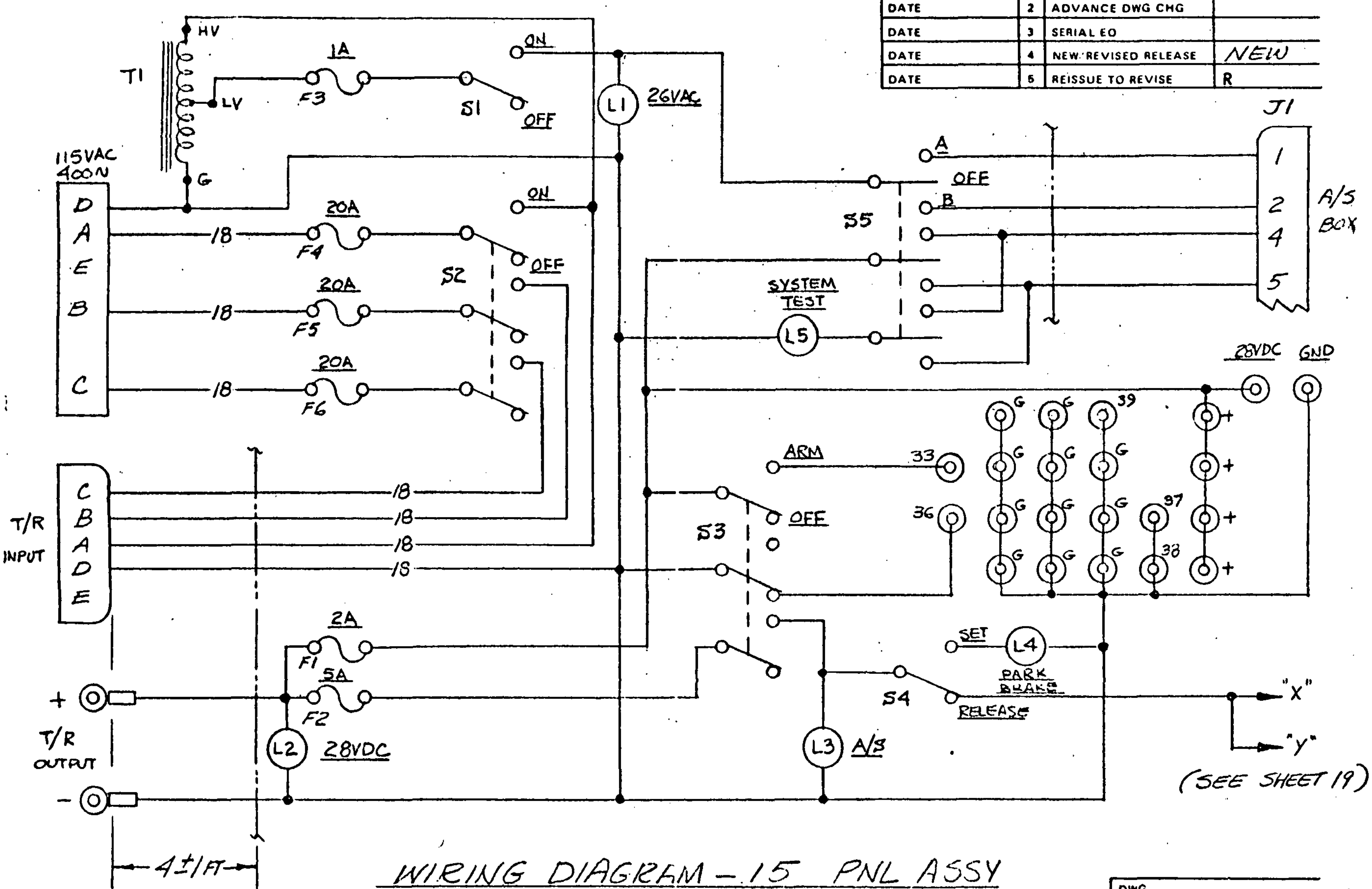

WIRING DIAGRAM – 15 PNL ASSY

(CONT'D ON SHTS 19 & 20)

DWG NO. Z 7935344

ENGINEERING ORDER

DAC 25-17098 (6-71)

DOUGLAS AIRCRAFT COMPANY
LONG BEACH, CALIFORNIA
MCDONNELL DOUGLAS
CORPORATION

SHEET	SIZE	DRAWING NUMBER
22		Z7935344

DATE	1	DRAWING CHANGED	
DATE	2	ADVANCE DWG CHG	
DATE	3	SERIAL EO	
DATE	4	NEW/REVISED RELEASE	NEW
DATE	6	REISSUE TO REVISE	R

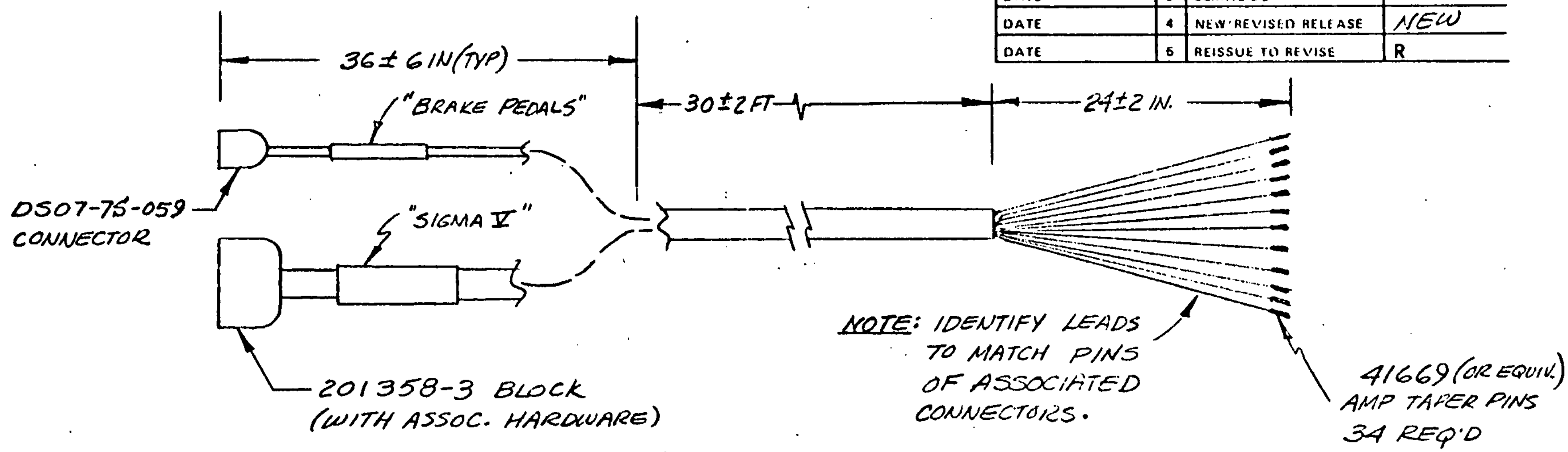

DETAIL -19 CABLE ASSY

(FOR WIRING, SEE SHEET 24)

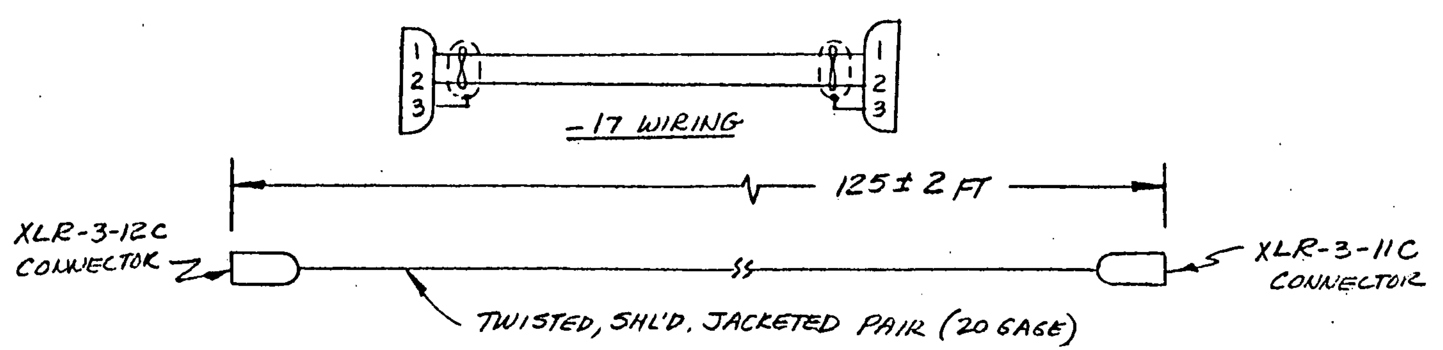

DETAIL -17 CABLE ASSY

(6 REQ'D)

DWG NO. Z7935344

ENGINEERING ORDER

DAC 25-17098 (6-71)

DOUGLAS AIRCRAFT COMPANY
LONG BEACH, CALIFORNIA
McDONNELL DOUGLAS CORPORATION

SHEET	SIZE	DRAWING NUMBER
23		Z 7935344

DATE	1	DRAWING CHANGED	
DATE	2	ADVANCE DWG CHG	
DATE	3	SERIAL EO	
DATE	4	NEW REVISED RELEASE	NEW
DATE	5	REISSUE TO REVISE	R

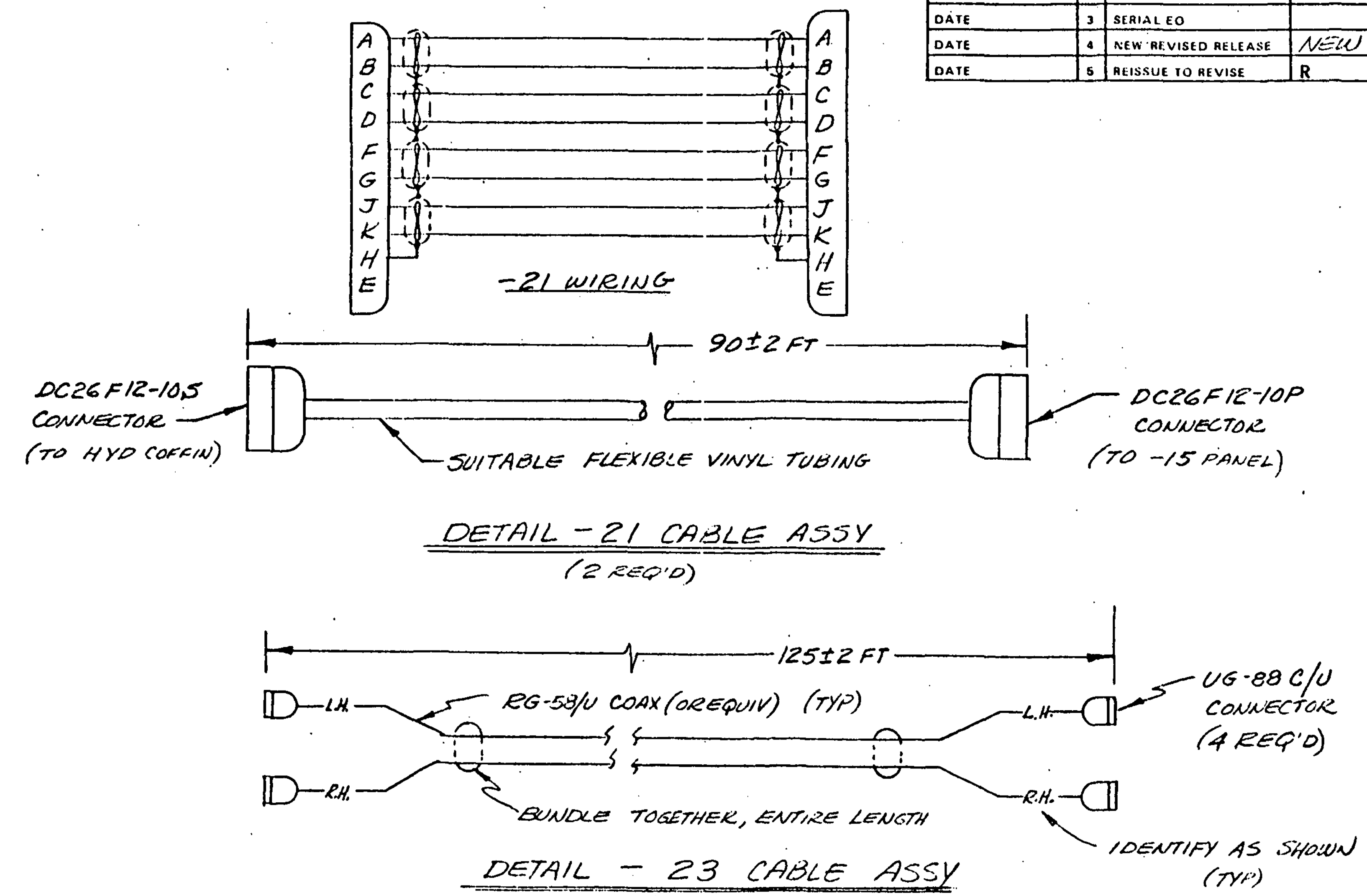

DWG NO. Z 7935344

ENGINEERING ORDER

DAC 25-1709B (6-71)

DOUGLAS AIRCRAFT COMPANY
LONG BEACH, CALIFORNIA
MCDONNELL DOUGLAS
CORPORATION

SHEET	SIZE	DRAWING NUMBER
24		Z 7935344

DATE	1	DRAWING CHANGED	
DATE	2	ADVANCE DWG CHG	
DATE	3	SERIAL EO	
DATE	4	NEW/REVISED RELEASE	NEW
DATE	5	REISSUE TO REVISE	R

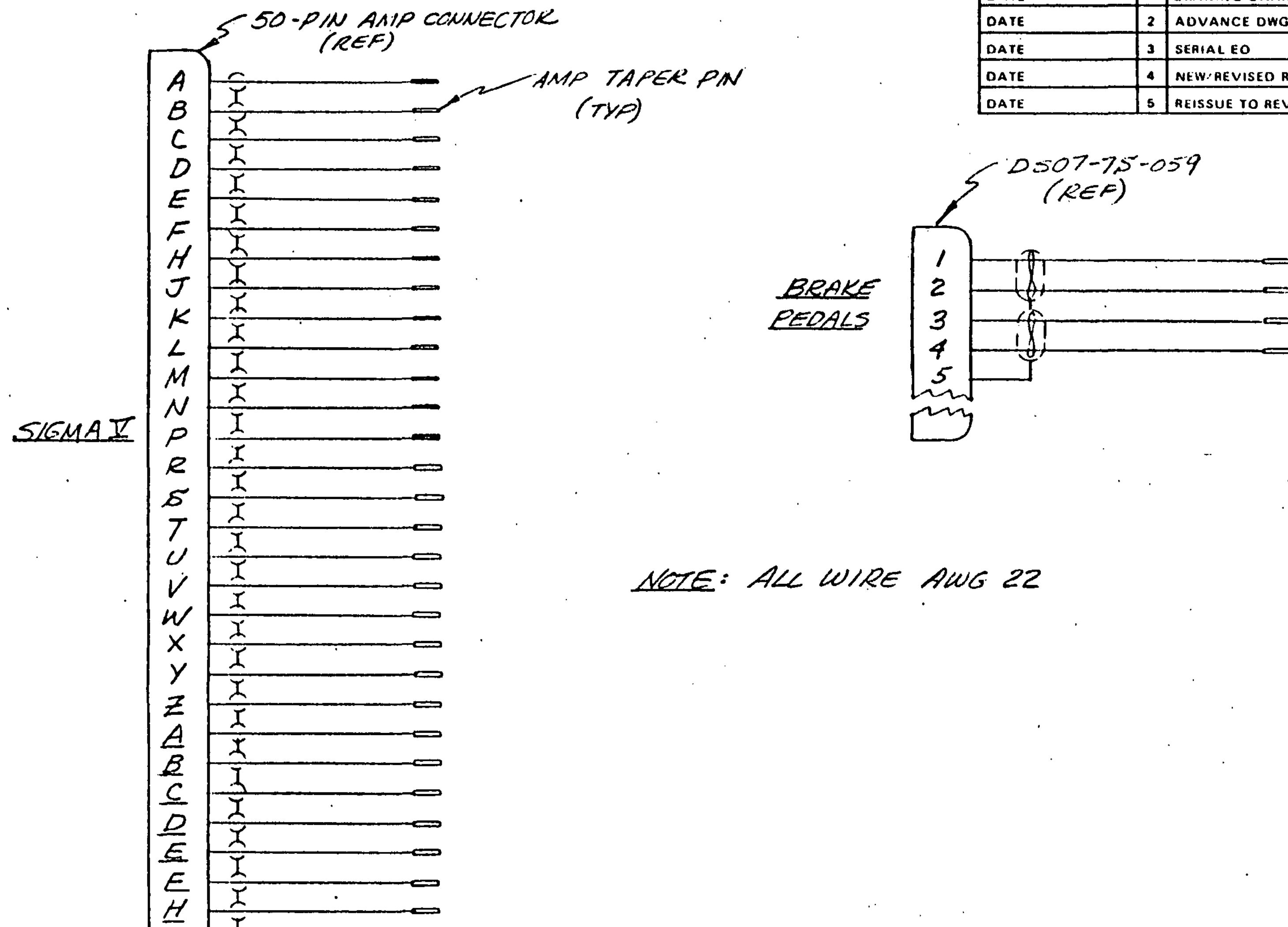

NOTE: ALL WIRE AWG 22

WIRING DIAGRAM -19 CABLE

DWG NO. Z 7935344

ENGINEERING ORDER

DAC 26-17098 (6-71)

DOUGLAS AIRCRAFT COMPANY
LONG BEACH, CALIFORNIA
MCDONNELL DOUGLAS
CORPORATION

SHEET	SIZE	DRAWING NUMBER
25		Z 7935344

DATE	1	DRAWING CHANGED	
DATE	2	ADVANCE DWG CHG	
DATE	3	SERIAL EO	
DATE	4	NEW REVISED RELEASE	NEW
DATE	5	REISSUE TO REVISE	R

* USE EXISTING EQUIP.

✓ PARTS ARE IN HOUSE; SEE DICK STORLEY OR BOB DEAN

	-23	-21	-19	-17	-15	-13	-11	-503	-501	PART NO.	PART NAME	VENDOR
✓								1	1	*	SINGLE-BAY CABINET	
✓									2	MODEL 6299A	DC POWER SUPPLY	HARRISON LABS
									1	Z (TBD)	BRAKE SERVO PANEL	
✓									1	Z 4888926	BRIDGE BALANCE PANEL	
✓									1	7600	AMPLIFIER RACK	PRESTON
									6	8300 DO	AMPLIFIER CARD	PRESTON
									6	-17	CABLE ASSY	
								1		-19	CABLE ASSY	
								2		-21	CABLE ASSY	
									1	-23	CABLE ASSY	
								1		-13	PANEL ASSY	
								1		-15	PANEL ASSY	
✓								1		*	ANTI-SKID BOX	
✓								1		6RW176YN3	POWER SUPPLY (T/R UNIT)	G.E.
✓								1		*	DC PWR SUPPLY (OPAD OR EQUIV)	
✓									6	Z 4802188-553	CABLE ASSY (STANDARD GREEN TRANSDUCER CABLE)	

DWG NO. Z 7935344

2

ENGINEERING ORDER

DAC 25-17098 (6-71)

DOUGLAS AIRCRAFT COMPANY
LONG BEACH, CALIFORNIA
MCDONNELL DOUGLAS CORPORATION

SHEET	SIZE	DRAWING NUMBER
26		Z 7935344

DATE	1	DRAWING CHANGED	
DATE	2	ADVANCE DWG CHG	
DATE	3	SERIAL EO	
DATE	4	NEW. REVISED RELEASE	NEW
DATE	5	REISSUE TO REVISE	R

PARTS ARE IN HOUSE; SEE DICK STORLEY OR BOB DEAN

-15	-13	-11	PART NO.		PART NAME	VENDOR
	1		-3	PANEL	MAKE FROM CAL CHASSIS NO. PWA-12 (UNPAINTED ALUM)	
	1		-5		PANEL - .125 X 5 X 16.5 6061-T6 ALUM	
1			-7	PANEL	MAKE FROM CAL CHASSIS NO. PWA-14 (UNPAINTED ALUM)	
1			-9		PANEL - .125 X 5 X 16 6061-T6 ALUM	
	1		-11		TIME DELAY ASSY	
	4		8469		SPACER	H.H. SMITH
4	6		8475		SPACER	H.H. SMITH
	2		TY-53X		TRANSFORMER (T1, T2)	TRIAD
1			P323B633		TRANSFORMER (115/26 V 400 ~)	WESTINGHOUSE
	1		DPD-40-34P-1B		CONNECTOR (COMCOR)	ITT-CANNON
6	5		1498	(BLUE)	BANANA JACK	H.H. SMITH
36	10		1498	(GREEN)	" "	"
5	1		1498	(RED)	" "	"
30			1498	(YEL)	" "	"

DWG NO. Z 7935344

ENGINEERING ORDER

DAC 25-1709B (6-71)

DOUGLAS AIRCRAFT COMPANY
LONG BEACH, CALIFORNIA
McDONNELL DOUGLAS
CODE IDENT NO. 88277
CORPORATION

SHEET	SIZE	DRAWING NUMBER
27		Z7935344

DATE	1	DRAWING CHANGED	
DATE	2	ADVANCE DWG CHG	
DATE	3	SERIAL EO	
DATE	4	NEW/REVISED RELEASE	NEW
DATE	5	REISSUE TO REVISE	R

-15	-13	-11	PART NO.	PART NAME	VENDOR
	40		1498 (BROWN)	BANANA JACK	H.H. SMITH
19	1		1498 (BLACK)	" "	"
2	4		MS24523-23 (OR EQUIV)	SPDT TOGGLE SW. -13: S2 THRU S5 -15: S1 & S4	
	1		MS24524-23 (OR EQUIV)	DPDT " " S1	
2			MS24525-23 (OR EQUIV)	4PDT " " S2 & S3	
1			MS24525-21 (OR EQUIV)	4PDT (CENT OFF) " S5	
4			MS25256-4-327	LAMP ASSY (GREEN) L1 THRU L4	
1			MS25256-2-327	" " (YELLOW) L5	
6			342838	FUSE HOLDER F1 THRU F6	LITTELFUSE
1			1A3AG	FUSE	
1			2A3AG	"	
1			5A3AG	"	
3			20A3AG	"	
	1		31-010	CONNECTOR (BULKHEAD BNC)	AMPHENOL

DWG NO. Z7935344

ENGINEERING ORDER

DAC 25-1709B (6-71)

DOUGLAS AIRCRAFT COMPANY
LONG BEACH, CALIFORNIA
MCDONNELL DOUGLAS

SHEET	SIZE	DRAWING NUMBER
28		Z 7935344

DATE	1	DRAWING CHANGED	
DATE	2	ADVANCE DWG CHG	
DATE	3	SERIAL EO	
DATE	4	NEW-REVISED RELEASE	NEW
DATE	5	REISSUE TO REVISE	R

✓ PARTS IN HOUSE; SEE DICK STORLEY OR BOB DEAN.

	-15	-11	PART NO.	PART NAME	VENDOR
	1		MS3102B-18-11P	CONNECTOR	
	1		DPAMA-40-33S	"	ITT/CANNON
	1		PT06E-22-55P(SR)	"	BENDIX
	1		AN3106B-16S-1S	"	
✓	1		200277-4	BLOCK	A-MP
	6		XLP-3-14	RECEPTACLE	ITT-CANNON
	2		DC22F12-10S	CONNECTOR	BURNDY
✓		2	KHP17D11	RELAY K1, K2	POTTER-BRUMFIELD
		2	2N2324	TRANSISTOR Q1, Q3	G.E.
		2	2N2647	TRANSISTOR Q2, Q4	G.E.
		4	100 Ω 1/2W	RESISTOR R4, R5, R9, R11	
		2	150 Ω 1/2W	RESISTOR R3, R10	
		2	680 Ω 1/2W	RESISTOR R6, R13	
		1	15 MFD 50VDC	CAPACITOR C1	
		2	9KH1	RELAY SOCKET (POTTER-BRUM.)	

DWG NO. Z 7935344

5

ENGINEERING ORDER

DAC 25-17098 (6-71)

DOUGLAS AIRCRAFT COMPANY
LONG BEACH, CALIFORNIA
McDONNELL DOUGLAS CORPORATION

SHEET	SIZE	DRAWING NUMBER
29		Z7935344

DATE	1	DRAWING CHANGED	
DATE	2	ADVANCE DWG CHG	
DATE	3	SERIAL EO	
DATE	4	NEW-REVISED RELEASE	NEW
DATE	5	REISSUE TO REVISE	R

* 33K & 30K IN PARALLEL.

\ PARTS IN HOUSE; SEE DICK STORLEY OR BOB DEAN

			-23	-21		-17	-11	PART NO.	PART NAME	VENDOR
							1	4MFD 50V	CAPACITOR C2	
\							1	CU-1041	POTENTIOMETER .1MEG-Ω R1	OHMITE
\							1	CU-2541	POTENTIOMETER .25MEG-Ω R2	OHMITE
							1	330K-Ω 1/2W	RESISTOR R7	
							1	62K-Ω 1/2W	" R8	
							1	180K-Ω 1/2W	" R12	
							1	*15.7K-Ω 1/2W	" R14	
							1	85H85WE (OR EQUIV)	CIRCUIT BOARD (1/16 x 3 x 6 1/2)	VECTOR
						1		XLR-3-11C	CONNECTOR	ITT-CANNON
						1		XLR-3-12C	"	"
				1				DC26F12-10P	"	BURNDY
				1				DC26F12-10S	"	"
			4					UG-88C/U	COAX CONN. (BNC)	
			AS REQ					RG-58/U	COAX CABLE	

DWG NO. Z7935344

6

ENGINEERING ORDER

DAC 25-1709B (6-71)

DOUGLAS AIRCRAFT COMPANY
LONG BEACH, CALIFORNIA
McDONNELL DOUGLAS
CODE IDENT NO. 88277 CORPORATION

SHEET	SIZE	DRAWING NUMBER
30		Z 7935344

DATE	1	DRAWING CHANGED	
DATE	2	ADVANCE DWG CHG	
DATE	3	SERIAL EO	
DATE	4	NEW/REVISED RELEASE	NEW
DATE	5	REISSUE TO REVISE	R

✓ PARTS IN HOUSE; SEE DICK STORLEY OR BOB DEAN.

	-19	-13	PART NO.	PART NAME	VENDOR
✓		1	DM 9601-7P	CONNECTOR	DEUTSCH
✓	1		D507-75-059	"	"
✓	1		201358-3	BLOCK	A-MP
		2	10 K Ω	RESISTOR	

DWG NO. Z 7935344

Section 5. ANALOG ANTISKID SIMULATOR VALIDATION

The validation consisted of matching Langley test-track test data (NASA TN D-8332) on the antiskid simulator.

The test conditions (speed, vertical load, maximum coefficient of friction, tire yaw angle, and commanded brake pressure) were set up on the simulator and runs were made. The drag loads decelerating the aircraft were adjusted to give the same deceleration and the torque gain was adjusted to give the same skid pressure level as on the test data. The brake characteristics utilized are shown in Figure C-5.

Two of the Langley tests were selected for correlation. The time history for the first, in which the tire was unyawed, is shown in Figure C-6. The actual test conditions are denoted on the figure. Figure C-7 presents the simulator run for the same conditions. The degree of correlation between the simulator and test data can be seen by comparing these two figures. Note the similarity in skid depth and in the levels of the brake pressure, brake torque and drag coefficient of friction just prior to the skids. The correlation between the simulator and test data is good, except that the pressure recovery immediately following a skid was quicker on the simulator. The time history of the second test, in which the tire was yawed 6°, is shown in Figure C-8 and the corresponding simulator run is shown in Figure C-9. Here, particularly note how well μ_s correlates, both unbraked and with 2000 psi applied (slip ratio = 10%). The comments made above about the degree of correlation for the other case apply here also for the initial skid. The subsequent shallow skids shown in the test data weren't duplicated on the simulator. These deep skids on the simulator are probably due to the adjustments made to achieve rougher cockpit motion.

Brake torque = f_1 (Speed) x f_2 (Pressure)

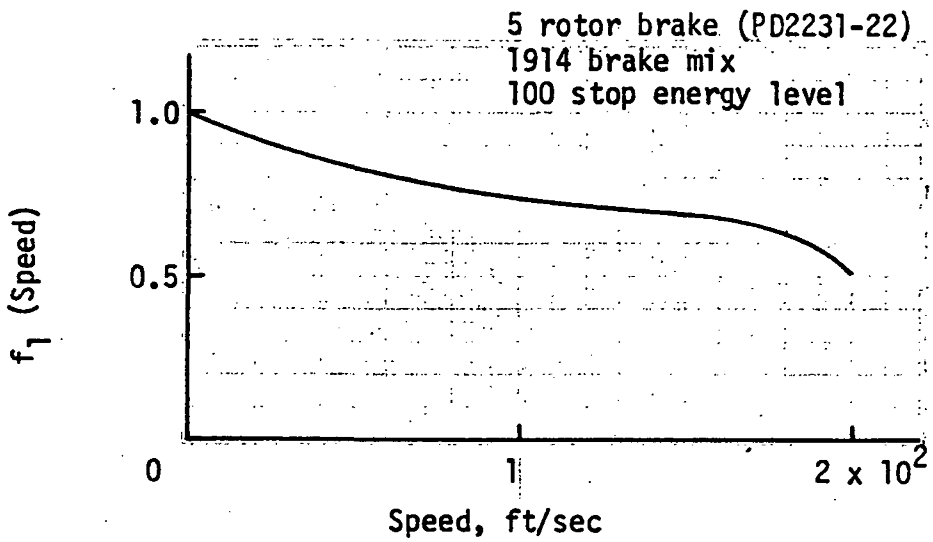

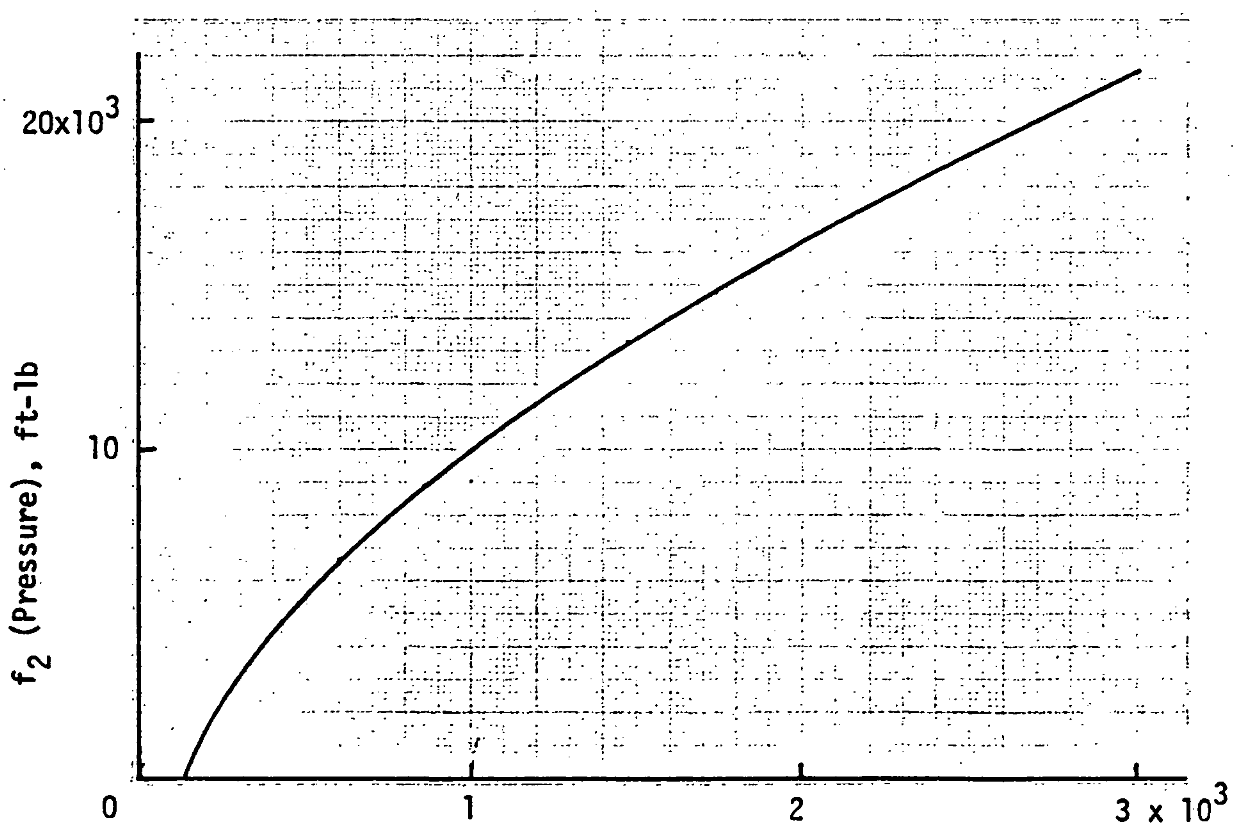

FIGURE C-5 BRAKE TORQUE/PRESSURE/SPEED RELATIONSHIP

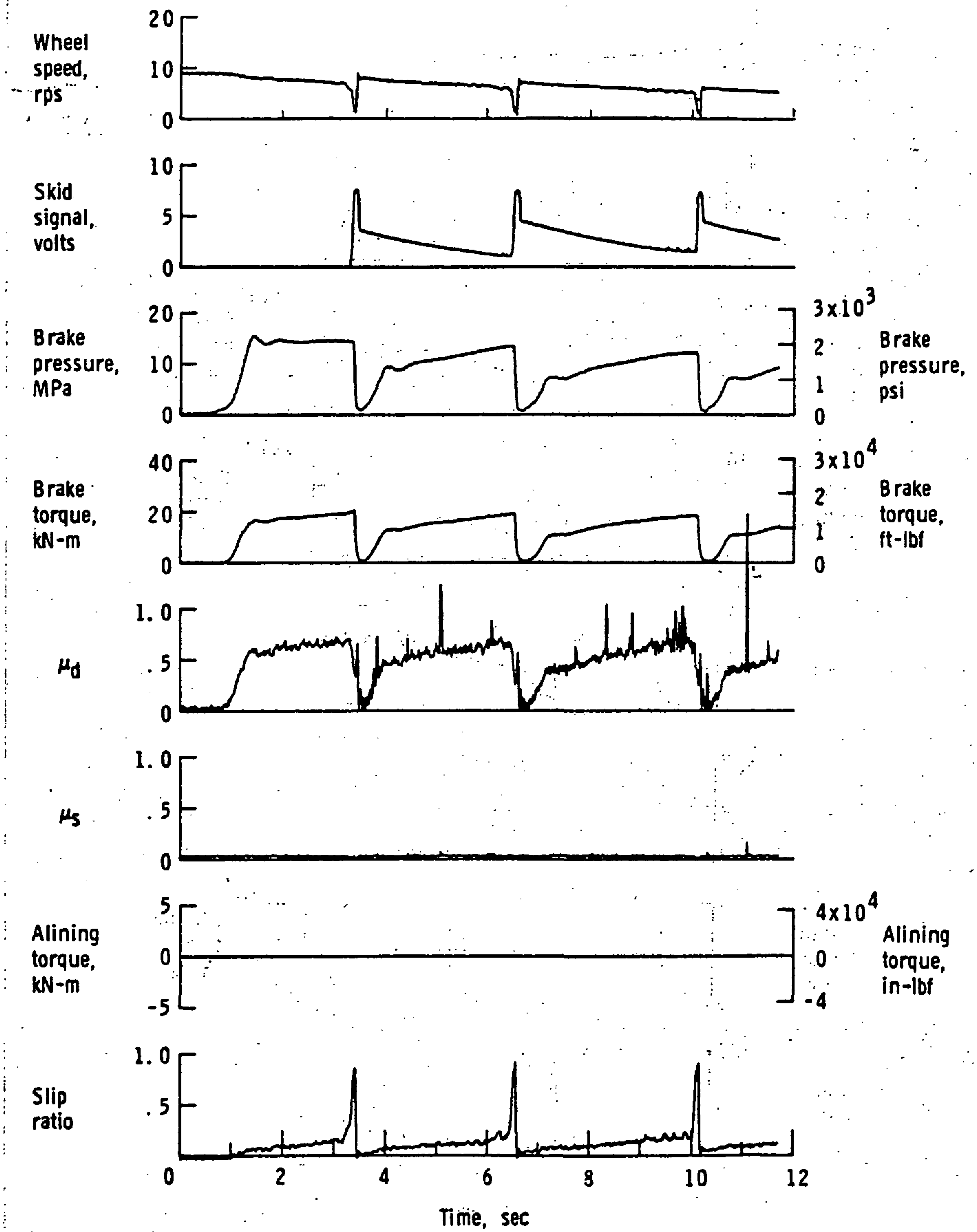

- Time histories for run 2; nominal carriage speed, 44 knots; vertical load, 59.6 kN (13 400 lbf); yaw angle, 0°; surface condition, dry; tire condition, new; brake pressure, 14 MPa (2000 lbf/in^2).

FIGURE C-6 TEST TIME HISTORY SELECTED FOR ANTISKID SIMULATOR VALIDATION -- UNYAWED TIRE

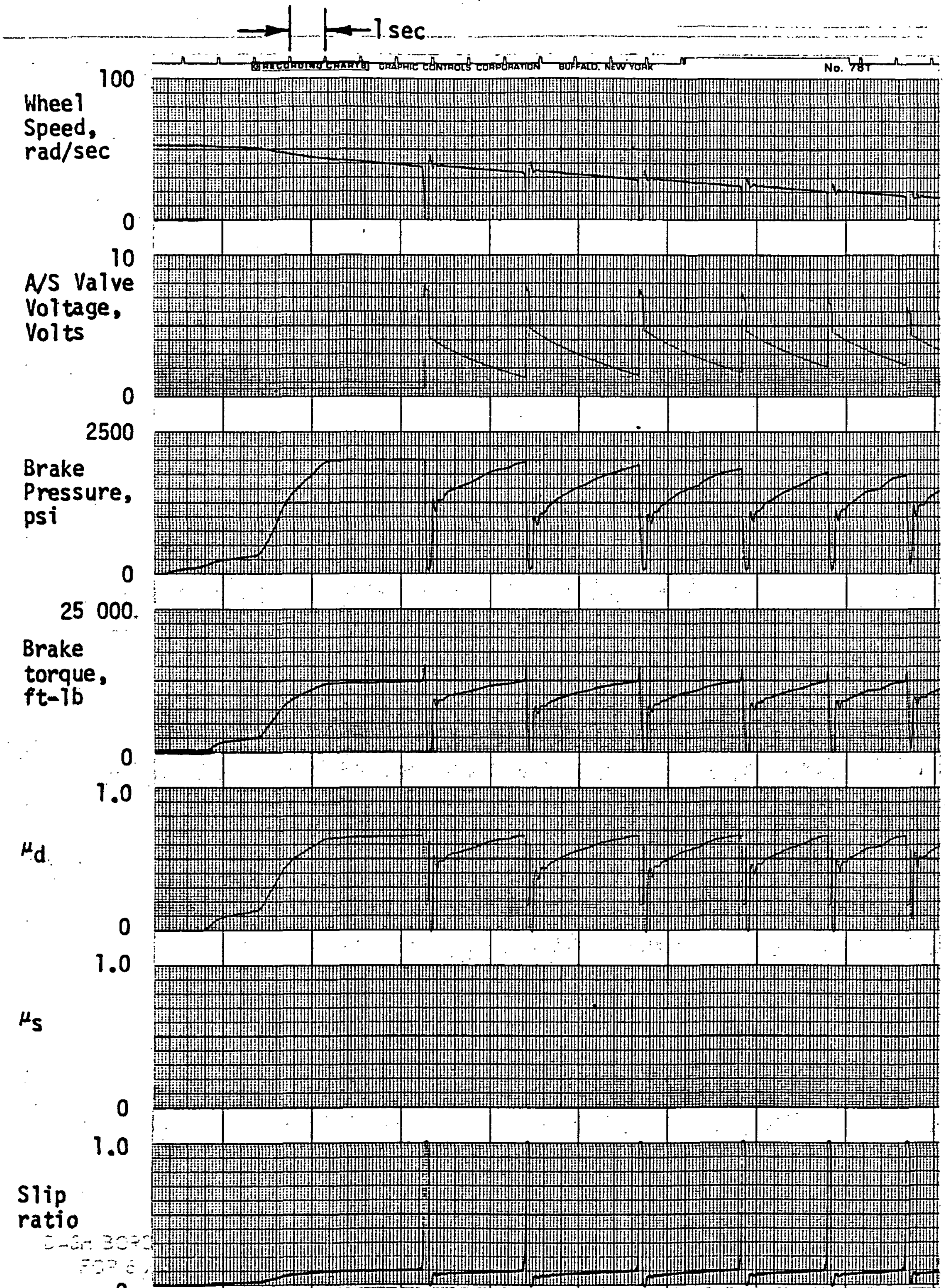

FIGURE C-7 ANTISKID SIMULATOR TIME HISTORY -- UNYAWED TIRE

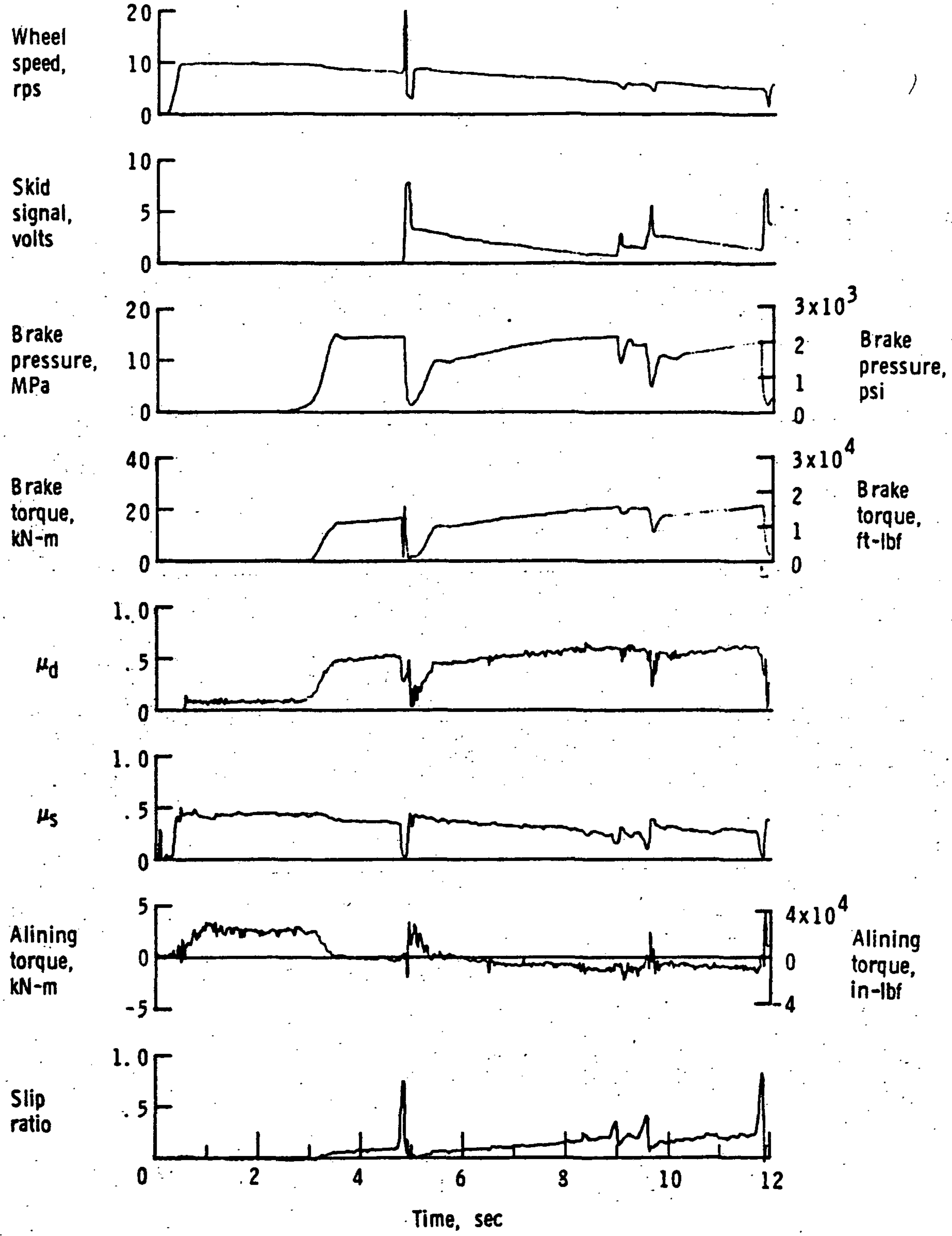

- Time histories for run 36; nominal carriage speed, 46 knots; vertical load, 83.6 kN (18 800 lbf); yaw angle, 6°; surface condition, dry; tire condition, new; brake pressure, 14 MPa (2000 lbf/in^2).

FIGURE C-8 TEST TIME HISTORY SELECTED FOR ANTISKID SIMULATOR VALIDATION -- YAWED TIRE

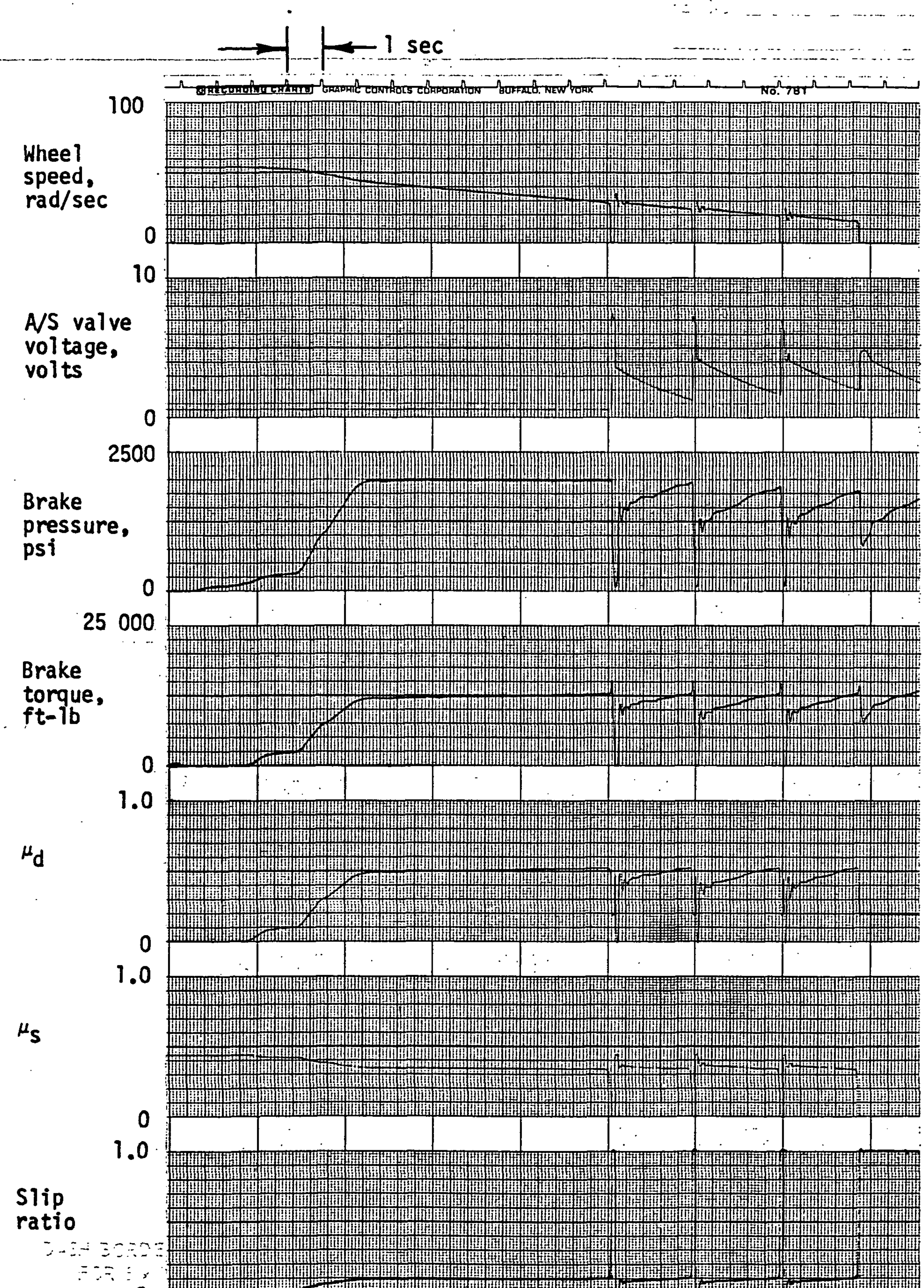

FIGURE C-9 ANTISKID SIMULATOR TIME HISTORY -- YAWED TIRE

APPENDIX D

COCKPIT SIMULATOR

The cockpit mounted on the motion base platform is sized and configured as a DC-10. This appendix outlines those changes that were made to the cockpit to more closely represent the DC-9 for the ground handling study.

Flight Instruments

DC-9 type instruments were installed on the Captain's side. These instruments were all types normally used in DC-9's except the vertical speed indicator which was a DC-10 type. The three DC-10 engine N_1 indicators were replaced with two DC-9 type EPR indicators. See Table D1 for list of instruments used. The First Officer's side remained in the DC-10 configuration.

Pilot Controls

The only changes made to the pilot controls were changes in the force gradients and the removal of the number three engine control lever. Figures D1 through D4 show the force versus position curves of the column, wheel, rudder pedals and toe brakes.

The spring rates of the column and wheel were changed to more closely match the DC-9. The force gradient of the rudder pedals was left the same as the DC-10. The force gradient of the toe brakes was adjusted using test pilot's comments. The curve shown is the gradient actually used.

As mentioned the number three (farthest right) engine control lever was removed leaving numbers one and two for independent twin engine control. A reverse thrust detent was added for the ground handling study. This addition is described in Appendix A Section 3 "Engine Model."

Pitch trim was provided through a thumb activated switch on the left hand side of the Captain's wheel and the right hand side of the First Officer's wheel.

Pilot Controls (Continued)

The speed brake and flap controls were DC-10 types but were active with the exception that the speed brake lever did not move with auto ground spoilers.

The nose wheel steering side controller "tiller" was not active for this study.

See Appendix A Section 2 "Aero and Control Systems" for additional descriptions of pilot controls.

Outside Visual Scene

The outside visual scene was provided by a Redifon Visual Flight Attachment (VFA). At the cockpit the VFA image is presented to the pilot by a T.V. monitor through large collimating lenses. The faces of the T.V. monitors are masked to provide the proper pilot eye cut off angle. For the DC-9 this angle is about 15.5° down from horizontal and was obtained in the DC-10 cockpit by moving the masks on the monitors up to a point where the cut off angle is correct, provided the eye is in the designated position. (See Figure D5.)

NOTE: It is very important for those "flying" the simulator (and the aircraft for that matter) to have their eyes in the proper position!

TABLE D1
EQUIPMENT USED FOR DC-9

VENDOR PART NO.	SERIAL NO.	NAME	VENDOR
2067635-0701 TYPE 1NA-51A	7526	RADIO ALTIMETER IND.	BENDIX
522-3907-001 TYPE 329B-7M	666	ALTITUDE INDICATOR (FLT DIR. INDICATOR)	COLLINS
522-3875-002 TYPE 33/A-6K	E-5	HOR. SITUATION IND. (COURSE INDICATOR)	COLLINS
A50D-10D KIT	4191	SIMULATED ALTIMETER	AEROSONIC
MS-45-1D KIT	8252	SIM. MACH/AIRSPD. IND.	MIDWAY
JG298H1	B-416	EPR INDICATOR	HONEYWELL
	B-432	EPR INDICATOR	HONEYWELL
2594468-902	2090895	VERTICAL SPD. IND.	SPERRY

DC-9 BRAKE SIMULATION MBS

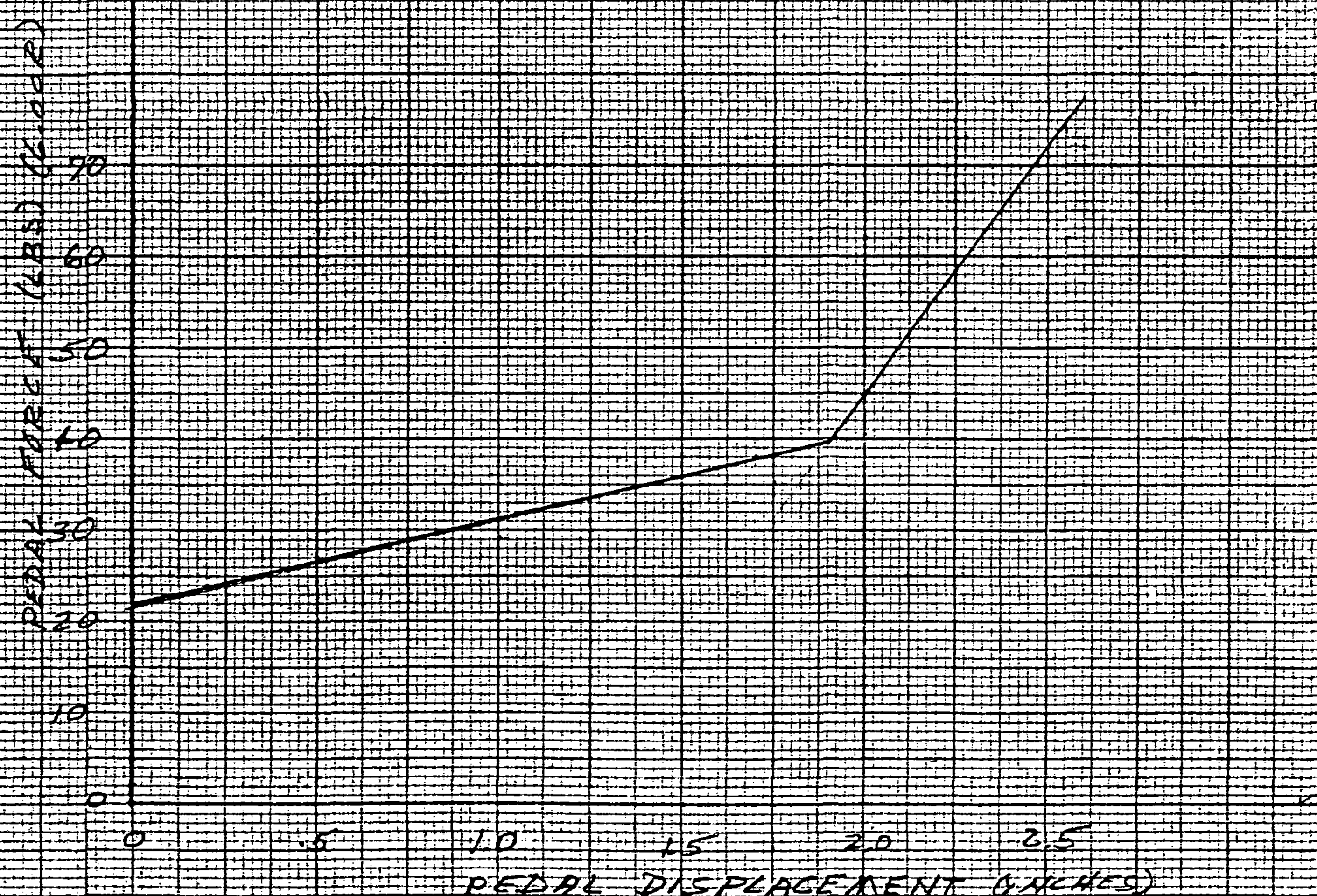

FIG. D1

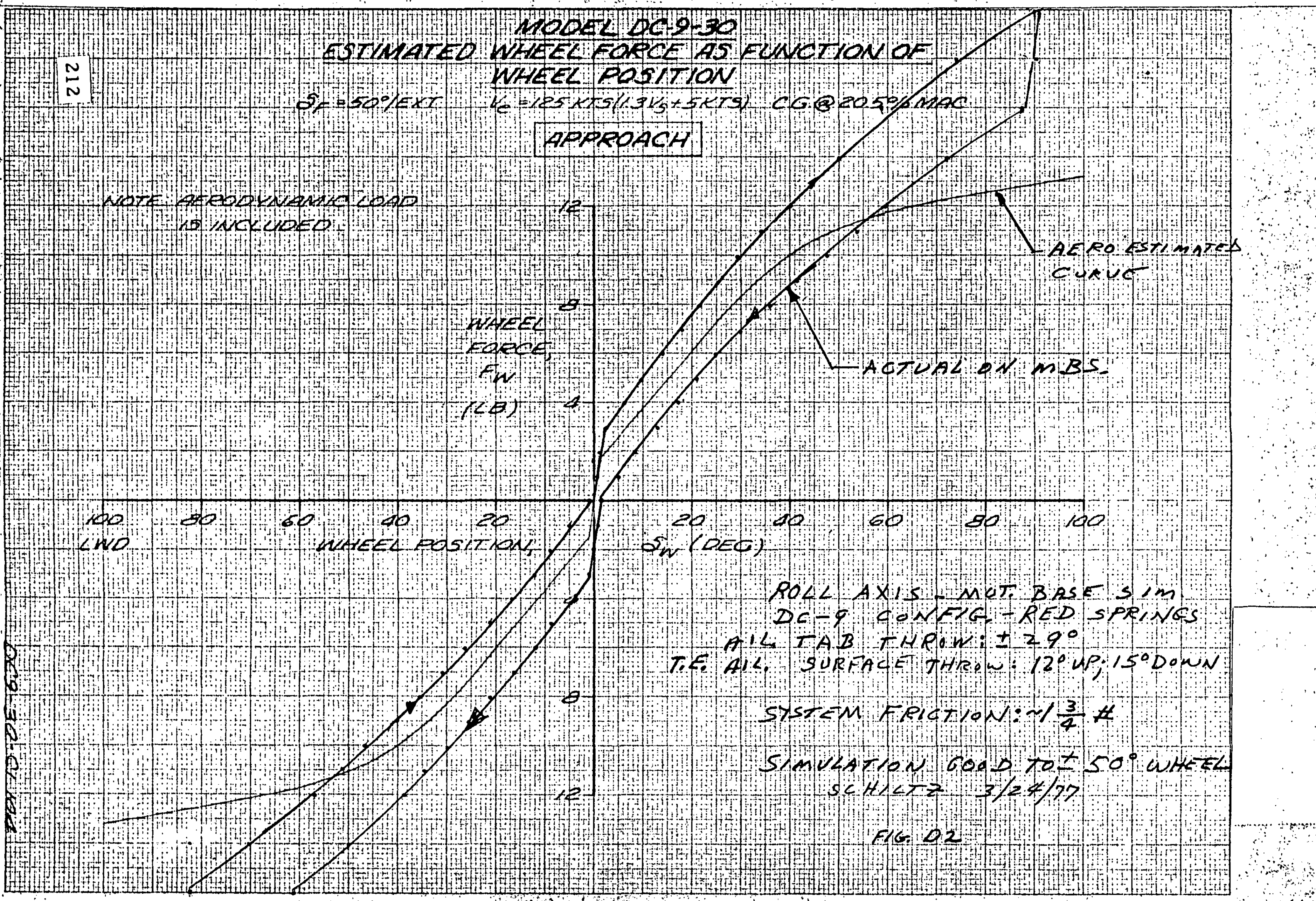
MODEL DC-9-30
ESTIMATED WHEEL FORCE AS FUNCTION OF
WHEEL POSITION
δ_F = 50°/EXT. V_c = 125 KTS (1.3 V_s + 5 KTS) CG @ 20.5% MAC
APPROACH
NOTE: AERODYNAMIC LOAD IS INCLUDED
WHEEL FORCE, F_W (LB)
12
8
4
4
8
12
100
80
60
40
20
20
40
60
80
100
LWD
WHEEL POSITION, δ_W (DEG)
AERO ESTIMATED CURVE
ACTUAL ON M.B.S.
ROLL AXIS - MOT. BASE SIM.
DC-9 CONFIG. - RED SPRINGS
AIL. TAB THROW: ± 29°
T.E. AIL. SURFACE THROW: 12° UP; 15° DOWN
SYSTEM FRICTION: ~1 3/4 #
SIMULATION GOOD TO ± 50° WHEEL
SCHILTZ 3/24/77

FIG. D2

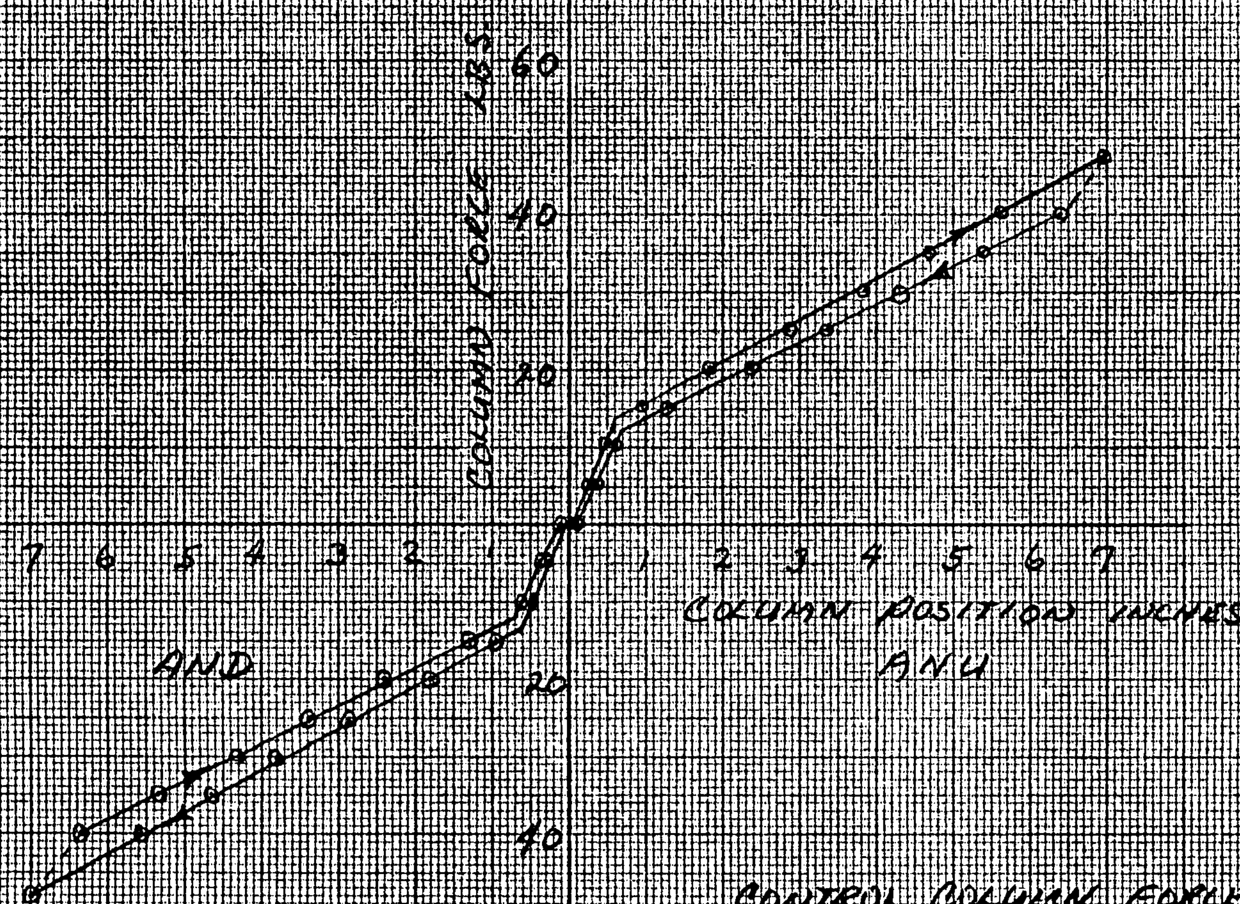

CONTROL COLUMN FORCE
VS.
POSITION
DC-9-10
FIG. D3


PEDAL FORCE ~ LB
RUDDER SURFACE ~ DEG
ANR
ANL
80
70
60
50
40
30
20
10
24 22 20 18 16 14 12 10 8 6 4 2
2 4 6 8 10 12 14 16 18 20 22 24
10
20
30
40
50
60
70
DC-10 COCKPIT SIMULATOR
RUDDER SYSTEM
3-14-70
LOADING FROM 1ST OFFICER'S PEDALS
⊙ ACTUAL
△ NOMINAL
FIG. D4

R.P.S.

(1)

DC9-40 DISTANCE FROM NOSE LANDING GEAR TO PILOT'S FORWARD VISION CUT-OFF POINT

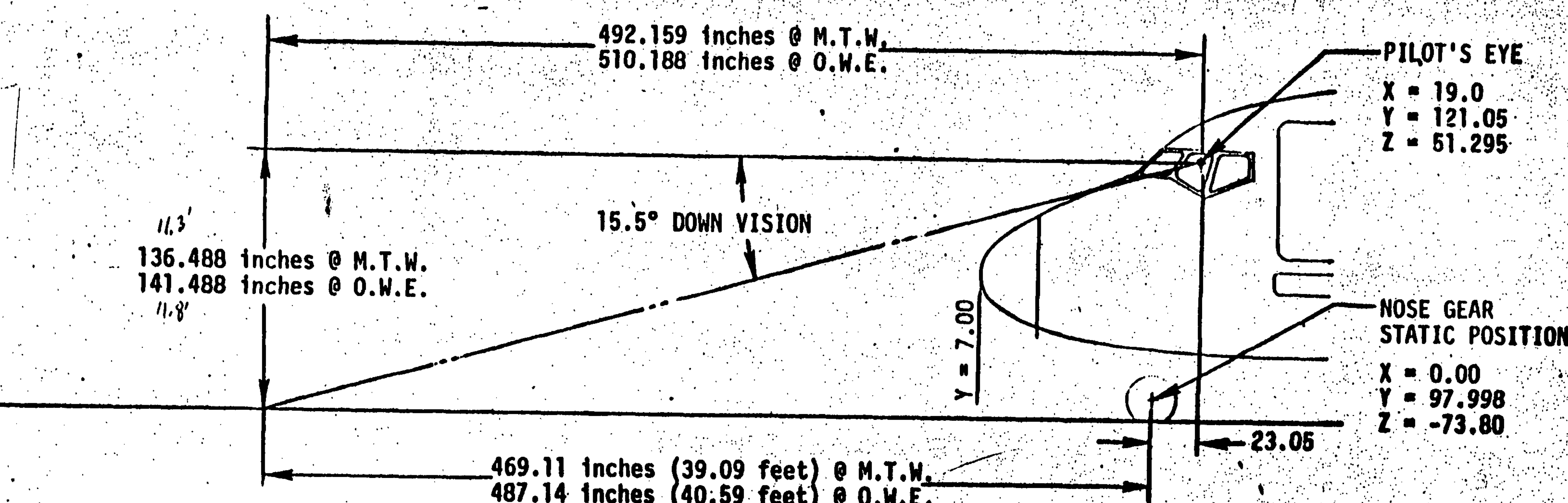

O.W.E. = OPERATING WEIGHT EMPTY
M.T.W. = MAXIMUM TAXI WEIGHT

DIMENSIONS ARE IN INCHES OR FEET

FIGURE D5

APPENDIX E

PROGRAMMING CONSIDERATIONS

This appendix covers some considerations in programming a digital computer to form a real-time solution to the airframe model. The term "real-time" in this context means that vehicle command inputs must be received and "next" airframe state variables calculated fast enough so that the various pilot displays can be updated with no perceptable "steps."

The DC-9-10 airframe model was programmed on the Systems Simulation Sigma V digital computer. An extended version of Fortran was used extensively as the programming language. All of the algorithms associated with the airframe simulation were solved at least once every 50 milli seconds. The single exception was a section of the strut routine (STRUTS) which was solved 7 times faster. The execution of the program took almost 100% of the 50 milli second frame.

When the simulation program was first assembled it took a few milli seconds longer than 50 to solve. This "overframing" condition was rectified by the following procedures:

1) All routines not specifically needed for RDC were taken out;
2) The beam noise was eliminated from the ILS model;
3) The turbulence filter parameters, which normally vary with speed and altitude, were calculated for a nominal speed and altitude and held constant during the real-time sequence. (See Sppendix A, Section 4 for description of the turbulence model);
4) The choice of 7 iterations per frame for a segment of the strut routine was due in part to timing considerations. (See Appendix A, Section 5);
5) Some other minor simplifications were made to the strut routine. (The statements preceded by an "X" in the Fortran listing of the STRUTS routine were left out).

The above five items were specific things done to the RDC program to make it "fit" in the frame time. Some general techniques used by the Douglas Systems Simulation group to effect time saving are described below:

- Simple Euler integration is used throughout the program with the only exception being some linear transfer funtions where finite difference equations are used.

- A special limited range arc tangent routine was implemented. This routine, which is good for resultant angles between $\pm$ 20 degrees, was used for solving angle of attack, side slip angle and the ILS deviations.

- No matrix arithmetic or general matrix subroutines are used for real-time calculations.

- An attempt is made to minimize subroutine CALL's. Fortran CALL statements invoke linkage routines which can be time consuming.

- A careful check is made to be sure that all calculations of constants are done "outside" the real-time loop.

Another point of interest to programmers is that in the solving of the X and Z axes moments of the aircraft a cross inertia term must be delt with. (See Appendix A, Section 1, Figure 1.2). For the RDC DC-9 model the P dot and r dot equations were solved using Cramer's rule to eliminate the "cross" terms. This technique seems to work quite well. However, in previous airframe simulations this same situation was handled by simply using the "past" value of one of the dot terms in the solution of current value of the other. This method also gave satisfactory results.

An important aspect of simulating an aircraft is providing the capability to place the simulated vehicle in different initial positions. A "trimming" process is necessary if it is desired to start the test run with the forces and moments balanced. A special trimming routine was implemented for this purpose. The desired aircraft configuration and position is input at the beginning of a series of runs. The calculations were made to trim the aircraft. These trim values were saved so each time the simulator was put in the reset mode they could be entered as initial conditions to the equations. A flow chart of the "trim" procedure is shown in Figure 1E.

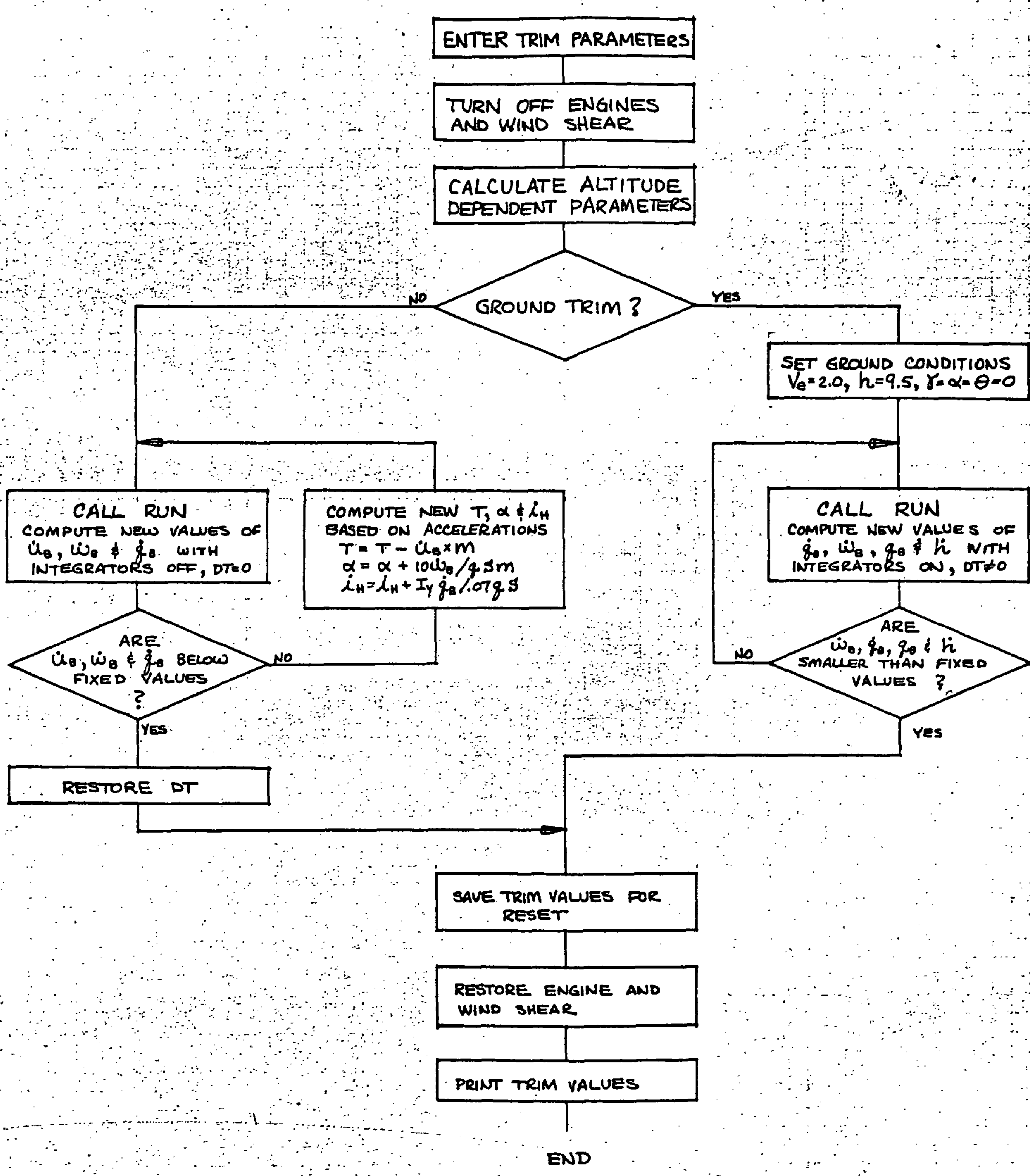
ENTER TRIM PARAMETERS
TURN OFF ENGINES AND WIND SHEAR
CALCULATE ALTITUDE DEPENDENT PARAMETERS
GROUND TRIM ?
NO
YES
SET GROUND CONDITIONS $V_e = 2.0$, $h = 9.5$, $\gamma = \alpha = \theta = 0$
CALL RUN
COMPUTE NEW VALUES OF $\dot{u}_B$, $\dot{w}_B$ & $\dot{q}_B$ WITH INTEGRATORS OFF, DT=0
COMPUTE NEW T, α & i_H BASED ON ACCELERATIONS
$T = T - \dot{u}_B \times m$
$\alpha = \alpha + 10\dot{w}_B / \bar{q}Sm$
$i_H = i_H + I_Y \dot{q}_B / .07\bar{q}S$
CALL RUN
COMPUTE NEW VALUES OF $\dot{q}_B$, $\dot{w}_B$, q_B & $\dot{h}$ WITH INTEGRATORS ON, DT≠0
ARE $\dot{u}_B$, $\dot{w}_B$ & $\dot{q}_B$ BELOW FIXED VALUES ?
NO
YES
ARE $\dot{w}_B$, $\dot{q}_B$, q_B & $\dot{h}$ SMALLER THAN FIXED VALUES ?
NO
YES
RESTORE DT
SAVE TRIM VALUES FOR RESET
RESTORE ENGINE AND WIND SHEAR
PRINT TRIM VALUES
END

VOLUME II REFERENCES

1. Expansion of Flight Simulator Capability for Study and Solution of Aircraft Directional Control Problems on Runways, Phase I, MDC Report A3304.

2. Expansion of Flight Simulator Capability for Study and Solution of Aircraft Directional Control Problems on Runways, Phase II, NASA CR-145044.

3. Russell V. Parrish, James E. Dieudonne, and Dennis J. Martin, Jr.,"Motion Software for a Synergistic Six-Degree-Of-Freedom Motion Base,"NASA TND-7350, 1973.

4. Harry Passmore and C. R. Korba,"DC-9 Landing Gear Math Model for Directional Control on Runway Flight Simulation,"MDC Report A4816, 1977.

5. Sandy M. Stubbs and John A. Tanner,"Behavior of Aircraft Antiskid Braking Systems on Dry and Wet Runway Surfaces,"NASA TND-8332, 1976.

6. Douglas Report No. LB-31624, "Estimated Aerodynamics Data For Stability and Control Calculations, Model DC-9 Jet Transport, Series 10," dated December 31, 1964 with latest revision February 23, 1967.

7. N. M. Barr, D. Gangass and D. R. Schaeffer, "Wind Models for Flight Simulation and Certification of Landing and Approach Guidance and Control Systems," Report No. FAA-RD-74-206 by Boeing Commercial Airplane Co., for U.S. Dept. of Transportation, December, 1974.

8. R. E. McFarland: NASA-Ames Program Specification, titled "Wind," Part No. NAPS-80, Computer Sciences Corporation NASA-Ames Site Operation.

9. R. V. Parrish, J. D. Rollins and Dennis J. Martin, Jr.: "Visual/Motion Simulation of CTOL Flare and Touchdown Comparing Data Obtained from Two Model Board Display Systems," AIAA Paper No. 76-010, April 26-28, 1976.

10. Redifon Report No. SD/846/S Issue 3, "Requirements for the Compatibility of a McDonnell Douglas Corporation Flight Simulator to the Redifon Rigid Model Visual Flight Attachment," January 12, 1971.

11. E. A. Mechtly, "The International System of Units, Physical Constants and Conversion Factors," second revision, NASA Report No. SP-7012, 1973.